Copyright

by

Margaret Ann Phillips

2011

The Dissertation Committee for Margaret Ann Phillips Certifies that this is the approved version of the following dissertation:

Polysaccharide Decoration of Complexation Hydrogel Networks for Oral Protein Delivery

Committee:

Nicholas A. Peppas, Supervisor

Jennifer Maynard

Krishnendu Roy

H. Grady Rylander, III

Christine Schmidt

Polysaccharide Decoration of Complexation Hydrogel Networks for Oral Protein Delivery

by

Margaret Ann Phillips, M.S.E, B.S. B.M.E

Dissertation

Presented to the Faculty of the Graduate School of

The University of Texas at Austin

in Partial Fulfillment

of the Requirements

for the Degree of

Doctor of Philosophy

The University of Texas at Austin

August, 2011

Dedication

For my family and friends

Acknowledgements

I would like to thank my family--my parents, Sean, Susie, Jenny, Rick, Matt, and Teresa—for their love and support over the last four years.

I would especially like to thank my advisor, Prof. Nicholas Peppas. This work would not have been possible without all of the time and hard work he spent to discuss and review my research. His guidance and support has made such an impact on my development as a scientist through his encouragement to seek out new learning opportunities. He taught me to really embrace the challenging parts of science.

I would like to thank my fellow Peppamers whose friendships were some of the best parts of my graduate school experience: Adam, Bill, Brandon, Carolyn, Cody, Daniel, David, Diana, Don, Justin, Marty, Mary, Melissa, Michael, Omar, Ruben, Shahana, Steve, Terry, Ana, Coro, Edgar, and Marta! Thank you for all of the wonderful moments and the assistance you offered me so generously.

I would especially like to thank Marty. Graduate school would not have been the same without him. He truly made this experience so special. Over the last four years, he has been a constant source of patience and support.

I would like to thank the members of my Ph.D. committee: Professor Jennifer Maynard of Chemical Engineering, Professors Krishnendu Roy, Grady Rylander, and Christine Schmidt of Biomedical Engineering. The input of my committee has been valuable, and the collaborations that followed have taught me so much.

I am very thankful for the opportunity to work with several outstanding undergraduates in the laboratory: Katy Bartlett, Amy Creecy, Asha Fleury, Julie Fogarty,

Jaclyn Huseman, Kristen Lutek, and Matt Winters. Their enthusiasm always brightened my day. Serving as their lab mentor was a truly rewarding experience.

My network of friends here in Austin truly helped make Austin a home for me. I would like to thank them for being an endless source of laughter, support, and memories.

Polysaccharide Decoration of Complexation Hydrogel Networks for Oral Protein Delivery

Publication No._____

Margaret Ann Phillips, Ph.D.

The University of Texas at Austin, 2011

Supervisor: Nicholas A. Peppas

Polysaccharide-decorated complexation hydrogels were investigated for use as oral insulin delivery systems. Several different polysaccharide modifications of poly(methacrylic acid-grafted-ethylene glycol) hydrogels were developed using dextran and pullulan. Polymerizable groups were added to the polysaccharides, dextran and pullulan, by methacrylation. These macromers were then copolymerized with methacrylic and poly(ethylene glycol) to form P(MAA-g-EG-co-Dextran) and P(MAA-g-EG-co-Pullulan) gels using a UV-initiated free radical polymerization. The synthesis of these materials was confirmed using Fourier transform-infrared spectroscopy.

The pH-responsive swelling of these systems was investigated using dynamic and equilibrium swelling measurements. Swelling of polysaccharide-modified hydrogels occurred with increasing pH. In acidic conditions, these materials were in a collapsed state while in neutral conditions these materials were swollen.

The ability to load insulin into these hydrogels using was demonstrated with loading efficiencies as high as 88% were observed for P(MAA-g-EG-co-Dextran 6000)

hydrogel microparticles. Almost zero release of insulin occurred in acidic conditions while an increase in pH was shown to trigger release.

The use of dextran and pullulan-modified complexation hydrogels for oral delivery applications was investigated using in vitro cellular viability assays and mucoadhesion experiments. These systems were shown to cause little cytotoxicity to an intestinal epithelium Caco-2 cell model over a range of concentrations as high as 1 mg/ml. The adherence of polysaccharide-modified hydrogels to reconstitituted mucin gels was quantified with the P(MAA-g-EG-co-Dextran 6000) performing the best.

Further evaluation of polysaccharide-modified complexation hydrogels for oral insulin delivery was evaluated through *in vitro* insulin drug transport studies using a mucus-producing Caco-2/HT29-MTX co-culture model. The results showed that the P(MAA-g-EG-co-Dextran 6000) allowed transport of insulin across the cell monolayers and did not adversely affect the integrity of the epithelial monolayer.

Table of Contents

List of Tables

List of Figures

Chapter 1:

Introduction

Protein drugs have already revolutionized treatment for a number of diseases, and the expected increase in protein-based pharmaceutics brings a new set of challenges for the pharmaceutics field. Due to their instability, size, and poor transport properties, protein drugs are predominantly administered by either intravenous or subcutaneous injection.

Patient compliance, the extent to which a patient adheres to the treatment, is already a concern in diabetes treatment with insulin and is likely to become a growing issue as protein drug treatments become more widely used. A number of studies have underscored the relationship of traditional subcutaneous injections with patient non-adherence, and it is estimated that over half of insulin-dependent adults intentionally skip injections [1, 2]. We believe that the development of an oral insulin formulation has the potential to address some of the issues associated with non-adherence (including the interference with daily activities, embarrassment, and injection pain) as well as reduce the adverse effects of subcutaneous administration.

Oral administration of drugs is also preferred over subcutaneous injection for other reasons. For example, oral administration is easier for patients, and it eliminates the need for needles and disposal of sharps. Orally delivered insulin would be advantageous over existing dosage forms because orally administered drugs absorbed in the intestine enter the hepatic portal vein. The hepatic portal vein carries the drug to the liver where it undergoes first pass metabolism. This pathway closely follows the pathways insulin naturally takes after secretion from the pancreas. As a result, orally administered insulin may more closely mimic the natural biodistribution of insulin. For

these reasons, the development of an oral insulin formulation could significantly impact the treatment of patients with diabetes.

Oral delivery of insulin and other protein drugs is not without challenges. Two of the greatest challenges to oral protein delivery is maintaining the bioactivity of the drug and achieving a therapeutic bioavailability. The secondary and tertiary structure of protein drugs can be denatured in the GI tract, reducing the therapeutic activity of the drug. Additionally, protein drugs can be degraded by proteolytic enzymes present in the stomach and the small intestine.

Improving the absorption of protein drugs is a major obstacle to maintaining high bioavailability using oral insulin delivery. Large, hydrophilic macromolecules such as insulin have low permeabilities across the intestinal epithelium. In order to overcome low absorption, a variety of methods have been explored. One of the most promising strategies is the use of mucoadhesive carriers which can interact with the intestinal mucosa and extend the residence time of the carrier and drug at the site of absorption.

Because protection of protein drugs from enzymes in the stomach followed by release in the small intestine is desirable, the use of protein drug carriers composed of anionic complexation hydrogel is a promising strategy for oral protein delivery. These hydrogels have been shown to effectively entrap protein drugs within their three-dimensional network. Anionic complexation hydrogels such as P(MAA-g-EG) have been used for pH-responsive protein delivery in the GI tract.

While these systems have been shown to be mucoadhesive, the incorporation of additional adhesion promoters such as wheat germ agglutinin has been shown to improve mucoadhesion. In this work, the incorporation of linear, neutral

polysaccharides into P(MAA-g-EG) hydrogels was investigated for mucoadhesive oral protein delivery.

REFERENCES

1. Peyrot, M., R. R. Rubin, D. F. Kruger and L. B. Travis, Correlates of Insulin Injection Omission. Diabetes Care, 2010, 33, 240-245.

2. Fu, A. Z., Y. Qiu and L. Radican, Impact of fear of insulin or fear of injection on treatment outcomes of patients with diabetes. Curr. Med. Res. Opin., 2009, 25, 1413-1420.

Chapter 2:

Background

Since the entrance of insulin as the first FDA-approved commercially available recombinant protein drug in 1982, protein drugs have become one of the fastest growing classes of new therapeutics. Because of the size of protein drugs and their stability, protein drugs are typically administered via injection systemically or intravenously.

Alternative methods of protein drug administration which do not require injection or intravenous access are highly desirable. The oral route is the most desirable administration method for drugs as it is easy for patients and does not require injection. However, there are several significant challenges to the successful development of oral protein drug formulations: the instability of protein drugs in the gastrointestinal (GI) tract, the low permeability of protein drugs, and a narrow absorption window in the intestine. This chapter is divided into three major sections to review the application, approach, and materials studied in this thesis by focusing on treatment of diabetes with insulin, oral protein drug delivery, and biomaterials containing polysaccharides.

2.1 Diabetes Mellitus and Insulin

According to the World Health Organization, chronic diseases including cancer, diabetes, and cardiovascular disease are the leading cause of death worldwide. The majority of deaths (80%) related to chronic diseases occurs in low to middle income nations [1]. A disproportionate increase in chronic diseases was predicted by WHO in low to middle income nations. Between 2005 and 2007, it was expected that deaths due to chronic diseases would increase by 17%. In comparison, a 3% decrease in deaths

due to nutritional deficiencies, infectious diseases, and maternal and prenatal conditions was predicted. This trend in increased chronic diseases in developing nations is expected to continue.

Diabetes is a particularly concerning chronic disease because it is becoming more prevalent both in the United States and abroad. In 2007, it was estimated that 23.6 million people in the United States or about 7.8% of the population were living with diabetes, and diabetes was the seventh leading underlying cause of death [2]. According to the World Health Organization, about 6% of the global population has diabetes. It is predicted that by 2025, diabetes treatment and prevention will cost the international community more than 300 billion US dollars and only a fraction of this expenditure, 20%, will be spent on patients outside the wealthiest countries [3].

Currently, the treatment and management of diabetes is challenging especially in poorer nations where control over diet, monitoring of blood glucose levels, and administration of drugs are less accessible. Limited access to insulin and limited health care resources are significant concerns for treatment of diabetics. For example, access to insulin in sub-Saharan Africa is still not available continuously.In a study on the availability of insulin, insulin was available only at the two national referral hospitals in Mali, at most hospitals in Mozambique, and at some smaller Referral Health Centers in Zambia [3].

In addition to concerns regarding insulin availability, cost is a significant constraint in the treatment of diabetes in developing nations. The cost of insulin is subsidized in some countries, but patients typically pay for their own syringes, which are often difficult to obtain and range in cost. In sub-Saharan Africa, syringes range in cost from $0.04 to $1.50 each.

With expected increases in diabetes globally and a disproportionate increase in chronic diseases in developing nations, diabetes management and treatment is a significant global challenge. Alternative methods to subcutaneous and intravenous administration of protein drugs are needed. More convenient administration methods, such as oral administration, would significantly impact the world through increased patient adherence, improved quality of life for patients, and may alleviate some expenses for patients in developing nations.

2.1.1 Physiology of Diabetes

Diabetes is a group of diseases associated with chronic hyperglycemia. The underlying cause of diabetes can be a problem with insulin production, insulin ineffectiveness, or both. Type 1 diabetes is characterized by an inability to produce insulin and is also referred to as juvenile diabetes. Type 2 diabetes, or adult-onset diabetes, is characterized insulin resistance and can include problems with insulin secretion. Gestational diabetes is diagnosed in hyperglycemic pregnant women who were non-diabetic prior to their pregnancy. Often, women diagnosed with gestational diabetes develop Type 2 diabetes. This section will focus on the physiology of normal glucose metabolism, the two most common types of diabetes (Type 1 and Type 2 diabetes), and treatment of diabetes.

Insulin

Insulin is a hormone produced in β-cells in the islets of Langerhans in the pancreas. The primary function of insulin is to control glucose levels and the metabolism of fats and steroids. Proper control of glucose is essential because glucose

is required for the synthesis of adenosine triphosphate (ATP) which is involved in almost every biological process.

Normal blood glucose levels are tightly maintained at approximately 90 mg/dL or 5 mmol/L by several hormones. These hormones, most notably insulin and glucagon, help balance glucose levels by regulating cellular glucose uptake in tissue and glucose output from the liver into the bloodstream in response to glucose absorption from nutrients (food) by the intestine and metabolic needs.

When glucose levels increase, insulin is released by β-cells in the eyes of Langerhans of the pancreas to return the blood glucose level to homeostasis by increasing glucose uptake by muscle and adipose tissue. Insulin binding to insulin receptors on adipocyte and muscle cell membranes stimulates the translocation of GLUT4, an insulin-dependent glucose transporter, from storage vesicles within the cell. Vesicles that store GLUT4 fuse with the cell membrane allowing GLUT4 to facilitate glucose uptake. Once glucose enters the cell, it is phosphorylated (by hexokinases), which prevents glucose from leaving the cell. Glucose-6-phosphate can undergo glycolysis. Energy released from glycolysis is used in the synthesis of ATP. Excess glucose-6-phosphate can by polymerized into glycogen for energy storage.

In addition to decreasing blood glucose levels by stimulating glucose uptake by peripheral tissues, insulin further decreases blood glucose levels by inhibiting glycogenolysis and gluconeogenesis in the liver and promoting glycogenesis. While insulin does not affect glucose uptake of the liver, it decreases glucose output by the liver by inhibiting glucose-6 phosphatase. Insulin activates the enzymes involved in glycogen synthesis including glycogen synthase and phosphofructokinase. The net effect is a further decrease in blood glucose levels towards normal levels.

Insulin's effect on glucose metabolism is paralleled by its involvement in lipid metabolism. In hepatocytes, glucose can be stored in glycogen or in fatty acids. Fatty acids are released from hepatocytes into the bloodstream and can be uptaken by adipocytes. Adipocytes can then convert uptaken fatty acids and glucose into triglycerides. Because insulin inhibits lipolysis, these triglycerides are stored in adipocytes leading to fat accumulation.

As blood glucose levels drop, glucagon secretion increases. Glucagon primarily acts on hepatocytes to stimulate production of glucose from breakdown on glycogen and gluconeogenesis, the synthesis of glucose from amino acids.

Naturally synthesized insulin is produced by enzymatic cleavage of proinsulin (molecular weight of 9 kDa) stored in vesicles in the Golgi apparatus. As these vesicles become maturing secretory granules, the vesicles leave the Golgi. During this process, proinsulin is then enzymatically converted into insulin (molecular weight of 5.8 kDa) and connecting peptide (C-peptide) by endopeptidases. As a result, insulin is secreted at a higher rate than proinsulin in normal patients.

Normal insulin secretion from β-cells occurs continuously at a baseline level but increases in response to elevated blood glucose levels. Insulin secretion following a spike in glucose levels occurs in a biphasic pattern. The first phase of insulin release occurs rapidly and lasts only a few minutes. This first phase release is caused by a glucose-dependent activation of voltage-dependent Ca^{2+} channels to increase intracellular Ca^{2+}. This influx of Ca^{2+} (in addition to an ATP requirement) causes some insulin storage vesicles to readily migrate to the β-cell membrane and secrete insulin. After this initial release of insulin, insulin release drops. The second phase release increases insulin once again due to insulin release from long-term storage vesicles.

Insulin release by β-cells can be influenced by other factors including amino acids and other hormones.

Type 1 Diabetes

Type 1 diabetes, often referred to as juvenile diabetes, accounts for 5-10% of all cases of diabetes [4]. Type 1 diabetes is fatal without treatment with insulin. Type 1 diabetics are deficient in insulin due to destruction of pancreatic β-cells, which produce insulin. Most cases, approximately 90%, of type 1 diabetes are caused by autoimmune destruction of β-cells [4, 5]. Autoantibodies for islet cells, insulin, tyrosine phosphatase, and glutamic acid decarboxylase are markers that may play a role in the development of autoimmune related diabetes [5].

The risk of type 1 diabetes is higher in families indicating that genetics also contribute to disease development [4]. However, environmental factors such as viral infections have been implicated as destroying or causing the destruction of β-cells [4, 5]. Other factors such as whether one was breast fed, diet, exposure to chemicals, and stress have also been identified as possible causes of type I diabetes [4].

Type 1 diabetes is typically diagnosed during childhood. Some cases of type 1 diabetes are diagnosed in adults, and it is acknowledged that type 1 diabetes can onset after childhood. Typically, symptoms arise suddenly and are severe. Some of the common symptoms of type 1 diabetes include frequent urination, thirst, extreme hunger, weight loss, tiredness, and irritability.

A patient is diagnosed with diabetes when they have a fasting plasma glucose level at or above 7.0 mmol/L; plasma glucose levels at or above 11.1 mmol/L in a glucose tolerance test; or a hemoglobin A1C at or above 6.5. At the time of diagnosis of type 1 diabetes, many diabetics already have some form of ketoacidosis caused by

unchecked fatty acid metabolism by lack of insulin, which causes the pH of the blood to become acidic.

Type 2 Diabetes

Type 2 diabetes is a result of insulin resistance and, or problems with insulin secretion. The causes of type 2 diabetes are not fully understood. Genetics do play a role in one's risk of developing diabetes, but environmental factors and lifestyle significantly affect diabetes development. For example, obesity, smoking, inactivity, and certain drugs can contribute to type 2 diabetes onset.

Type 2 diabetes disease progression typically begins with development of insulin resistance. Development of insulin resistance, or an inability to respond to insulin, includes hyperinsulinemia in the fasted state but also increased postprandial insulin. Hyperinsulinemia is caused by a combination of increased insulin secretion by β-cells (due to blood glucose levels) or due to decreased liver uptake of insulin [6].

Excess circulating fatty acids from lipolysis of triglycerides in adipose tissue are both an effect of insulin resistance and contributor to insulin resistance. Increased fatty acids increase glucose output from the liver as well as reduce insulin's inhibitory effect on glucose output by the liver. Because insulin inhibits fatty acid production, an increased amount of fatty acids in muscle provides more substrate rendering insulin less effective, but increased fatty acids also affect downstream signaling the continues to reduce insulin activity [7]. There are a variety of other physiological changes that occur as a result of insulin resistance which are discussed more in depth in Eckel et al. [7].

Continued exposure of β-cells to elevated glucose levels and fatty acid levels affects insulin secretion. Normally, elevated fatty acids can stimulate insulin secretion, but β-cell insulin secretion decreases after prolonged exposure to high fatty acid levels

[6, 7]. Defects in insulin secretion can also be caused by decreases in insulin receptors on β-cells [7]. One of the hallmarks of irregular insulin secretion is a much higher secretion rate of proinsulin and insulin precursors than insulin [5]. The higher secretion rates of proinsulin and insulin precursors are caused when vesicles in β-cells are secreted prior to insulin cleavage. This occurs when these vesicles bypass the Golgi apparatus and are secreted from the cell directly from the endoplasmic reticulum. Insulin secretion by this altered mechanism occurs constitutively rather than in a biphasic pattern associated with normal insulin secretion. In this case, the secretion of insulin is not regulated but is constitutive.

Although most people with type 2 diabetes have no apparent symptoms, symptoms may occur insidiously. Type 2 diabetes symptoms include the symptoms of type 1 diabetes as well as frequent infections, blurred vision, hypertension, slow healing cuts and bruises, tingling or numbness in the hands or feet, recurring skin, gum, or bladder infections.

Complications of Diabetes

Diabetes can cause a range of serious complications resulting in disability or even death [5]. Some of the complications that are associated with diabetes are cataracts, retinopathy, glaucoma, nephropathy, neuropathy, heart attack, stroke, blockage of blood vessels in legs and feet, and gum disease.

As a result, diabetics are typically monitored for management of diabetes, lifestyle, and onset of complications. Monitoring of weight and body mass index can indicate the patient's lifestyle, and abdominal obesity can indicate an increased risk of cardiovascular disease. A good indicator of blood glucose management over the preceding 2-3 months is glycosylated hemoglobin (HbA1c) [8]. As hemoglobin is

exposed to plasma glucose, it becomes glycosylated. The extent to which hemoglobin A is glycosylated is an indicator of blood glucose levels over the preceding 2-3 months [8].

Long-term management of diabetes includes management of the various complications of the disease. Complications to diabetes are numerous and can significantly impact a patient's physical and mental heath. For example, diabetics have a high risk of depression [8]. Diabetes is associated with an increased risk of kidney damage, which can be detected by several tests. The ratio of microalbumin to creatinine levels in the urine levels may indicate kidney problems. In addition, measurement of the estimated glomerular filtration rate (e-GFR) can indicate issues with the kidney that may be brought on by diabetes or may be a side effect of some prescription drugs. Diabetics with a low e-GFR may be placed on statins or their medications may be switched.

Because diabetes affects both the circulatory and nervous systems, monitoring for several related complications is very important. Blood pressure measurements can indicate a variety of issues including onset of diabetic neuropathy [8]. As high cholesterol and triglycerides are a complication of diabetes, cholesterol and triglyceride levels are monitored to reduce the risks of cardiovascular diseases and stroke. Additional vascular and neural issues may be identified in an annual foot exam. The combination of neural and vascular issues can result in blindness. Early detection of retinopathy may be monitored using digital retinal photography and is especially recommended for newly diagnosed type 2 diabetics [8].

2.1.2 Treatment of Diabetes

Treatment of Non-Insulin-Dependent Type 2 Diabetes

Many type 2 diabetes patients are not on dependent insulin, and there are several treatment strategies for these patients. The treatment of type 2 diabetes begins with lifestyle modification. Patients are recommended to exercise and adjust their diet to reduce caloric intake, cholesterol, and sodium. Because obesity is a risk factor for type 2 diabetes, patients are typically recommended to lose weight.

For patients whose blood glucose levels are not controlled by lifestyle changes, there are a variety of drugs available which include insulin sensitizers, insulin secretagogues, and agents to slow carbohydrate absorption (from digestion) [4]. Metformin and thiazolidinediones are often used as insulin sensitizers. Metformin specifically reduces glucose produced by the liver and improves insulin-mediated glucose usage at the cellular level (improving insulin sensitivity). Thiazolidinediones improve insulin sensitivity by increasing glucose usage through peroxisome proliferator-activated receptors although the specific mechanism is still not clear [4].

Improved insulin secretion is achieved with sulfonylureas or non-sulfonylureas. Sulfonylureas (metformin) bind to sulfonylurea receptors of β-cells. Binding triggers depolarization of the β-cell membrane which causes secretion of insulin granules. Non-sulfonylureas increase insulin secretion at mealtimes. These drugs, such as repaglinide and nateglinide, bind sulfonylurea receptors but act on much shorter time scales than the sulfonylureas.

Reduction or delay of carbohydrate absorption in the intestine can also lower blood glucose levels. One mechanism for doing this is through the use of α-glucosidase (AG) inhibitors. Inhibiting the enzymatic metabolism of disaccharides and complex

carbohydrates leads to lower postprandial blood glucose increases and can lead to decreased insulin secretion.

Because these drugs typically lead to weight gain (and can cause edema and hypoglycemia), diabetes treatments that do not result in weight gain are highly desirable. Incretins are gastrointestinal hormones secreted during eating that cause insulin secretion before blood glucose levels rise. As a result, incretins are targets for diabetes management. Glucagon-like peptide 1 (GLP-1) may be involved in β-cell health, appetite suppression, and slow gastric emptying [4]. Although the role of GLP-1 in metabolism is still being studied, GLP-1 therapy is a target of type 2 diabetes treatment because GLP-1 levels tend to be lower in obese people and in type 2 diabetics. Exenatide is a GLP-1 analogue that must be administered by injection as a type 2 diabetes treatment without a side effect of weight gain. Exenatide and other GLP-1 mimics must be administered by injection because they can be degraded by dipeptidyl peptidase-4 (DPP-4). As a result, a DPP-4 inhibitor, sitagliptin, is being used to increase GLP-1 in patients.

Insulin Therapy for Diabetics

Type 1 and some type 2 diabetics require insulin replacement therapy. There are several types of insulin and various insulin regimens. For example, there are animal insulins, short-acting insulins, very rapid-acting insulin analogues, intermediate-acting insulins, long-acting insulin zinc suspensions, long-acting insulin analogues, and pre-mixed insulin mixtures. A discussion of the action of each of these insulins can be found in several references [4, 8].

For very young type 1 diabetes patients, the most common treatment is the 'basal-bolus' regimen consisting of multiple subcutaneous injections (multiple daily

injections, MDI) of a short-acting insulin and a long-acting insulin to maintain basal levels [5, 8].

Insulin Administration

Insulin may be administered by syringe and needles, with insulin pens, by insulin pumps, or by inhalation. Subcutaneous insulin injections can be done in the abdomen, the thighs, and upper arms. Patients must be careful to rotate the injection site, but over time lipohypertrophy still can occur. Lipohypertrophy is problematic in that it decreases insulin transport or absorption and is a cosmetic issue for patients [8].

Insulin pens are an alternative to the traditional syringe subcutaneous method. Insulin pens are pre-filled devices that allow a metered dose from an insulin cartridge. The dose is administered via a disposable pen needle which fits on the end of the device. Currently, Novo Nordisk, Sanofi-Aventis, and Eli Lilly have insulin pens on the market. These devices are particularly popular in Europe and Asia and are growing in popularity in the United States.

Insulin pumps are an alternative to subcutaneous administration. Insulin pumps generally replace slow-acting insulin with a continuous infusion of rapid-acting insulin. The most common insulin pumps use an external pump to administer insulin through a cannula implanted under the skin. Pumps are loaded with insulin either by pre-filled cartridges or manually from vials of insulin. There are also completely implantable pumps, which are implanted in the peritoneal cavity and controlled by an external device.

The only FDA approved route of administration not requiring needles was Pfizer's Exubera. Exubera was withdrawn from the market after only one year. The failure of Exubera is one of the biggest failures in the pharmaceutics industry with

approximately $1 billion lost [9]. The failure of Exubera was due to a variety of contributing factors. Exubera was not user-friendly, it was not supported by insurance companies, and it was expensive. More importantly, it was not demonstrated that Exubera improved metabolic control over subcutaneous injection [9].

The inhaler device was somewhat large and offered little discreteness for patients. In addition, it could take a long time (up to minutes) to administer a large dose of insulin by inhalation. Administration of a desired dose was challenging as the insulin dose was contained in blister packs. To change the dosage of insulin, the number and combination of blister packs had to be changed. On top of this, the dosage of insulin in the Exubera blister packs was reported in different units than patients and physicians normally used (mg versus international units (IU)) [9].

In addition to convenience and ease of use questions, the safety of Exubera was not certain. During clinical trials, Exubera was shown to adversely affect lung function (Exubera). The affects on lung function did not appear to worsen over the course of Exubera usage, and were shown to reverse when Exubera use was terminated [9]. As a result, the FDA required lung function of patients taking Exubera to be monitored regularly.

Since Exubera was not covered by insurance companies, the patient was required to pay for the costs of lung function tests on top of the costs of Exubera. The long-term effects on the lungs and the progression of diabetes related complications were not known. In ongoing clinical Exubera studies, Pfizer reported an increased number of newly diagnosed lung cancer. Even though there was no clear correlation (based on statistics) between Exubera use and lung cancer, Nektar chose to stop development of their own inhaled insulin formulation [9].

2.2 Oral Protein Delivery

Protein drugs have become the fastest growing class of new pharmaceutics since the FDA approval of recombinant insulin in 1982. The field of protein therapeutics has experienced tremendous growth in part due to recombinant biotechnology but also the inherent advantages of proteins drugs over small drugs. Proteins carry out complex functions, interact with biomolecules specifically with reduced risk of side effects, and have low immunogenicity [10].

The first accounts of protein drugs in the treatment of diseases were in the form of tissue extracts. For example, the first protein-based vaccine was developed in 1796 for small pox by Jenner using extracts from cowpox blisters of milkmaids. Over a century later in 1922, the first protein drug, insulin, was discovered by Banting et al. in treatment of diabetes in humans with pancreatic extracts from dogs [11]. A method for extraction of pure insulin from bovine pancreas extracts was later developed. The safety, quantity, and activity of these insulin extracts were determined by quantifying its effects on rabbit blood glucose levels. Manufacturing of insulin by synthetic chemical means was made possible by the work of Fred Sanger on sequencing insulin during the mid 1940s and 1950s.

It was not until the 1970s that the foundation for modern protein therapeutic production and engineering was established. In 1977, somatostatin was the first protein to be cloned into *Escherichia coli* by insertion of the somatostatin gene into the pBR322 plasmid [12]. A year later, the first recombinant protein, insulin, was reported by Genentech. Goeddel et al. synthesized insulin from two separately cloned polypeptide chains demonstrating for the first time synthetic recombinant technology to produce a therapeutic protein [13]. Over the next decade, protein therapeutics including human growth hormone and interferon-α were reported. Meanwhile, several other major

breakthroughs, notably the discovery of polymerase chain reactions (PCR) for DNA amplification and the development of chemical DNA sequencing methods transformed biotechnology. These technologies along with the 1982 FDA approval of the recombinant form of insulin set the stage for protein drug development.

Recombinant DNA technology has had a significant impact on the discovery of new drugs but has also contributed to the safety and efficacy of protein drugs. For example, recombinant production of protein drugs reduced supply and immunological issues associated with protein drugs which were previously harvested then purified from blood or tissues. Moreover, protein engineering has led to improved drug half-lives and activity over native forms. The impact of biotechnology is already apparent in the more than 130 protein drugs approved by the Food and Drug Administration (FDA) [10]. Protein-based pharmaceutics are expected to continue to expand. It is estimated that by 2015 the protein drug market will exceed $150 billion US dollars (Global Industry Analysts, Inc.).

While protein drugs have revolutionized treatment for a number of diseases, the expected increase in protein-based pharmaceutics brings a new set of challenges for the pharmaceutics field. Due to their instability, size, and poor transport, protein drugs are predominantly administered by either intravenous or subcutaneous injection.

Patient compliance, the extent to which a patient adheres to the treatment, is already a huge issue in diabetes treatment with insulin and is likely to become a growing issue as protein drug treatments become more widely used. A number of studies have underscored the relationship of traditional subcutaneous injections with patient non-adherence, and it is estimated that over half of insulin-dependent adults intentionally skip injections [14, 15]. We believe that the development of an oral insulin formulation has the potential to address some of the issues associated with non-adherence

(including the interference with daily activities, embarrassment, and injection pain) as well as the adverse effects of subcutaneous administration. The development of an oral insulin formulation could significantly impact the treatment of patients with diabetes.

The successful development of oral protein delivery systems will significantly impact health care costs and the quality of patients' lives as small improvements in the ease of subcutaneous administration have translated to measurable improvements in patient adherence and decreased health care costs in the case of insulin pen injectors [16].

Orally administered drugs follow the same route through the digestive system as food. The digestive system breaks down food, absorbs nutrients, and excretes waste. For oral drug delivery systems, the physiology of the digestive system can hinder performance but can potentially be exploited to improve drug delivery. Enzymes present throughout the GI tract can act on drugs causing a loss of bioactivity, the ability of the drug to carry out its function. On the other hand, the large surface area and high vascularization of the small intestine is advantageous in drug absorption, but the mucosa of the small intestine can serve as a barrier to drug absorption. In order for an oral delivery system to be effective, the drug of interest must retain its activity and a high bioavailability--be absorbed in quantities large enough to elicit a pharmacological effect.

Protein drugs are particularly challenging to successfully deliver orally due to their instability in acidic environments, their susceptibility to proteolysis by enzymes in the GI tract, and their large size. For example, the structure of protein drugs and the amino acid sequence of the protein drug define its bioactivity. The stability of proteins in the GI tract is particularly problematic. Protein degradation can be due to either chemical or physical instability. Physical changes can result in denaturation, disruption

of the secondary or tertiary structure of the protein in an irreversible or reversible process. Denaturation can occur as a result of aggregation, precipitation, adsorption, or unfolding. Chemical degradation can occur from deamidation, oxidation, racemisation, proteolysis, and disulfide interchange [17].

The large molecular weight of protein drugs limits absorption. Protein drugs must cross the intestinal lining by penetrating an unstirred water layer and then passing across the cellular lining of the intestine. The mucus and glycocalyx of the intestine can further cause degradation of protein drugs [18]. Diffusion of large molecules is limited across the cell membrane. Additionally, large protein drugs cannot easily pass between cells due to tight junctions between adjacent cells. These junctions are estimated to have pore sizes as small as 10 Å. As a result, protein drug absorption is much more challenging than small molecule delivery.

Insulin is a good candidate for oral delivery because oral administration of insulin has the potential to more closely mimic natural insulin biodistribution. Insulin is secreted by β-cells in the pancreas and enters the hepatic portal vein passing into the hepatic portal system. The majority of insulin is metabolized in the liver where it regulates glucose output. Because drug absorbed into the bloodstream of the GI tract enters the hepatic portal system and passes to the liver, orally delivered insulin would mimic the natural pathway for insulin distribution. With many drugs, first pass metabolism by the liver can be a significant drawback to oral delivery, but this is a more natural route for insulin delivery. Furthermore, passage of insulin through the liver allows the overall biodistribution of insulin to more closely resemble that of natural insulin biodistribution. Subcutaneous administration of insulin generates an equal concentration of insulin in peripheral circulation and in the hepatic portal system. Yet, insulin biodistribution is naturally higher in the liver than elsewhere.

Not only does oral insulin administration have the potential to more closely mimic normal insulin secretion, an oral insulin formulation could significantly impact patients. One of the major side effects of subcutaneous administration of insulin is lipohypertrophy which has a cosmetic effect but also can reduce insulin absorption. Oral insulin delivery may not alleviate the need for subcutaneous injections completely, but it could significantly reduce the number of necessary injections for insulin-dependent diabetics. Generally, oral formulations are easier and more convenient to administer than the more invasive subcutaneous route. Improvement of the method of administration is hypothesized to improve patient compliance leading towards overall better management of diabetes and an improved quality of life for the patient.

2.2.1 The Oral Route

Both the anatomy and physiology of the digestive system reflect its range of functions through contrasting, tailored environments. The digestive system is composed of the mouth, the esophagus, the stomach, the small intestine, the large intestine, the liver, and the pancreas. This organ system functions in concert to digest food, absorb nutrients, and prevent pathogens from entering the bloodstream.

In the stomach, enzymes, such as pepsin and gelatinase, break down proteins and other compounds in food. Enzymatic digestion is facilitated by the acidic environment of the stomach which has a pH of approximately 2.0 in the fasted state. The time scale for gastric emptying can be as long as 2.5 hours but is dependent on a number of signals.

Next, food passes to the small intestine. The small intestine is approximately 2.5 cm wide and 6.5 m long extending from the pylorus to the ileocecal valve where it connects to the large intestine. Overall, the small intestine has a relatively neutral pH

between 7 and 8. The overall transit time for chyme in the small intestine varies depending on a number of factors but is on average 3-4 hours.

As food passes from the stomach to small intestine through the pylorus, it enters the duodenum and is mixed with bile and pancreatic juices. The duodenum is the first 20-30 cm segment of the small intestine. The majority of the duodenum forms a loop around the pancreas. One of the functions of the duodenum is to raise the pH of chyme after it leaves the stomach. Duodenal luminal contents have a pH between 6 and 6.5. Generally, the transit time through the duodenum is rapid and can occur as fast as 1 minute [19].

Chyme travels from the duodenum past the duodenojejunal flexure to the jejunum, the middle section of the small intestine, which is approximately 2.5 m in length and is about 4 cm wide. The structure of the jejunum is composed of mucosal folds, valvulae conniventes. These folds increase the surface area of the jejunum to improve nutrient absorption and may also aide in the mixing of chyme. The jejunum has fewer enzymes in the luminal content than what is present in the duodenum. However, there are enzymes associated with the brush border of epithelial cells that compose the majority of the cellular lining. The jejunum is more highly vascularized than the ileum and is more absorptive than the ileum. As chyme passes through the jejunum, the pH rises to between 6.0 and 7.0. The transit time through the jejunum is considerably longer than the duodenal transit time and is on average 3-4 h. The ileum is about 3.6 m in length and is narrower (3.75 cm) than the jejunum. The ileum has less pronounced valvulae conniventes and is less vascularized. Then, chyme passes through the ileocecal valve to the large intestine. The pH of the digestive tract continues to rise between 7.0 and 7.5 in the large intestine, which regulates ion and fluid absorption.

The microanatomy of the small intestine allows for the high absorption and transport of nutrients providing about 90% of the body's nutrients. The small intestine wall has a surface area of approximately 200 m^2 (Wilson TH 1962, Intestinal Absorption Saunders, Philadelphia) 600 times greater than a hollow cylinder of the same dimensions because of intestinal villi, which are finger-like projections of tissue covering the luminal surface of the small intestine. Intestinal villi are highly vascularized as shown in Figure 1; each villus has its own capillary system feeding into an arteriole and venule pair and its own lacteal feeding into the lymphatic system. The surface area of the small intestine and its close coupling with vasculature give the small intestine its absorptive properties. *Because the small intestine is the site where most absorption takes place, it is the ideal release site for orally delivered proteins.*

The absorptive properties of the small intestine are counterbalanced with physiological barriers for prevention of pathogen entry. The interface of the intestinal wall and the lumen is composed of the mucosa, glycocalyx, and the brush border of the intestinal epithelial cells which is the predominant cell type in the small intestine. Columnar epithelial cells are polarized cells that have a brush border (microvilli) on their apical surface.

The main component of the mucosa is water (up to 95% by weight), mucin (less than 5% by weight), and inorganic salts (approximately 1% by weight). Mucin itself is an O-linked glycoprotein. Branched regions of mucin are covered in highly branched oligosaccharide chains (2 to 19 residues). About 25% of the amino acids in these regions are linked to an oligosaccharide chain [20]. Most of these oligosaccharide chains terminate with fucose, sialic acid, and sulfate esters of galactose and N-acetylglucosamine [21].

Below the mucosa is the glycocalyx, a filamentous glycoprotein network that is anchored to the microvilli. The thickness of the glycocalyx ranges from 400 nm up to 500 nm [22, 23]. The glycocalyx is anchored to the brush border of microvilli, the projections of the apical side of intestinal enterocytes. The brush border has mostly digestive and absorptive functions. Enzymes responsible for peptide and saccharide digestion and membrane transporters that facilitate absorption of small molecules such as glucose are closely associated with microvilli.

In addition to columnar epithelial cells, mucus-secreting goblet cells, M cells, and enteroendocrine cells are found in the cell lining of the small intestine. M cells are part of Peyer's patches which are found throughout the cell lining of the lower small intestine. These structures appear as thickened portions of the cell lining and contain lymphocytes, macrophages, and dendritic cells. Peyer's patches have distinctly different properties than surrounding tissues and have been used as specific targets for vaccine delivery applications.

Absorption Mechanisms

Molecules that diffuse across the mucosa and the glycocalyx must cross the intestinal epithelium before entering the bloodstream. In order for absorption to take place, nutrients and even pathogens must penetrate the mucosa, which can be compared to an unstirred water layer. After passing through the mucus layer, a drug must cross through the glycocalyx, and reach the epithelial layer. Transport across the epithelium can occur by either a paracellular route, between cells, or a transcellular route, across cells.

In paracellular transport, the molecule may simply diffuse between the tight junctions of adjacent cells. Typically, paracellular transport is controlled by the

permeability of the tight junctions between neighboring epithelial cells. It has been shown that the permeability of the tight junctions is dependent on divalent cations such as Ca^{2+} and Mg^{2+}. As the concentration of divalent cations decreases, the permeability of the tight junctions increases.

In contrast, transcellular transport allows transport through the cell. In order for molecules to transport across the intestinal epithelium by transcellular mechanisms, the molecule must cross the cell membrane. Permeation across the epithelium of the intestinal lining is bi-directional allowing for absorption and exorption. However, flow in the intestine favors absorption rather than exorption [17]. The intestinal wall can be compared to a semi-permeable porous lipid membrane. Water and polar small molecules can transport easily whereas hydrophilic molecules cannot pass as easily.

There are several mechanisms by which molecules can transport across the intestinal epithelial lining. For molecules that can easily pass through lipid membrane, diffusion is the primary mechanism of diffusion, which can be described by Fick's law. However, protein drugs are large, often hydrophilic macromolecules that cannot easily diffuse across a cell membrane.

Several forms of carrier-mediated transport can occur to facilitate the transport of more polar, hydrophilic molecules. Facilitated diffusion, sometimes referred to as facilitated transport or facilitated passive transport, involves an integral membrane protein which allows the passage of molecules across the cell membrane without an energy expenditure at the cellular level. Counter transport is similar to facilitated diffusion in that a carrier protein is involved. However, in counter transport, the transport of one molecule from the luminal side of the membrane is coupled with facilitated transport of a second molecule in the opposite direction. Active transport

allows facilitated passage of molecules across the cell membrane but requires energy. Generally, active transport moves a molecule against a gradient.

Pinocytosis is another mechanism by which molecules may cross the apical side of intestinal epithelium. Pinocytosis allows transport of molecules by formation of an invagination in cell membrane. The invagination engulfs nearby molecules and then breaks off the cell membrane forming a vesicle. The vesicle enters the cytoplasm and can empty its contents or can fuse with the opposite side of the cell membrane and empty its contents. Although this is a promising mechanism for transport of large molecules, the regulatory mechanisms of pinocytotic transport are not well understood.

2.2.3 Approaches to Oral Protein Delivery

An oral formulation for a protein drug must preserve the drug's structure, protect the drug from proteolysis, and allow for the drug to be absorbed into the bloodstream. A variety of approaches to oral protein delivery have been proposed to meet these needs. Of these, there are several predominant strategies for oral protein delivery: co-administering additional compounds for altering the physiology of the GI tract, modifying the drug, and delivering the drug using a carrier.

The large size of protein drugs on the order of 10 to 100 kDa limits their ability to diffuse across GI tract tissues. The permeability of the intestinal epithelium has been shown to be lowest in the colon and highest in the upper small intestine. Even in the upper small intestine, where the intestinal epithelium is most permeable and over 90% of nutrients are absorbed, protein drug absorption is still low in comparison to smaller molecular weight drug counterparts.

Permeation enhancers

The co-administration of compounds, which alter conditions in the GI tract has been investigated for improvement of protein bioavailability. Permeation enhancers typically enhance intestinal permeability by disrupting the epithelium's tight junctions. A variety of permeation enhancers have been studied including surfactants, fatty acids, medium chain glycerides (usually monoglycerides and diglycerides of caprylic and capric acid), steroidal detergents, acylcarnitines and alkanoylcholines, N-acetylated-α-amino acids and N-acetylated non-α-amino acids, and chitosans and other mucoadhesive polymers [24].

Permeation enhancers have been studied as excipients in oral protein formulations in a number of studies to allow passage of these large drugs across the epithelium. For example, oral delivery of the nonapeptide leuprolide was shown to increase 4-fold in bioavailability with the addition of sodium salicylate as a permeation enhancer [25]. The effect of tetradecylmaltoside (TDM) on the intestinal absorption of low molecular weight heparins increased bioavailability [26]. The presence of trimethyl chitosan (TMC) in gas empowered drug delivery systems was shown to improve insulin absorption in rabbits [27].

Fetih et al. compared the effects of several permeation enhancers on carboxyfluorescein oral delivery at different sites of the intestine. Their studies showed the greatest effect of permeation enhancers on the colonic delivery. In addition, they found that n-dodecyl-β-D-maltopyranoside had the greatest effect on absorption in the colon [28].

While permeation enhancers have been shown to improve oral protein bioavailability [29], they have also been shown to damage the intestinal epithelium. This damage has been suggested to be reversible but only after the removal of the

permeation enhancer [29, 30]. Yang et al. showed that the effect of the permeation enhancer TDM on transepithelial electrical resistance of monolayers of $C2_{BBe}1$ (a Caco-2 clone) was dependent on the concentration of the permeation enhancer but full recovery took nearly 30 h after removal [26]. The disruption of tight junctions and damage to the epithelium associated with permeation enhancers may also diminish the immunoprotective function of the intestinal epithelium in preventing pathogen entry.

Protease Inhibitors

The use of protease inhibitors to reduce degradation of protein drugs in the GI tract has also been investigated. Because protease inhibitors can reduce enzymatic degradation of protein drugs, protease inhibitors have been used to improve bioavailability and by maintaining the bioactivity of more of the drug. If more bioactive protein drug is available for absorption, a higher bioavailability can be achieved.

A number of studies have shown that protease inhibitors affect bioavailability and protein degradation. For example, Aoki et al. demonstrated that protease inhibitors effectively reduced the activity of a variety of enzymes linked to protein drug degradation [18]. Other studies have confirmed the effects of protease inhibitors on bioavailability *in vivo*. Morishita et al. studied the effects of several protease inhibitors on insulin delivery in the small intestine. They observed an improved hypoglycemic effect over insulin controls indicating a greater the absorption of active insulin in the presence of protease inhibitor. In contrast, Yamamoto et al. only observed a noticeable effect of protease inhibitor on insulin delivery in the large intestine and not the small intestine. They cited variability in enzyme presence and activity between the small and large intestine for the discrepancy between their findings and literature. They also hypothesized that a key difference in experimental methods between the studies in

which the lumen was washed in one study and not washed in the other as a contributing factor in the two studies [31, 32].

The use of protease inhibitors to improve oral protein formulations has several main drawbacks. First, the variability in the performance based on enzyme quantity and activity raises serious concerns over predictable dosing and patient-to-patient variability in absorption. The long-term effects of continued exposure to protease inhibitors, which may include changes to food digestion, have not been fully investigated.

Conjugation of protein drugs

Instead of altering properties of the GI tract, the conjugation of other molecules, such as poly(ethylene glycol) (PEG) or a transporter molecule, have been used to impart enhanced properties to the protein drug. The conjugation of PEG to a protein drug through the process of PEGylation can lead to improved resistance to degradation as well as an extended half-life in the bloodstream. PEG is relatively resistant to protein binding and hence may impart enzyme-resistant properties to a protein drug through conjugation. In general, it is thought that the hydrophilicity of PEG causes water molecules to be closely associated with the polymer forming a hydration layer. This hydration layer acts as a barrier and interferes with protein adsorption. For example, PEG-insulin conjugates have been developed for oral delivery applications to improve enzyme resistance of insulin. Tuesca et al. demonstrated *in vivo* bioactivity of PEG-insulin conjugates and a prolonged circulation time in comparison to insulin after intravenous administration [33].

The modification of protein drugs by conjugation to transporter molecules has been investigated in order to improve protein absorption. In this method, the protein drug is conjugated to molecules absorbed via receptor-mediated endocytosis. The

conjugation of the transporter molecule and the protein drug allows for absorption of the protein drug by the same absorption pathway as the transporter molecule. For example, transporter molecules of transferrin and vitamin B-12 have been investigated for conjugation to protein drugs. Vitamin B-12 has been used to form conjugates with granulocyte-colony stimulating factor, erythropoietin [34], leutinizing hormone [35], and insulin [36]. It has been shown that these conjugates transport across Caco-2 cell layers using the vitamin B-12 absorption pathway [34]. Orally administered B-12-insulin conjugates in the diabetic rat model had a 4.7-fold greater decrease in the area under the blood glucose curve in comparison to orally administered insulin indicating that B-12 conjugation improved oral bioavailability of active insulin [36].

Conjugation to transferrin has also been used to improve insulin transport. The transferrin molecule typically transports iron across the intestinal epithelium via receptor-mediated endocytosis. Conjugates of insulin and transferrin have been shown to improve drug transport in comparison to native insulin in intestinal epithelial cell models [37, 38]. Insulin-transferrin conjugation was also shown to have increased transport over insulin in a mucus-producing co-culture model of Caco-2 and HT29-MTX cells [39]. These studies have suggested that the ability for transferrin to be uptaken by the transferrin receptor is imparted to the conjugate by competitive inhibition experiments [37, 38].

With the administration of protein-transporter conjugates, the long-term effects of chronic administration still need to be evaluated. Furthermore, the effects of administering additional transferrin and vitamin B-12 on iron absorption and vitamin B-12 absorption, respectively, have not been investigated. Transferrin and vitamin B-12 facilitated transport mechanisms could also affect cell signaling but have not yet been investigated.

Enteric Coatings

Protein drugs have also been encapsulated in polymeric delivery vehicles of two kinds: enteric coatings and polymer networks. The main advantage of using a polymer coating or matrix to encapsulate a protein drug is to protect the protein drug from degradation in the stomach. Enteric coatings, such as the Eudragit® systems, are non-crosslinked polymers that dissolve to release the drug. Typically, enteric coatings dissolve at a neutral pH to allow protection of the drug in the stomach at low pH. Because dissolution of the coating occurs at specific pH values, coatings can be selected such that release occurs in one segment of the small intestine.

One of the distinct disadvantages of this strategy is that enteric coatings can only improve the amount of bioactive protein drugs available for absorption but do not facilitate the absorption process. As a result, protease inhibitors and permeation enhancers have been used in conjunction with enteric coatings to achieve improved pharmacological availabilities [30, 40, 41]. A strategy combining an enteric coating and either a protease inhibitor or a permeation enhancer raises additional concerns over long-term safety.

2.2.4 Polymeric Carriers for Oral Protein Delivery

In order to maintain bioactivity but also improve absorption, polymeric carriers have been developed. A variety of designs have been studied including degradable matrices, thiomers, and environmentally responsive polymer networks. Typically, the protein drug is entrapped in the polymer network, and release is controlled by diffusion. Diffusion of proteins through a polymer network is strongly dependent on the mesh size (ξ) of the polymer network, the hydrodynamic radius of the protein, and the strength of polymer-drug interactions.

Degradable Carriers

In the case of degradable polymers, drug diffusion out of the carrier is dependent on the extent of degradation. For the oral delivery of protein drugs, degradable carriers can limit release prior to degradation but allow for increased release with degradation. The ideal degradable system would remain intact in the stomach and start degrading in either the small or large intestine. Degradation products from breakdown of the carrier may interact with GI tissue, be absorbed, or be excreted. Characterization of the effect of degradation products on the GI tract is a critical challenge to oral delivery using degradable carriers.

A variety of degradable carriers have been investigated for oral protein delivery. Of the most widely studied degradable polymer carriers is poly(lactide-co-glycolide), or PLGA. For example, PEG-coated PLGA nanoparticles were shown to deliver intact tetanus toxoid orally [42]. Insulin delivery from PLGA particles co-loaded with insulin and magnetite nanoparticles were shown to decrease blood glucose levels even though bioavailabilities were less than 2% [43]. PLGA was also used to deliver an insulin-sodium oleate complex orally generating a decrease in blood glucose [44]. In another study, PLGA particles with and without an enteric coating of hypromellose phthalate achieved bioavailabilities of 6.27% and 3.68% [45]. Oral formulations composed of PLGA-COOH with olive oil filler were used to orally deliver glucagon-like peptide-1. This formulation had a positive effect after an oral glucose challenge [46]. These studies demonstrated that a variety of PLGA-based particles effectively deliver pharmacologically active protein drugs via the oral route.

Another degradable polymer carrier that has been studied extensively in drug delivery applications is poly(epsilon-caprolactone) yet there are few studies that demonstrate oral protein delivery *in vivo*. Poly(epsilon-caprolactone)/Eudragit

nanoparticles were shown to decrease blood glucose levels after oral delivery of either aspart-insulin [47] and insulin [48]. For the insulin delivery system, the bioavailability of insulin was calculated to be 13% [48].

Mucoadhesive Delivery

One strategy for improving oral delivery of challenging molecules, such as proteins, is the use of mucoadhesive drug carriers. Mucoadhesion is a form of bioadhesion that involves a mucus substrate. The use of mucoadhesive carriers to interact with mucus at the site of absorption was proposed to prolong the residence time of carriers at the site of absorption. Extension of the residence time would allow for an increase in drug bioavailabilty.

There are five main theories that describe the mechanisms of bioadhesion. Often, adhesion is described as a combination of these mechanisms. The electronic theory of adhesion involves the transfer of electrons between the polymer and the tissue. The adjacent electrons form a double layer of charge at the interface causing adhesion between the two materials based on charge attraction. Adsorption theory describes adhesion as occurring based on secondary forces such as hydrogen bonding van der Waals forces. Unlike electronic theory and adsorption theory, the theory of wettability typically describes a system in which one substrate is a liquid and the other substrate is a solid. Wettability describes adhesion based on the ability of the liquid to spread on the surface of the solid. Chain interpenetration theory describes the mechanism of adhesion between polymer gels and tissue. Polymer chains can diffuse across the interface. These interpenetrating polymer chains anchor the two substrates together causing adhesion between the polymer and biological substrate.

Mucoadhesive Hydrogel Carriers

Specifically engineered carriers with the ability to form interactions with the intestinal environment have made improvements in oral drug delivery. For example, carriers have been designed to exhibit mucoadhesive interactions with the intestinal lining. These interactions are believed to enhance the residence time of the carrier in the intestine so that there is a greater period of time for controlled release at the intestinal lining where absorption takes place. Improving the residence time of the carrier and extending the time period over which release can occur in the small intestine is desirable, because protein drug released beyond the small intestine, in the colon for example, has a lower absorption and can result in a lower overall bioavailability of the drug.

Surface decoration of the carrier as shown in Figure 4 has been suggested as a means to enhance cellular interactions between the carrier and the intestine by forming mucoadhesive interactions. Synthetic polymers such as PEG have been used to promote mucoadhesion by interpenetration of PEG chains into the mucosa. The ability of PEG tethers to promote adhesive-like behavior by chain interpenetration into the mucosa has been confirmed both experimentally and theoretically [41, 49, 50]. Additionally, PEG chains have been used in other drug delivery applications for protecting drug delivery systems from immune recognition and shielding drugs from enzymatic degradation [51, 52].

While the mechanism behind mucoadhesion of PEG tethers is due to penetration of the PEG chains into the mucosa and interactions between PEG chains and the mucosa, other systems have been studied that can form more specific interactions. For example, polymer carriers have been decorated with lectins, which are proteins that bind specific carbohydrates, in order to bind to carbohydrate residues found on mucus

glycoproteins. The decoration of wheat germ agglutinin onto P(MAA-g-EG) microspheres was shown to improve the bioavailability of orally delivered insulin (Wood et al). Likewise, this concept of binding components of the mucosa has been applied to forming covalent interactions. Thiol groups have been added to carriers to form thiomers that can form covalent bonds between thiol groups of the carrier and cysteine groups in mucus glycoproteins [53]. *In vivo* studies on the oral delivery of insulin showed that thiolated polymers reduced the blood glucose more than non-thiolated polymers [54].

Chitosan-based drug delivery systems are some of the most studied systems for oral delivery of macromolecules and are the subject of several extensive reviews [55, 56]. One of the prevailing reasons that chitosan has been the focus of so many studies is chitosan's ability to interact with intestinal mucus through charge attraction. Oral delivery of insulin using chitosan nanoparticles achieved a pharmacological activity ranging from 14% to 15.6% [57]. Lower pharmacological availabilities were observed for oral delivery using nanoparticles composed of a chitosan shell and alginate core. However, insulin pharmacological activity was higher when delivered using the nanoparticles (3.4% and 6.8%) in comparison to free insulin (1.6%) [58]. Pharmacological availabilities as high as 5.4% were obtained from insulin oral delivery using carriers of nanoparticles composed of dextran sulfate/chitosan [59]. Calcitonin oral delivery was also demonstrated using liposomes composed of protease inhibitor-chitosan conjugates [60].

Complexation Hydrogels

For controlled release of orally delivered protein drugs, hydrogels have become attractive candidates for carrier design. Hydrogels are crosslinked, three-dimensional

networks composed of hydrophilic polymers. Hydrogels have the ability to swell and imbibe water. Hydrogels are water insoluble and typically exhibit good biocompatibility. One of the unique properties of hydrogels is that hydrogels can be tailored to swell in response to various stimuli including pH, ionic strength, electric field, and temperature. Control of swelling is synonymous with control of diffusion into and out of the hydrogel network.

Control of diffusion processes of a carrier material allows for temporal and even spatial control of the release of protein drugs. This ability to tailor hydrogels is particularly advantageous for oral protein delivery. For oral delivery of protein drugs, release of the protein drug should be minimal in the stomach where degradation is likely to occur. Drug release in the intestine at the absorption site will allow for the maximal amount of active drug to be available for absorption. Hydrogels with pH-dependent swelling can be used to release the protein drug based on the increase in pH between the stomach and the intestine based on complexation behavior.

To use this pH transition from the stomach to the small intestine as a trigger for release, anionic complexation hydrogels have been developed which rely on the complexation properties of the cross-linked polymeric carrier to control release. Anionic complexation hydrogels, such as poly(methacrylic acid-grafted-ethylene glycol) (P(MAA-g-EG)), are composed of a methacrylic acid (MAA) backbone and grafts of PEG. In acidic conditions, the carboxylic acid residues of MAA are protonated and form hydrogen bonds with the etheric groups of PEG. Hydrogen bonds between adjacent polymer chains form physical crosslinks causing the polymer to be in a collapsed state. As a result, diffusion into and out of the polymer network is limited. An entrapped protein drug is shielded from degradation, and release is prevented in the stomach. The physical crosslinks formed by the hydrogen bonding breaks down in the more neutral

pH values of the small intestine. With an increase in pH, the carboxylic acids become deprotonated. Deprotonation causes hydrogen bonding to break down. Meanwhile, steric repulsions between polymer chains cause the polymer network to relax, and the polymer mesh size to increase. With this process comes macroscopic swelling. The protein drug is allowed to diffuse out of the polymer network and release in the small intestine.

P(MAA-g-EG) hydrogels were developed by Peppas and co-workers and have been investigated for oral delivery. Peppas et al. have demonstrated successful loading of a number of protein drugs including insulin, calcitonin [61, 62], growth hormone [62], interferon-beta [61], and chemotherapeutics. These hydrogels effectively protect protein drugs in acidic conditions and from proteolytic degradation [63]. The ability of P(MAA-g-EG) to retain protein drugs and shield them from proteolytic degradation allows for delivery of bioactive drug. Control of release based on the pH change from the stomach to the small intestine allows for site-specific delivery of the payload.

In addition to protecting the bioactivity of protein drugs, P(MAA-g-EG) carriers have been shown to improve absorption of insulin. The ability to improve absorption stems from the ability of these carriers to interact with intestinal mucosa as well as interact with the tight junctions of enterocytes. The mechanism of mucoadhesion of P(MAA-g-EG) is that of chain interpenetration where PEG diffuse into the mucosa. The ability to interact with the intestinal mucosa has been shown to be dependent on the size of the particles and the composition of the polymer. Prolonging the residence time of the carrier allows for an extended time period for the drug to release from the carrier and to be absorbed. One of the other benefits of mucoadhesive delivery systems is a reduction in the path length towards absorption.

The ability of P(MAA-g-EG) carriers to influence paracellular transport is largely based on experimental evidence from *in vitro* studies. Confocal studies on insulin transport across Caco-2 monolayers showed that insulin transport was predominantly paracellular [64]. P(MAA-g-EG) carriers can reversibly open tight junctions by chelating Ca^{2+}. Since tight junction proteins are dependent on Ca^{2+}, the junctions loosen with depletion of Ca^{2+} concentrations. Studies by Peppas and co-workers have shown the recovery of tight junction integrity using transepithelial electrical resistance (TEER) [65].

In vivo, P(MAA-g-EG) systems have improved bioavailability over orally administered insulin. The hypoglycemic effect of orally delivered insulin from P(MAA-g-EG) was first studied by Lowman et al. Oral insulin bioavailability from these systems was found to be 3.40% in healthy rats and 2.44% in diabetic rats for a 25 IU/kg dose [66]. Higher bioavailabilities of 12.8% were observed in optimized systems [67]. The size of P(MAA-g-EG) microparticles was shown to affect drug bioavailability with smaller particles performing better [67].

2.3 Polysaccharides As Biomaterials

Carbohydrates are the most abundant natural biomaterials, more abundant than nucleic acids and peptides. They form polymers with a number of repeat units including monosaccharides, disaccharides, oligosaccharides, and polysaccharides. Carbohydrates decorate a variety of molecules to form glycolipids, glycosaminoglycans, glycoproteins, and proteoglycans. Additionally, they are important components of many other biomolecules including ribonucleic acid (RNA) and deoxyribonucleic acid (DNA). Because of their integration into so many biomolecules, carbohydrates play essential roles in cellular communication, inflammation, infection, development, and disease [68-71].

While the goals of genomics and proteomics, which look at the biological information 'stored' in the genetic code of organisms and the amino acid sequences of proteins, are familiar, glycomics is a much more recent topic in biotechnology. Glycomics seeks to understand glycans as bioinformatics molecules [71-73]. Researchers theorize that the coding capacity of polysaccharides is far greater than that of nucleic acids and amino acids because of the numerous ways that polysaccharides can form glycosidic bonds with one another and the different isomers these molecules may assume [68, 69, 71, 73]. There is a tremendous amount of information to be gained from polysaccharide sequences and their interactions with proteins and nucleic acids [70]. Glycomics seeks to understand the role that polysaccharides play in cellular processes for advancing biotechnology.

Many fields within biotechnology stand to gain enormous rewards from glycomics research. More information on polysaccharides' roles in cell signaling, development, inflammation, and disease states is anticipated to be generated by glycomics. The applications of this knowledge in drug delivery and tissue engineering are innumerable.

2.3.2 The Role of Carbohydrates in Adhesion

Carbohydrate interactions are typically weak [69, 74-76]. However, they can be enhanced by multivalent interactions where multiple saccharides are involved[77-80]. Two phenomena are at play in multivalent carbohydrate interactions: chelate effect where multiple interactions occur after an initial interaction and ligand-induced protein clustering [69, 77, 81]. These properties and effects of carbohydrate interactions with other biomolecules make polysaccharides versatile biomaterials. With recent advances

in glycomics, the critical roles of carbohydrates in physiology are becoming even more apparent.

Cellular processes of adhesion and recognition are often mediated by carbohydrate-carbohydrate and carbohydrate-protein interactions [82]. Single carbohydrate-carbohydrate interactions are considered weak interactions. Of the few studies that have quantified these, carbohydrate-carbohydrate interactions have been shown to have dissociation constants (K_d) of 1 x 10^{-4} M [83]. However, the adhesion forces of glycan-glycan interactions are considerably strong with 190-310 pN adhesion forces which are in the range of antibody-antigen interactions (244 pN) [82]. It is generally thought that the strength of carbohydrate interactions increases with multivalency as more carbohydrate interactions occur in close proximity [84]. For example, monovalent carbohydrate-protein interactions have affinities of $K_a = 10^{3-4}$ M^{-1} and increase 2 to 6 fold with multivalency [81].

2.3.1 Lectins and Analysis of Carbohydrates

Advances in carbohydrate research have largely been driven by the use of lectins. Lectins are proteins with affinities for specific saccharide residues. Many proteins classified as lectins are found decorating cell surfaces and are involved in many cell-carbohydrate interactions. Studies have shown that selectins, a subclass of lectins, mediate lymphocyte rolling and adhesion [85]. In addition, lectins have been shown to play a role in cancer cell migration [86, 87].

Because of their specificity for saccharide units, lectins have also been used to study the roles of carbohydrates in biology. One of the primary uses of lectins has been to understand glycosylation patterns. Labeled lectins have been used for imaging carbohydrates in cellular matrices, on the surface of cells, and intracellularly. Recent

microarray technology has been used to develop lectin microarrays. These powerful new tools require only small amounts of carbohydrate ligands and can be used for quantitative, simultaneous detection of different carbohydrates. These microarrays have been used to study the cell surface glycome of bacteria and mammalian cells [88, 89].

2.3.3 Carbohydrate Biomaterials for Applications in Tissue Engineering

Polysaccharide biomaterials have been investigated for a variety of tissue engineering applicationsand scaffold engineering is almost synonymous with tissue engineering. Selection of the biomaterials in scaffold design plays an integral role in the overall success of the implant by modulating cellular adhesion, cellular proliferation, and the inflammatory response. Biodegradable materials are especially attractive materials for tissue engineering scaffolds because they may help to limit a chronic foreign body response that could ensue from a permanent implant [90]. Polysaccharide biomaterials have, therefore, been used in a variety of tissue engineering fields: cartilage, cardiovascular, neural, and hepatics.

Cartilage Engineering Applications

Cartilage is a connective tissue that provides support to other tissue and can also cushion joints. Hyaline cartilage is the most predominant form of cartilage, which is present at joints. Natural hyaline cartilage repair is very slow because cartilage is avascular. Articular cartilage is composed of chondrocytes (cells) and the extracellular matrix they produce. The primary components of the cartilage ECM are type II collagen and GAGs which include hyaluronic acid, chondroitin sulfate, dermatan sulfate, keratin sulfate, and heparin sulfate [91]. The phenotype of chondrocytes determines the ECM

that they produce [91, 92]. Maintaining chondrocyte expression of the appropriate ECM components is essential in properly producing articular cartilage. (A more in depth review of issues in cartilage repair may be found in [Ref. [91]]).

Tissue engineering schemes have proposed using bioactive scaffolds to support chondrocyte growth and control chondrocyte phenotype [93]. Scaffolds may be designed to support ingrowth of chondrocytes from surrounding tissues or may be used to encapsulate implanted chondrocytes. Material selection for these scaffolds must be careful as the scaffold's properties can influence chondrocyte expression and the produced cartilage [91, 92]. Because glycosaminoglycans (GAGs) are a major component of the chondrocyte extracellular matrix, GAGs and GAG-like materials have been mimicked in chondrocyte scaffold design [92]. As a result, several polysaccharide-based biomaterials have been investigated for chondrocyte scaffolding including alginate, chitosan, and hyaluronic acid.

Alginate has been used in several studies to evaluate its potential use in cartilage scaffolds. Diduch et al used agarose, alginate, and type I collagen to encapsulate marrow stromal cells (which produce cartilage like chondrocytes) [94]. This study recommended alginate as the optimal material selection for this application because alginate had better mechanical properties than agarose and maintained the chondrocyte-like morphology of marrow stromal cells [94]. Caterson et al examined poly(lactic acid) and alginate constructs for marrow stromal cell growth. Results from this study indicated that the poly(lactic acid)/alginate constructs supported chondrogenesis and limited fibrous capsule formation over poly(lactic acid) [95]. Iwasaki et al. formed an alginate-chitosan hybrid material that increased chondrocyte adhesion (over alginate controls) and did not influence chondrocyte morphology [96].

This study demonstrated that the addition of chitosan to alginate materials improved the material properties for application in cartilage tissue engineering.

Chitosan scaffolds have been the focus of multiple studies because of their GAG-like structure that may mimic the cartilage ECM. Lu et al. used *in vivo* studies of chitosan implants to assess its use in cartilage therapeutics. Chitosan was injected into the knees of Wistar rats [97]. Subsequent results were promising: chitosan increased the number of chondrocytes in the articular cavity and maintained the thickness of epiphyseal cartilage better than controls [97]. This study showed that chitosan was biocompatible causing no inflammation and may contribute to chondrogenesis and hence cartilage repair [97].

Modified chitosans have also been investigated for cartilage tissue engineering, and Sechriest et alinvestigated chitosan for cartilage repairing applications. They found that membranes of chitosan and chondroitin sulfate-A (a chondroitin sulfate precursor) maintained chondrocyte phenotype by showing that chondrocytes cultured on these surfaces predominantly produced type II collagen [98]. By creating new materials with chondroitin sulfate-A and chitosan, Sechriest et al were able to influence chondrocyte expression towards producing the appropriate type of collagen for articular cartilage ECM. More recently, Masuko et al. modified chitosan with a peptide sequence containing RGDS, an adhesion promoting peptide sequence [99]. Their work demonstrated that conjugated chitosan-RGDSGGC materials increased chondrocyte and fibroblast adhesion and proliferation [99]. Masuko et al also proposed that their procedure for conjugating RGDSGGC to chitosan could be used to conjugate other peptides and proteins to chitosan. This research demonstrated that tailoring a polysaccharide scaffold with peptides added more control over cellular adhesion. It

suggests that further modifications of polysaccharides with other materials such as proteins may add another method towards controlling chondrocyte behavior.

Hyaluronic acid has also been investigated for chondrocyte scaffolding. Unlike chitosan, hyaluronic acid is a natural component of the extracellular matrix (ECM) of chondrocytes. It has been suggested that hyaluronic acid is an ideal candidate material for chondrocyte scaffolding based on its natural presence in the ECM as well as its biodegradability and biocompatibility.

Advances have been made in synthesis of hyaluronic acid materials and novel modification methodologies have been explored that may expand the potential uses of hyaluronic acid in cartilage engineering. Bulpitt and Aeschlimann developed several methods, notably amine and aldehyde functionalization, for covalent coupling of proteins to hyaluronic acid [100]. Crosslinked hyaluronic acids were implanted in a rat subcutaneous model to show that the cross-linker and functionalization of the hyaluronic acid affected inflammation and cartilage generation. Bulpitt and Aeschlimann's work was novel in that it allowed functionalization and *in situ* polymerization of hyaluronic acid materials. More recently, Burdick et al. developed a photopolymerizable hyaluronic acid that supported chondrocyte growth and neocartilage formation [100]. Burdick et al. improved upon Bulpitt and Aeschlimann's work by simplifying the synthesis process with photopolymerization that could be carried out *in situ*.

Other studies have shown that hyaluronic acid-containing biomaterials are biocompatible and contribute to cartilage regeneration *in vivo* [101, 102]. With improvement of its synthesis process and its natural occurrence in cartilage, hyaluronic acid has been shown to be an important biomaterial in cartilage tissue engineering.

Vascular Applications

Like cartilage tissue engineering, carbohydrate-based biomaterials have been used in a number of cardiovascular tissue engineering applications. The use of tissue engineering scaffolds to repair capillaries and larger blood vessels is one of the main foci of cardiovascular tissue engineering. Tissue engineering constructs for vascular implants may be implanted to recruit the formation of new blood vessels or may be implanted as part of a support of tissue generation ex vivo. Some of the current vascular implants include but are not limited to stents and blood vessel grafts. The main challenges to implant design in cardiovascular tissue engineering include thrombosis, inflammation, re-endothelialization, and smooth muscle cell hyperplasia.

Polysaccharide-based biomaterials have been investigated for several different implants. For example, Matthew et al. investigated chitosan scaffolds for small-diameter blood vessel grafts showing that tubular scaffolds desirable for cardiovascular implants could be created with a nonporous luminal layer and a porous external layer [103]. SEM images verified that heparin could be incorporated into the chitosan scaffold by rehydrating the scaffold in a solution containing heparin [103]. A subsequent study expanded on this heparin-chitosan complex. Chitosan scaffolds containing additional GAGs were evaluated. *In vitro* cellular studies showed that the spreading and growth rate of smooth muscle cells and endothelial cells could be controlled by the GAG-chitosan complexes [104]. Smooth muscle cell spreading was more restricted on chitosan and chitosan-GAG structures than that of endothelial cells which may be additionally beneficial for cardiovascular applications where smooth muscle cell control is of the utmost importance. These same implants were examined *in vivo* through evaluation tissue ingrowth 14 days following subcutaneous implantation of GAG-chitosan scaffolds. Of these, heparin-chitosan samples developed a granulation

layer containing new vasculature [104]. The demonstrated ability of chitosan-based biomaterials to elicit different *in vitro* responses of cardiovascular cells as well as their ability to support tissue ingrowth and angiogenesis *in vivo* shows that these polysaccharide biomaterials may be further used in cardiovascular implants.

Neural Applications

Development of a degradable conduit to facilitate neural regeneration and repair is one of the primary goals in neural tissue engineering today. The material properties of such a construct are essential to the implant's success. Based on their biocompatibility and mechanical similarities to soft tissue, several polysaccharide-based biomaterials have been investigated for use in such scaffolds for nerve repair.

Zhang et al. have investigated chitosan biomaterials for use in nerve guidance channels. Their work has focused primarily on using chitosan to create polymer blends with several proteins to form new materials. In one study, gelatin incorporation into chitosan films increased the film's hydrophilicity and elastic properties. Differentiation of PC12 cells *in vitro* showed that, indeed, the combined film had an improved affinity for neural cells over chitosan controls [105]. Albumin, collagen, and poly-L-lysine were also blended with chitosan. Results indicated that poly-L-lysine blended chitosan films were the most effective in improving PC12 cell adhesion, differentiation, and extension over chitosan controls [106]. It was proposed that increasing the hydrophilicity of the chitosan films with GAGs and poly-L-lysine was responsible for an increased neural cell affinity.

Other combination materials using chitosan have been investigated. For example, Gu et al. studied nerve grafts composed of poly(glycolic acid) (PGA) fibers on the inner-surface and an outer layer of chitosan. Six months following implant in a

canine severed sciatic nerve model, the implants had degraded and nerve tissue had formed to reconnect the severed nerve. Dogs that received the chitosan-PGA scaffold recovered similarly to dogs that received an autologous nerve graft. Gu et al proposed that the success of the grafts was due in part to the chitosan component which allowed blood vessel in-growth, allowed nutrients to enter the graft, and served as a barrier to keep out other cells [107]. This study clearly demonstrated that chitosan may be used in neural tissue engineering schemes and illustrates the clinical significance of polysaccharide biomaterials.

Hyaluronic acid as a nerve guidance channel component has been investigated by Schmidt et al. Their work has taken a novel approach to neural biomaterials development combining natural materials with electrically conductive materials to stimulate neural regeneration chemically, mechanically, and electrically [108]. They developed films of photocrosslinkable hyaluronic acid and polypyrrole that maintained the electrical conductivity of polypyrrole. PC12 adhesion and morphology were comparable to controls. These films were also shown to be biocompatible *in vivo* 6 weeks after subcutaneous implantation using a rat model. This study also showed that hyaluronic acid-containing biomaterials have the unique ability to stimulate angiogenesis near the site of the implant [108]. With the capacity to electrically stimulate neurite extension, the ability to mechanically support nerve growth, and the capability to promote angiogenesis, these biomaterials are advanced material solutions in neural tissue engineering.

Hepatic Applications

Hepatic tissue engineering has already begun to incorporate protein-carbohydrate interactions into scaffold design. Hepatic tissue itself is one of the most

complex tissues found in the body structurally because of its large amount of vasculature. Control of cell morphology and differentiation as well as blood vessel ingrowth is essential for hepatic tissue scaffolds. Cho et al. and Griffith et al. have done pioneering work towards hepatic tissue engineering. Their work has centered around the fact that liver cells are known to express lectins (asialyglycoprotein receptor (ASGP-R)) with galactose affinities [109, 110]. Therefore, their research has used galactose-containing scaffolds as a natural control mechanism for tissue engineering of hepatic tissue.

Cho et al. have examined several galactosylated materials. In one study, they used galactosylated chitosan/ alginate scaffolds for hepatic cell growth [111]. In additional work, they have examined the effect that different carbohydrate-containing materials may have on hepatic cell morphology and spreading [112]. A nice review of their work may be found in [Ref. [111]]. They have shown that their carbohydrate-containing scaffold performed better than alginate controls. Results suggest that carbohydrate-containing scaffolds are a possible choice for a hepatic tissue scaffold.

Griffith et al. have focused on a synthetic scaffolds modified with galactose. They have synthesized poly(ethylene oxide) star polymers modified with galactose for hepatic tissue engineering [113, 114]. Results showed that galactose modification led to specific mediation between the polymer substrate and ASGP-R of hepatic cells [113]. Galactose modified polymers improved hepatic cell attachment and growth and proved formidable scaffolds for hepatic tissue engineering [113, 114].

2.3.4 Carbohydrates in Drug Delivery

Carrier Systems

Chitosan has been used in several successful drug delivery studies with one of the most important being gene therapy delivery systems [115-118]. Chitosan has the distinct advantage to complex with DNA because of its positive charge and DNA's negative charge. Roy et al developed chitosan nanoparticles to deliver gene therapy-based vaccines [119]. Chitosan particles containing a genetic vaccine (against peanut allergy) were orally administered to mice. In sensitization studies, the resulting anaphylaxis of vaccinated mice with the chitosan drug delivery system was much lower than samples which were vaccinated with only the gene (without the chitosan carrier) and controls that were not vaccinated at all [119]. Roy et al showed promising results that chitosan drug delivery systems can successfully deliver gene-based therapies orally. Senel et al examined chitosan for protein drug delivery across buccal mucosa. Their results suggested that chitosan enhanced the permeability of transforming growth factor-β [120]. Janes et al outline several other drugs that chitosan was used as a carrier for. These included bovine serum albumin and insulin [121].

Alginates have been studied for drug delivery as well [122]. Bouhadir et al oxidized sodium aliginate to form a new monomer [123]. They were able to engineer this polysaccharide delivery system to release three different model drugs in a controlled fashion via three different mechanisms of release: diffusion, ionic dissociation, degradation of a covalent bond [123]. Alginate has been used to release a variety of proteins as well including but not limited to fibroblast growth factor, bovine serum albumin, nerve growth factor, and interleukin-2 [124].

While this is just a miniscule sampling of the research on carbohydrate-based drug carriers, several reviews discuss polysaccharide drug delivery systems including amylose, dextran, and pectin in more detail [125, 126].

Targeted Delivery

Lectin-carbohydrate interactions are beginning to be exploited for targeted drug delivery. The strength of their interactions with carbohydrates increases significantly with multivalency as outlined earlier in the paper. Both lectins and their polysaccharide counterparts may be used for targeting and adhesion [127]. In designing these targeting modalities for drug delivery systems, carbohydrates may be used to target lectins or vice verse. The exciting research into drug polysaccharide targeting systems shows promise for transforming drug delivery.

Several lectin-mediated drug delivery systems have been developed that use lectins to target specific tissues and systems [127, 128]. Umamaheshwari et al. demonstrated that lectin-modified nanoparticles could be used to prevent *H. pylori* infection of human stomach cells [129]. Lectins have been used to target drug delivery to epithelial M-cells and Caco-2 cells [65, 130-133]. Wood et al used wheat germ agglutinin (a lectin) to target an insulin complexation hydrogel drug delivery system to carbohydrate residues found in intestinal mucosa. Results showed enhanced permeability towards insulin transport and indicated that wheat germ agglutinin led to improved bioavailability of insulin [132].

Xu et al also investigated lectin-mediated oral delivery of insulin. In addition to wheat germ agglutinin, Xu et al also investigated tomato lectin and Ulex europaeus agglutinin 1 (UEA1) [134]. Liposomes were modified with lectins and loaded with insulin. *In vivo* drug delivery studies showed that lectins increased insulin delivery over

controls. Of the lectin modifications examined by Xu et al, wheat germ agglutinin performed the best [134].

Delivery of imaging modalities to cancer via lectins has been investigated by Hama et al [135, 136]. Hama et al showed that avidin conjugated-BODIPY could be used to bind asialo-receptors on cancer cell lines and used fluorescence emission to detect cancerous cells. Nine different cancer cell lines were observed: ovarian, colon, pancreatic, gastric, breast, and prostate. Images from each culture showed that lectins may be used to target cancer cells for delivery imaging systems.

Drug delivery systems that use carbohydrateshave also been studied [137-139]. Cho et al have investigated galactose containing particles to target the asialoglycoprotein receptors (containing a lectin domain) on hepatic cells. Their research investigated poly(L-lactic acid) particles coated with polystyrene and galactose for targeted drug delivery of trans-retinoic acid [138].

Another team of researchers investigated lectin-ligand chemistry as a means to deliver anti-inflammatory drugs to the blood vessel lining by targeting P-selectin which plays a significant role in blood vessel inflammation [140]. P-selectin is expressed by endothelial cells and supports neutrophil rolling mediated by Sialyl-Lewis$_x$ (sLe$_x$), a sialylated and fucosylated carbohydrate. These drug delivery systems were designed to mimic this neutrophil rolling to deliver anti-inflammatory drugs. PLGA microparticles were synthesized and decorated with sLe$_x$ through avidin-biotin chemistry [140]. Laminar flow studies showed that drug delivery system supported rolling on P-selectin coated surfaces and that it was dependent on the density of carbohydrates on the PLGA microspheres [140]. This study took an innovative approach to anti-inflammatory drug delivery systems and indicates that carbohydrate-decorated drug delivery systems may be used to target lectins on cell surfaces in other therapies as well. Both systems

described used carbohydrates to target lectins on cell surfaces for cell-specific drug delivery.

Other Polysaccharide-Related Targeting Strategies

Bertozzi et al. have proposed an innovative strategy for drug delivery using polysaccharides. They have used polysaccharides to selectively modify cell surfaces so that these modified cells may be targeted by drug delivery systems [141, 142]. They utilized natural oligosaccharide (metabolism and) synthesis to incorporate a ketone containing N-levulinoyl mannosamine into sialic acids on cell surfaces instead of the N-acetylmannosamine. Biotin was then bound to these ketone groups on sialic acid, and Avidin-coupled toxins were used to target and kill the cells that were biotinylated [141]. They suggested that their methodology for engineering the cell surface for drug targeting may be further developed to selectively target tumor cells which tend to express high levels of sialic acid.

2.3.5 Carbohydrate-Mediated Adhesion in the Intestine

Studies have shown that carbohydrates are involved in adhesion processes involving both carbohydrates and proteins, and that many occur at the intestinal wall. For example, many bacteria that colonize the small intestine rely on polysaccharides on their surfaces for adhesion to the intestinal wall. Gram-negative bacteria, which are often pathogenic, adhere to the mucosa with lipolysaccharides (LPS) found on their membranes. While LPS interacts strongly with the intestinal wall, LPS have been shown to be immunogenic [143-145].

O-linked polysaccharides are known to play roles in cellular adhesion especially in cancer (Fukuda 2002). Studies have suggested that O-linked polysaccharides can

serve as ligands for cell binding via selectins, but to our knowledge, there are no studies linking this class of polysaccharides to adhesive interactions with the intestinal wall [146].

Teichoic acids are polysaccharides found in the cell wall of Gram-positive bacteria (often non-pathogenic). Research has shown that teichoic acid is involved in the adhesion of bacteria to stomach epithelial cells. A more recent study investigating a Caco-2 model showed that lipoteichoic acids of L. johnsii La1 were involved in adhesion to the intestinal epithelial cell model (Granato, et al). Several studies have investigated the role of teichoic acid in septic shock and immune responses highlighting that the bacterial source is a determining factor in immunogenicity [147-149].

The presence of hyaluronic acid (HA) in the extracellular matrix and the expression of hyaluronic acid on a wide variety of cell types make HA an attractive candidate for in vivo applications. HA has been shown to be a suitable tissue engineering construct for intestinal epithelial cells [150]. Because intestinal epithelial cells adhered to the HA substrate, HA may be a good candidate for facilitating carrier interactions with the intestinal wall. It is important to note that HA served as a substrate for Caco-2 cells, meaning that the basolateral side of the polarized cells adhered well to HA.

Drug delivery systems of pectin, which contains polygalacturonic acid, have been investigated for ocular and colonic delivery [151, 152]. In addition, rheological studies have shown that pectin can interact with mucin [153]. These interactions depended on mucin concentration but also on the degree of esterification of pectin [153].

Galectins, a type of lectin, have affinities for β-galactosides and are expressed on the apical side of the intestinal epithelium. To the best of our knowledge, the ability of β -galactosides to interact with the intestinal epithelium in a receptor-ligand fashion

has not yet been investigated. However, galectin-3 is expressed on the apical side of intestinal epithelial cells and has been shown to bind glycosaminoglycans containing β - galactose [154-157].

Dextran and pullulan are neutral polysaccharides composed of glucose units. These polysaccharides have been used in a variety of drug delivery applications. Dextran is especially well characterized for *in vivo* applications and is considered non-immunogenic. These polysaccharides are not considered to be strongly mucoadhesive. However, they are typically long, mostly linear, hydrophilic chains. Their structure would allow for the tethers of dextran and pullulan to diffuse into the mucosa and promote carrier interactions with the intestinal wall via chain interpenetration.

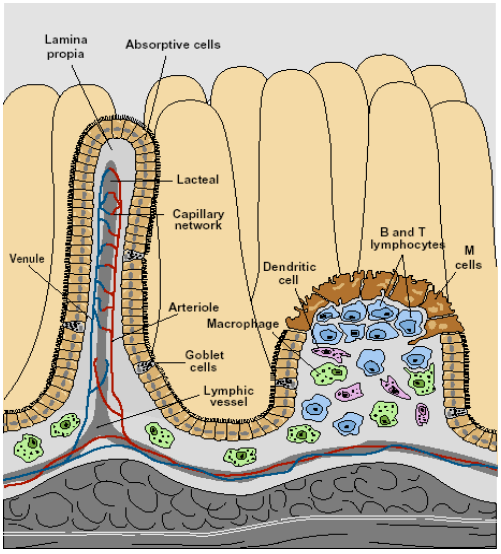

Figure 2.1 Schematic of the intestinal epithelium.

Each intestinal villus has its own arteriole and venule pair as well as a lacteal. The cell lining is composed mostly of epithelial cells [158].

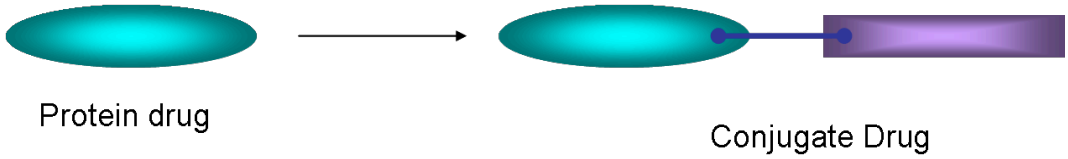

Figure 2.2 Schematic representation of a protein drug conjugate.

Protein drugs (green) may be conjugated to another molecule (purple) via a covalent bond (blue) to improve drug stability or transport.

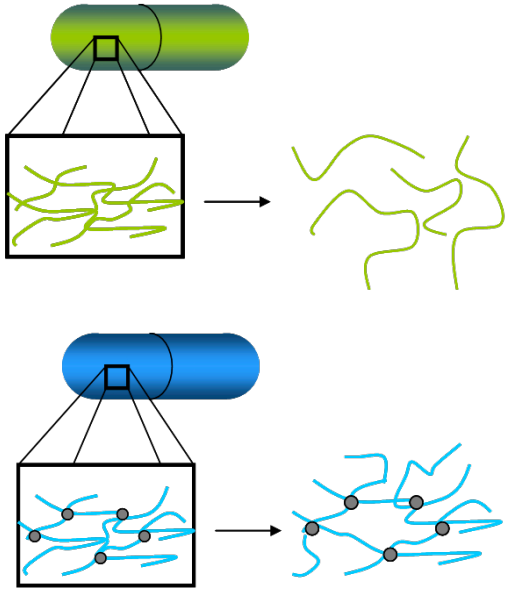

Figure 2.3 Comparison of enteric coatings and crosslinked polymer matrices for oral drug delivery systems.

Enteric coatings are non-crosslinked polymers which allow them to fully dissolve while crosslinked polymer networks are covalently held together and will not dissolve.

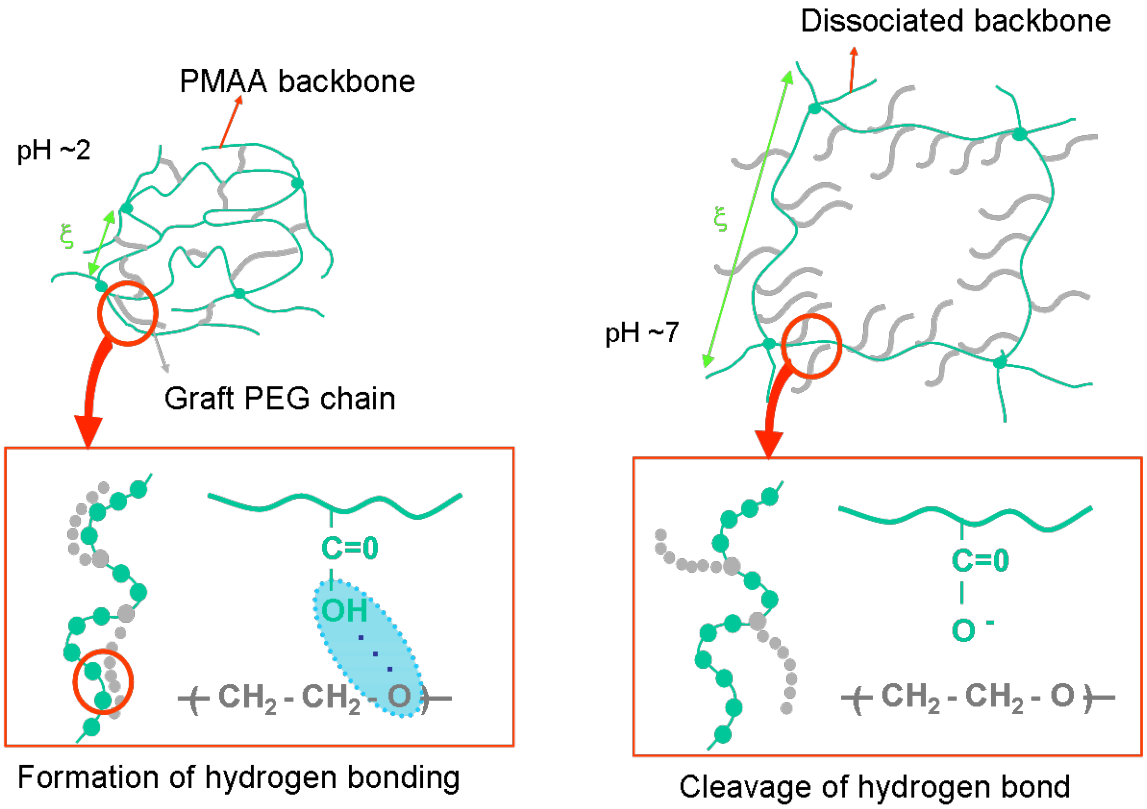

Figure 2.4 Complexation behavior of P(MAA-g-EG) hydrogels.

In acidic conditions, P(MAA-g-EG) hydrogels are in a collapsed state with a small mesh size due to hydrogen bonding between carboxylic acid groups and etheric groups. At neutral pH, deprotonation of the carboxylic acid groups leads to electrostatic and steric repulsions which causes swelling and increases the mesh size of the polymer network.

2.4 REFERENCES

1. World Health Organization *Preventing Chronic Diseases: A Vital Investment*. 2006,

2. National diabetes fact sheet: general information and national estimates on diabetes in the United States. 2007,

3. *Diabetes Atlas*. International Diabetes Federation, Brussels, 2006, 387.

4. Poretsky, L., Principles of Diabetes of Diabetes Mellitus. 2010, 868.

5. Bilous, R. and R. Donnelly, *Handbook of Diabetes*. John Wiley & Sons Ltd., Chichester, 2010,

6. Lewis, G. F., A. Carpentier, K. Adeli and A. Giacca, Disordered fat storage and mobilization in the pathogenesis of insulin resistance and type 2 diabetes. *Endocr. Rev.*, 2002, 23, 201-229.

7. Eckel, R. H., S. M. Grundy and P. Z. Zimmet, The metabolic syndrome. *Lancet*, 2005, 365, 1415-1428.

8. Holt, T. and S. Kumar, *ABC of Diabetes*. John Wiley & Sons Ltd, Chichester, 2010, 114.

9. Heinemann, L., The Failure of Exubera: Are We Beating a Dead Horse? 2008, 2, 518-529.

10. Leader, B., Q. J. Baca and D. E. Golan, Protein therapeutics: A summary and pharmacological classification. *Nat. Rev. Drug Discov.*, 2008, 7, 21-39.

11. Banting, F. G., C. H. Best, J. B. Collip, W. R. Campbell and A. A. Fletcher, Pancreatic Extracts in the Treatment of Diabetes Mellitus. *Can. Med. Assoc. J.*, 1922, 12, 141-146.

12. Itakura, K., T. Hirose, R. Crea, A. D. Riggs, H. L. Heyneker, F. Bolivar and H. W. Boyer, Expression in Escherichia coli of a Chemically Synthesized Gene for the Hormone Somatostatin. *Science*, 1977, 198, 1056-1063.

13. Goeddel, D. V., D. G. Kleid, F. Bolivar, H. L. Heyneker, D. G. Yansura, R. Crea, T. Hirose, A. Kraszewski, K. Itakura and A. D. Riggs, Expression in Escherichia coli of chemically synthesized genes for human insulin. *P. Natl. Acad. Sci. U.S.A.*, 1979, 76, 106-110.

14. Peyrot, M., R. R. Rubin, D. F. Kruger and L. B. Travis, Correlates of Insulin Injection Omission. *Diabetes Care*, 2010, 33, 240-245.

15. Fu, A. Z., Y. Qiu and L. Radican, Impact of fear of insulin or fear of injection on treatment outcomes of patients with diabetes. *Curr. Med. Res. Opin.*, 2009, 25, 1413-1420.

16. Lee, W. C., S. Balu, D. Cobden, A. V. Joshi and C. L. Pashos, Medication adherence and the associated health-economic impact among patients with type 2 diabetes mellitus converting to insulin pen therapy: An analysis of third-party managed care claims data. *Clin. Ther.*, 2006, 28, 1712-1725.

17. Csaky, T. Z., Intestinal Permeation and Permeability: an Overview. 1984, 61-88.

18. Aoki, Y., M. Morishita and K. Takayama, Role of the mucous/glycocalyx layers in insulin permeation across the rat ileal membrane. *Int. J. Pharm.*, 2005, 297, 98-109.

19. Hwang, S.-J., H. Park and K. Park, Gastric Retentive Drug-Delivery Systems. *Crit. Rev. Ther Drug Carrier Syst.*, 1998, 15, 243-284.

20. Shogren, R., T. A. Gerken and N. Jentoft, Role of Glycosylation on the Conformation and Chain Dimensions of O-Linked Glycoproteins - Light-Scattering-Studies of Ovine Submaxillary Mucin. *Biochemistry*, 1989, 28, 5525-5536.

21. Macadam, A., The Effect of Gastrointestinal Mucus on Drug Absorption. *Adv. Drug Deliv. Rev.*, 1993, 11, 201-220.

22. Maury, J., A. Bernadac, A. Rigal and S. Maroux, Expression and Glycosylation of the Filamentous Brush-Border Glycocalyx (FBBG) during Rabbit Enterocyte Differentiation along the Crypt-Villus Axis. *J. Cell Sci.*, 1995, 108, 2705-2713.

23. Frey, A., K. T. Giannasca, R. Weltzin, P. J. Giannasca, H. Reggio, W. I. Lencer and M. R. Neutra, Role of the glycocalyx in regulating access of microparticles to apical plasma membranes of intestinal epithelial cells: Implications for microbial attachment and oral vaccine targeting. *J. Exp. Med.*, 1996, 184, 1045-1059.

24. Aungst, B. J., Intestinal Permeation Enhancers. *J. Pharm. Sci.*, 2000, 89, 429-442.

25. Zheng, Y. Q., Y. H. Qiu, M. Y. F. Lu, D. Hoffman and T. L. Reiland, Permeability and absorption of leuprolide from various intestinal regions in rabbits and rats. *Int. J. Pharm.*, 1999, 185, 83-92.

26. Yang, T. Z., J. J. Arnold and F. Ahsan, Tetradecylmaltoside (TDM) enhances in vitro and in vivo intestinal absorption of enoxaparin, a low molecular weight heparin. *J. Drug Target.*, 2005, 13, 29-38.

27. Sadeghi, A. M. M., M. R. Avadi, S. Ejtemaimehr, S. Abashzadeh, A. Partoazar, F. Dorkoosh, M. Faghihi, M. Rafiee-Tehrani and H. E. Junginger, Development of a Gas Empowered Drug Delivery system for peptide delivery in the small intestine. *J. Control. Release*, 2009, 134, 11-17.

28. Fetih, G., S. Lindberg, K. Itoh, N. Okada, T. Fujita, F. Habib, P. Artersson, M. Attia and A. Yamamoto, Improvement of absorption enhancing effects of n-dodecyl-

beta-D-maltopyranoside by its colon-specific delivery using chitosan capsules. *Int. J. Pharm.*, 2005, 293, 127-135.

29. Swenson, E. S., W. B. Milisen and W. Curatolo, Intestinal Permeability Enhancement- Efficacy, Acute Local Toxicity, and Reversibility. *Pharm. Res.*, 1994, 11, 1132-1142.

30. Hastewell, J., S. Lynch, R. Fox, I. Williamson, P. Skeltonstroud and M. Mackay, Enhancement of Human Calcitonin Absorption Across the Rat Colon In-vivo. *Int. J. Pharm.*, 1994, 101, 115-120.

31. Morishita, M., I. Morishita, K. Takayama, Y. Machida and T. Nagai, Novel Oral Microspheres of Insulin with Protease Inhibitor Protecting Enzymatic Degradation. *Int. J. Pharm.*, 1992, 78, 1-7.

32. Yamamoto, A., T. Taniguchi, K. Rikyuu, T. Tsuji, T. Fujita, M. Murakami and S. Muranishi, Effects of Various Protease Inhibitors on the Intestinal Absorption and Degradation of Insulin in Rats. *Pharm. Res.*, 1994, 11, 1496-1500.

33. Tuesca, A. D., C. Reiff, J. I. Joseph and A. M. Lowman, Synthesis, Characterization and In Vivo Efficacy of PEGylated Insulin for Oral Delivery with Complexation Hydrogels. *Pharm. Res.*, 2009, 26, 727-739.

34. Russell-Jones, G. J., S. W. Westwood and A. D. Habberfield, Vitamin-B-12 Mediated Oral Delivery Systems for Granulocyte-colony-stimulating Factor and Erythropoieitin. *Bioconjugate Chem.*, 1995, 6, 459-465.

35. Russell-Jones, G. J., S. W. Westwood, P. G. Farnworth, J. K. Findlay and H. G. Burger, Synthesis of LHRH Antagonists Suitable for Oral-Administration via the Vitamin-B-12 Uptake System. *Bioconjugate Chem.*, 1995, 6, 34-42.

36. Petrus, A. K., A. R. Vortherms, T. J. Fairchild and R. P. Doyle, Vitamin B-12 as a carrier for the oral delivery of insulin. *ChemMedChem*, 2007, 2, 1717-1721.

37. Shah, D. and W. C. Shen, Transcellular delivery of an insulin-transferrin conjugate in enterocyte-like Caco-2 cells. *J. Pharm. Sci.*, 1996, 85, 1306-1311.

38. Kavimandan, N. J., E. Losi and N. A. Peppas, Novel delivery system based on complexation hydrogels as delivery vehicles for insulin-transferrin conjugates. *Biomaterials*, 2006, 27, 3846-3854.

39. Shofner, J. P., M. A. Phillips and N. A. Peppas, Cellular Evaluation of Synthesized Insulin-Transferrin Bioconjugates for Oral Insulin Delivery Using Intelligent Complexation Hydrogels. *Macromol. Biosci.*, 2010, 10, 299-306.

40. Morishita, I., M. Morishita, K. Takayama, Y. Machida and T. Nagai, Enteral Insulin Delivery by Microspheres in 3 Different Formulations Using Eudragit-L-100 and Eudragit-S100. *Int. J. Pharm.*, 1993, 91, 29-37.

41. Sahlin, J. J. and N. A. Peppas, Enhanced hydrogel adhesion by polymer interdiffusion: Use of linear poly(ethylene glycol) as an adhesion promoter. *J. Biomater. Sci.-Polym. Ed.*, 1997, 8, 421-436.

42. Tobio, M., A. Sanchez, A. Vila, I. Soriano, C. Evora, J. L. Vila-Jato and M. J. Alonso, The role of PEG on the stability in digestive fluids and in vivo fate of PEG-PLA nanoparticles following oral administration. *Colloid Surf. B-Biointerfaces*, 2000, 18, 315-323.

43. Cheng, J. J., B. A. Teply, S. Y. Jeong, C. H. Yim, D. Ho, I. Sherifi, S. Jon, O. C. Farokhzad, A. Khademhosseini and R. S. Langer, Magnetically responsive polymeric microparticles for oral delivery of protein drugs. *Pharm. Res.*, 2006, 23, 557-564.

44. Sun, S. P., N. Liang, H. Z. Piao, H. Yamamoto, Y. Kawashima and F. D. Cui, Insulin-S.O (sodium oleate) complex-loaded PLGA nanoparticles: Formulation, characterization and in vivo evaluation. *J. Microencapsul.*, 27, 471-478.

45. Cui, F. D., A. J. Tao, D. M. Cun, L. Q. Zhang and K. Shi, Preparation of insulin loaded PLGA-Hp55 nanoparticles for oral delivery. *J. Pharm. Sci.*, 2007, 96, 421-427.

46. Joseph, J. W., J. Kalitsky, S. St-Pierre and P. L. Brubaker, Oral delivery of glucagon-like peptide-1 in a modified polymer preparation normalizes basal glycaemia in diabetic db/db mice. *Diabetologia*, 2000, 43, 1319-1328.

47. Damge, C., M. Socha, N. Ubrich and P. Maincent, Poly(epsilon-Caprolactone)/Eudragit Nanoparticles for Oral Delivery of Aspart-Insulin in the Treatment of Diabetes. *J. Pharm. Sci.*, 99, 879-889.

48. Damge, C., P. Maincent and N. Ubrich, Oral delivery of insulin associated to polymeric nanoparticles in diabetic rats. *J. Control. Release*, 2007, 117, 163-170.

49. Huang, Y. B., I. Szleifer and N. A. Peppas, A molecular theory of polymer gels. *Macromolecules*, 2002, 35, 1373-1380.

50. Huang, Y. B., W. Leobandung, A. Foss and N. A. Peppas, Molecular aspects of muco- and bioadhesion: Tethered structures and site-specific surfaces. *J. Control. Release*, 2000, 65, 63-71.

51. Molineux, G., Pegylation: engineering improved pharmaceuticals for enhanced therapy. *Cancer Treat. Rev.*, 2002, 28, 13-16.

52. Owens, D. E. and N. A. Peppas, Opsonization, biodistribution, and pharmacokinetics of polymeric nanoparticles. *Int. J. Pharm.*, 2006, 307, 93-102.

53. Leitner, V. M., M. K. Marschutz and A. Bernkop-Schnurch, Mucoadhesive and cohesive properties of poly(acrylic acid)-cysteine conjugates with regard to their molecular mass. *Eur. J. Pharm. Sci.*, 2003, 18, 89-96.

54. Deutel, B., M. Greindl, M. Thaurer and A. Bernkop-Schnuerch, Novel insulin thiomer nanoparticles: In vivo evaluation of an oral drug delivery system. *Biomacromolecules*, 2008, 9, 278-285.

55. George, M. and T. E. Abraham, Polyionic hydrocolloids for the intestinal delivery of protein drugs: Alginate and chitosan - a review. *J. Control. Release*, 2006, 114, 1-14.

56. Bowman, K. and K. W. Leong, Chitosan nanoparticles for oral drug and gene delivery. *Int. J. Nanomed.*, 2006, 1, 117-128.

57. Pan, Y., Y. J. Li, H. Y. Zhao, J. M. Zheng, H. Xu, G. Wei, J. S. Hao and F. D. Cui, Bioadhesive polysaccharide in protein delivery system: chitosan nanoparticles improve the intestinal absorption of insulin in vivo. *Int. J. Pharm.*, 2002, 249, 139-147.

58. Sarmento, B., A. Ribeiro, F. Veiga, P. Sampaio, R. Neufeld and D. Ferreira, Alginate/Chitosan nanoparticles are effective for oral insulin delivery. 2007, 24, 2198-2206.

59. Sarmento, B., A. Ribeiro, F. Veiga, D. Ferreira and R. Neufeld, Oral bioavailability of insulin contained in polysaccharide nanoparticles. 2007, 8, 3054-3060.

60. Werle, M. and H. Takeuchi, Chitosan-aprotinin coated liposomes for oral peptide delivery: Development, characterisation and in vivo evaluation. *Int. J. Pharm.*, 2009, 370, 26-32.

61. Kamei, N., M. Morishita, H. Chiba, N. J. Kavimandan, N. A. Peppas and K. Takayama, Complexation hydrogels for intestinal delivery of interferon beta and calcitonin. *J. Control. Release*, 2009, 134, 98-102.

62. Carr, D. A., M. Gomez-Burgaz, M. C. Boudes and N. A. Peppas, Complexation Hydrogels for the Oral Delivery of Growth Hormone and Salmon Calcitonin. *Ind. Eng. Chem. Res.*, 2010, 49, 11991-11995.

63. Yamagata, T., M. Morishita, N. J. Kavimandan, K. Nakamura, Y. Fukuoka, K. Takayama and N. A. Peppas, Characterization of insulin protection properties of complexation hydrogels in gastric and intestinal enzyme fluids. *J. Control. Release*, 2006, 112, 343-349.

64. Kavimandan, N. J. and N. A. Peppas, Confocal microscopic analysis of transport mechanisms of insulin across the cell monolayer. *Int. J. Pharm.*, 2008, 354, 143-148.

65. Wood, K. M., G. M. Stone and N. A. Peppas, The effect of complexation hydrogels on insulin transport in intestinal epithelial cell models. *Acta Biomater.*, 2010, 6, 48-56.

66. Lowman, A. M., M. Morishita, M. Kajita, T. Nagai and N. A. Peppas, Oral delivery of insulin using pH-responsive complexation gels. *J. Pharm. Sci.*, 1999, 88, 933-937.

67. Morishita, M., T. Goto, N. A. Peppas, J. I. Joseph, M. C. Torjman, C. Munsick, K. Nakamura, T. Yamagata, K. Takayama and A. M. Lowman, Mucosal insulin delivery systems based on complexation polymer hydrogels: effect of particle size on insulin enteral absorption. *J. Control. Release*, 2004, 97, 115-124.

68. Rudiger, H., H. C. Siebert, D. Solis, J. Jimenez-Barbero, A. Romero, C. W. von der Lieth, T. Diaz-Maurino and H. J. Gabius, Medicinal chemistry based on the sugar code: Fundamentals of lectinology and experimental strategies with lectins as targets. 2000, 7, 389-416.

69. Bertozzi, C. R. and L. L. Kiessling, Chemical glycobiology. 2001, 291, 2357-2364.

70. Ratner, D. M., E. W. Adams, M. D. Disney and P. H. Seeberger, Tools for glycomics: Mapping interactions of carbohydrates in biological systems. 2004, 5, 1375-1383.

71. Hirabayashi, J., Y. Arata and K. Kasai, Glycome project: Concept, strategy and preliminary application to Caenorhabditis elegans. *Proteomics*, 2001, 1, 295-303.

72. Freeze, H. H., Genetic defects in the human glycome. *Nat. Rev. Genet.*, 2006, 7, 537-551.

73. Gabius, H. J., H. C. Siebert, S. Andre, J. Jimenez-Barbero and H. Rudiger, Chemical biology of the sugar code. *Chembiochem*, 2004, 5, 741-764.

74. Spillmann, D. and M. M. Burger, Carbohydrate-carbohydrate interactions in adhesion. *J. Cell. Biochem.*, 1996, 61, 562-568.

75. David, A., P. Kopeckova, T. Minko, A. Rubinstein and J. Kopecek, Design of a multivalent galactoside ligand for selective targeting of HPMA copolymer-doxorubicin conjugates to human colon cancer cells. 2004, 40, 148-157.

76. Roy, R., Syntheses and some applications of chemically defined multivalent glycoconjugates. 1996, 6, 692-702.

77. Mammen, M., S. K. Choi and G. M. Whitesides, Polyvalent interactions in biological systems: Implications for design and use of multivalent ligands and inhibitors. *Angew. Chem.-Int. Edit.*, 1998, 37, 2755-2794.

78. Yarema, K. J. and C. R. Bertozzi, Chemical approaches to glycobiology and emerging carbohydrate-based therapeutic agents. *Curr. Opin. Chem. Biol.*, 1998, 2, 49-61.

79. Mann, D. A., M. Kanai, D. J. Maly and L. L. Kiessling, Probing low affinity and multivalent interactions with surface plasmon resonance: Ligands for concanavalin A. 1998, 120, 10575-10582.

80. Sigal, G. B., M. Mammen, G. Dahmann and G. M. Whitesides, Polyacrylamides bearing pendant alpha-sialoside groups strongly inhibit agglutination of

erythrocytes by influenza virus: The strong inhibition reflects enhanced binding through cooperative polyvalent interactions. *J. Am. Chem. Soc.*, 1996, 118, 3789-3800.

81. Burke, S. D., Q. Zhao, M. C. Schuster and L. L. Kiessling, Synergistic formation of soluble lectin clusters by a templated multivalent saccharide ligand. *J. Am. Chem. Soc.*, 2000, 122, 4518-4519.

82. Bucior, I., S. Scheuring, A. Engel and M. M. Burger, Carbohydrate-carbohydrate interaction provides adhesion force and specificity for cellular recognition. *J. Cell Biol.*, 2004, 165, 529-537.

83. Patel, T. R., S. E. Harding, A. Ebringerova, M. Deszczynski, Z. Hromadkova, A. Togola, B. S. Paulsen, G. A. Morris and A. J. Rowe, Weak self-association in a carbohydrate system. *Biophys. J.*, 2007, 93, 741-749.

84. Bucior, I. and M. M. Burger, Carbohydrate-carbohydrate interaction as a major force initiating cell-cell recognition. *Glycoconjugate J.*, 2004, 21, 111-123.

85. Lawrence, M. B. and T. A. Springer, Neutrophils Roll on E-Selectin. *J. Immunol.*, 1993, 151, 6338-6346.

86. Camby, I., M. Le Mercier, V. Mathieu, L. Ingrassia, F. Lefranc and R. Kiss, Galectin-1 as potential therapeutic target for cancer progression. *Drug Future*, 2008, 33, 1057-1069.

87. Thijssen, V., R. Postel, R. Brandwijk, R. P. M. Dings, I. Nesmelova, S. Satijn, N. Verhofstad, Y. Nakabeppu, L. G. Baum, J. Bakkers, K. H. Mayo, F. Poirier and A. W. Griffioen, Galectin-1 is essential in tumor angiogenesis and is a target for antiangiogenesis therapy. *Proc. Natl. Acad. Sci. U. S. A.*, 2006, 103, 15975-15980.

88. Hsu, K. L., K. T. Pilobello and L. K. Mahal, Analyzing the dynamic bacterial glycome with a lectin microarray approach. *Nat. Chem. Biol.*, 2006, 2, 153-157.

89. Pilobello, K. T., D. E. Slawek and L. K. Mahal, A ratiometric lectin microarray approach to analysis of the dynamic mammalian glycome. *Proc. Natl. Acad. Sci. U. S. A.*, 2007, 104, 11534-11539.

90. Kim, B. S. and D. J. Mooney, Development of biocompatible synthetic extracellular matrices for tissue engineering. *Trends Biotechnol.*, 1998, 16, 224-230.

91. Temenoff, J. S. and A. G. Mikos, Review: tissue engineering for regeneration of articular cartilage. *Biomaterials*, 2000, 21, 431-440.

92. Suh, J. K. F. and H. W. T. Matthew, Application of chitosan-based polysaccharide biomaterials in cartilage tissue engineering: a review. *Biomaterials*, 2000, 21, 2589-2598.

93. Vacanti, C. A., R. Langer, B. Schloo and J. P. Vacanti, Synthetic-Polymers Seeded With Chondrocytes Provide A Template For New Cartilage Formation. *Plast. Reconstr. Surg.*, 1991, 88, 753-759.

94. Diduch, D. R., L. C. M. Jordan, C. M. Mierisch and G. Balian, Marrow stromal cells embedded in alginate for repair of osteochondral defects. *Arthroscopy*, 2000, 16, 571-577.

95. Caterson, E. J., L. J. Nesti, W. J. Li, K. G. Danielson, T. J. Albert, A. R. Vaccaro and R. S. Tuan, Three-dimensional cartilage formation by bone marrow-derived cells seeded ion polylactide/alginate amalgam. *J. Biomed. Mater. Res.*, 2001, 57, 394-403.

96. Iwasaki, N., S. T. Yamane, T. Majima, Y. Kasahara, A. Minami, K. Harada, S. Nonaka, N. Maekawa, H. Tamura, S. Tokura, M. Shiono, K. Monde and S. I. Nishimura, Feasibility of polysaccharide hybrid materials for scaffolds in cartilage tissue engineering: Evaluation of chondrocyte adhesion to polyion complex fibers prepared from alginate and chitosan. *Biomacromolecules*, 2004, 5, 828-833.

97. Lu, J. X., F. Prudhommeaux, A. Meunier, L. Sedel and G. Guillemin, Effects of chitosan on rat knee cartilages. *Biomaterials*, 1999, 20, 1937-1944.

98. Sechriest, V. F., Y. J. Miao, C. Niyibizi, A. Westerhausen-Larson, H. W. Matthew, C. H. Evans, F. H. Fu and J. K. Suh, GAG-augmented polysaccharide hydrogel: A novel biocompatible and biodegradable material to support chondrogenesis. *J. Biomed. Mater. Res.*, 1999, 49, 534-541.

99. Masuko, T., N. Iwasaki, S. Yamane, T. Funakoshi, T. Majima, A. Minami, N. Ohsuga, T. Ohta and S. I. Nishimura, Chitosan-RGDSGGC conjugate as a scaffold material for musculoskeletal tissue engineering. *Biomaterials*, 2005, 26, 5339-5347.

100. Burdick, J. A., C. Chung, X. Q. Jia, M. A. Randolph and R. Langer, Controlled degradation and mechanical behavior of photopolymerized hyaluronic acid networks. *Biomacromolecules*, 2005, 6, 386-391.

101. Solchaga, L. A., J. S. Temenoff, J. Z. Gao, A. G. Mikos, A. I. Caplan and V. M. Goldberg, Repair of osteochondral defects with hyaluronan- and polyester-based scaffolds. *Osteoarthritis Cartilage*, 2005, 13, 297-309.

102. Aigner, J., J. Tegeler, P. Hutzler, D. Campoccia, A. Pavesio, C. Hammer, E. Kastenbauer and A. Naumann, Cartilage tissue engineering with novel nonwoven structured biomaterial based on hyaluronic acid benzyl ester. *J. Biomed. Mater. Res.*, 1998, 42, 172-181.

103. Madihally, S. V. and H. W. T. Matthew, Porous chitosan scaffolds for tissue engineering. *Biomaterials*, 1999, 20, 1133-1142.

104. Chupa, J. M., A. M. Foster, S. R. Sumner, S. V. Madihally and H. W. T. Matthew, Vascular cell responses to polysaccharide materials: in vitro and in vivo evaluations. *Biomaterials*, 2000, 21, 2315-2322.

105. Cheng, M. Y., J. U. Deng, F. Yang, Y. D. Gong, N. M. Zhao and X. F. Zhang, Study on physical properties and nerve cell affinity of composite films from chitosan and gelatin solutions. *Biomaterials*, 2003, 24, 2871-2880.

106. Cheng, M. Y., W. L. Cao, Y. Cao, Y. D. Gong, N. M. Zhao and X. F. Zhang, Studies on nerve cell affinity of biodegradable modified chitosan films. *J. Biomater. Sci.-Polym. Ed.*, 2003, 14, 1155-1167.

107. Wang, X. D., W. Hu, Y. Cao, J. Yao, J. Wu and X. S. Gu, Dog sciatic nerve regeneration across a 30-mm defect bridged by a chitosan/PGA artificial nerve graft. *Brain*, 2005, 128, 1897-1910.

108. Collier, J. H., J. P. Camp, T. W. Hudson and C. E. Schmidt, Synthesis and characterization of polypyrrole-hyaluronic acid composite biomaterials for tissue engineering applications. *J. Biomed. Mater. Res.*, 2000, 50, 574-584.

109. Lee, Y. C., R. R. Townsend, M. R. Hardy, J. Lonngren, J. Arnarp, M. Haraldsson and H. Lonn, Binding Of Synthetic Oligosaccharides To The Hepatic Gal Galnac Lectin - Dependence On Fine-Structural Features. *J. Biol. Chem.*, 1983, 258, 199-202.

110. Townsend, R. R., M. R. Hardy, T. C. Wong and Y. C. Lee, Binding Of N-Linked Bovine Fetuin Glycopeptides To Isolated Rabbit Hepatocytes - Gal/Galnac Hepatic Lectin Discrimination Between Galbeta(1,4)Glcnac And Galbeta(1,3)Glcnac In A Triantennary Structure. *Biochemistry*, 1986, 25, 5716-5725.

111. Cho, C. S., S. J. Seo, I. K. Park, S. H. Kim, T. H. Kim, T. Hoshiba, I. Harada and T. Akaike, Galactose-carrying polymers as extracellular matrices for liver tissue engineering. *Biomaterials*, 2006, 27, 576-585.

112. Kim, S. H., T. Hoshiba and T. Akaike, Effect of carbohydrates attached to polystyrene on hepatocyte morphology on sugar-derivatized polystyrene matrices. *J. Biomed. Mater. Res. Part A*, 2003, 67A, 1351-1359.

113. Lopina, S. T., G. Wu, E. W. Merrill and L. GriffithCima, Hepatocyte culture on carbohydrate-modified star polyethylene oxide hydrogels. *Biomaterials*, 1996, 17, 559-569.

114. Griffith, L. G. and S. Lopina, Microdistribution of substratum-bound ligands affects cell function: hepatocyte spreading on PEO-tethered galactose. 1998, 19, 979-986.

115. Dang, J. M. and K. W. Leong, Natural polymers for gene delivery and tissue engineering. *Adv. Drug Deliv. Rev.*, 2006, 58, 487-499.

116. Green, D. W., S. Mann and R. O. C. Oreffo, Mineralized polysaccharide capsules as biomimetic microenvironments for cell, gene and growth factor delivery in tissue engineering. *Soft Matter*, 2006, 2, 732-737.

117. Prabaharan, M. and J. F. Mano, Chitosan-based particles as controlled drug delivery systems. 2005, 12, 41-57.

118. Lim, S. T., G. P. Martin, D. J. Berry and M. B. Brown, Preparation and evaluation of the in vitro drug release properties and mucoadhesion of novel microspheres of hyaluronic acid and chitosan. *J. Control. Release*, 2000, 66, 281-292.

119. Roy, K., H. Q. Mao, S. K. Huang and K. W. Leong, Oral gene delivery with chitosan-DNA nanoparticles generates immunologic protection in a murine model of peanut allergy. 1999, 5, 387-391.

120. Senel, S., M. J. Kremer, S. Kas, P. W. Wertz, A. A. Hincal and C. A. Squier, Enhancing effect of chitosan on peptide drug delivery across buccal mucosa. *Biomaterials*, 2000, 21, 2067-2071.

121. Janes, K. A., P. Calvo and M. J. Alonso, Polysaccharide colloidal particles as delivery systems for macromolecules. *Adv. Drug Deliv. Rev.*, 2001, 47, 83-97.

122. Augst, A. D., H. J. Kong and D. J. Mooney, Alginate hydrogels as biomaterials. *Macromol. Biosci.*, 2006, 6, 623-633.

123. Bouhadir, K. H., E. Alsberg and D. J. Mooney, Hydrogels for combination delivery of antineoplastic agents. 2001, 22, 2625-2633.

124. Gombotz, W. R. and S. F. Wee, Protein release from alginate matrices. *Adv. Drug Deliv. Rev.*, 1998, 31, 267-285.

125. Sinha, V. R. and R. Kumria, Polysaccharides in colon-specific drug delivery. 2001, 224, 19-38.

126. Vandamme, T. F., A. Lenourry, C. Charrueau and J. Chaumeil, The use of polysaccharides to target drugs to the colon. 2002, 48, 219-231.

127. Gabor, F. and M. Wirth, Lectin-mediated drug delivery: fundamentals and perspectives. *STP Pharma Sci.*, 2003, 13, 3-16.

128. Gabor, F., M. Stangl and M. Wirth, Lectin-mediated bioadhesion: binding characteristics of plant lectins on the enterocyte-like cell lines Caco-2, HT-29 and HCT-8. *J. Control. Release*, 1998, 55, 131-142.

129. Umamaheshwari, R. B. and N. K. Jain, Receptor mediated targeting of lectin conjugated gliadin nanoparticles in the treatment of Helicobacter pylori. *J. Drug Target.*, 2003, 11, 415-424.

130. Jepson, M. A., M. A. Clark and B. H. Hirst, M cell targeting by lectins: a strategy for mucosal vaccination and drug delivery. 2004, 56, 511-525.

131. Clark, M. A., B. H. Hirst and M. A. Jepson, Lectin-mediated mucosal delivery of drugs and microparticles. 2000, 43, 207-223.

132. Wood, K., Molecular design of advanced oral protein delivery systems using complexation hydrogels. 2006,

133. Wood, K. M., G. M. Stone and N. A. Peppas, Wheat germ agglutinin functionalized complexation hydrogels for oral insulin delivery. *Biomacromolecules*, 2008, 9, 1293-1298.

134. Zhang, N., Q. N. Ping, G. H. Huang and W. F. Xu, Investigation of lectin-modified insulin liposomes as carriers for oral administration. *Int. J. Pharm.*, 2005, 294, 247-259.

135. Hama, Y., Y. Urano, Y. Koyama, M. Kamiya, M. Bernardo, R. S. Paik, M. C. Krishna, P. L. Choyke and H. Kobayashi, In vivo spectral fluorescence imaging of submillimeter peritoneal cancer implants using a lectin-targeted optical agent. *Neoplasia*, 2006, 8, 607-U2.

136. Hama, Y., Y. Urano, Y. Koyama, P. L. Choyke and H. Kobayashi, Targeted optical imaging of cancer cells using lectin-binding BODIPY conjugated avidin. *Biochem. Biophys. Res. Commun.*, 2006, 348, 807-813.

137. Eniola, A. O. and D. A. Hammer, Characterization of biodegradable drug delivery vehicles with the adhesive properties of leukocytes - II: effect of degradation on targeting activity. *Biomaterials*, 2005, 26, 661-670.

138. Park, I. K., T. H. Kim, Y. H. Park, B. A. Shin, E. S. Choi, E. H. Chowdhury, T. Akaike and C. S. Cho, Galactosylated chitosan-graft-poly(ethylene glycol) as hepatocyte-targeting DNA carrier. *J. Control. Release*, 2001, 76, 349-362.

139. Nishikawa, M., A. Kamijo, T. Fujita, Y. Takakura, H. Sezaki and M. Hashida, Synthesis And Pharmacokinetics Of A New Liver-Specific Carrier, Glycosylated Carboxymethyl-Dextran, And Its Application To Drug Targeting. *Pharm. Res.*, 1993, 10, 1253-1261.

140. Eniola, A. O. and D. A. Hammer, Artificial polymeric cells for targeted drug delivery. *J. Control. Release*, 2003, 87, 15-22.

141. Mahal, L. K., K. J. Yarema and C. R. Bertozzi, Engineering chemical reactivity on cell surfaces through oligosaccharide biosynthesis. 1997, 276, 1125-1128.

142. Luchansky, S. J., S. Goon and C. R. Bertozzi, Expanding the diversity of unnatural cell-surface sialic acids. *Chembiochem*, 2004, 5, 371-374.

143. Raetz, C. R. H. and C. Whitfield, Lipopolysaccharide endotoxins. *Annu. Rev. Biochem.*, 2002, 71, 635-700.

144. Ulevitch, R. J. and P. S. Tobias, Receptor-Dependent Mechanisms of Cell Stimulation by Bacterial-Endotoxicin. *Annu. Rev. Immunol.*, 1995, 13, 437-457.

145. Wells, C. L., R. P. Jechorek, S. B. Olmsted and S. L. Erlandsen, Effect of LPC on Epithelial Integrity and Bacterial Uptake in the Polarized Human Enterocyte-Like Cell-Line Caco-2. *Circ. Shock*, 1993, 40, 276-288.

146. Fukuda, M., Roles of mucin-type O-glycans in cell adhesion. *Biochim. Biophys. Acta-Gen. Subj.*, 2002, 1573, 394-405.

147. Finney, S. J., P. B. Anning, T. V. Cao, M. Perretti, T. W. Evans and A. Burke-Gaffney, Butanol-extracted lipoteichoic acid induces in vivo leukocyte adhesion. *Biochem. Biophys. Res. Commun.*, 2007, 364, 831-837.

148. Granato, D., F. Perotti, I. Masserey, M. Rouvet, M. Golliard, A. Servin and D. Brassart, Cell surface-associated lipoteichoic acid acts as an adhesion factor for attachment of Lactobacillus johnsonii La1 to human enterocyte-like Caco-2 cells. *Appl. Environ. Microbiol.*, 1999, 65, 1071-1077.

149. Schar-Zammaretti, P. and J. Ubbink, The cell wall of lactic acid bacteria: Surface constituents and macromolecular conformations. *Biophys. J.*, 2003, 85, 4076-4092.

150. Esposito, A., A. Mezzogiorno, A. Sannino, A. De Rosa, D. Menditti, V. Esposito and L. Ambrosio, Hyaluronic acid based materials for intestine tissue engineering: A morphological and biochemical study of cell-material interaction. *J. Mater. Sci.-Mater. Med.*, 2006, 17, 1365-1372.

151. Bigucci, F., B. Luppi, L. Monaco, T. Cerchiara and V. Zecchi, Pectin-based microspheres for colon-specific delivery of vancomycin. *J. Pharm. Pharmacol.*, 2009, 61, 41-46.

152. Sriamornsak, P. and N. Wattanakorn, Rheological synergy in aqueous mixtures of pectin and mucin. *Carbohydr. Polym.*, 2008, 74, 474-481.

153. Ludwig, A., The use of mucoadhesive polymers in ocular drug delivery. *Adv. Drug Deliv. Rev.*, 2005, 57, 1595-1639.

154. Gunning, A. P., R. J. M. Bongaerts and V. J. Morris, Recognition of galactan components of pectin by galectin-3. *Faseb J.*, 2009, 23, 415-424.

155. Iwaki, J., T. Minamisawa, H. Tateno, J. Kominami, K. Suzuki, N. Nishi, T. Nakamura and J. Hirabayashi, Desulfated galactosaminoglycans are potential ligands for galectins: Evidence from frontal affinity chromatography. *Biochem. Biophys. Res. Commun.*, 2008, 373, 206-212.

156. Delacour, D., C. I. Cramm-Behrens, H. Drobecq, A. Le Bivic, H. Y. Naim and R. Jacob, Requirement for galectin-3 in apical protein sorting. *Curr. Biol.*, 2006, 16, 408-414.

157. Delacour, D., C. Greb, A. Koch, E. Salomonsson, H. Leffler, A. Le Bivic and R. Jacob, Apical sorting by galectin-3-dependent glycoprotein clustering. *Traffic*, 2007, 8, 379-388.

158. Daugherty, A. L. and R. J. Mrsny, Regulation of the intestinal epithelial paracellular barrier. *Pharm. Sci. Tech. Today*, 1999, 2, 281-287.

Chapter 3:

Objectives

With the completion of the human genome project and advances in protein engineering, protein drugs are poised to become more widely used for disease treatment. Protein drugs, such as insulin, calcitonin, growth hormone, and interferon-β, have traditionally been administered by injection because of their large molecular weights and the dependence of their bioactivity on structure. While injection has been an effective administration route for protein drugs, administration via the oral route is more desirable. Avoidance of needles or sharps waste, convenience in travel, and ease of administration are some of the reasons behind the need for an oral formulation as an alternative to administration by injection.

However, the oral administration of protein drugs has major challenges. The activity of the protein drug must be maintained in the GI tract, and therapeutic levels of the active drug must make their way into the bloodstream leading to a therapeutic bioavailability. To meet these challenges, an oral delivery system must protect the drug in the stomach from proteolytic enzymes and acid but allow absorption of the drug in either the small or large intestine. The target site of absorption is the small intestine which is typically preferred for absorption of hydrophilic proteins due to a more permeable epithelium than the colon.

We propose orally delivered protein drugs using an anionic complexation hydrogel composed of a methacrylic acid backbone with grafts of poly(ethylene glycol) and carbohydrate tethers. Poly(methacrylic acid-grafted-ethylene glycol), P(MAA-g-EG), gels are particularly suited for oral protein delivery because they have the ability to swell dependent on pH allowing for drug release to be triggered by a change in pH. For

example, in more acidic environments, diffusion into and out of P(MAA-g-EG) gels is limited due to physical crosslinks composed of hydrogen bonds between methacrylic acid and ethylene glycol. In the neutral conditions of the small intestine P(MAA-g-EG) gels swell allowing for diffusion of entrapped drugs out of the gel. These properties allow for protection of the protein in the stomach but release in the small intestine.

In this work, we seek to enhance the interactions between P(MAA-g-EG) gels and the intestinal wall to improve bioavailability using tethers composed of carbohydrates. A biomimetic approach based on the mediation of carbohydrates and polysaccharides in many adhesion and recognition processes is used to improve interactions of the carrier and intestinal wall. Improved interactions between the carrier and the intestinal wall will increase the residence time of the carrier allowing more time for the protein drug to release at the site of absorption. Furthermore, previous studies have shown that P(MAA-g-EG) carriers modified to interact with the intestinal lining have increased protein bioavailability.

The hypothesis of this thesis is that the addition of carbohydrate tethers to P(MAA-g-EG) gels will enhance carrier interactions with the intestinal lining leading to an improvement in bioavailability of protein drugs. In this research, we will focus on creating carbohydrate tethers from a variety of polysaccharides. These polysaccharides will then be covalently incorporated into P(MAA-g-EG) gels. The properties of these materials will be optimized for the oral delivery of insulin which we will use as a model protein. Furthermore, we will evaluate the *in vitro* performance of these systems.

Towards the development and evaluation of P(MAA-g-EG) gels decorated with carbohydrate tethers for oral protein delivery, we have several aims:

- To investigate the incorporation of polysaccharides into the bulk of P(MAA-g-EG) hydrogels

- To study these systems for pH-responsive delivery of protein drugs
- To evaluate and optimize the properties of these hydrogels for mucoadhesive oral delivery of proteins.

We present our work on developing and optimizing carbohydrate decorated-P(MAA-g-EG) hydrogel microparticles and nanoparticles for oral protein delivery. Our work towards these aims is organized by the material used. Chapter 4 presents our work on the design of complexation hydrogels with polysaccharides incorporated throughout the material and discusses the potential for these hydrogels as oral protein delivery systems. The pH-responsive swelling of these systems is investigated in Chapter 5. The evaluation of the loading and release of insulin from these hydrogels as well as the evaluation of the cytotoxicity of these systems is presented in Chapter 6. Our work on characterizing interactions of polysaccharide-modified P(MAA-g-EG) hydrogels with cells and mucus membranes for oral protein delivery is in Chapter 7. *In vitro* evaluation of the insulin transport and the effect on epithelial monolayers is discussed in Chapter 8. Finally, Chapter 8 presents a parallel project in which we investigated the use of P(MAA-g-EG) for the oral delivery of ovalbumin.

Chapter 4:

Synthesis and Characterization of Complexation Hydrogels Containing Polysaccharides

4.1 Introduction

Maintaining bioactivity of protein drugs and improving absorption of orally administered protein drugs are the two major challenges to oral protein bioavailability. Disruption of the secondary structure of protein drugs and degradation by enzymes in the stomach are significant issues for maintaining the function of protein drugs. Because disruption of the structure of these drugs significantly affects bioactivity, protein drugs must be protected from the environment of the GI tract [1]. Achieving a therapeutic bioavailability in the bloodstream is dependent on the absorption of the protein drug along the GI tract [1]. However, absorption of large undigested macromolecules such as proteins is uncommon. Both the mucosa and glycocalyx serve as physical barriers between the lumen of the intestine and the epithelium, while the tight junctions of the epithelium limit passive diffusion.

To overcome these challenges to oral protein delivery, polymeric drug delivery systems composed of anionic complexation hydrogels were synthesized for the oral delivery of protein drugs [2-15]. P(MAA-g-EG) hydrogels have been shown to be effective in maintaining the bioactivity of protein drugs in the GI tract. These hydrogels protect protein drugs from degradation in acidic stomach conditions due to hydrogen bonding between PMAA and PEG polymer chains [15, 16]. Hydrogen bonding between adjacent polymer chains act as physical crosslinks—limiting diffusion into and out of the mesh. The pH-dependent dissociation of these physical crosslinks allows control of drug

release at higher pH. For example, the release of protein drugs from P(MAA-g-EG) networks at pH values of the intestine has been demonstrated [17, 18].

The ability of protein drugs to be absorbed from the GI tract after release is essential. The absorption of insulin delivered via P(MAA-g-EG) microparticles has been confirmed *in vivo* through measurement of serum insulin levels and a measured reduction in blood glucose levels [8]. The decrease in blood glucose level proves the absorbed insulin is pharmacologically active. The amount of drug absorbed has been measured in terms of its bioavailability. Increased bioavailability is highly desirable as a higher bioavailability results in more efficient delivery with less wasted drug. For delivery of insulin from P(MAA-g-EG) microparticles, a bioavailability as high as 12% has been achieved in rodent models indicating that these systems are promising candidates for an oral insulin delivery system [17].

One promising strategy for improving bioavailability of protein delivery is improving mucoadhesion of the carrier in the upper small intestine. Increases in drug absorption from mucoadhesive carriers have been attributed to a prolonged carrier residence time at the site of absorption allowing for more release and hence absorption of the drug locally [5, 19]. Several methods of improving mucoadhesion of the polymeric drug delivery systems have been studied including incorporation of thiolated polymer [20, 21], incorporation of cationic polymers such as chitosan [22, 23], addition of polymer tethers [24], and the addition of lectins [25, 26].

Because many polysaccharides are considered biocompatible and may degrade *in vivo*, polysaccharides such as chitosan, dextran, alginate, and hyaluronic acid have been used in a variety of drug delivery and tissue engineering applications. Many polysaccharide based biomaterials have been investigated for oral delivery including

materials formed by ionic crosslinking of polysaccharides and covalent crosslinking of polysaccharides in both homopolymers and copolymers.

Hydrogel networks have been formed from polymerizable polysaccharides and used in a wide variety of biomedical applications. The most common method of polymerizing hydrogel networks of polysaccharides is by free radical polymerization of vinyl groups added along the backbone of the polysaccharide. For example, acrylation and methacrylation of dextran has been developed for polymerization of dextran hydrogels or copolymers [27-30]. Photopolymerizable chitosans have also been developed for a number of applications in drug delivery and tissue engineering. Likewise, hyaluronic acid gels have been prepared for tissue engineering and wound healing applications [31-34].

Dextrans have been investigated for a number of drug delivery applications. For example, crosslinked hydrogel networks of dextran have been studied [35]. Co-polymers of dextran and methacrylic acid have been shown to exhibit pH-sensitivity. Furthermore, dextran has been investigated for applications involving mucoadhesion.

In the work presented in this chapter, a synthesis method for polysaccharide decorated-complexation hydrogels for the oral delivery of insulin is presented. This strategy involves polymerizing dextrans, with a molecular weight of 6000 Daltons (Dex 6) or 100000 (Dex 100), and pullulans, with a molecular weight of 75000 Daltons (Pul 75), to form hydrogel networks with polysaccharide and PEG tethers. These gels, poly(methacrylic acid-double grafted-ethylene glycol-X) (P(MAA-g-EG-co-X)) with X denoting the polysaccharide graft, consisted of a crosslinked polymer network with a poly(methacrylic acid) backbone and grafts of PEG and either Dex 6, Dex 100, or Pul 75).

4.2 Materials and Methods

4.2.1 Functionalization of Polysaccharides with Polymerizable Vinyl Groups

Methacrylation of Dextrans

The synthesis procedure for methacrylation of dextran was adapted from van-Dijk Wolthius et al [36]. Briefly, Dextran (3 g, Sigma Aldrich) with a molecular weight of either 6000 or 100,000 was dissolved in anhydrous dimethyl sulfoxide (DMSO, Sigma Aldrich) to yield a concentration of 100 mg/ml. After dissolution, dimethylaminopyridine (DMAP, Sigma Aldrich) was added at a concentration of 20 mg/ml. Glycidyl methacrylate (GMA, Sigma Aldrich) was slowly added dropwise at a ratio of 8 mol% in relation to total saccharide units. The reaction was allowed to proceed at room temperature for 48 hours. The reaction was quenched by neutralizing the basic solution with 1 N hydrochloric acid (HCl). To remove any excess reagent, the solution was dialyzed against water for at least one week in a 3500 Da molecular weight cut-off dialysis tube (Spectrapor). The water was changed twice a day. The resulting product was lyophilized. The lyophilized product was white to cream in color and was fluffy in texture.

Methacrylation of Pullulan

A methacrylate group was added to pullulan by a similar procedure. Pullulan with an average molecular weight of 75,000 (Sigma) was solubilized in DMSO. DMAP was added to the pullulan solution. After dissolution of DMAP, glycidyl methacrylate was added drop wise to the solution. The solution was stirred at room temperature for 48 hours. The reaction was stopped by addition of 1 N hydrochloric acid. The viscous liquid was placed in a dialysis tube with a molecular weight cut-off of 3500 Da. The dialysis tube was cut longer than the recommended length (for the given volume) to

prevent the osmotic pressure from breaking the dialysis tube. The product was dialyzed against Ultrapure water for at least a week. The water was changed twice each day. During replacement of the dialysate, the dialysis bag and clips were carefully inspected.

4.2.2 Hydrogel Synthesis

Polymerization of P(MAA-g-EG) Hydrogels

P(MAA-g-EG) films were prepared by a free radical UV-initiated polymerization. The monomers, crosslinker, and initiator are shown in Figure 4.2. Briefly, a 1:1 (by weight) solution of ethanol and water was prepared. To the solvent, an equal mass of monomers was added. The monomers consisted of methacrylic acid (MAA, Sigma Aldrich) and poly(ethylene glycol) monomethyl ether monomethacrylate (PEGMMA, Polysciences Inc) with an average molecular weight of 1000 Da combined in a ratio of 1 mole methacrylic acid to 1 mole ethylene glycol. To the monomers and solvent, a crosslinker and initiator were then added.

The crosslinker poly(ethylene glycol) dimethacrylate (PEGDMA, Polysciences Inc.) with an average molecular weight of 400 Da was added to comprise a desired percent of the total monomer, the percent crosslinker. The initiator, Irgacure 184, was added to be 0.1 wt% of the total monomer weight. The pre-polymer solution was sonicated for 20 minutes. The solution was then purged with nitrogen for 30 minutes inside a glove box which was purged for the same amount of time.

The pre-polymers solution was then placed in a mold consisting of two glass slides and a Teflon spacer. The mold was placed under an ultraviolet (UV) light with an intensity of 16-17 mW/cm^2 for 30 minutes. The film was then washed in ultrapure water for 7 days and the water was exchanged twice daily to remove any unreacted

components. Films were dried in a vacuum oven and then crushed and sieved to achieve diameters less than 53 μm.

Polymerization of P(MAA-g-EG-Dex) Hydrogels

In order to solubilize dextran in the pre-polymer solution, modifications were made to the P(MAA-g-EG) synthesis outlined previously. The solvent was changed from a 1:1 water to ethanol solution to a 73% 0.1 N sodium hydroxide and 27% ethanol solution. MAA was first solubilized in sodium hydroxide, followed by Dex-acrylate or Dex-methacylate, PEGMMA, PEGDMA, ethanol, and then Irgacure 184.

The solution was sonicated for 20 minutes or until the reactants were fully dissolved. The solution was then placed in a glove box and purged for 30 minutes with ntirogen. Next, the solution was pipetted into a glass mold in the oxygen free environment. The polymerization was initiated by UV light with an intensity of 16-17 mW/cm^2 and allowed to proceed for 30 minutes.

Polymerization of P(MAA-g-EG-Pl) Hydrogels

Pullulan-methacrylate was polymerized into complexation hydrogels using the same method used for dextran-methacrylates and dextran-acrylates. The amounts of each component were determined relative to the chosen mass of PEGMMA (2.0 g). For each mole of ethylene glycol, one mole of MAA was used. The molar feed ratio of the crosslinker, PEGDMA, relative to the total moles of monomer was 1%. A solvent, equal in weight to the total monomers, consisted of 73% 0.1 N NaOH and 27% ethanol. Pullulan-methacrylate (1 % by weight of the total mass of monomers) was dissolved in 0.1 N sodium hydroxide (73 % by weight of the total mass of solvent). Methacrylic acid was added and allowed to dissolve. Ethanol, PEGMMA, and PEGDMA were slowly added along with Irgacure 184. The solution was sonicated for at least 20 minutes until

all of the components were fully dissolved, then placed in a glove box and purged with nitrogen for 20 minutes. Following purge, the solution was placed between two glass slides separated by a Teflon spacer. The polymerization was carried out for 30 minutes under UV light. The resulting polymer film was washed in ultrapure water for 5-7 days. The water was changed twice each day.

4.2.3 Fourier Transform Infrared Spectroscopy

Fourier transform infrared spectroscopy was used to evaluate the functional groups of the various materials prepared in this chapter. Hydrogel films were dried in ambient conditions for at least 24 hours and placed in a vacuum oven maintained at 37^{o}C for at least 24 hours. Dried films were then crushed with a mortar and pestle to obtain microparticles less the 90 μm in diameter. Microparticles used for FTIR were placed back in the vacuum oven for a minimum of 24 hours. Potassium bromide was dried by heating over 100 ^{o}C for more than 2 hours. A dry hydrogel sample (2 mg) was mixed with KBr (198 mg) for a total mass of 200 mg using a small, agate mortar and pestle. A 13 mm pellet was prepared from the sample powder using a laboratory press and a 13mm steel die and placed in an FT-IR sample holder. Measurements were taken using a Nicolet FT-IR with a resolution of 4 cm^{-1} and 64 scans.

4.3 Results and Discussion

4.3.1 Hydrogel Synthesis

In order to covalently incorporate polysaccharides into an anionic complexation hydrogel with a poly(methacrylic acid) (PMAA) backbone and PEG tethers, polymerizable groups were first added to the polysaccharides. There are a variety of methods for adding functional groups to polysaccharides. The most popular method involves the oxidation of the polysaccharide using periodates. The addition of

methacrylate polymerizable using glycidyl methacrylate groups was first reported by van-Dijk Wolthius et al [36]. This method uses a base catalyst (DMAP) and an epoxide (GMA) to react with hydroxyl groups on the polysaccharide. This method has been used by a number of other researchers and adapted for addition of methacrylate groups to pullulan.

The hydrogel system was designed to create long macromolecular tethers composed of polysaccharides. As a result, a low degree of substitution of the polysaccharide was desired. Because we were interested in adding only a few polymerizable groups per chain, analysis of the polysaccharide component was very difficult. For example, feed ratios of GMA that would result in a degree of substitution of 8% were chosen. Most uses of methacryloyl dextran have been formation of dextran hydrogels requiring relatively larger degrees of substitution as high as 20-30%. Degrees of substitution as low as 1 have been reported in literature for dextrans using the same reaction mechanism.

In order to synthesize P(MAA-g-EG-co-Dextran) and P(MAA-g-EG-co-Pullulan) hydrogels, the synthesis method of P(MAA-g-EG) was modified. Typically, P(MAA-g-EG) hydrogels are polymerized in a solvent consisting of 50 wt% water and 50 wt% ethanol. It is well known that alcohols such as ethanol and methanol can be used for precipitation of polysaccharides such as dextran and serve as anti-solvents. As a result, a solvent system with a reduced amount of ethanol was used.

The combination of both PEG and dextran was an additional challenge. Phase separations were observed with higher ethanol concentrations in the polymerization solvent and especially at pH values lower than the pKa of methacrylic acid. It was observed that the replacement of water with 0.1 N NaOH and reduction of ethanol in

the polymerization eliminated phase separation and allowed for the polymerization of a homogeneous hydrogel film.

The difficulty in obtaining a homogenous monomer mixture was likely due to phase separations between PEG and dextran. It has been reported in literature that PEG and dextran are partially miscible in aqueous solution [37-39]. However, in polymer blends, PEG and dextran were shown to be immiscible [40]. Moriyama and Yui [35] successfully synthesized hydrogels composed of PEG and dextran but showed regions of phase separation within the materials. These phase separations resulted in regions composed predominantly of either PEG or dextran. Some degree of favorable interactions between the two polymers has been shown in FT-IR studies.

In designing these systems, the dependence of dextran-PEG separations on molecular weight was taken into consideration. Because separation between PEG and dextran is more pronounced as the molecular weight of the polymers increases [38], the synthesis method was developed using the highest molecular weight dextran (100 kDa). For all of the compositions reported in this thesis, the polymerization reaction solutions were optimized so that the solutions obtained after sonication were clear with no observable phase separations occurring during polymerization.

4.3.2 FT-IR Spectroscopy

FT-IR is a technique that allows identification of organic functional groups based on energy absorption. This technique is commonly used for identification of organic compounds, identification of polymer composition, as well as studying molecular interactions. In this work, FT-IR was used to confirm synthesis of various hydrogels.

The synthesis of P(MAA-g-EG) hydrogel films and copolymers with polysaccharides was verified by FT-IR. Figure 4.3 shows the spectra of P(MAA-g-EG) and

P(MAA-g-EG-co-Dextran 6000 (1%)). A comparison of the two shows few differences in absorbance peak locations indicating matching functional groups. For example, the presence of carbonyl groups is clearly evident in the range of 1700-1750 cm-1 as well as etheric groups in the 1090-1180 cm^{-1} region. A peak corresponding to methyl group vibration appears from 2890-3050 cm^{-1}. Other studies have reported hydrogen bonding can shift a peak from 1700 to 1730 cm^{-1} [41]. In this work, distinct peaks occurring at 1700 and 1733 cm^{-1} are observed for both P(MAA-g-EG) and P(MAA-g-EG-co-Dextran 6000). The ratio of these two peaks changes with addition of the polysaccharide comonomer suggesting increased hydrogen bonding of carbonyl groups.

Likewise in Figure 4.3, hydroxyl group stretching is evident in the 3300-3500 range cm^{-1}. The copolymer containing dextran 6000 shifts the center of the hydroxyl group vibration as shown in Figure 4.6 and Table 4.1 from 3481 cm^{-1} to 3446 cm^{-1}. A shift in the peak in hydroxyl group stretching region was also observed in PEG and dextran polymer blends due to hydrogen bonding [40].

The absorbance spectra of P(MAA-g-EG-co-Dextran 100000 (1%)) and P(MAA-g-EG) in Figure 4.7 indicate the presence of methacrylic acid and ethylene glycol in both polymers. For example, both carbonyl groups (1700-1750 cm^{-1}) and etheric groups (1090-1180 cm^{-1}) are present in both samples corresponding to methacrylic acid and PEG, respectively. A shift in the hydroxyl group stretching shown in Figure 4.8 similar to that observed for the P(MAA-g-EG-co-Dextran 6000) system indicates the presence of Dextran 100000 in the hydrogel. The center of the absorbance peak corresponding to hydroxyl group stretching decreases in wavenumber (3481 cm^{-1} to 3467 cm^{-1}) (Table 4.2). This decrease is smaller than the shift observed in P(MAA-g-EG-co-Dextran 6000) which may indicate that hydrogen bonding occurs to a lesser extent in the system with the higher molecular weight dextran. Similar to P(MAA-g-EG-co-Dextran 100000)

samples, the hydroxyl group stretching was observed at lower wavenumbers for pullulan copolymers shifting the peak from 3481 to 3469 cm^{-1} (Table 4.3).

4.4 CONCLUSIONS

In this work, a novel method for synthesizing complexation hydrogels containing poly(methacrylic acid), poly(ethylene glycol), and polysaccharides was developed. The incorporation of all comonomers was verified using FT-IR spectroscopy.

Glycidyl Methacrylate

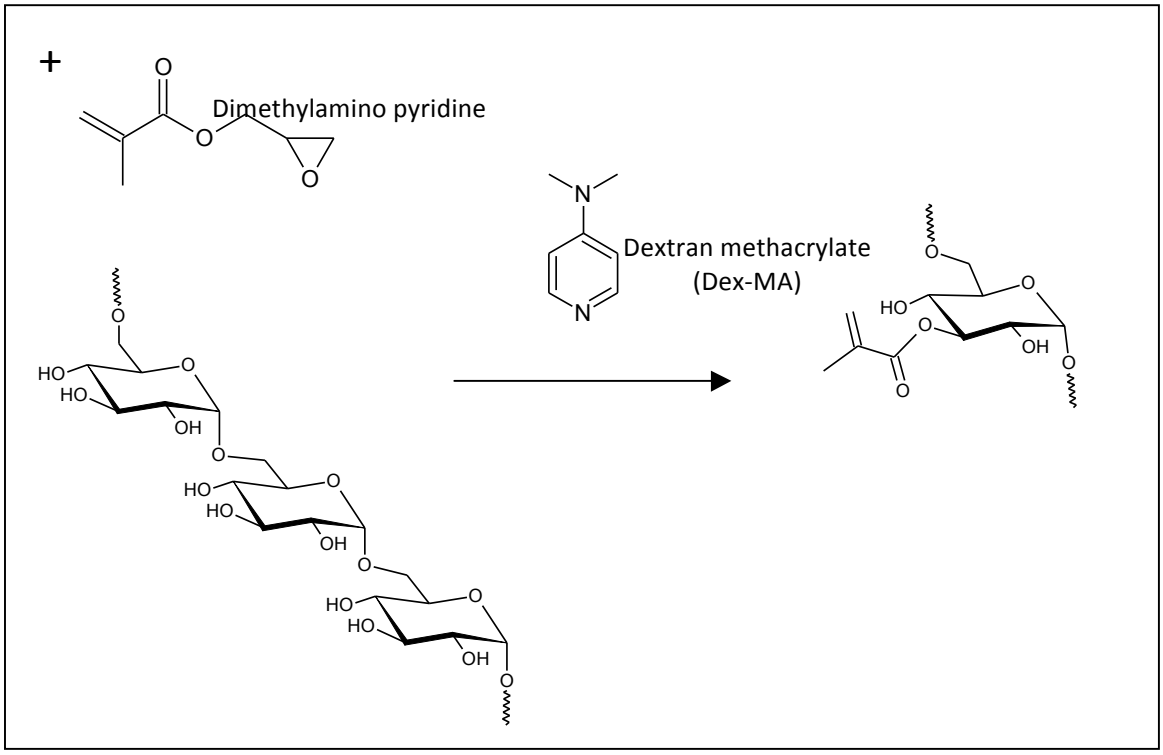

Figure 4.1. Reaction scheme for methacrylation of dextran.

Methacrylate groups were covalently attached to dextran by transesterification using glycidyl methacrylate and dimethylaminopyridine.

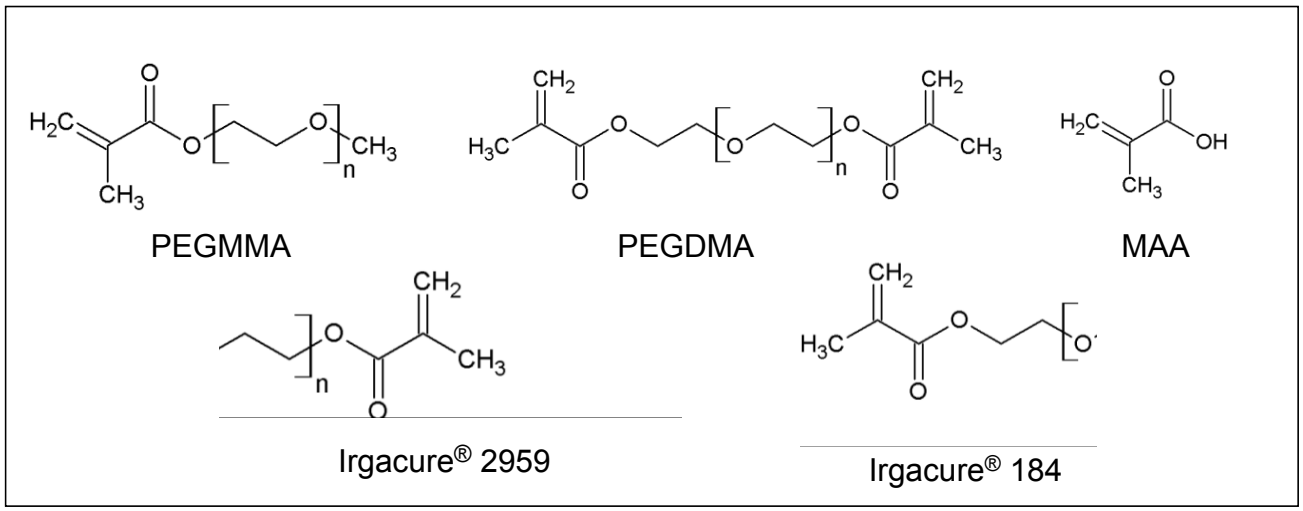

Figure 4.2. Components for P(MAA-g-EG) hydrogels.

P(MAA-g-EG) hydrogels were polymerized using methacrylic acid (MAA), poly(ethylene glycol) monomethyl ether monomethacrylate (PEGMMA), poly(ethylene glycol dimethacrylate) (PEGDMA), and an initiator.

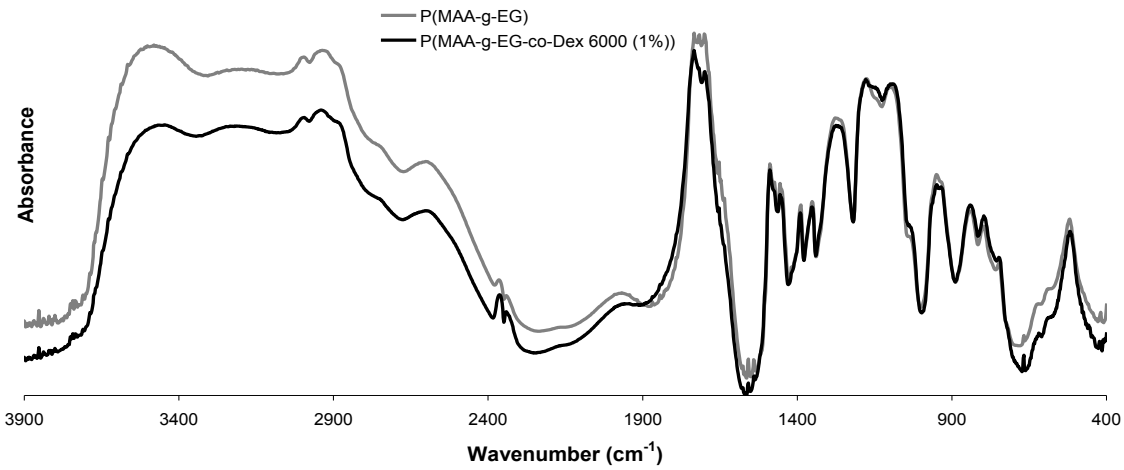

Figure 4.3. FT-IR spectra of P(MAA-g-EG) hydrogels and P(MAA-g-EG-co-Dextran 6000 (1%)) hydrogels.

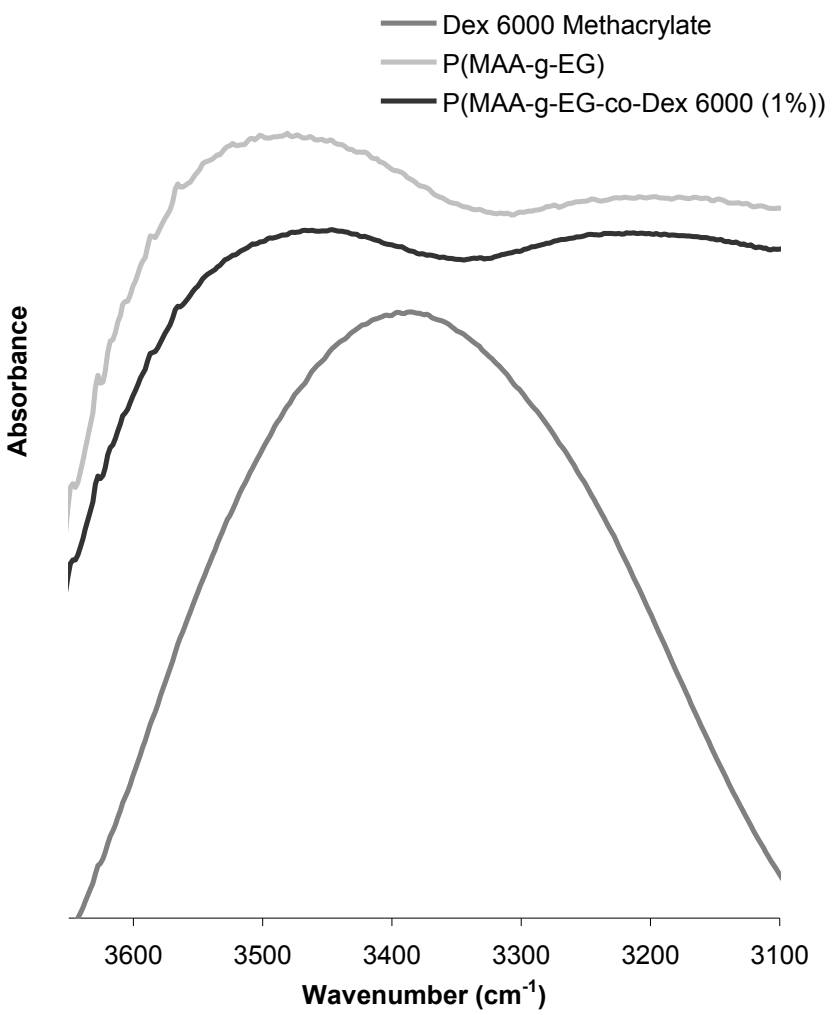

Figure 4.4. FT-IR absorbance spectra of Dextran 6000-Methacrylate, P(MAA-g-EG), and P(MAA-g-EG-co-Dextran 6000 (1%)) in the 3100-3600 cm^{-1} range.

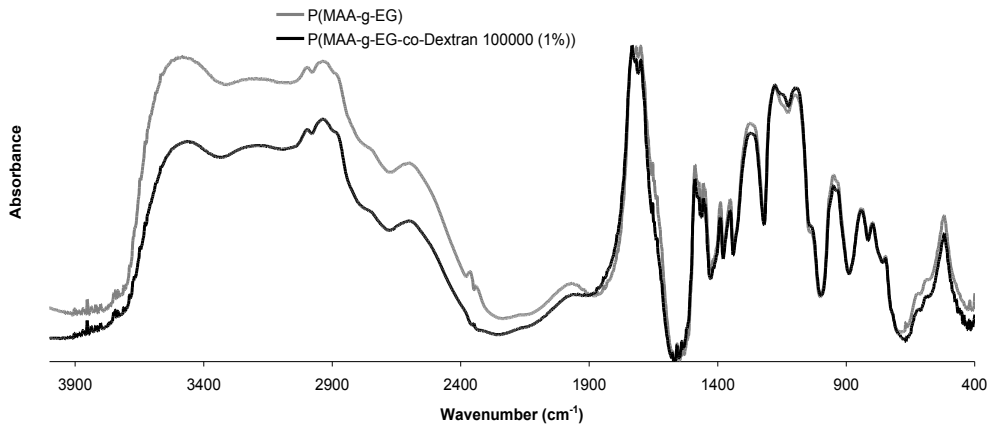

Figure 4.5. FT-IR spectra of P(MAA-g-EG) hydrogels and P(MAA-g-EG-co-Dextran 100000 (1%)) hydrogels.

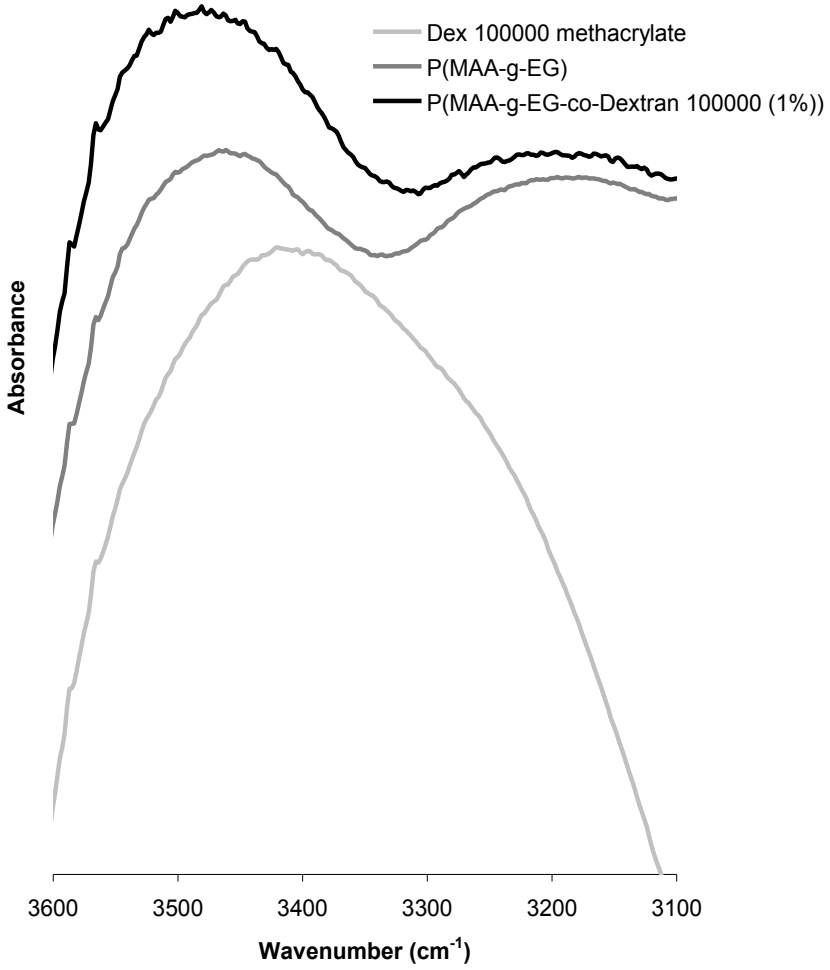

Figure 4.6. FT-IR absorbance spectra of Dextran 100000-Methacrylate, P(MAA-g-EG), and P(MAA-g-EG-co-Dextran 100000 (1%)) in the 3100-3600 cm^{-1} range.

Table 4.1. FT-IR absorbance peak locations corresponding to hydroxyl stretching for P(MAA-g-EG), P(MAA-g-EG-co-Dextran 6000 (1%), and Dextran 6000-methacrylate.

	Hydroxyl group stretching (cm^{-1})
P(MAA-g-EG)	3481
P(MAA-g-EG-co-Dextran 6000 (1%))	3446
Dextran 6000-methacrylate	3385

Table 4.2. FT-IR absorbance peak locations corresponding to hydroxyl stretching for P(MAA-g-EG), P(MAA-g-EG-co-Dextran 100000 (1%), and Dextran 100000-methacrylate.

	Hydroxyl group stretching (cm^{-1})
P(MAA-g-EG)	3481
P(MAA-g-EG-co-Dextran 100000 (1%))	3467
Dextran 100000-methacrylate	3421

Table 4.3. FT-IR absorbance peak locations corresponding to hydroxyl stretching for P(MAA-g-EG), P(MAA-g-EG-co-Dextran 100000 (1%), and Dextran 100000-methacrylate.

	Hydroxyl group stretching (cm^{-1})
P(MAA-g-EG)	3481
P(MAA-g-EG-co-Pullulan (1%))	3469
Pullulan methacrylate	3381

4.5 REFERENCES

1. Blanchette, J., N. Kavimandan and N. A. Peppas, Principles of transmucosal delivery of therapeutic agents. *Biomed. Pharmacother.*, 2004, 58, 142-151.

2. Betancourt, T., J. Pardo, K. Soo and N. A. Peppas, Characterization of pH-responsive hydrogels of poly(itaconic acid-g-ethylene glycol) prepared by UV-initiated free radical polymerization as biomaterials for oral delivery of bioactive agents. *J. Biomed. Mater. Res. Part A*, 93A, 175-188.

3. Carr, D. A. and N. A. Peppas, Assessment of poly(methacrylic acid-co-N-vinyl pyrrolidone) as a carrier for the oral delivery of therapeutic proteins using Caco-2 and HT29-MTX cell lines. *J. Biomed. Mater. Res. Part A*, 2010, 92A, 504-512.

4. Fisher, O. Z. and N. A. Peppas, Quantifying tight junction disruption caused by biomimetic pH-sensitive hydrogel drug carriers. *J. Drug Deliv. Sci. Technol.*, 2008, 18, 47-50.

5. Goto, T., M. Morishita, N. J. Kavimandan, K. Takayama and N. A. Peppas, Gastrointestinal transit and mucoadhesive characteristics of complexation hydrogels in rats. *J. Pharm. Sci.*, 2006, 95, 462-469.

6. Kavimandan, N. J., E. Losi and N. A. Peppas, Novel delivery system based on complexation hydrogels as delivery vehicles for insulin-transferrin conjugates. *Biomaterials*, 2006, 27, 3846-3854.

7. Kavimandan, N. J. and N. A. Peppas, Confocal microscopic analysis of transport mechanisms of insulin across the cell monolayer. *Int. J. Pharm.*, 2008, 354, 143-148.

8. Morishita, M., M. Goto, K. Takayama and N. A. Peppas, Oral insulin delivery systems based on complexation polymer hydrogels. *J. Drug Deliv. Sci. Technol.*, 2006, 16, 19-24.

9. Morishita, M., T. Goto, K. Nakamura, A. M. Lowman, K. Takayama and N. A. Peppas, Novel oral insulin delivery systems based on complexation polymer hydrogels: Single and multiple administration studies in type 1 and 2 diabetic rats. *J. Control. Release*, 2006, 110, 587-594.

10. Morishita, M. and N. A. Peppas, Is the oral route possible for peptide and protein drug delivery. *Drug Discov. Today*, 2006, 11, 905-910.

11. Peppas, N. A., J. B. Thomas and J. McGinty, Molecular Aspects of Mucoadhesive Carrier Development for Drug Delivery and Improved Absorption. *J. Biomater. Sci.-Polym. Ed.*, 2009, 20, 1-20.

12. Serra, L., J. Domenech and N. A. Peppas, Design of poly(ethylene glycol)-tethered copolymers as novel mucoadhesive drug delivery systems. *Eur. J. Pharm. Biopharm.*, 2006, 63, 11-18.

13. Shofner, J. P., M. A. Phillips and N. A. Peppas, Cellular Evaluation of Synthesized Insulin/Transferrin Bioconjugates for Oral Insulin Delivery Using Intelligent Complexation Hydrogels. *Macromol. Biosci.*, 10, 299-306.

14. Wood, K. M., G. M. Stone and N. A. Peppas, The effect of complexation hydrogels on insulin transport in intestinal epithelial cell models. *Acta Biomater.*, 2010, 6, 48-56.

15. Yamagata, T., M. Morishita, N. J. Kavimandan, K. Nakamura, Y. Fukuoka, K. Takayama and N. A. Peppas, Characterization of insulin protection properties of complexation hydrogels in gastric and intestinal enzyme fluids. *J. Control. Release*, 2006, 112, 343-349.

16. Lowman, A. M. and N. A. Peppas, Molecular analysis of interpolymer complexation in graft copolymer networks. *Polymer*, 2000, 41, 73-80.

17. Lowman, A. M., M. Morishita, M. Kajita, T. Nagai and N. A. Peppas, Oral delivery of insulin using pH-responsive complexation gels. *J. Pharm. Sci.*, 1999, 88, 933-937.

18. Besheer, A., K. M. Wood, N. A. Peppas and K. Mader, Loading and mobility of spin-labeled insulin in physiologically responsive complexation hydrogels intended for oral administration. *J. Control. Release*, 2006, 111, 73-80.

19. Achar, L. and N. A. Peppas, Preparation, Characterization And Mucoadhesive Interactions Of Poly(Methacrylic Acid) Copolymers With Rat Mucosa. *J. Control. Release*, 1994, 31, 271-276.

20. Leitner, V. M., G. F. Walker and A. Bernkop-Schnurch, Thiolated polymers: evidence for the formation of disulphide bonds with mucus glycoproteins. *Eur. J. Pharm. Biopharm.*, 2003, 56, 207-214.

21. Deutel, B., M. Greindl, M. Thaurer and A. Bernkop-Schnuerch, Novel insulin thiomer nanoparticles: In vivo evaluation of an oral drug delivery system. *Biomacromolecules*, 2008, 9, 278-285.

22. Roy, K., H. Q. Mao, S. K. Huang and K. W. Leong, Oral gene delivery with chitosan-DNA nanoparticles generates immunologic protection in a murine model of peanut allergy. *Nat. Med.*, 1999, 5, 387-391.

23. Pan, Y., Y. J. Li, H. Y. Zhao, J. M. Zheng, H. Xu, G. Wei, J. S. Hao and F. D. Cui, Bioadhesive polysaccharide in protein delivery system: chitosan nanoparticles improve the intestinal absorption of insulin in vivo. *Int. J. Pharm.*, 2002, 249, 139-147.

24. Sahlin, J. J. and N. A. Peppas, Enhanced hydrogel adhesion by polymer interdiffusion: Use of linear poly(ethylene glycol) as an adhesion promoter. *J. Biomater. Sci.-Polym. Ed.*, 1997, 8, 421-436.

25. Wood, K. M., G. M. Stone and N. A. Peppas, Wheat germ agglutinin functionalized complexation hydrogels for oral insulin delivery. *Biomacromolecules*, 2008, 9, 1293-1298.

26. Zhang, N., Q. N. Ping, G. H. Huang and W. F. Xu, Investigation of lectin-modified insulin liposomes as carriers for oral administration. *Int. J. Pharm.*, 2005, 294, 247-259.

27. Kim, S. H. and C. C. Chu, Synthesis and characterization of dextran-methacrylate hydrogels and structural study by SEM. *J. Biomed. Mater. Res.*, 2000, 49, 517-527.

28. De Smedt, S. C., A. Lauwers and D. J., Characterization of the Network Structure of Dextran Glycidyl Methacrylate Hydrogels by Studying the Rheological and Swelling Behavior. *Macromolecules*, 1995, 28, 5082-5088.

29. vanDijkWolthuis, W. N. E., J. J. KettenesvandenBosch, A. vanderKerkvanHoof and W. E. Hennink, Reaction of dextran with glycidyl methacrylate: An unexpected transesterification. *Macromolecules*, 1997, 30, 3411-3413.

30. De Groot, C. J., M. J. A. Van Luyn, W. N. E. Van Dijk-Wolthuis, J. A. Cadee, J. A. Plantinga, W. Den Otter and W. E. Hennink, In vitro biocompatibility of biodegradable dextran-based hydrogels tested with human fibroblasts. *Biomaterials*, 2001, 22, 1197-1203.

31. Collier, J. H., J. P. Camp, T. W. Hudson and C. E. Schmidt, Synthesis and characterization of polypyrrole-hyaluronic acid composite biomaterials for tissue engineering applications. *J. Biomed. Mater. Res.*, 2000, 50, 574-584.

32. Leach, J. B., K. A. Bivens, C. N. Collins and C. E. Schmidt, Development of photocrosslinkable hyaluronic acid-polyethylene glycol-peptide composite hydrogels for soft tissue engineering. *J. Biomed. Mater. Res. Part A*, 2004, 70A, 74-82.

33. Bulpitt, P. and D. Aeschlimann, New strategy for chemical modification of hyaluronic acid: Preparation of functionalized derivatives and their use in the formation of novel biocompatible hydrogels. 1999, 47, 152-169.

34. Burdick, J. A., C. Chung, X. Q. Jia, M. A. Randolph and R. Langer, Controlled degradation and mechanical behavior of photopolymerized hyaluronic acid networks. *Biomacromolecules*, 2005, 6, 386-391.

35. Moriyama, K. and N. Yui, Regulated insulin release from biodegradable dextran hydrogels containing poly(ethylene glycol) (vol 42, pg 237, 1996). *J. Control. Release*, 1997, 45, 209-209.

36. Van Dijk-Wolthuis, W. N. E., O. Franssen, H. Talsma, M. J. van Steenbergen, J. J. Kettenes-van den Bosch and W. E. Hennink, Synthesis, Characterization, and Polymerization of Glycidyl Methacrylate Derivitized Dextran. *Macromolecules*, 1995, 28, 6317-6322.

37. Albertsson, P. A., Particle Fractionation in Liquid Two-Phase Systems: The Composition of Some Phase Systems and the Behaviour of Some Model Particles in them Application to the Isolation of Cell Walls from Microorganisms. *Biochim. Biophys. Acta*, 1958, 27, 378-395.

38. Diamond, A. D. and J. T. Hsu, Phase Diagrams for Dextran-PEG Aqueous Two-Phase Systems at 22 Degrees C. *Biotechnol. Tech.*, 1989, 3, 119-124.

39. Stenekes, R. J. H., O. Franssen, E. M. G. van Bommel, D. J. A. Crommelin and W. E. Hennink, The preparation of dextran microspheres in an all-aqueous system: Effect of the formulation parameters on particle characteristics. *Pharm. Res.*, 1998, 15, 557-561.

40. Barsbay, M. and A. Guner, Miscibility of dextran and poly(ethylene glycol) in solid state: Effect of the solvent choice. *Carbohyd. Polym.*, 2007, 69, 214-223.

41. Torres-Lugo, M. and N. A. Peppas, Preparation and characterization of P(MAA-g-EG) nanospheres for protein delivery applications. *J. Nanopart. Res.*, 2002, 4, 73-81.

Chapter 5:

Analysis of Complexation Behavior of Polysaccharide-Modified Hydrogels

5.1 Introduction

Changes in the molecular structure of hydrogels can have a significant impact on the properties of the resulting material. For example, the addition of more hydrophobic or more hydrophilic comonomers during polymerization with crosslinking agents may change the ability of the hydrogel to swell in aqueous solvents. Additionally, the mesh size of the hydrogel network in a particular environment may change. For biological applications, changes in the hydrogel's ability to swell and the mesh size of the network are very important. Both hydrogel swelling and mesh size are commonly used in controlled drug delivery, and their effects on drug release have been extensively studied [1-3].

The molecular structure of a hydrogel network includes crosslinking of the network, chain entanglements, and interpolymer interactions as well as the polymer chain lengths between any of these junctions. The molecular structure of hydrogels can be changed by the addition of comonomers [4] that experience intermolecular interactions such as hydrogen bonding [5]. The distance between junctions and network flexibility is often increased as the amount of crosslinker decreases [3, 6].

In this research, polysaccharides were incorporated into the structure of P(MAA-g-EG) complexation hydrogels. The maintenance of interpolymer complexation for pH-responsive oral protein delivery would be highly desirable for this application. One of the major concerns addressed in the subsequent studies is whether the polysaccharide tethers significantly change pH-responsive swelling. For example, dextran and pullulan

can potentially participate in hydrogen bonding between adjacent polymer chains due to their hydroxyl groups and etheric groups.

In this chapter, the effect of large polysaccharide comonomers on pH-dependent swelling is analyzed for P(MAA-g-EG) hydrogels using dynamic and equilibrium swelling studies along with analysis of the hydrogel mesh sizes using physical data and the Peppas-Merrill equation. Because these systems were designed for applications in pH-responsive oral protein delivery, the goal of this work was to confirm pH-dependent swelling and evaluate swelling behavior as it relates to oral insulin delivery.

5.2. Materials and Methods

P(MAA-g-EG) hydrogels were modified with polysaccharide tethers of dextran or pullulan. Photopolymerizable vinyl groups were added to the polysaccharide tethers first and the resulting monomers were added to the polymerization and incorporated into the hydrogel network. The synthesized hydrogel films were then used to evaluate pH-responsive swelling.

5.2.1 Functionalization of Polysaccharides with Polymerizable Vinyl Groups

Addition of Polymerizable Groups to Dextrans and Pullulans

The synthesis procedure for methacrylation of dextran was adapted from published procedures [7]. Either dextran (3 g, Sigma Aldrich) with an average molecular weight of either 6000 Da or 100,000 Da or pullulan (Sigma Aldrich) with an average molecular weight of 75,000 Da was dissolved in anhydrous dimethyl sulfoxide (DMSO, Sigma Aldrich) to yield a concentration of 100 mg/ml. After dissolution, dimethylamino pyridine (DMAP, Sigma Aldrich) was added at a concentration of 20 mg/ml. Glycidyl methacrylate (GMA, Sigma Aldrich) was slowly added drop wise at a ratio of 8 mol% of the total saccharide units. The reaction was allowed to proceed at room temperature

for 48 hours. The reaction was quenched by neutralizing the DMAP with 1 N hydrochloric acid (HCl). The product was dialyzed against water for at least one week in a 3500 molecular weight cut-off dialysis tube (Spectrapor). The water was changed twice a day for 7 days and then lyophilized.

For formation of hydrogels using dextran with an acrylate group, dextran with a molecular weight of 100,000 Da was solubilized in ultrapure water and placed in an ice bath. After 30 minutes, acryloyl chloride (Acros Organic) was then added to the solution, and the solution was allowed to stir for two hours. The product, acryl-Dex, was dialyzed for 48 hours against ultrapure water in a 3,500 molecular weight cut-off dialysis membrane (Spectrapor). The product was then frozen and lyophilized.

5.2.2 Hydrogel Synthesis

Polymerization of P(MAA-g-EG) Hydrogels

P(MAA-g-EG) films were prepared by a free radical, UV-initiated polymerization. This polymerization was carried out in solution with a solvent of 50 wt % ethanol and 50 wt % water. To the solvent, an equal mass of monomers was added. The monomers consisted of methacrylic acid (MAA, Sigma Aldrich) and poly(ethylene glycol) monomethyl ether monomethacrylate (PEGMMA, Polysciences Inc) with an average molecular weight of 1000 Da combined in a ratio of 1 mol methacrylic acid to 1 mol ethylene glycol. To the monomers and solvent, a crosslinker and initiator were then added.

A crosslinking agent poly(ethylene glycol) dimethacrylate (PEGDMA, Polysciences Inc.) with an average molecular weight of 400 Da, was added at a crosslinking feed ratio of 0.75 mol% . The UV-initiator, Irgacure 184, was 0.1 wt% of the total mass of the monomers. The pre-polymer solution was sonicated for 20 minutes and placed in a

sealed glove box. The solution were purged with nitrogen for 30 minutes. The solution was then placed in a mold consisting of two glass slides and a Teflon spacer. The mold was placed under an ultraviolet (UV) light with an intensity of 16-17 mW/cm^2 for 30 minutes. The film was then washed in ultrapure water for 7 days and the water was exchanged twice daily to remove any unreacted components.

Polymerization of P(MAA-g-EG-Dex) and P(MAA-g-EG-co-Pul) Hydrogels

The reaction solvent was changed from a 1:1 water to ethanol solution to a 73 wt % 0.1 N sodium hydroxide and 27 wt % ethanol solution. MAA was first solubilized in sodium hydroxide, followed by the polysaccharide, PEGMMA, PEGDMA, ethanol, and then Irgacure 184. The solution was sonicated for 20 minutes or until the reactants were fully dissolved. The reaction was carried out as described in the previous section for P(MAA-g-EG).

5.2.3 Swelling Studies

Two types of hydrogel swelling studies, dynamic and equilibrium, were used to measure pH-responsive swelling of polysaccharide-modified hydrogels.

Dynamic Swelling Studies

Hydrogel disks with a diameter of 15 mm were punched from hydrogel films that had been washed in ultrapure water for 5-7 days to remove any unreacted components. The hydrogel disks were dried overnight in a vacuum oven. The initial mass of the dried disks was recorded before the swelling study.

Dimethylglutaric acid (DMGA, Sigma Aldrich, St. Louis, MO) buffers (0.01 M) were prepared with constant ionic strength and different pHs. The buffer pH was adjusted between 3.2 and 7.6 to simulate GI tract fluids. For dynamic swelling studies,

disks were placed in a series of dimethyl glutaric acid (DMGA) buffers of increasing pH (pH = 3.2 to 7.6) at 37 ^{o}C and constant ionic strength for 5 minutes. Each disk was placed first in the buffer with a pH of 3.2 for 5 minutes. The disks were removed from the swelling media, and excess water was removed. The mass of the disk was measured, and the disk was placed in the next buffer. This process was repeated until the disks had been allowed to swell in each of the 10 buffers with different pH for 5 minutes. The mass swelling ratios of the films after each 5 minute incubation period were calculated.

Equilibrium Swelling Studies

Equilibrium swelling studies were performed on P(MAA-g-EG) gels modified with polysaccharides. Disks (15 mm in diameter) were cut from hydrogel films immediately following polymerization. The mass of the hydrogel in the relaxed state was measured in air. The mass of the hydrogel in a non-solvent in the relaxed state was then obtained in heptanes using a hanging basket system apparatus. The hydrogel disks were washed in ultrapure water for 5-7 days with a twice daily replacement of the water. The hydrogel disks were then allowed to dry at room temperature for at least 24 hours and then placed in a vacuum oven maintained at 37 ^{o}C to continue drying.

The initial mass of the dry hydrogel disks was recorded both in air and in heptanes using the hanging basket apparatus. Gels were then incubated in 50 ml of 0.01 M DMGA buffers with various pHs (pH = 3.2 to 7.6) maintained at 37^{o}C and constant ionic strength for 24 hours. The disks were carefully removed from the swelling media. Excess water was wicked from the surface of the hydrogels prior to measurements. The mass of the gels in the swollen state was recorded in air and in heptanes using the same methods for relaxed stated and dry state measurements. The

final mass of the swollen gels was used to calculate the equilibrium mass swelling ratio. Measurements of the mass of the hydrogel disks in air and the mass of the disks in a non-solvent were obtained for each disk in the relaxed state, the dry state, and the swollen state.

5.3. Results and Discussion

Because the complexation behavior of these hydrogels is an essential property for use as an oral protein delivery system, we verified the pH-dependent swelling by comparing the swelling of these hydrogels in different simulated physiological fluids. In this work, polysaccharide-modified hydrogels were examined using several measurements including the mass swelling ratio, the polymer volume fraction in the relaxed state, and the polymer volume fraction in the swollen state.

The mass swelling ratio of these gels was analyzed using dynamic and equilibrium swelling.

The swelling of P(MAA-g-EG-co-Dextran 100000) gels with different amounts of dextran in the gel was investigated using dynamic swelling studies. For dynamic swelling studies shown in Figure 5.1, hydrogels polymerized with Dextran 100000 have increased swelling in comparison to P(MAA-g-EG) controls. Three different dextran 100,000 feed ratios were examined to determine if an increase in the amount of polysaccharide in the polymer affected swelling. While all gels had higher swelling ratios than P(MAA-g-EG), no specific trend was observed in relation to increasing the polysaccharide content.

In contrast to dynamic swelling measurements, equilibrium swelling studies measure the extent of hydrogel swelling at equilibrium. These studies typically require

incubation periods on the order of hours to days. Additionally, these studies are very relevant for analysis of hydrogel drug delivery systems composed of microparticles. Because complexation hydrogels used for drug delivery systems are commonly in the form of microparticles, the equilibrium swelling of the films is a more accurate representation of microparticle swelling in response to pH changes. Microparticles swell much faster than films due to their significantly smaller size. Estimation for the time required for water to diffuse dry, glassy microparticles is on the order of minutes. Both Wood and Carr have shown estimates for this time scale [8, 9]. In both calculations, a diffusion coefficient of 10^{-6} cm^2/s was assumed, and 100 µm was used as an approximate diffusion path length for a particle with a 100 µm diameter. Here, the approximate calculation is shown based on a microparticle with a 200 µm diameter (100 µm radius) because diffusion occurs radially inward.

$$t = \frac{r^2}{D} = \frac{(100\,\mu m)^2}{10^{-6}\,cm^2/s} \approx 100 \quad s \quad < \quad 2 \quad \min \tag{5.1}$$

From this expression, the approximate swelling of a microparticle from the dry, glassy state occurs on the order of minutes. (It is important to note that the diffusion coefficient in this analysis in Equation 5.1 is merely an estimate and is typically time variant.) Because diffusion of aqueous solvents into micro-scale hydrogels occurs on such short time scales, the time to reach a swelling equilibrium on the micro-scale is also short.

To better understand how microparticles composed of polysaccharide-modified complexation hydrogels swell with pH for oral delivery applications, the equilibrium swelling of these gels was analyzed in simulated physiological fluids. The equilibrium mass swelling ratios of each of these polysaccharide-modified hydrogels were compared to unmodified P(MAA-g-EG). Comparison of modified gels to unmodified P(MAA-g-EG)

allow the effects of the large polysaccharide tethers to be more fully evaluated. In addition, P(MAA-g-EG) systems are well characterized for oral delivery applications, and its swelling properties have been extensively studied. Results from this study show the addition of polysaccharide tethers increased the swelling ratio in comparison to unmodified P(MAA-g-EG) materials. The equilibrium mass swelling ratios of P(MAA-g-EG-co-Dextran 6000) and P(MAA-g-EG-co-Dextran 100000(1%)) gels were significantly higher than P(MAA-g-EG) gels (Figures 5.2 and 5.3). Similarly, P(MAA-g-EG-co-Pullulan) gels reached a greater equilibrium mass swelling ratio than P(MAA-g-EG) as shown in Figure 5.4, but the difference was not as pronounced as observed for the P(MAA-g-EG-co-Dextran) materials.

One of the concerns with polysaccharide tethers is their hydrophilicity and ability to hydrogen bond. The hydrophilic nature of polysaccharides may cause increased swelling at low pH which is not desirable for these applications. A comparison of all three gels shows that each had similar swelling ratios at pH values below 4.5 (Figure 5.4). As the pH increased, we observed more significant differences in the swelling behavior of the gels. P(MAA-dg-EG-co-Dextran 6000) showed the overall greatest mass swelling ratio (Figure 5.5). Gels of P(MAA-dg-EG-co-Pullulan) had lower swelling ratios than P(MAA-dg-EG-co-Dextran 6000) and P(MAA-g-EG-co-Dextran 100000) at pH 7.6 in the swollen state. The general trend of the swelling curves show that as the molecular weight of the polysaccharide gel component decreased, the swelling ratio increased for pHs beyond the pKa of methacrylic acid which is reported between a pH of 4.8 and 4.9 [10].

All three of these polysaccharides are very hydrophilic. These data demonstrate that the polysaccharide is not disrupting complexation behavior as the glycosidic bonds along the backbone of the polysaccharide and the hydroxyl groups on each saccharide

mer unit can participate in hydrogen bonding with the methacrylic acid and PEG components of the gel. Each gel was prepared with the same mass of polysaccharide (and hence the same molar feed ratio of glucose mer units).

In order to gain insight into whether these gels could be used to load and release a protein drug, measurements of the volume fraction of the hydrogel in the relaxed state and swollen state were determined. The volume fraction of the polymer in the relaxed state ($\nu_{2,r}$) was calculated using the Equation 5.2 using the mass of the hydrogels (W) in either the dry or relaxed state denoted by a subscript d or r, respectively. The mass in air or in a non-solvent is denoted by subscripts a or n, respectively).

$$\nu_{2,r} = \frac{W_{a,d} - W_{n,d}}{W_{a,r} - W_{n,r}} \tag{5.2}$$

The polymer volume fractions for each of the hydrogels in the relaxed state are shown in Figure 5.5. In general, the volume fraction in the relaxed state of the hydrogels is similar falling in the range of 0.527 to 0.599.

The equilibrium polymer volume fraction in the swollen state, $\upsilon_{2,s}$, was measured as a function of pH and calculated using the mass of the hydrogel disk in the dry and swollen states in either air or a non-solvent (Equation 5.3).

$$\nu_{2,s} = \frac{W_{a,d} - W_{n,d}}{W_{a,s} - W_{n,s}} \tag{5.3}$$

Based on calculations from Equation 5.3, the equilibrium polymer volume fractions in the swollen state $\upsilon_{2,s}$ of the different polymer compositions are compared. In Figure 5.6, the equilibrium polymer volume fraction in the swollen state, $\upsilon_{2,s}$ decreases as pH increases for P(MAA-g-EG-co-Dextran 100000) and P(MAA-g-EG) hydrogels. There are some subtle differences in the equilibrium polymer volume fraction in the swollen state $\upsilon_{2,s}$for the formulations. Notably, at low pH, P(MAA-g-EG-co-Dextran 100,000 (1%)) has the highest $\upsilon_{2,s}$ while P(MAA-g-EG-co-Dextran 100000

(2%)) has a lower $\upsilon_{2,s}$ than P(MAA-g-EG). In acidic conditions, it is highly desirable to have an increased $\upsilon_{2,s}$ that indicates that there is less solvent present in the hydrogel. Less solvent in the hydrogel corresponds to a lower degree of swelling and suggests that entrapped molecules, such as a protein drug, may be better protected from the environment surrounding the gel. Likewise, a decrease in the polymer volume fraction at neutral conditions is desirable for applications in oral protein drug delivery.

For example, P(MAA-g-EG-co-Pullulan) gels exhibit decreased equilibrium polymer volume fraction in the swollen state $\upsilon_{2,s}$ with increased pH (Figure 5.7). A decrease in the polymer volume fraction indicates a greater degree of swelling and increased diffusion into and out of the gel. In comparing P(MAA-g-EG-co-Dextran 6000) gels to P(MAA-g-EG), the dextran-modified hydrogels have the lowest $\upsilon_{2,s}$ (Figure 5.8). The polysaccharide-modified hydrogels, therefore, have swelling properties that are desirable for oral protein drug delivery applications.

These trends in $\upsilon_{2,s}$ are expected based on equilibrium swelling studies. In all cases, the swelling ratio and the volume fraction of the polymer in the swollen state are inversely related. As the mass of water imbibed increases the mass of the hydrogel, the polymer network swells. As a result, the fraction of the volume that is the polymer network is decreased in relation to the volume accounted for by the imbibed water.

The Peppas-Merrill equation can be used to estimate the molecular weight between crosslinks, $\overline{M_c}$, and hence the mesh size, ξ, of a hydrogel network. This equation is a modification of Flory-Rehner theory to account for the presence of a solvent during crosslinking. To obtain the molecular weight between crosslinks, the following equation is used.

$$\frac{1}{\overline{M_c}} = \frac{2}{\overline{M_n}} - \frac{\left(\bar{v}/V_1\right)\left[\ln\left(1-\upsilon_{2,s}\right)+\upsilon_{2,s}+\chi_1{\upsilon_{2,s}}^2\right]}{\nu_{2,r}\left[\left(\frac{\upsilon_{2,s}}{\upsilon_{2,r}}\right)^{1/3}-\frac{\upsilon_{2,s}}{2\upsilon_{2,r}}\right]} \tag{5.4}$$

The volume fraction of the polymer in the swollen state, $\upsilon_{2,s}$, and the volume fraction of the polymer in the relaxed state, $\upsilon_{2,r}$, (Equations 5.2 and 5.3) are used in the Peppas-Merrill equation (Equation 5.4).

The Flory interaction parameter for polysaccharide-modified P(MAA-g-EG) can be calculated by a weighted average of the Flory interaction parameters for MAA and PEG assuming that there is not a significant contribution from the polysaccharide using the molar feed ratio in the polymerization of methacrylic acid and poly(ethylene glycol) where χ for methacrylic acid is given by Equation 5.5 [11, 12] and χ for PEG is 0.436.

$$\chi = 0.44 + 0.6\upsilon_{2,s} \tag{5.5}$$

In this work, χ was determined for the experimental data using Equation 5.5. For swelling measurements below pH 5.2, the χ values were greater than 0.5 while χ was less than 0.5 at more neutral pH. The Flory interaction parameter indicates how well the solvent and polymer interact. A Flory interaction parameter less than 0.5 indicates favorable interactions between the polymer and the solvent. Generally, solvents with a χ less than 0.5 are considered good solvents while solvents with χ greater than 0.5 are considered poor solvents.

The Flory interaction parameter plays a significant role in the $\overline{M_c}$ analysis using the Peppas-Merrill equation because one of the assumptions is that there is a favorable interaction between the solvent and the polymer (χ <0.5). As a result of χ calculations based on the data presented in this chapter, the Peppas-Merrill equation is a more representative analysis for the hydrogels in the swollen state above the swelling transition point (pH > 5).

The specific volume of the polymer can be calculated using Equation 5.6 based on the mass of the hydrogels in air and heptane in the dry state and the density of the non-solvent, ρ_n.

$$\bar{\upsilon} = \frac{1}{\rho_n}\frac{W_{a,d} - W_{a,n}}{W_{a,d}} \tag{5.6}$$

In this analysis, the molar volume of the solvent (V_1) is assumed to be the molar volume of water (18.1 cm^3/mol) because water is the major component of the buffers used during the swelling measurements.

In the case of these gels, it is not possible to measure the number average molecular weight, $\overline{M_n}$, of the polymer chains using traditional gel permeation chromatography. Because the polysaccharides may have more than one polymerizable group per molecule, they can act as crosslinkers. In typical $\overline{M_n}$ determinations, the polymer samples are prepared by polymerization under normal reaction conditions but with the omission of the crosslinker. The reason the crosslinker is not used is that it can affect the hydrodynamic diameter of the polymer chains which is correlated to molecular weight. Additionally, crosslinked polymer chains may not elute from the GPC set-up resulting in a skewed molecular weight.

The mesh size of the hydrogel network can be calculated from the $\overline{M_c}$ of the hydrogel. The mesh size of the hydrogel is advantageous in analyzing the space available for diffusion of molecules into and out of the gel in the swollen state.

$$\xi = \alpha\left(\overline{r_0^2}\right)^{1/2} = \upsilon_{2,s}^{-1/3}\left(\frac{2C_n\overline{M_c}}{M_r}\right)^{1/2} \cdot l \tag{5.7}$$

For example, Equation 5.7 allows the approximation of the length associated with the $\overline{M_c}$ where α is the elongation ratio of gel and $\left(\overline{r_0^2}\right)^{1/2}$ is the root mean square

end-to-end distance of the polymer in the unperturbed state. Based on the following assumptions, the right-hand side of the Equation 5.7 can be obtained.

For example, the root mean square end-to-end distance of the polymer in the unperturbed state, $\left(\overline{r_0^2}\right)^{1/2}$, can be calculated using the following expression:

$$\left(\overline{r_0^2}\right)^{1/2} = \sqrt{C_n}\left(\overline{r^2}\right)^{1/2} \quad (5.8)$$

Equation 5.8 uses the characteristic ratio, C_n, of the polymer and root mean square end-to-end distance of the polymer in the freely jointed state, $\left(\overline{r^2}\right)^{1/2}$, to calculate the root mean square end-to-end distance of the polymer in the unperturbed state. Using Equation 5.9, the root mean square end-to-end distance of the polymer in the unperturbed state, $\left(\overline{r^2}\right)^{1/2}$, can be calculated from the bond length of the polymer backbone (l), which is predominantly carbon-carbon bonds (1.54 Å) for these materials, and the number of bonds associated with the $\overline{M_c}$ estimated in Equation 5.4.

$$\left(\overline{r^2}\right)^{1/2} = l\sqrt{n} \quad (5.9)$$

The final assumption used to arrive at the expression in Equation 5.7 is that the gel swelling is isotropic. Isotropic swelling of the gel allows the elongation ratio to be calculated based on the volume swelling ratio of polymer using Equation 5.10.

$$\alpha = \upsilon_{2,s}^{-1/3} \quad (5.10)$$

In this work, we have analyzed the mesh size, ξ, for a range of $\overline{M_n}$ using the Equation 5.4 and 5.7. Similar analyses have been previously published in which the $\overline{M_c}$ for hydrogels was analyzed in terms of $\overline{M_n}$ and was shown to increase with increasing $\overline{M_n}$ before reaching a plateau $\overline{M_c}$. Therefore, the mesh size was determined with respect to molecular weight between crosslinks with varying $\overline{M_n}$ as shown in Figures 5.11-5.12 for all three polymer formulations. The $\overline{M_c}$ for the polymers was calculated for a pH of 7.6 and used for calculation of ξ. For P(MAA-g-EG-co-Dextran 100000 (1%)) and P(MAA-g-EG-co-Dextran 6000) gels, the mesh size was larger than the mesh size of

P(MAA-g-EG) gels. In Figure 5.11, the opposite is true for P(MAA-g-EG-co-Pullulan). These results indicate that at neutral conditions, the mesh size of the gel increases more for dextran-modified P(MAA-g-EG) than for unmodified gels with corresponding $\overline{M_n}$. Generally, polymerization of P(MAA-g-EG) gels has resulted in $\overline{M_n}$ greater than 75 kDa. From the calculations presented in Figures 5.9-5.11, the mesh size of the hydrogels is sufficient to allow release of insulin, which has a diameter of 12-13 Å in monomeric form, rapidly at neutral pH.

The incorporation of large biomolecules into hydrogels is a new topic in the field of biomaterials, and the influence of large pendant polymer tethers on the molecular structure of hydrogels is not yet well understood. Despite a limited understanding of large biomolecular tethers on the molecular structure of hydrogel networks, the polymerization of biomolecules into hydrogels has become a popular strategy for imparting biological functionality into hydrogels for biological applications. For example, avidin [13] and biotin [14] have been polymerized into hydrogel networks for further modification after gel formation.

Tissue engineering scaffolds incorporating larger macromolecules into the synthetic hydrogel matrix have also been developed. Immobilization of vascular endothelial growth factor in PEG hydrogels has been shown to promote endothelialization [15, 16].

In drug delivery application, enzymes have also been immobilized in three-dimensional hydrogels for detection of glucose and for pulsatile release of insulin in response to elevated glucose levels [17, 18]. In other applications, such as molecular imprinting and recognition, the presence of large macromolecules during polymerization has been utilized as a means to synthesize crosslinked polymers with recognitive properties. Polymerization of a hydrogel network in the presence of a

template molecule impacts the molecular structure of hydrogel network allowing subsequent recognition of the template molecule. Template recognition by imprinted hydrogels has been attributed to the formation of nanocavities around the template molecule [19]. These nanocavities allow preferential recognition of the template molecule based on structural changes in the hydrogel [20, 21].

Crosslinking, polymerization kinetics, interpolymer interactions, and mesh size are parameters that are affected by the addition of comonomers during hydrogel polymerization. These same parameters are likely to be influenced by the polymerization of large molecule tethers into hydrogel networks although how these parameters change is likely specific for the size, shape, and composition of tether. The size of synthetic copolymer tethers has been shown to affect swelling properties of hydrogels. For example, large biomolecules may physically interfere with crosslinking and may thereby influence mesh size. Likewise, interactions, such as hydrogen bonding, between neighboring polymer chains may be disrupted by large tethers.

These large tethers may also form new interactions with adjacent polymer chains through hydrogen bonding, van der Waals forces, and hydrophobic-hydrophobic interactions. The affect that large comonomers have on complexation hydrogels in which the mesh size changes with pH, for example, is unknown yet very important in certain applications including oral protein delivery.

5.4 Conclusions

Based on analysis of the swelling of these hydrogels modified with either dextran or pullulan, pH-responsive swelling is conserved in the presence of the polysaccharide comonomers. These systems form collapsed structures with minimal swelling in acidic

conditions and swell significantly in more neutral conditions. Analysis of the mesh size indicates that these gels could sufficiently entrap and release drugs as large as protein drugs including insulin. In comparison to unmodified P(MAA-g-EG) hydrogels, polysaccharide-modified P(MAA-g-EG) hydrogels exhibited similar trends in swelling. Several differences such as increased $\upsilon_{2,s}$ at low pH and decreased $\upsilon_{2,s}$ at neutral pH suggest that polysaccharide-modified P(MAA-g-EG) gels may have some advantages for oral delivery with respect to their complexation and decomplexation behavior.

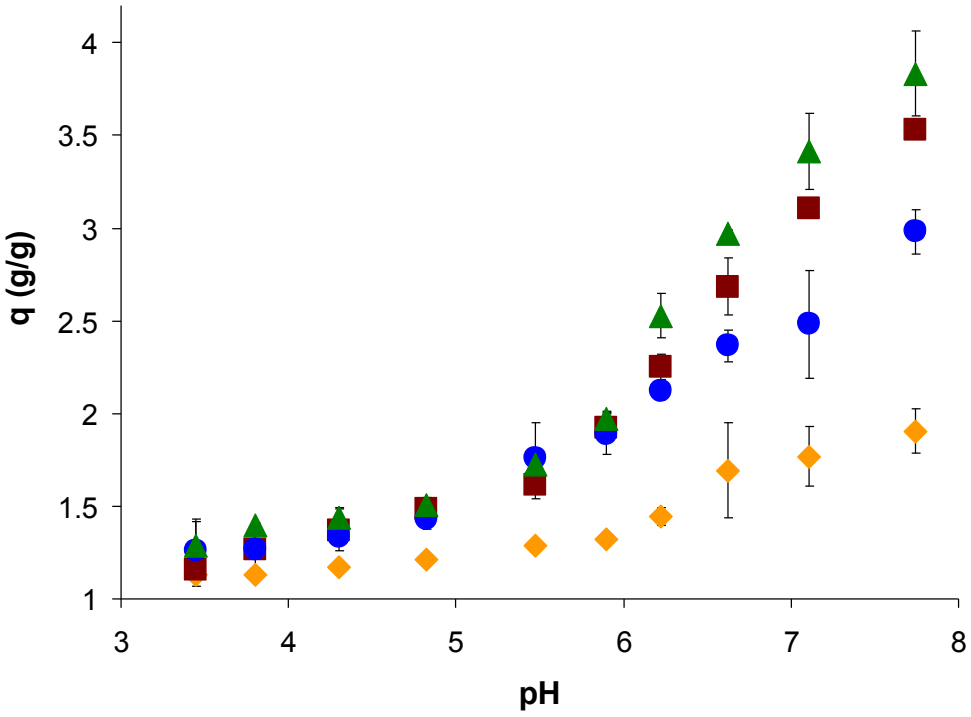

Figure 5.1 Dynamic weight swelling behavior of P(MAA-g-EG) and P(MAA-dg-EG-Dex100) gels with varying amounts of dextran including 0.5 wt %, 1 wt%, and 2 wt %.

Data reported are the mean ± standard deviation.

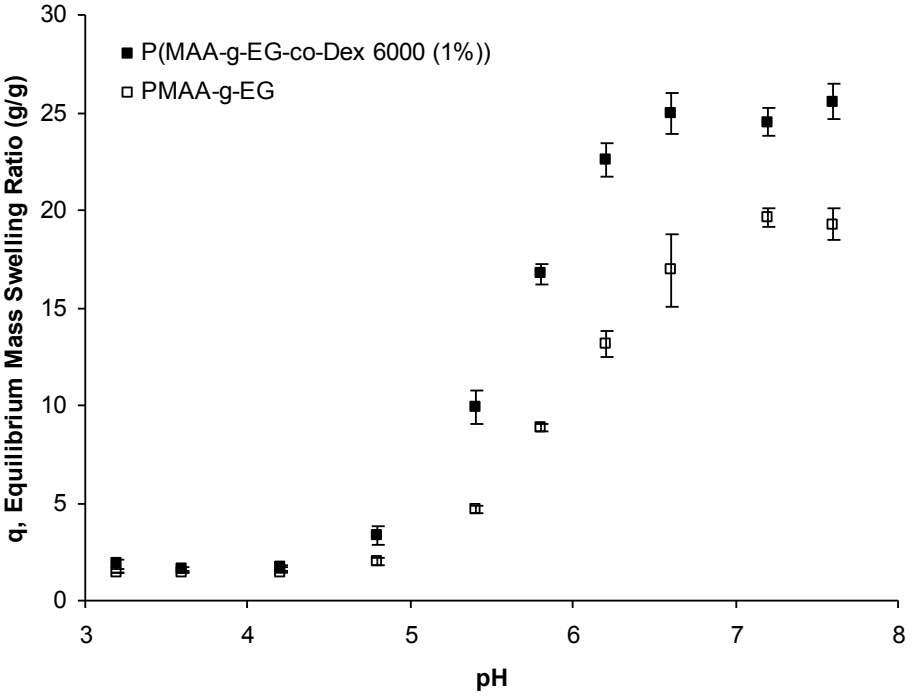

Figure 5.2 Equilibrium weight swelling ratios of P(MAA-dg-EG-co-Dextran 6000 (1%)) hydrogels and P(MAA-g-EG) hydrogels in DMGA buffer at different pH.

Data reported are the mean ± standard deviation.

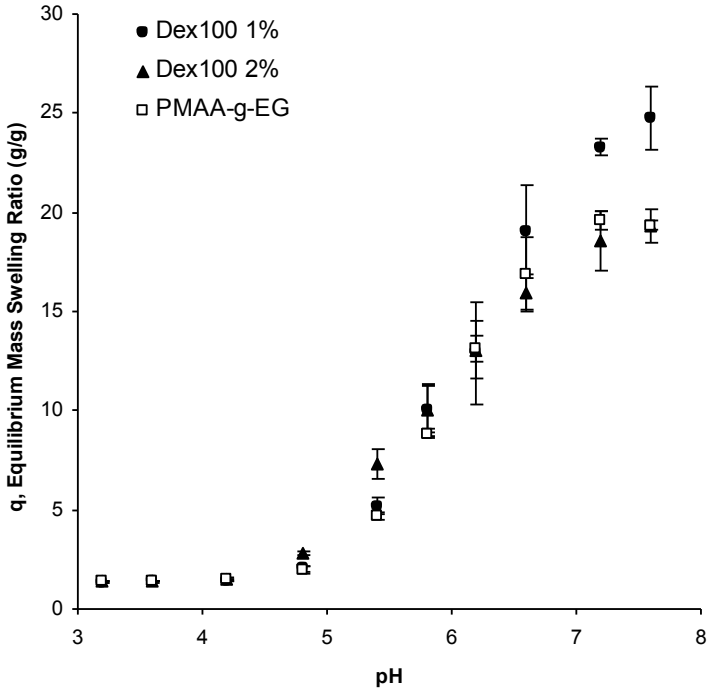

Figure 5.3 Equilibrium weight swelling ratios of P(MAA-dg-EG-co-Dextran 100000 (1%)), P(MAA-g-EG-co-Dextran 100000 (2%)), and P(MAA-g-EG) hydrogels at different pH.

Data reported are the mean ± standard deviation.

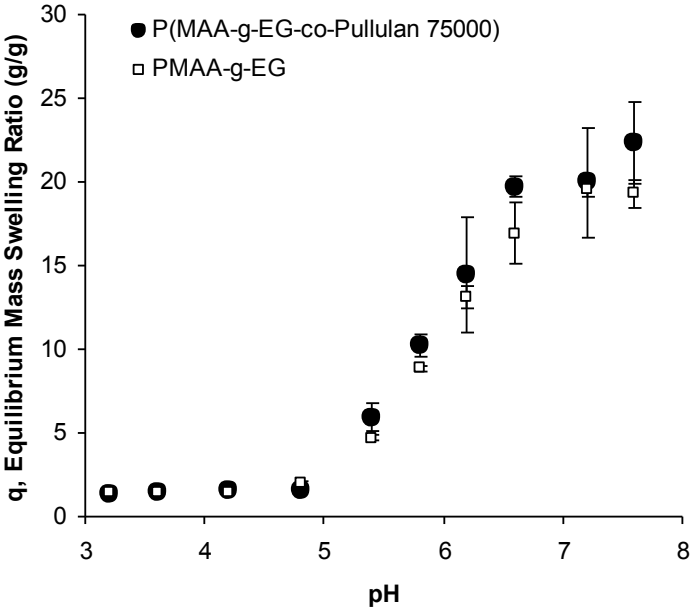

Figure 5.4 Equilibrium weight swelling ratios of P(MAA-g-EG-co-Pullulan) and P(MAA-g-EG) hydrogels in DMGA buffer with different pH values.

Data reported are the mean ± standard deviation.

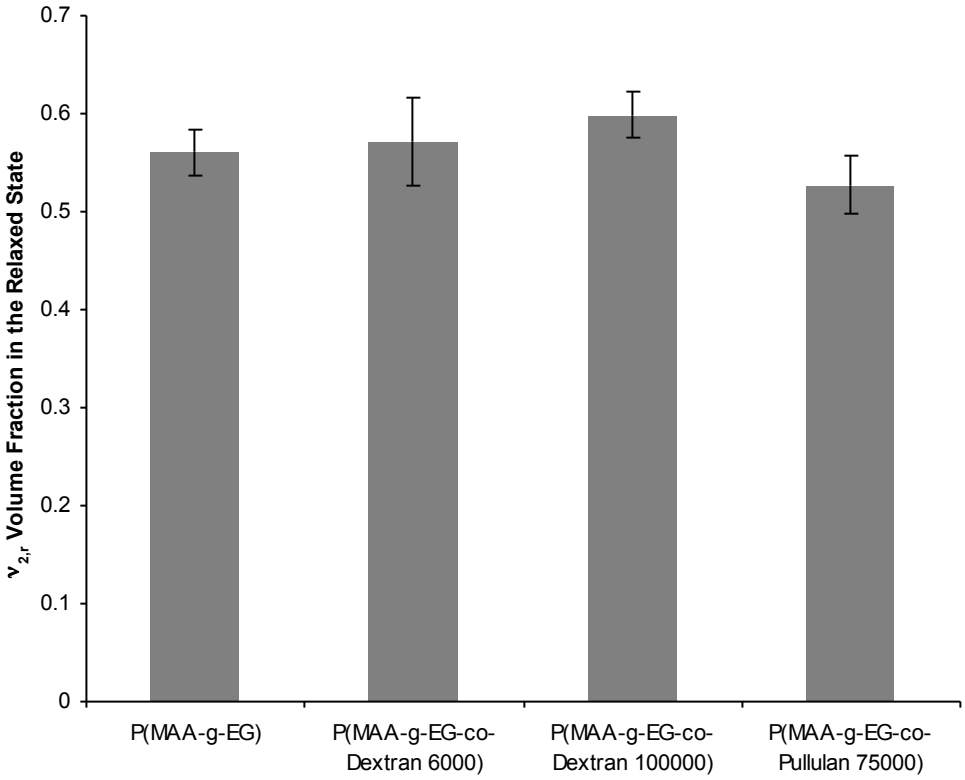

Figure 5.5 Polymer volume fraction of hydrogels in the relaxed state at 37 ^{o} C.

Data reported are the mean ± standard deviation.

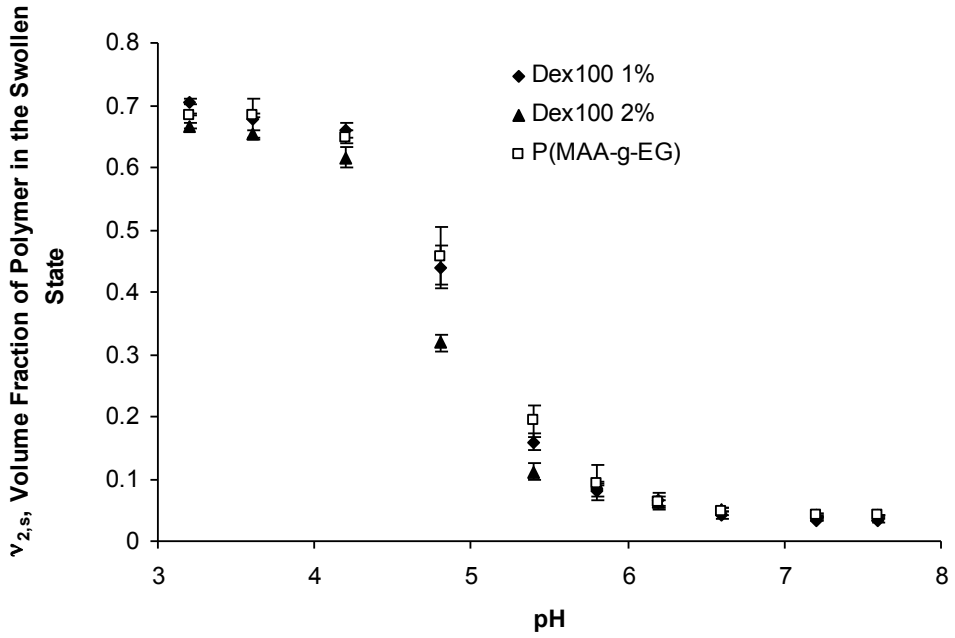

Figure 5.6 Volume fraction of P(MAA-dg-EG-co-Dex 100) in the swollen state at equilibrium after incubation in DMGA buffers of varying pH.

Data reported are the mean ± standard deviation.

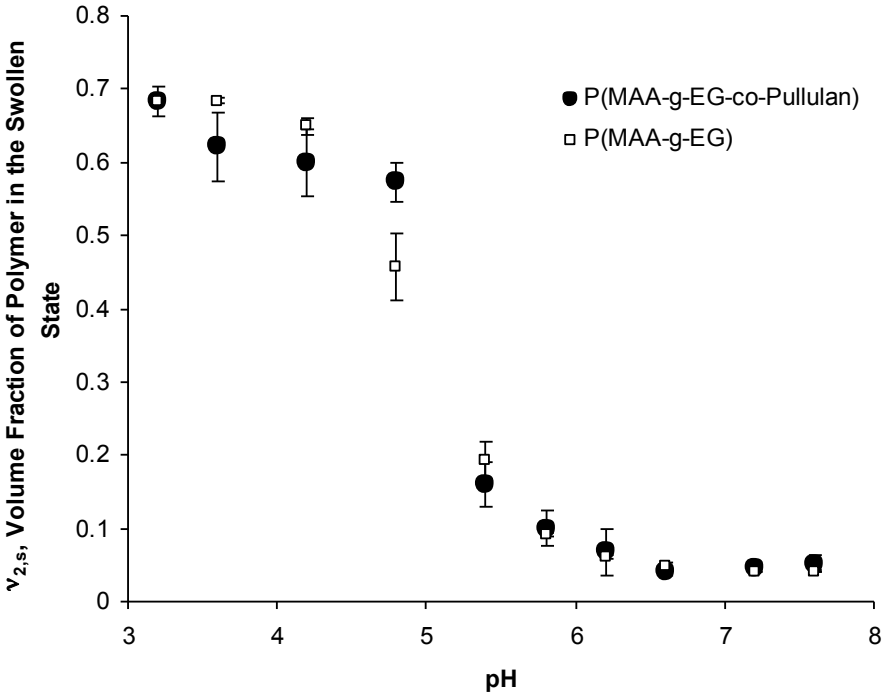

Figure 5.7 Volume fraction of P(MAA-dg-EG-co-Pullulan in the swollen state at equilibrium after incubation in DMGA buffers of varying pH.

Data reported are the mean ± standard deviation.

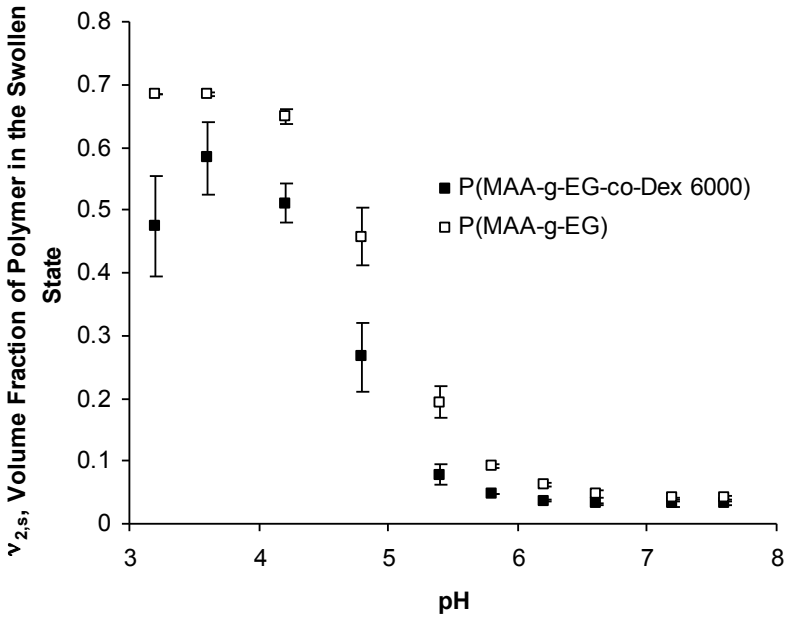

Figure 5.8 Volume fraction of P(MAA-dg-EG-co-Dex 6000) in the swollen state at equilibrium after incubation in DMGA buffers of varying pH.

Data reported are the mean ± standard deviation.

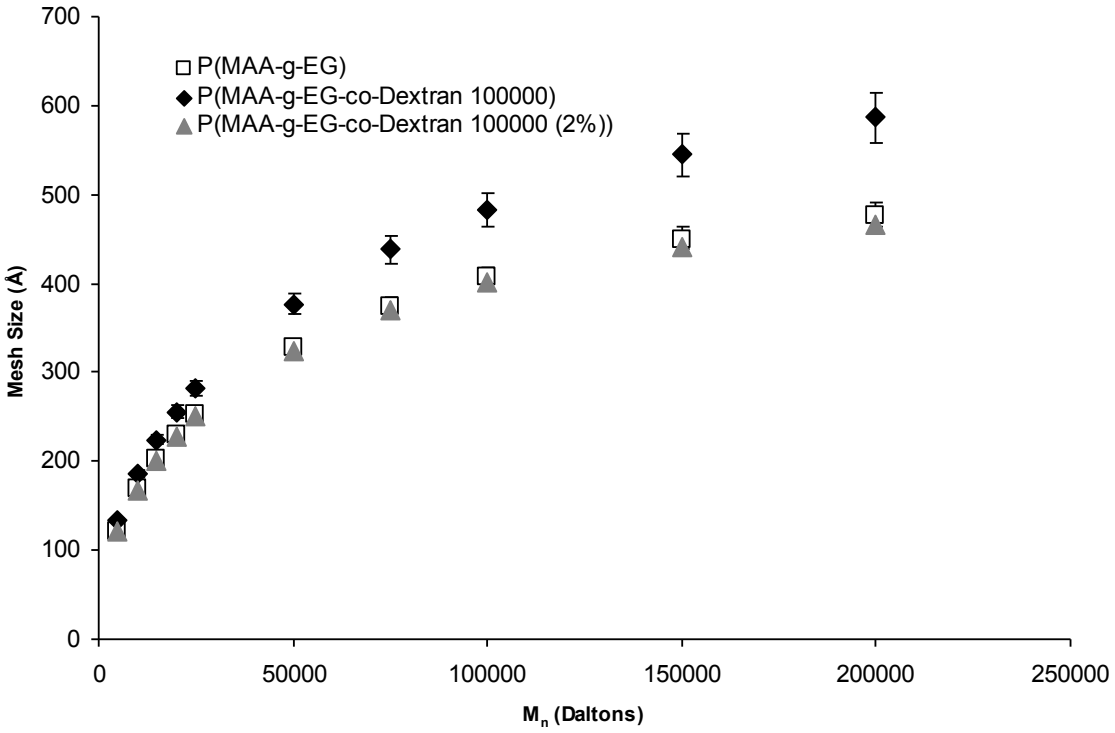

Figure 5.9 Estimated mesh size for P(MAA-dg-EG-co-Dex 100000) hydrogels in comparison to P(MAA-g-EG) at pH 7.6 for various polymer number average molecular weights.

Data reported are the mean ± standard deviation.

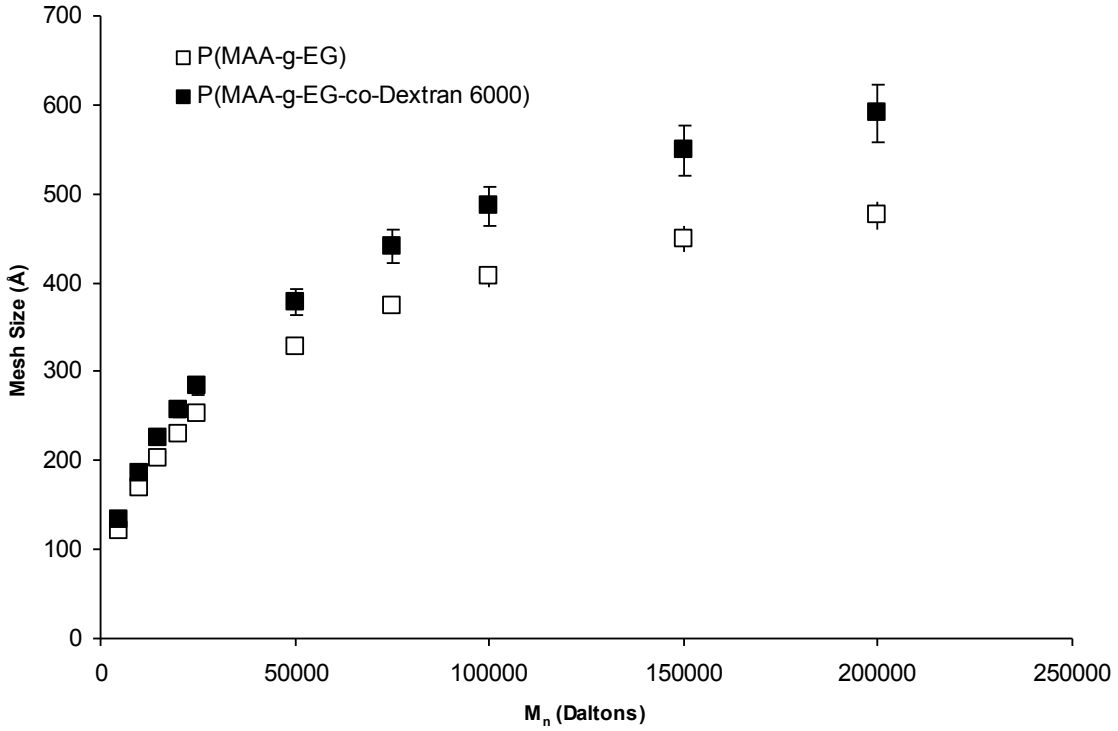

Figure 5.10 Estimated mesh size for P(MAA-dg-EG-co-Dex 6000) and P(MAA-g-EG) hydrogels at pH 7.6 for various polymer number average molecular weights.

Data reported are the mean ± standard deviation.

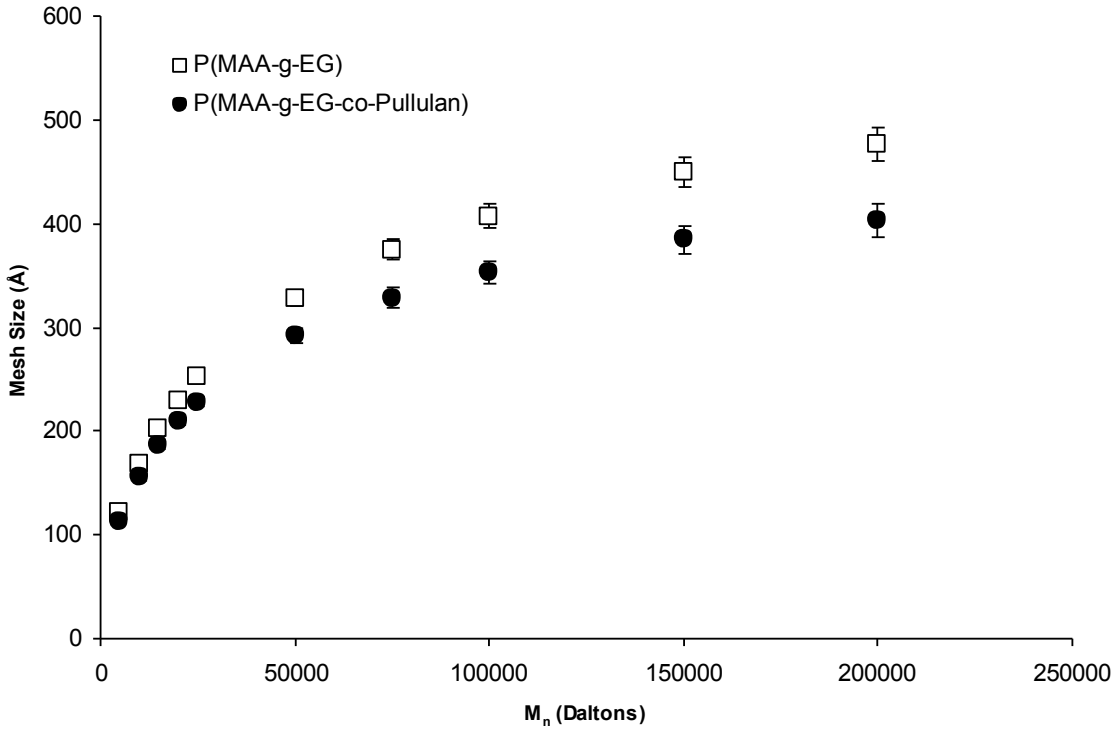

Figure 5.11 Estimated mesh size for P(MAA-dg-EG-co-Pullulan) and P(MAA-g-EG) hydrogels for various polymer number average molecular weights.

Hydrogels were swollen at pH 7.6, and the mesh size was calculated. Data reported are the mean ± standard deviation.

5.5 REFERENCES

1. amEnde, M. T., D. Hariharan and N. A. Peppas, Factors influencing the drug and protein transport and release from ionic hydrogels. React. Polym., 1995, 25, 127-137.

2. Carr, D. A., M. Gomez-Burgaz, M. C. Boudes and N. A. Peppas, Complexation Hydrogels for the Oral Delivery of Growth Hormone and Salmon Calcitonin. Ind. Eng. Chem. Res., 2010, 49, 11991-11995.

3. Tuesca, A., K. Nakamura, M. Morishita, J. Joseph, N. Peppas and A. Lowman, Complexation hydrogels for oral insulin delivery: Effects of polymer dosing on in vivo efficacy. J. Pharm. Sci., 2008, 97, 2607-2618.

4. Cakal, E. and S. Cavus, Novel Poly(N-vinylcaprolactam-co-2-(diethylamino)ethyl methacrylate) Gels: Characterization and Detailed Investigation on Their Stimuli-Sensitive Behaviors and Network Structure. Ind. Eng. Chem. Res., 2010, 49, 11741-11751.

5. Madsen, F. and N. A. Peppas, Complexation graft copolymer networks: swelling properties, calcium binding and proteolytic enzyme inhibition. Biomaterials, 1999, 20, 1701-1708.

6. Carr, D. A. and N. A. Peppas, Assessment of poly(methacrylic acid-co-N-vinyl pyrrolidone) as a carrier for the oral delivery of therapeutic proteins using Caco-2 and HT29-MTX cell lines. J. Biomed. Mater. Res. Part A, 2010, 92A, 504-512.

7. Van Dijk-Wolthuis, W. N. E., O. Franssen, H. Talsma, M. J. van Steenbergen, J. J. Kettenes-van den Bosch and W. E. Hennink, Synthesis, Characterization, and Polymerization of Glycidyl Methacrylate Derivitized Dextran. Macromolecules, 1995, 28, 6317-6322.

8. Wood, K. M., Molecular design of advanced oral protein delivery systems using complexation hydrogels. 2006, Ph.D., Thesis. Academic, DepartmentThe University of Texas at Austin.

9. Carr, D. A., Molecular Design of Biomaterial Systems for the Oral Delivery of Therapeutic Proteins. 2008, Ph.D., 225, Thesis. Academic, DepartmentThe University of Texas at Austin.

10. Peppas, N. A., K. M. Wood and J. O. Blanchette, Hydrogels for oral delivery of therapeutic proteins. Expert Opin. Biolog. Ther., 2004, 4, 881-887.

11. Eichenbaum, G. M., P. F. Kiser, A. V. Dobrynin, S. A. Simon and D. Needham, Investigation of the swelling response and loading of ionic microgels with drugs and proteins: The dependence on cross-link density. Macromolecules, 1999, 32, 4867-4878.

12. Hasa, J. and M. Ilavsky, Deformational, Swelling and Potentiometric Behavior of Ionized Poly(Methacrylic Acid) Gels. 2. Experimental Results. J. Polym. Sci., Part B: Polym. Phys., 1975, 13, 263-274.

13. Wood, K. M., G. M. Stone and N. A. Peppas, Wheat germ agglutinin functionalized complexation hydrogels for oral insulin delivery. Biomacromolecules, 2008, 9, 1293-1298.

14. Behravesh, E., V. I. Sikavitsas and A. G. Mikos, Quantification of ligand surface concentration of bulk-modified biomimetic hydrogels. Biomaterials, 2003, 24, 4365-4374.

15. Mann, B. K., R. H. Schmedlen and J. L. West, Tethered-TGF-beta increases extracellular matrix production of vascular smooth muscle cells. Biomaterials, 2001, 22, 439-444.

16. Leslie-Barbick, J. L., J. J. Moon and J. L. West, Covalently-immobilized vascular endothelial growth factor promotes endothelial cell tubulogenesis in poly(ethylene glycol) diacrylate hydrogels. J. Biomater. Sci., 2009, 20, 1763-1779.

17. Podual, K., F. J. Doyle and N. A. Peppas, Glucose-sensitivity of glucose oxidase-containing cationic copolymer hydrogels having poly(ethylene glycol) grafts. J. Control. Release, 2000, 67, 9-17.

18. Podual, K., F. J. Doyle and N. A. Peppas, Preparation and dynamic response of cationic copolymer hydrogels containing glucose oxidase. Polymer, 2000, 41, 3975-3983.

19. Kryscio, D. R. and N. A. Peppas, Mimicking Biological Delivery Through Feed back-Controlled Drug Release Systems Based on Molecular Imprinting. Aiche J., 2009, 55, 1311-1324.

20. Bergmann, N. M. and N. A. Peppas, Molecularly imprinted polymers with specific recognition for macromolecules and proteins. Prog. Polym. Sci., 2008, 33, 271-288.

21. Bergmann, N. M. and N. A. Peppas, Configurational Biomimetic Imprinting for Protein Recognition: Structural Characteristics of Recognitive Hydrogels. Ind. Eng. Chem. Res., 2008, 47, 9099-9107.

Chapter 6:

Loading and Release of Insulin from Polysaccharide-Modified Hydrogels

6.1 Introduction

Analysis of the loading and release of drugs from controlled release systems is essential in evaluating and optimizing their performance *in vitro*. In the case of oral protein drug delivery of therapeutics such as insulin, the bioactivity of the protein drug must be preserved in the GI tract and sufficient absorption of the drug into the bloodstream must take place.

The use of anionic complexation hydrogels of P(MAA-g-EG) to orally deliver insulin has been investigated by Peppas and co-workers [1-4]. One of the unique properties of P(MAA-g-EG) systems that lends itself to oral protein delivery applications is their complexation behavior. Hydrogen bonding between the PMAA backbone and PEG tethers in acidic conditions similar to the stomach allows limited diffusion into and out of the gel [5]. Release is caused by the dissociation of these hydrogen bonds and subsequent swelling at higher pH. *In vitro* loading studies have shown that insulin can be loaded into P(MAA-g-EG) hydrogels [6]. These studies have previously demonstrated pH-triggered release of insulin from P(MAA-g-EG) hydrogels [7]. In addition, P(MAA-g-EG) systems have been shown to maintain the bioactivity of protein drugs in physiological fluids present in the GI tract [8].

Modifications to P(MAA-g-EG) hydrogels have been previously investigated and were shown to influence the loading and release of protein drugs. For example, in the work of Shofner and Peppas [9], changing the length of the crosslinker in P(MAA-g-EG) gels allowed optimization of insulin-transferrin loading and release. Wood et al. [7] examined functionalization of P(MAA-g-EG) with wheat germ agglutinin (WGA) using

avidin-biotin binding. Lower loading efficiencies were observed for modified microparticles. It was hypothesized that the presence of the large avidin molecules in the hydrogels were interfering with release. It is also possible that large pendant groups changed the mesh size of the hydrogel network.

In this work, the influence of polysaccharide-modifications on loading and release of insulin from complexation hydrogels modified with large pendant polysaccharides was examined. One of the concerns addressed in this work is whether these large tethers limit drug diffusion out of the gel or interfere with hydrogen bonding in acidic conditions resulting in less protection of the protein drug. Specifically, polysaccharide-modified P(MAA-g-EG) complexation hydrogels were investigated to evaluate the effect of dextran and pullulan comonomers on the loading and release of insulin *in vitro*. The insulin loading was examined for several different polymer formulations including P(MAA-g-EG-co-Dextran 6000), P(MAA-g-EG-co-Dextran 100000), P(MAA-g-EG-co-Pullulan 75000), and P(MAA-g-EG) as a control. Furthermore, the insulin release profiles for several formulations are presented to evaluate the potential use of polysaccharide-modified P(MAA-g-EG) complexation hydrogels for the oral delivery of insulin.

6.2 Materials and Methods

6.2.1 Loading Studies

P(MAA-dg-EG-co-Dextran 6000), P(MAA-dg-EG-co-Dextran 100000), and P(MAA-dg-EG-co-Pullulan 75000) microparticles were prepared with size between 53 and 75 μm. Hydrogel films with corresponding compositions were dried overnight in air at room temperature and then placed in a vacuum oven maintained at 37 °C for further drying. Microparticles were crushed from these dry hydrogel films using a mortar and

pestle and then passed through a sieve to obtain the desired microparticle diameters. All formulations were synthesized with 0.75 mol% of PEGDMA (with an average molecular weight of 400 Da). Each polymer was synthesized with a polysaccharide feed ratio of 1 wt% unless indicated otherwise. Additional formulations of P(MAA-g-EG-co-Dextran 100000) were prepared with dextran feed ratios of 0.5 wt%, 1 wt%, and 2 wt % to examine the effect of polysaccharide feed.

Loading studies were carried out in silanized glassware prepared using Sigmacote (Sigma Aldrich) according to the manufacturers recommendations. First, a 0.5 mg/ml solution of bovine insulin (Sigma Aldrich, St. Louis, MO) in pH 7.4 phosphate buffered saline (PBS) was prepared by solubilizing bovine insulin in PBS with a pH of 5 and raising the pH with the addition of 0.1 N sodium hydroxide. A 200 µl sample of the insulin stock solution was taken and passed through a 0.22 µm PVDF syringe filter (Millipore). While stirring the insulin solution, dry microparticles were slowly added to obtain a final microparticle concentration of 2 mg/ml. The solutions were covered to prevent evaporation.

The particles were allowed to imbibe drug for 2 hours with continuous stirring. Then, a 200 µl sample of the loading solution was taken before collapsing the microparticles. The particles were collapsed by the addition of 1N HCl, and an additional 200 µl sample of the loading solution was collected. The collapsed particles were filtered with a 22 µm filter. The microparticles were washed with water (30% of the loading volume) to remove any insulin adsorbed to the surface of the particles. Particles were lyophilized and stored at -80 ºC until use.

During the loading process, the initial insulin and final insulin concentration were sampled and measured by aqueous high throughput liquid chromatography (HPLC).

6.2.2 Release of Insulin

Insulin release from polysaccharide-modified P(MAA-g-EG) hydrogels was evaluated during *in vitro* release studies. Release studies were carried out using a USP 2 dissolution apparatus.

All glassware including the release vessels were coated with Sigmacote to prevent protein adsorption to the glassware. Prior to the release study, the water bath of the dissolution apparatus was pre-heated to 37 °C. In these studies, a 1 mg/ml solution of loaded microparticles was prepared. For example, 30 mg of insulin-loaded particles were added to 30 ml of 1X PBS at 37 °C and were stirred with impellers rotating at 100 rpm. The release solutions were sampled at 0, 5, 10, 15, 30, 60, and 120 minutes after the addition of the microparticles. As the 200 μl samples were removed, the sample volume was replaced with pre-warmed PBS. The concentration of insulin in each sample was determined by HPLC.

6.2.2 Dynamic Insulin Release

The pH-responsive release of insulin from P(MAA-g-EG-Dextran 100000) hydrogels was evaluated. This release study followed the preceding procedure using an initial solvent of 30 ml of 0.01 M DMGA with a pH of 3.2. After addition of the microparticles, the release solution was sampled at 5, 10, 15, 30, and 60 min. At 60 min, 100 μl of 3 N sodium hydroxide was added to bring the pH of the release solution up to 7.2. The release solution was sampled using a 1 ml syringe and needle at 0, 5, 10, 15, 30, 60, 120 min following the addition of the base. Each sample was then passed through a 0.2 μm PVDF syringe filter. The concentration of each sample was determined by HPLC.

6.2.4 High Throughput Liquid Chromatography

HPLC was used to determine the concentration of insulin in loading and release studies. A Waters Alliance HPLC unit equipped with a Symmetry C4 5 µm column was used to run gradient elution in the reverse direction. The mobile phase consisted of 70% water with 0.1% trifluoroacetic acid (TFA) and 30% acetonitrile with 0.08% TFA. The column temperature was 40 ºC. A gradient was run in the reverse direction from 30% to 60% acetonitrile over a 6 minute time period. The sample run time was 10 minutes, and the sample injection volume was 20 µl. The protein concentration was measured by UV absorbance at 220 nm.

6.3 Results and Discussion

The loading and release of insulin from polysaccharide-modified P(MAA-g-EG) hydrogels were investigated *in vitro* to evaluate the use of these hydrogels as oral protein drug delivery systems. Complexation hydrogel microparticles have been shown to successfully entrap and release insulin, human growth hormone, salmon calcitonin, interferon-β, PEG-insulin, and insulin-transferrin conjugates.

The loading of P(MAA-g-EG) complexation hydrogels with protein drugs wasaccomplished by allowing swelling of the hydrogel microparticles in a solution of the protein drug at neutral pH. The loading of protein drugs in anionic complexation hydrogels was attributed to equilibrium partitioning as well as favorable interactions between the protein drug and the hydrogel. After several hours of incubation in the protein drug, collapsing the hydrogel by addition of an acid entrapped the drug in the hydrogel network. The addition of an acid caused protonation of PMAA and allowed the formation of hydrogen bonding with PEG. These hydrogen bonds form physical crosslinks around the entrapped protein drug.

The addition of large molecular tethers of polysaccharides could potentially interfere with loading by limiting diffusion of drug into the hydrogel network and reduce the overall efficiency of loading.

The efficiency of loading can by calculated based on the mass of the drug loaded as a fraction of the initial mass of the protein drug using Equation 6.1.

$$Loading \quad Efficiency(\%) = \frac{C_{initial} \cdot V_{initial} - C_{final} \cdot V_{final}}{C_{initial} \cdot V_{final}} \cdot 100 \tag{6.1}$$

In this case, the concentration of each sample and the volume were used to determine the loading efficiency. Other protein loading studies [7, 10] of complexation hydrogels have done the loading efficiency calculation with a small difference. These studies report the loading efficiency as shown in Equation 6.2.

$$Loading \quad Efficiency(\%) = \frac{C_{initial} \cdot -C_{final}}{C_{initial}} \cdot 100 \tag{6.2}$$

The caveat between the two calculations is due to a difference in the experimental methods. In other studies, samples of the loading solution were taken and the volume replaced with buffer so that concentration alone could be used to calculate the loading efficiency because the volume was kept constant [7, 10]. However, the final concentrations were typically adjusted to account for the mass of protein drug removed in prior samples that could not be replaced through the addition of buffer. Experimental and measurement errors can propagate and influence the overall loading efficiency. For example, an inaccurate measurement of the protein drug concentration prior to collapse of the microparticles will result in an inaccurate mass to be accounted for in subsequent calculations and will change the calculated loading efficiency. Whereas, in the study and calculations presented in this work, the protein drug concentration prior to collapse and the final protein drug concentration are calculated independently of each other.

Insulin loading of polysaccharide-modified hydrogels was examined to understand the influence of polysaccharide tethers on the efficiency of loading of bovine insulin. Loading studies showed that the polysaccharide modifications to P(MAA-g-EG) hydrogels affected loading and that this was dependent on the type of polysaccharide, either Dextran 6000, Dextran 100000, or Pullulan 75000 as shown in Figure 6.1.

In these studies, bovine insulin was imbibed at neutral pH, and the microgels were collapsed by addition of HCl. Prior to collapse of the microparticles, the amount of insulin loaded into the gels was similar and greater than 80%. However, when the gels were collapsed, the P(MAA-g-co-EG-Dextran 100000) and P(MAA-g-co-EG-Pullulan 75000) loading efficiencies dropped (Figure 6.1). The smaller molecular weight dextran copolymers, P(MAA-g-EG-co-Dextran 6000), had better loading efficiencies following collapse of the microgels.

The values of the P(MAA-g-EG-co-Dextran 6000) loading efficiency were not statistically different than P(MAA-g-EG) loading efficiencies after addition of HCl (using a student t-test with $p>0.05$). The hydrogel formulations containing the higher molecular weight polysaccharides of Dextran 100000 and Pullulan 75000 appeared to squeeze most of the drug out of the polymer network. Collapse of the microparticles by formation of hydrogen bonds within the polymer network may have caused large polysaccharides to reorient towards the core of the microparticles, thereby displacing some of the loaded insulin.

It is also possible that during loading a large percentage of the loaded insulin may have been associated with the surface of the microparticles and then dissociated or desorbed from the microparticles once the microparticles collapsed.

To better understand the influence of large polysaccharide tethers on the loading efficiency of insulin three formulations of P(MAA-g-EG-co-Dextran 100000) were compared. The three formulations consisted of three different feed ratios of Dextran 100000 in the polymerization feed which were 0.5 wt%, 1 wt%, and 2 wt%. The loading efficiencies of the different P(MAA-g-EG-co-Dextran 100000) are compared in Figure 6.2. The formulations are denoted by the polysaccharide and content such as 0.5% Dextran 100000.

A comparison of insulin loading in polysaccharide-modified hydrogels with different Dextran 100000 contents shows that insulin is loaded prior to collapse of the microparticles but that the final loading efficiency is much lower (Figure 6.2). The final loading efficiencies of Dextran 100000-modified hydrogels were similar with the 18.4%, 22.3%, or 22.7% corresponding to the 0.5 wt%, the 1 wt%, and 2 wt% formulations, respectively. Only the 0.5 wt% Dextran 100000 formulation was statistically different (ANOVA, $p < 0.05$) from the others.

To examine the affect of the polysaccharide tethers on the release of insulin, the release profiles for each hydrogel formulation was compared against P(MAA-g-EG) hydrogel controls. In these studies, microparticles were slowly added to PBS buffer with a pH of 7.4. At this pH, these hydrogels readily swell (Chapter 5). It was expected that loaded insulin should readily release from the polysaccharide-modified hydrogels. Release data shown in Figure 6.3 confirms this hypothesis.

All of the polysaccharide-modified hydrogels release insulin faster than P(MAA-g-EG) (Figure 6.3). Of the formulations tested, the P(MAA-g-EG-co-Dextran 100000) released insulin the fastest with the majority of release occurring in the first 5 minutes. The percentage of insulin released from P(MAA-g-EG-co-Dextran 6000) released insulin faster than P(MAA-g-EG) but was the slowest of all polysaccharide-modified

formulations as shown in Figure 6.3. Similarly, P(MAA-g-EG-co-Pullulan 75000) gels released insulin faster than the P(MAA-g-EG) control.

The release profiles of insulin from polysaccharide-modified hydrogels are steeper with increasing molecular weight of the hydrogel (Figure 6.2). A faster drug release would be expected for hydrogels containing large, hydrophilic molecular weight tethers. Swelling data presented in Chapter 5 which showed increased swelling ratios of polysaccharide-modified hydrogels over P(MAA-g-EG) at neutral pH supports this hypothesis. As the microgels hydrate, the network expands due to the influx of water. Greater swelling is associated with increased diffusion. Swelling of these hydrogels is estimated to occur rapidly, on the order of minutes, which may explain the rather fast release of insulin from these gels.

The much faster release of insulin from P(MAA-g-EG-co-Dextran 100000) gels may also be explained by dissolution of insulin that was loaded on the surface of the hydrogel. . These gels were generously washed following collapse of the microgels and filtered to remove any adsorbed protein. This technique of washing the microparticles after loading has been used during loading of proteins in hydrogels especially by the Peppas lab [10]. However, strong interactions between the protein and the surface of the gels may explain both the quick release of insulin and the decreased loading efficiencies obtained after collapse of the microparticles.

A dynamic release study was performed to analyze insulin release from P(MAA-g-EG-co-Dextran 100000) gels in response to pH. There was concern that the presence of the large polysaccharide tethers may disrupt hydrogen bonding during complexation and may hence leave the entrapped protein drug less protected from GI tract fluids. In addition, the ability of the polysaccharide-modified hydrogels to release insulin in response to increased pH was unknown.

In this study, P(MAA-g-EG-co-Dextran 100000) microparticles were placed in a release medium of DMGA buffer with a pH of 3.2. At this pH, these hydrogels are in a collapsed state (Chapter 5), and insulin release from these microparticles would not be desirable for oral protein delivery. After 1 hour, the pH was neutralized to 7.4 using sodium hydroxide to simulate the pH increase between the stomach and the small intestine. At this pH, the P(MAA-g-EG-co-Dextran 100000) hydrogels swell and were hypothesized to release insulin.

The results from this study presented in Figure 6.4 show that virtually no insulin is released at acidic conditions. Based on the HPLC spectra, only 1 sample showed any insulin was released in the 1 hour acid incubation period which was less than 3 %. The shift in pH to more neutral conditions results in insulin release shown in Figure 6.4. The pH increase is marked by the position of the y-axis in Figure 6.4. This data shows that within the first 30 minutes following the increase in pH, most of the insulin is released. This release time period is highly desirable for oral protein delivery in the upper small intestine based on GI transit times. In addition, HPLC spectra of the release showed that the elution time of insulin was nearly constant (4.59 min ± 0.01 min) indicating that insulin denaturation was not an issue.

6.4 CONCLUSIONS

The data presented in this work show that polysaccharide-modified hydrogels are promising materials for oral insulin delivery systems. These systems can be used to entrap insulin, protect insulin in acidic conditions, release insulin in response to changes in pH, and the release profile can be controlled by the amount and type of polysaccharide tether.

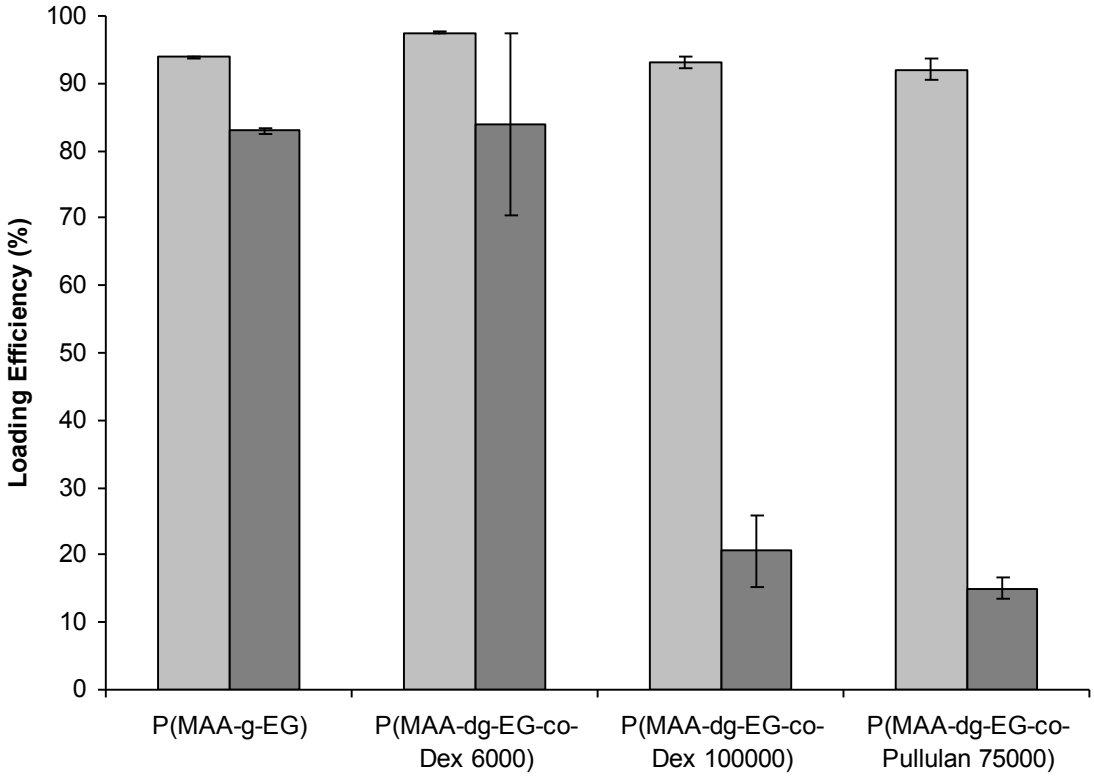

Figure 6.1. Loading efficiency of insulin in unmodified P(MAA-*g*-EG) hydrogels and modified hydrogels of P(MAA-g-EG-co-Dextran 6000), P(MAA-g-EG-co-Dextran 100000), and P(MAA-g-EG-co-Pullulan 75000) during the loading process and after the addition of acid to collapse the microparticles.

Data are presented as mean ± standard deviation.

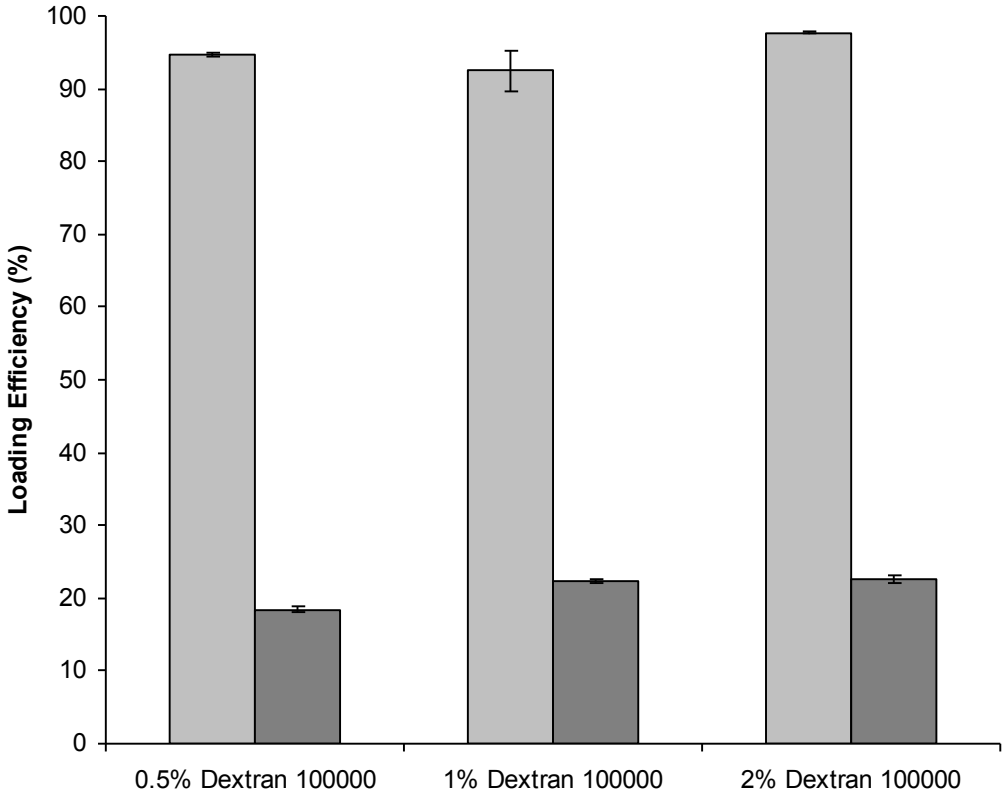

Figure 6.2. Insulin loading efficiencies for P(MAA-g-EG-co-Dextran) hydrogel microparticles with Dextran 100000 feed ratios of 0.5%, 1%, and 2% during loading and following addition of acid to collapse the hydrogels. The microparticles had diameters between 90 and 120 µm.

Data are presented as mean ± standard deviation.

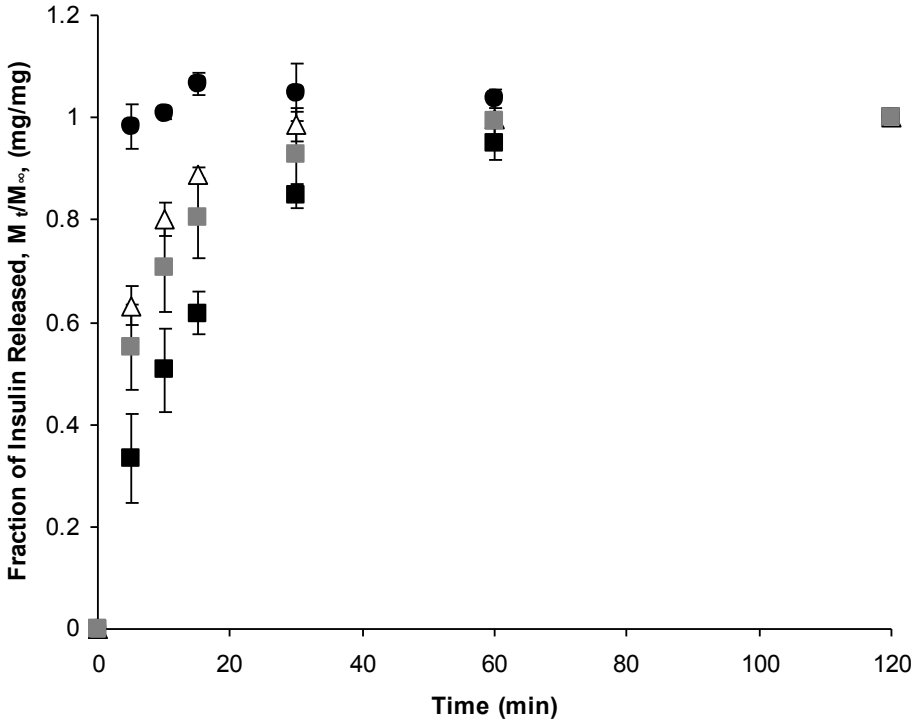

Figure 6.3. Cumulative release of insulin in pH 7.4 PBS buffer from microparticles of P(MAA-g-EG), P(MAA-g-EG-co-Dextran 6000), P(MAA-g-EG-co-Dextran 100000), and P(MAA-g-EG-co-Pullulan 75000) with diameters between 53 and 75 µm.

Data are presented as mean ± standard deviation.

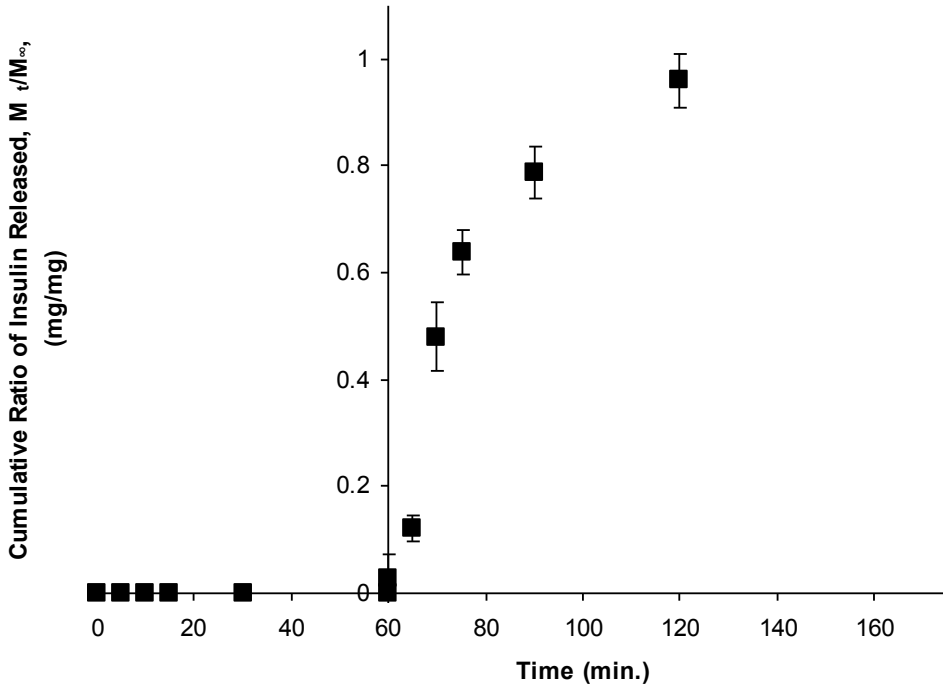

Figure 6.4. Cumulative release of insulin in pH 7.4 PBS buffer from microparticles of P(MAA-*g*-EG-co-Dextran 100000) with diameters between 90 and 120 µm.

Data are presented as mean ± standard deviation.

6.5 REFERENCES

1. Kavimandan, N. J., E. Losi and N. A. Peppas, Novel delivery system based on complexation hydrogels as delivery vehicles for insulin-transferrin conjugates. Biomaterials, 2006, 27, 3846-3854.

2. Lowman, A. M., M. Morishita, M. Kajita, T. Nagai and N. A. Peppas, Oral delivery of insulin using pH-responsive complexation gels. J. Pharm. Sci., 1999, 88, 933-937.

3. Morishita, M., T. Goto, K. Nakamura, A. M. Lowman, K. Takayama and N. A. Peppas, Novel oral insulin delivery systems based on complexation polymer hydrogels: Single and multiple administration studies in type 1 and 2 diabetic rats. J. Control. Release, 2006, 110, 587-594.

4. Wood, K. M., G. M. Stone and N. A. Peppas, The effect of complexation hydrogels on insulin transport in intestinal epithelial cell models. Acta Biomater., 2010, 6, 48-56.

5. Lowman, A. M. and N. A. Peppas, Molecular analysis of interpolymer complexation in graft copolymer networks. Polymer, 2000, 41, 73-80.

6. Besheer, A., K. M. Wood, N. A. Peppas and K. Mader, Loading and mobility of spin-labeled insulin in physiologically responsive complexation hydrogels intended for oral administration. J. Control. Release, 2006, 111, 73-80.

7. Wood, K. M., G. M. Stone and N. A. Peppas, Wheat germ agglutinin functionalized complexation hydrogels for oral insulin delivery. Biomacromolecules, 2008, 9, 1293-1298.

8. Yamagata, T., M. Morishita, N. J. Kavimandan, K. Nakamura, Y. Fukuoka, K. Takayama and N. A. Peppas, Characterization of insulin protection properties of complexation hydrogels in gastric and intestinal enzyme fluids. J. Control. Release, 2006, 112, 343-349.

9. Shofner, J. P., Oral Delivery of Protein-Transporter Bioconjugates Using Intelligent Complexation Hydrogels. 2008, Ph.D., 325, Thesis, Department of Chemical Engineering, The University of Texas at Austin.

10. Carr, D. A., M. Gomez-Burgaz, M. C. Boudes and N. A. Peppas, Complexation Hydrogels for the Oral Delivery of Growth Hormone and Salmon Calcitonin. Ind. Eng. Chem. Res., 2010, 49, 11991-11995.

Chapter 7:

Investigation of Mucoadhesion and Cytotoxicity of Polysaccharide-Modified Complexation Hydrogels

7.1 Introduction

In the design of oral protein drug delivery systems, it is very important to evaluate how these materials may interact with tissues of the GI tract. For example, materials that are cytotoxic are not desirable for a safe and effective therapeutic delivery system. How the drug delivery system interacts with the intestinal mucosa can not only affect safety but it can also influence drug absorption. Drug delivery systems that interact favorably with the intestinal mucosa through mucoadhesion are highly desirable as mucoadhesive drug delivery systems are associated with prolonged carrier residence times in the upper small intestine and improved bioavailabilities.

In order to evaluate how oral drug delivery systems will interact with biological tissues, a variety of tests to measure cytoxicity and mucoadhesion can be done *in vitro.* For evaluation of the cytotoxicity of microparticle and nanoparticle drug delivery systems, cell proliferation assays are commonly used such as 3-(4,5-dimethylthiazol-2-yl)-5-(3-carboxymethoxyphenyl)-2-(4-sulfophenyl)-2H-tetrazolium (MTS) [1-3]. Likewise, the mucoadhesion of drug delivery systems can be evaluated using a wide variety of experimental techniques *in vitro* [4-8].

Complexation hydrogels of P(MAA-g-EG) have been extensively studied for oral drug delivery systems by Peppas and coworkers. For these systems, there is strong experimental evidence of the correlation between the mucoadhesive measurements *in vitro* [9] and confirmed mucoadhesive behavior in the small intestine [10]. Cellular

cytotoxicity studies have indicated that these systems do not significantly affect cell viability. To date, issues with cytotoxicity have not been observed *in vivo*.

Therefore, *in vitro* evaluations of polysaccharide-modified P(MAA-g-EG) hydrogels are essential for developing an understanding of how these materials may interact with the upper small intestine. In this work, the cellular compatibility and mucoadhesion of polysaccharide-decorated complexation hydrogels are evaluated *in vitro* to asses how these materials may interact with biological tissue in the upper small intestine.

7.2 Materials and Methods

7.2.1 General Cell Culture

Caco-2 cells (ATCC, Rockwell, MD) were grown in Dulbecco's modified Eagle medium (DMEM, Mediatech, Herndon, VA) with high glucose and sodium pyruvate. The DMEM media was supplemented with 10 % heat inactivated fetal bovine serum (FBS, Cambrex, East Rutherford, NJ), 1 % non-essential amino acids (Mediatech), penicillin, streptomycin, and amphotericin B. Freshly thawed cells were grown in DMEM media with 20% FBS until the first passage.

Caco-2 cells were allowed to grow in a humidified incubator maintained at 37 ^{o}C and 5% CO_2. The cell media was refreshed every other day. Cells were passaged prior to 90% confluency. To passage cells, the media was removed and the cells were washed with pre-warmed Dulbecco's phosphate buffered saline without Ca^{2+} and without Mg^{2+}. Trypsin was placed on the cells and allowed to incubate for 10 minutes. Then, fresh, pre-warmed media was added to inhibit trypsin activity. A small volume of cells was removed and counted. Cells were resuspended then seeded at a density of 3.0 x 10^3 cells/cm^2.

7.2.2 Preparation of Materials

In this study, P(MAA-g-EG), P(MAA-g-EG-co-Dextran 6000), P(MAA-g-EG-co-Dextran 100000), and P(MAA-g-EG-co-Pullulan 75000) were synthesized using the procedure described in Chapter 4. Several different P(MAA-g-EG-co-Dextran 100000) hydrogels were prepared with different feed ratios of Dextran. For the cytotoxicity study, unmodified and polysaccharide-modified microparticles were obtained by crushing and sieving dry hydrogel films of the same composition.

7.2.3 Cell Viability Assay

Caco-2 cells with 20 to 35 passages were seeded on 96-well plates at a seeding density of 1.4×10^4 cells/cm^2. The cells were allowed to grow for at least 48 hours. Once cells reached approximately 90% confluency, the assay was started.

One hour before the experiment, the media from the cells was removed and replaced with only 150 µl. Microparticle samples were prepared first by exposing the gels to UV light to ensure sterility. Then, microparticle suspensions four times the desired concentration were prepared. For example, 4 mg/ml, 2 mg/ml, 1 mg/ml, and 0.5 mg/ml solutions were prepared by serial dilution in Hank's Balanced Salt Solution (HBSS). Then, 50 µl of the microparticle suspensions was added to each well to bring the final volume to 200 µl and the final microparticle concentrations to 1 mg/ml, 0.5 mg/ml, 0.25 mg/ml, and 0.125 mg/ml. In this study, 50 µl of HBSS was added to the wells instead of 50 µl of a microparticle suspension.

The cells were incubated for 2 hours. The microparticle solutions were removed from each well followed by 3 washes with HBSS. A CellTiter 96® Aqueous MTS assay was then performed according to the manufacturer's directions (Promega, Madison, WI). The MTS solution was incubated with the cells for 90 minutes before the optical

absorbance at 490 nm of the samples was recorded using a UV-Vis plate reader. The ratio of viable cells relative to control wells was calculated.

7.2.4 Preparation of Fluorescently Labeled Microparticles

The fluorescently labeled microparticle formulations of P(MAA-g-EG), P(MAA-g-EG-co-Dextran 6000), P(MAA-g-EG-co-Dextran 100000), and P(MAA-g-EG-co-Pullulan 75000) were synthesized from fluorescently labeled hydrogel films. Briefly, the fluorescent hydrogels were prepared using the same polymerization conditions outlined in Chapter 4 with the addition of fluorecein-o-methacrylate (Sigma Aldrich) at a molar feed ratio of 0.1 mol%. The fluorescently labeled hydrogels were protected from light and washed for 5-7 days with the water being refreshed twice a day. The fluorescently labeled hydrogels were then dried. Microparticles were obtained by crushing and sieving the dry fluorescent hydrogel films.

7.2.5 Mucoadhesion Experiments

For mucoadhesion experiments, mucin gels were prepared from reconstituted porcine mucin (2 wt%) (Sigma Aldrich) and (3 wt %) hydroxyl ethyl cellulose (Sigma Aldrich) in PBS in tissue culture plates. In the work presented here, 48-well plates (Corning) were used and the initial volume of the mucin solution added to each well was 100 µl/well. Suspensions of fluorescently labeled complexation hydrogels were prepared in PBS (pH 7.4) at a concentration of 0.25 mg/ml. The reconstituted mucin gels were prepared immediately before use and allowed to sit for 15 minutes prior to the experiment. Next, a 300 µl sample of the fluorescently labeled microparticles was added to each reconstituted mucin gel. The samples were allowed to incubate for 30 minutes before removing the samples from each well. Each well was then washed 3

times with a 300 µl volume of PBS. As a control, each hydrogel formulation was placed in a well without a reconstituted mucin gel.

To quantify the adherence of the microparticles to the reconstituted mucin gels, the samples were imaged using fluorescence microscopy. At least 3 images were obtained from randomly selected positions in the well. The number of fluorescent microparticles per image was quantified and the average number of particles per image was obtained. For these studies, all sample sizes were greater than 10.

7.3 Results and Discussion

The use of polysaccharide-decorated P(MAA-g-EG) hydrogels microparticles for oral protein drug delivery systems applications was investigated *in vitro* by measuring cell viability after exposure to these materials as well as the materials' mucoadhesion. *In vitro* measurements allow a variety of materials to be tested and the design optimized prior to *in vivo* studies.

In this work, an MTS cell viability assay was used to compare the fraction of viable Caco-2 cells relative to controls. Caco-2 cells were chosen as an enterocyte model because enterocytes compose almost 90% of the cells comprising the intestinal epithelium. For these studies, MTS cell viability assays were used to quantify cell viability based on dehydrogenase activity of living cells. Dehydrogenase activity was detected based on production of formazan reduced from 3-(4,5-dimethylthiazol-2-yl)-5-(3-carboxymethoxyphenyl)-2-(4-sulfophenyl)-2H-tetrazolium (MTS) in the presence of phenazine methosulfate.

Based on cell viability measurements obtained, polysaccharide-decorated P(MAA-g-EG) microparticles do not significantly affect cell viability. Figure 7.1 shows the fraction of viable cells relative to controls for P(MAA-g-EG-Dextran 6000), P(MAA-g-EG-

Dextran 100000), P(MAA-g-EG-Pullulan 75000), and P(MAA-g-EG). For all formulations investigated, the cell viability was greater than 1 indicating that the ratio of formazan production from samples was greater than control wells. These values indicate that the control wells had fewer viable cells than the wells exposed to microparticles. It is possible that the addition of the pH-responsive microparticles changed the pH of the cell media and affected enzyme activity. In other MTS assays on P(MAA-g-EG), this was not observed, but in the study by Wood et al. [4], the pH of the P(MAA-g-EG) microparticle suspensions was adjusted to a pH value of 7.4 prior to incubation with cells.

In order to better understand the influence of the polysaccharide content on cell viability, microparticles with different amounts of Dextran 100000 tethers were also tested. Figure 7.2 shows that the relative cell viability for Dextran 100000 materials had similar cellular viabilities to P(MAA-g-EG) materials. All concentrations of 0.5%, 1%, and 2% Dextran 100000 were not significantly lower than control wells. However, the 2% Dextran 100000 0.125 mg/ml suspensions had a significantly higher fraction of viable cells than controls. In analyzing the data from these samples, the ratio of viable cells relative to the controls is a bimodal distribution, which explains the large error bar associated with this sample.

The mucoadhesion of polysaccharide-modified P(MAA-g-EG) to reconstituted mucin gels was determined in vitro. There are a variety of assays that have been developed for measuring adhesion to intestinal mucus. The method presented in this work was developed because we wanted to quantify the mucoadhesion of swollen hydrogels to mucus, and we wanted to avoid unnecessary use of animal resources. For example, the use of harvested intestinal mucosa for more traditional mucoadhesion studies such as the falling liquid film method would require a significant amount of

tissue. Based on the amount of tissue that would need to be harvested, we chose to use reconstituted mucin as an alternative to harvested tissue and recommend a mucoadhesive study in situ in conjunction with in vivo bioavailability studies.

Several other alternative methods have been developed for the in vitro evaluation of mucoadhesion including a tensile test [6] to measure the work of adhesion as well as a flow test. The tensile test allows the measurement of the work of adhesion based on the force required to separate two plates, one of which is coated with mucin or excised tissue and the other with the material of interest. Thomas et al. used this method to quantify the mucoadhesion of nanogels composed of complexation hydrogels. One of the disadvantages of this method is that the nanogels are not in the hydrated state. Because hydration of the polysaccharide tethers may influence their ability to diffuse into the mucosa, this method was not used.

Other studies by Mikos and Peppas [7] examined the adhesion of hydrogel microgels using a flow chamber. In this set-up, the microparticle was placed on a mucus substrate and maintained at a constant temperature. Then, nitrogen air was flowed across the surface of the mucus. Both the time and flow rate required to dislodge the particle were measured. One of the disadvantages of this method is that analysis of the forces exerted on the microparticles was based on smooth, spherical particles. In the case of the materials developed in this thesis, the microparticles are irregular in shape.

Wood et al. [4] used an in vitro method to quantify mucoadhesion using fluorescently-labeled complexation hydrogels. Mucin was adsorbed on 96-well plates, and microparticles were incubated on these plates. After incubation, non-adhered microparticles were removed, and the fluorescence intensity of each well was used to determine the percentage of adhered particles relative to the initial concentration of microparticles. This study was used primarily to study the effects of wheat germ

agglutinin on the adhesion of complexation hydrogels. The alternative method was chosen based on the difficulty in obtaining fluorescence measurements without the impact of light scattering by microparticles. In addition, the mechanism of adhesion of polysaccharide-modified hydrogels was hypothesized to be caused by the diffusion of polysaccharides into the mucus gel. Measurement of adsorbed microparticles would not account for this mechanism of adhesion.

In the results obtained from these experiments, shown in Figure 7.3, the mucoadhesion measurements of polysaccharide-modified hydrogels is compared to unmodified P(MAA-g-EG) microparticles. Of the material formulations tested, the P(MAA-g-EG-co-Dextran 6000) formulation had the highest number of adhered microparticles per area. Although this was not statistically different than P(MAA-g-EG) controls, the results are promising. P(MAA-g-EG-co-Pullulan 75000) microparticles were the least adherent of the formulations tested (Figure 7.3). Likewise, there were fewer adherent P(MAA-g-EG-co-Dextran 100000) microparticles than P(MAA-g-EG) microparticles. The decrease in adhesion may be a result of the large tethers, which may require a longer time-scale for diffusion into the mucus gel to occur. To the best of our knowledge, the diffusion coefficients of dextran and pullulan in mucin solutions are unknown. However, the diffusion coefficient of FITC-Dextran with a molecular weight of 40 kDa is 1.87 x 10-7 μm2/s [11] while a 150 kDa FITC-Dextran has a diffusion coefficient of 2.06 x 10-11 μm2/s in water. Longer time scales for tether penetration in mucus may not be desirable for oral protein drug delivery as microparticles may contact the GI tract for only a brief time period in which the particles either adhere or desorb. Overall, results from this study show that all formulations adhere to reconstituted mucin gels preferentially over tissue culture plates in which less than 1 adhered microparticle per area was observed for any given formulation.

7. 4 CONCLUSIONS

Based on the in vitro assessments of polysaccharide-modified hydrogels, these materials appear to be promising for the oral delivery of protein drugs. These materials do not cause a significant increase in cell death as measured by an MTS assay and a Caco-2 enterocyte model. In addition, these materials were shown to adhere to reconstituted mucin gels. The ability to adhere to mucus membranes and cause limited cell death is highly desirable for oral protein drug delivery systems.

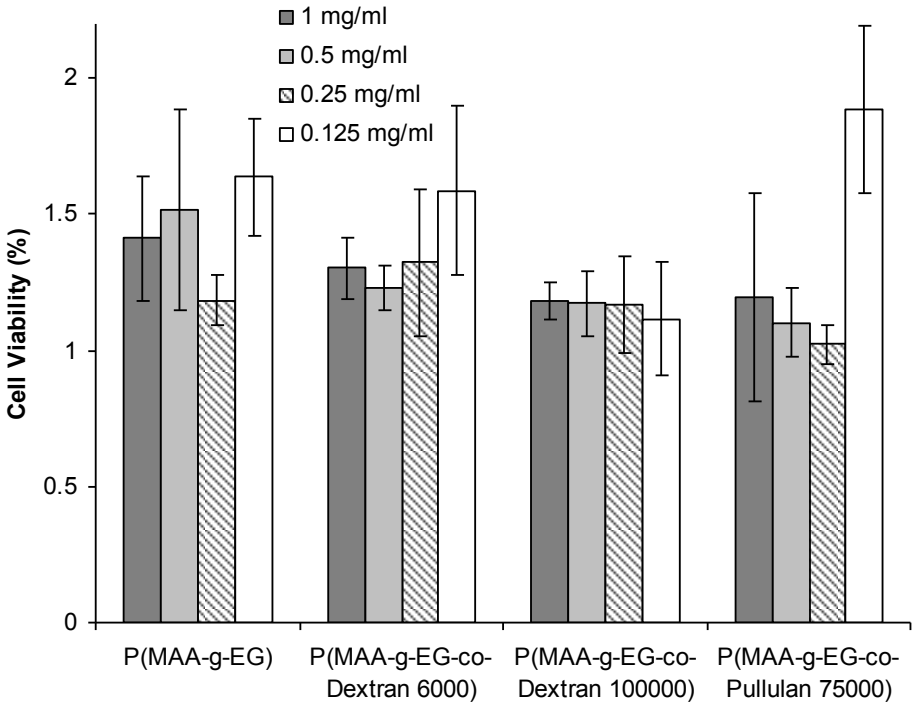

Figure 7.1 Fraction of viable cells relative to control wells for various microparticle formulations including P(MAA-g-EG), P(MAA-g-EG-co-Dextran 6000), P(MAA-g-EG-co-Dextran 100000), and P(PMAA-g-EG-co-Pullulan 75000) over a range of concentrations (1 mg/ml, 0.5 mg/ml, 0.25 mg/ml, and 0.125 mg/ml).

Data are represented by mean ± standard deviation.

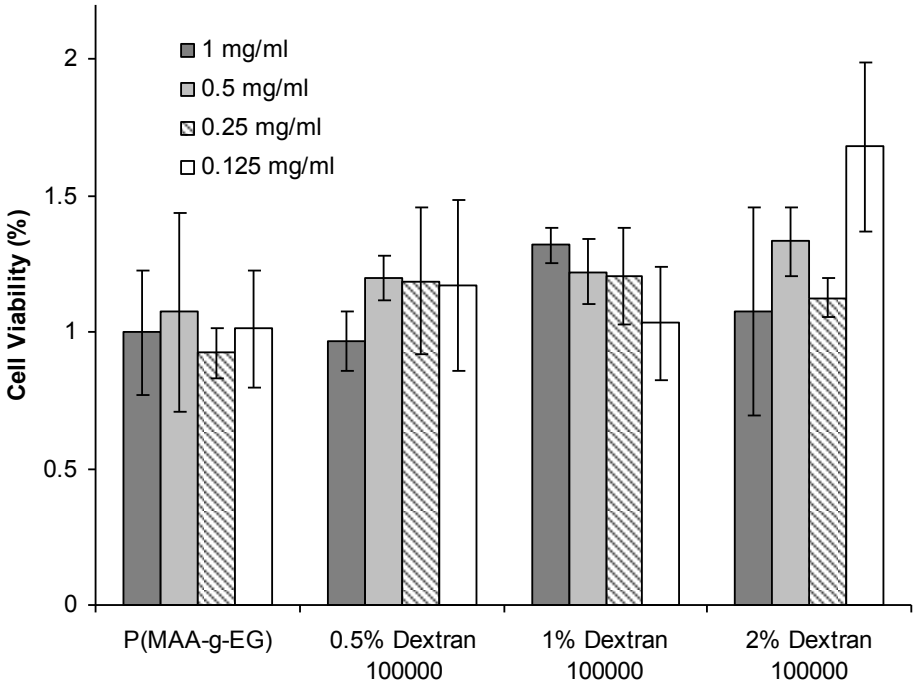

Figure 7.2 Fraction of viable cells relative to control wells for various P(MAA-g-EG-co-Dextran 100000) microparticle formulations with Dextran 100000 feed ratios of 0.5 %, 1%, and 2% in comparison to P(MAA-g-EG) microparticles. A range of concentrations was investigated including 1 mg/ml, 0.5 mg/ml, 0.25 mg/ml, and 0.125 mg/ml.

Data are represented by mean ± standard deviation.

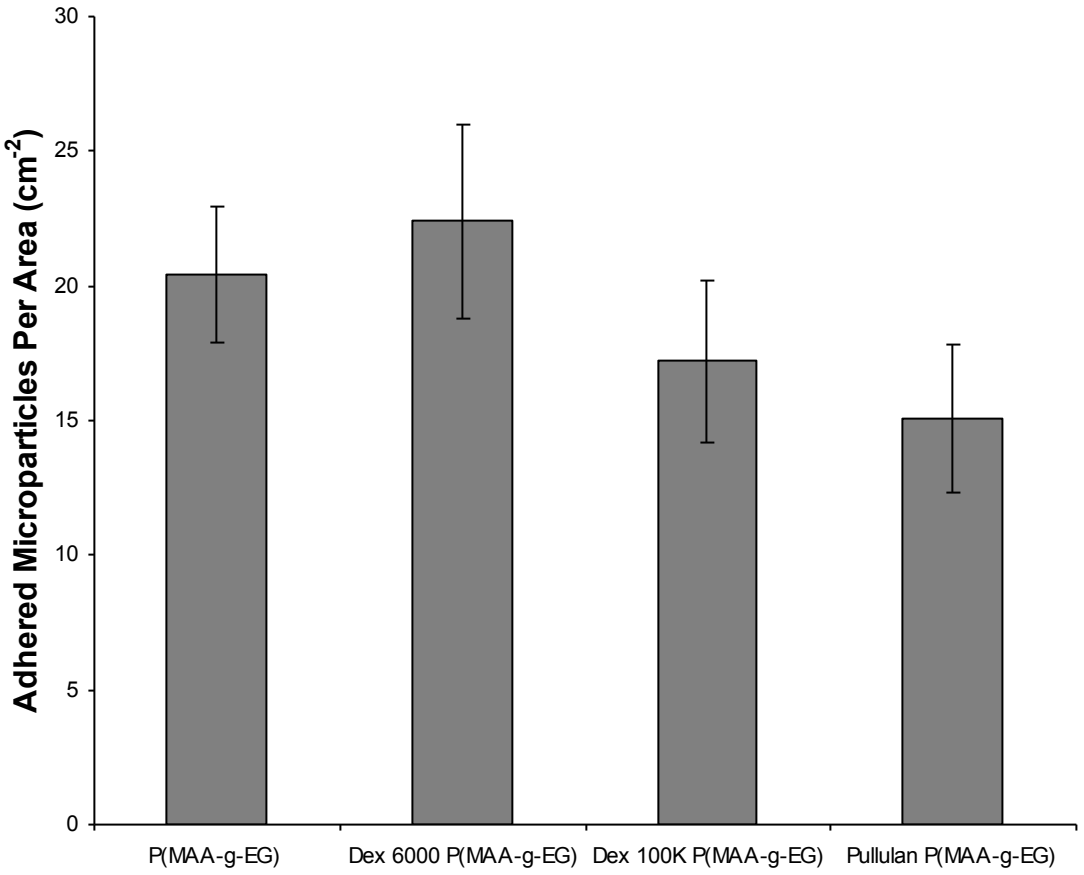

Figure 7.3 Mucoadhesion of fluorescently labeled polysaccharide-modified complexation hydrogel microparticles of P(MAA-g-EG), P(MAA-g-EG-co-Dextran 6000), P(MAA-g-EG-co-Dextran 100000), and P(PMAA-g-EG-co-Pullulan 75000) to reconstituted mucin gels is quantified by the number of adherent microparticles per area.

Data are represented by mean ± standard deviation.

7.5 REFERENCES

1. Betancourt, T., J. Pardo, K. Soo and N. A. Peppas, Characterization of pH-responsive hydrogels of poly(itaconic acid-g-ethylene glycol) prepared by UV-initiated free radical polymerization as biomaterials for oral delivery of bioactive agents. *J. Biomed. Mater. Res. Part A*, 93A, 175-188.

2. Carr, D. A. and N. A. Peppas, Assessment of poly(methacrylic acid-co-N-vinyl pyrrolidone) as a carrier for the oral delivery of therapeutic proteins using Caco-2 and HT29-MTX cell lines. *J. Biomed. Mater. Res. Part A*, 2010, 92A, 504-512.

3. Wood, K. M., G. M. Stone and N. A. Peppas, The effect of complexation hydrogels on insulin transport in intestinal epithelial cell models. *Acta Biomater.*, 2010, 6, 48-56.

4. Wood, K. M., G. M. Stone and N. A. Peppas, Wheat germ agglutinin functionalized complexation hydrogels for oral insulin delivery. *Biomacromolecules*, 2008, 9, 1293-1298.

5. Sahlin, J. J. and N. A. Peppas, Enhanced hydrogel adhesion by polymer interdiffusion: Use of linear poly(ethylene glycol) as an adhesion promoter. *J. Biomater. Sci.-Polym. Ed.*, 1997, 8, 421-436.

6. Thomas, J. B., J. H. Tingsanchali, A. M. Rosales, C. M. Creecy, J. W. McGinity and N. A. Peppas, Dynamics of poly(ethylene glycol)-tethered, pH responsive networks. *Polymer*, 2007, 48, 5042-5048.

7. Mikos, A. G. and N. A. Peppas, Bioadhesive Analysis Of Controlled-Release Systems .4. An Experimental-Method For Testing The Adhesion Of Microparticles With Mucus. 1990, 12, 31-37.

8. Deascentiis, A., J. L. Degrazia, C. N. Bowman, P. Colombo and N. A. Peppas, Mucooadhesion of Poly(2-Hydroxy Ethyl Methacrylate) is Improved when Linear

Poly(Ethylene Oxide) Chains are Added to the Polymer Network. *J. Control. Release*, 1995, 33, 197-201.

9. Achar, L. and N. A. Peppas, Preparation, Characterization And Mucoadhesive Interactions Of Poly(Methacrylic Acid) Copolymers With Rat Mucosa. *J. Control. Release*, 1994, 31, 271-276.

10. Goto, T., M. Morishita, N. J. Kavimandan, K. Takayama and N. A. Peppas, Gastrointestinal transit and mucoadhesive characteristics of complexation hydrogels in rats. *J. Pharm. Sci.*, 2006, 95, 462-469.

11. Seksek, O., J. Biwersi and A. S. Verkman, Translational Diffusion of Macromolecule-sized Solutes in Cytoplasm and Nucleus. *J. Cell. Biol.*, 1997, 138, 131-142.

Chapter 8:

In Vitro Drug Transport Studies and Measurement of Transepithelial Electrical Resistance in an Intestinal Epithelium Model

8.1 INTRODUCTION

In developing and optimizing drug delivery systems, *in vitro* tests are useful tools for selecting which formulations are the most likely to be successful *in vivo*. For oral delivery applications, drug absorption across the mucosa and intestinal wall into the bloodstream is a major factor contributing to the performance of the drug delivery system *in vivo*. The absorption of large molecular weight drugs such as proteins is especially important because these drugs typically have low bioavailabilities [1, 2]. Furthermore, interactions between the oral drug delivery systems and the mucosa are very important as many materials can disrupt the tight junctions of the intestinal epithelium. Damage to the epithelium can allow pathogens to cross the lining of the intestine. Therefore, *in vitro* evaluation of an oral delivery system's effect on the opening of the tight junctions or damage to the epithelium is highly desirable from a safety standpoint. However, reversible interactions that cause temporary opening of the tight junctions is hypothesized to improve absorption of low-solubility and large drugs [3-5].

The most widely used *in vitro* model to study oral drug delivery systems consists of Caco-2 cells which are human colon adenocarcinoma cells. These cells have the ability to differentiate into columnar epithelial cells with polarized membranes. On the apical side of these cells, the cells can produce a brush border and secrete enzymes associated with the intestinal epithelium. While Caco-2 cells have many similar properties to native intestinal epithelia, these cells are of colonic origin. One of the

disadvantages of the Caco-2 cell model is that it is a single cell model with an overall lower permeability than native human tissue of the small intestine. A lower permeability means that transport of molecules from the apical to basolateral side is slower than in normal tissue. As a result, drug permeability across these cells is often lower than what is observed in normal tissue.

As an alternative to Caco-2 cell models, a co-culture model consisting of Caco-2 cells and HT29-MTX goblet cells has been developed by Hilgendorf et al [6]. This model has several advantages over the Caco-2 model. First, the absorptive properties of Caco-2/HT29-MTX monolayers are more similar to native tissue including the electrical resistance. Additionally, the incorporation of mucus-secreting goblet cells into the model allows the effects of mucus on drug absorption to be studied *in vitro*.

In addition to analyzing drug absorption across intestinal epithelium cell models, understanding the effect of the oral drug delivery systems on the integrity of the intestinal epithelium is essential in designing more effective systems. For example, the structure of the epithelium can be characterized by analyzing the tight junctions of enterocytes. Disruption of the cellular monolayer corresponds to opening of the tight junctions between adjacent cells which can be measured by the transepithelial electrical resistance (TEER) of the cell monolayer. TEER studies have been used to better understand the interactions between drug delivery systems and GI tract tissue *in vitro*.

In the research presented in this chapter, polysaccharide-modified hydrogels are evaluated for potential use as oral protein drug delivery systems using drug transport and TEER measurements *in vitro*. Insulin transport across Caco-2/HT29-MTX cells in the presence of P(MAA-g-EG-co-Dextran 6000) was compared to transport in the presence of unmodified P(MAA-g-EG) microparticles. Furthermore, P(MAA-g-EG-co-Dextran 6000) and P(MAA-g-EG) microparticles that were loaded with insulin were also studied.

The effect of all of these systems on the TEER of Caco-2/HT29-MTX cells was also measured.

8.2 Materials and Methods

8.2.1 General Cell Culture

Caco-2 cells (ATCC, Rockwell, MD) and HT29-MTX cells (which were a generous gift from Prof. Thecla Lesuffleur, INSERM, Paris, France) were grown in Dulbecco's modified Eagle medium (DMEM, Mediatech, Herndon, VA) with high glucose and sodium pyruvate. The DMEM media was supplemented with 10 % heat inactivated fetal bovine serum (FBS, Cambrex, East Rutherford, NJ), 1 % non-essential amino acids (Mediatech), penicillin, streptomycin, and amphotericin B. Freshly thawed cells were grown in DMEM media with 20% FBS until the first passage.

Caco-2 cells and HT29-MTX cells were grown separately in a humidified incubator maintained at 37 ^{o}C and 5% CO_2. The cell media was refreshed every other day. Cells were passaged prior to 90% confluency. To passage cells, the media was removed and the cells were washed with pre-warmed Dulbecco's phosphate buffered saline without Ca^{2+} and without Mg^{2+}. Trypsin was placed on the cells and allowed to incubate for 10 minutes. Then, fresh, pre-warmed media was added to inhibit trypsin activity. A small volume of cells was removed and counted. Caco-2 cells were resuspended then seeded at a density of 3.0 x 10^3 cells/cm^2 whereas HT29-MTX cells were seeded at a density of 2 x 10^4 cells/cm^2.

8.2.2 Material Preparation

P(MAA-g-EG) and P(MAA-g-EG-co-Dextran 6000) hydrogel microparticles with diameters between 53 and 75 μm were prepared as described in previous chapters. P(MAA-g-EG) and P(MAA-g-EG-co-Dextran 6000) microparticles were loaded with insulin

as outlined in Chapter 6. Insulin-loaded particles were lyophilized and stored at -80 ^{o}C until use.

8.2.3 Caco-2/HT29-MTX Co-Culture

Caco-2 and HT29-MTX co-cultures were formed by combining both cell types and seeding them on the same tissue culture substrate. For the studies presented in this work, cells were seeded on polycarbonate Transwell® permeable supports (Corning, Lowell, MA) with a pore size of 0.4 μm. Transwell® plates (with 12-wells) were seeded using equal numbers of Caco-2 and HT29-MTX cells. The total cell seeding density was 1.0×10^5 cells/cm^2 with 5×10^4 Caco-2 cells/cm^2 and 5×10^4 HT29-MTX cells/cm^2. The co-cultures were allowed to grow for 21-24 days to allow differentiation and formation of a confluent monolayer. The cell media was refreshed every other day.

8.2.4 Transepithelial Electrical Resistance Measurements

The formation and integrity of tight junctions of the cell monolayers was monitored using transepithelial electrical resistance measurements (TEER) with a chopstick electrode (World Precision Instrument, Sarasota, FL). During TEER measurements, the temperature of the cell cultures were maintained at 37 ^{o}C using a heated mat. The chopstick electrode was placed in the Transwell® plate such that the longer electrode was placed in contact with the bottom of the lower Transwell® chamber, which allowed consistent positioning of the electrode. The shorter electrode was carefully positioned in the upper chamber so that it did not damage the membrane or touch the sides of the chamber. The electrical resistance between the two electrodes was recorded.

8.2.5 Drug Transport Studies

Transport studies were used to measure insulin permeability across Caco-2/HT29-MTX monolayers after constant TEER measurements were obtained (Figure 8.1). For drug transport studies, the TEER measurement for each cell monolayer was recorded. The media was removed and replaced with pre-warmed HBSS. The cells were allowed to equilibrate for one hour, and TEER measurements were recorded initially then at 15, 30, 45, and 60 minutes.

For transport studies, the cell media consisted of HBSS with Ca^{2+} and Mg^{2+} with 0.5 mg/ml bovine serum albumin to prevent protein adsorption to the Transwell® plates in both the upper and lower chambers. The control used in transport studies was a 0.2 mg/ml solution of insulin in a 0.5 mg/ml solution of BSA in HBSS. P(MAA-g-EG-co-Dextran 6000) and P(MAA-g-EG) microparticle samples were suspended in HBSS for a final microparticle concentration of 1 mg/ml along with 0.2 mg/ml bovine insulin and 0.5 mg/ml bovine serum albumin. Samples consisting of insulin-loaded microparticles were selected so that their insulin loading efficiency was approximately 85-88% with a final drug to polymer mass ratio of 17-18 % which allowed the ratio of insulin to polymer (0.2 mg/ml to 1 mg/ml) to be approximately matched. These microparticles were suspended in HBSS with 0.5 mg/ml so that the final polymer concentration was 1 mg/ml and the concentration of the entrapped drug would be 0.2 mg/ml if it was completely released.

Once the samples were added to the apical side of the cell monolayers, a 100 µl sample from the apical chamber was removed along with a 100 µl sample from the lower chamber. The volume of the lower chamber was replaced with pre-warmed 0.5 mg/ml of BSA in HBSS. The TEER of the cell monolayer was also recorded. At 30 minutes, 60 minutes, and 120 minutes, the TEER was recorded and a 100 µl sample from

the basolateral chamber was removed. An additional 100 µl of 0.5 mg/ml BSA in HBSS was added to the lower chamber to return the volume to 1.5 ml. After 3 hours, the TEER was recorded and a sample was removed from both the apical and basolateral chambers.

The cells were washed with HBSS three times to remove microparticles. Once the cells were washed, fresh DMEM media was added to each well and the TEER values were monitored for 24 hours.

8.2.6 Measurement of Drug Concentrations with ELISA

In order to measure the amount of insulin transported across the cell monolayers, the concentration of the insulin was measured using an enzyme-linked immunosorbent assay (ELISA assay) for bovine insulin (Mercodia AB, Uppsala, Sweden). The samples obtained from the basolateral chamber during transport studies were diluted prior to the ELISA assay by a dilution factor of 100 in HBSS. The assay procedure was followed according to the manufacturer's directions. The concentration of insulin in each sample was determined by measuring the optical absorbance at a wavelength of 450 nm using a UV-Vis plate reader.

8.2.7 Measurement of Drug Concentrations with HPLC

To measure the insulin concentrations in samples taken from the upper chamber during the transport study, HPLC was used. A Waters Alliance HPLC unit equipped with a Symmetry C4 5 µm column was used to run gradient elution in the reverse direction. The mobile phase consisted of 95% water with 0.1% trifluoroacetic acid (TFA) and 5% acetonitrile with 0.08% TFA. The column temperature was 40 ^{o}C. A gradient was run in the reverse direction from 5% to 60% acetonitrile over 18 minutes. The sample run time

was 22 minutes, and the sample injection volume was 20 µl. The protein concentration was measured by UV absorbance at 220 nm.

8.3 Results and Discussion

The use of polysaccharide-modified P(MAA-g-EG) microparticles as oral insulin delivery systems was evaluated *in vitro* through drug transport studies and TEER measurements of an intestinal epithelial cell model. In this work, P(MAA-g-EG-co-Dextarn 6000) and P(MAA-g-EG-co-Dextran 100000) were compared to unmodified P(MAA-g-EG) microparticles and insulin alone. Furthermore, insulin transport across Caco-2/HT29-MTX cell monolayers from insulin-loaded P(MAA-g-EG-co-Dextran 6000) and P(MAA-g-EG) microparticles was studied. The effect on the TEER of the cell monolayers was also investigated.

In this research, polysaccharide tethers were incorporated into P(MAA-g-EG) complexation hydrogels to promote mucoadhesion of the carrier in the upper small intestine. Because these systems were designed to interact with mucus, a Caco-2/HT29-MTX co-culture mucus-secreting co-culture was chosen as the intestinal epithelial cell model. The use of Caco-2/HT29-MTX models for evaluating insulin permeability *in vitro* in the presence of complexation hydrogels has been studied for several carrier and drug formulations by Peppas and co-workers [4, 7, 8]. Other studies have used Caco-2 cell models to study hydrogel drug delivery systems [4, 5, 9-11].

Prior to transport studies the formation of the tight junctions between adjacent cells was monitored by TEER as shown in Figure 8.1. The TEER of the cell monolayers (R_{tissue}) was calculated using Equation 8.1 by subtracting the average TEER from blank wells consisting only of media (R_{blank}) from the measured TEER ($R_{measured}$).

$$R_{tissue} = R_{measured} - R_{blank} \quad (8.1)$$

The TEER of the co-culture monolayer increased steadily over the first 10 days and then reached a plateau of approximately 200 Ω·cm^2. These TEER measurements are higher than the ones reported by Wood et al. [4] which were less than 200 Ω·cm^2 but still much lower than Caco-2 cultures which have TEER values of approximately 350-400 Ω·cm^2.

Prior to transport studies, the TEER of the Caco-2/HT29-MTX co-culture was measured once the media was replaced with HBSS. The cells were allowed to equilibrate in new media for 1 h to ensure that the replacement of the media with HBSS was not a factor in the transport study. The results are shown in Figure 8.2 over the one hour equilibration period. After replacement of the media, the TEER values returned, and there was no indication of damage to the epithelium.

For drug transport studies, the ratio of microparticles to insulin was chosen based on results obtained from loading studies presented in Chapter 6. The maximal insulin loading efficiencies around 90% resulted in drug to polymer ratios of around 18 wt%. As a result, microparticles concentrations of 1 mg/ml and insulin concentrations of 0.2 mg/ml were chosen for comparison.

During the transport study, the TEER values were monitored. The TEER values were measured using a chopstick electrode and an EVOM epithelial voltohmmeter. The chopstick electrode allows measurement of the electrical resistance of the cell monolayer using an applied AC current. Typically, TEER measurements obtained with a chopstick electrode vary 10-30 Ω. One of the advantages of this measurement is that AC current is used and does not have adverse effects on cell monolayers that DC current does.

For all samples, the measured TEER decreased over the course of the transport study as shown in Figure 8.3. Throughout the transport experiment, the TEER fluctuates close to the initial TEER. This indicates that the microparticle drug delivery systems (at concentrations of 1 mg/ml) do not adversely affect the tight junctions. A decrease in TEER measurements of Caco-2 and Caco-2/HT29-MTX monolayers during exposure to anionic complexation hydrogels was expected based on published research [4, 5]. In previous results, the TEER measurements of cell monolayers treated with insulin did not change significantly [4]. In addition, we monitored the pH of the apical and basolateral chambers over the course of the experiment by placing 1 µl droplets on pH paper. Throughout the experiment, the pH of both chambers was approximately a pH value of 7.

To analyze the transport of insulin across the Caco-2/HT29-MTX monolayers, the apparent permeability (P_{app}) was calculated based on the initial concentration of insulin in the apical chamber (C_o), the surface area of the cell monolayer (A), and the steady-state flux of the drug from the apical to the basolateral chambers across the cell layer (dQ/dt) as shown in Equation 8.2.

$$P_{app} = \left(\frac{dQ}{dt}\right)\frac{1}{A \cdot C_0} \tag{8.2}$$

The apparent permeability of insulin across the cell monolayers when insulin was mixed with either P(MAA-g-EG-co-Dextran 6000) microparticles or P(MAA-g-EG) as shown in Table 8.1. The apparent permeability of insulin in the presence of P(MAA-g-EG-co-Dextran 6000) was comparable to insulin alone. Unmodified P(MAA-g-EG) microparticles had higher apparent permeabilities than insulin alone as well as P(MAA-g-EG-co-Dextran 6000) mixtures. The transport profile of insulin into the basolateral chamber is shown in Figure 8.4 for the insulin control as well as the mixtures of insulin

with either P(MAA-g-EG) or P(MAA-g-EG-co-Dextran 6000). The concentration of insulin in the basolateral chamber increases linearly with respect to time for all samples. The insulin transport in the presence of P(MAA-g-EG-co-Dextran 6000) is similar to the insulin control. However, the insulin transport is highest for unmodified P(MAA-g-EG) microparticle mixtures.

The observed difference between insulin transport in the presence of P(MAA-g-EG) in comparison to P(MAA-g-EG-co-Dextran 6000) may be a result of polymer-drug and polymer-cell interactions. The dextran systems may interact more favorably with the mucus layer secreted by the Goblet cells thereby forming a layer of adhered particles atop the mucus layer. An adhered layer of microparticles above the cells is an additional barrier to diffusion of insulin across the mucus layer. Furthermore, the large hydrophilic co-macromonomers that may effectively charge shield the P(MAA) components of the hydrogel. In the case of insulin and P(MAA-g-EG), the negative charge of the P(MAA-g-EG) gel discourages polymer-drug interactions at neutral pH because both insulin and P(MAA-g-EG) have a negative charge. Interactions between insulin and P(MAA-g-EG-co-Dextran 6000) may be more favorable than diffusion through negatively charged mucus.

The apparent permeability of insulin across Caco-2/HT29-MTX monolayers from insulin-loaded formulations was investigated. The apparent permeability of insulin released from P(MAA-g-EG-co-Dextran 6000) microparticles was comparable to insulin alone (5.58×10^{-8} cm/s and 5.52×10^{-8} cm/s) as shown in Table 8.2. However, insulin's apparent permeability from insulin-loaded P(MAA-g-EG) microparticles was much higher (21.85×10^{-8} cm/s). In comparing the insulin permeability measured for P(MAA-g-EG) and insulin (that was not loaded), the P(MAA-g-EG) has a much greater impact on permeability causing the permeability to quadruple. The insulin transport profiles for

the formulations loaded with insulin shown in Figure 8.4 increase linearly with respect to time. The flux of insulin across the monolayer is relatively low in comparison to the insulin-polymer mixtures. Due to the lower concentration of the released drug in the apical compartment in comparison to the drug-polymer mixtures, higher apparent permeabilities were obtained. On average, the concentration of the drug in the apical chamber was 0.1 mg/ml for insulin-loaded samples. It is important to note that the apparent permeability of insulin released from loaded P(MAA-g-EG-co-Dextran 6000) was greater than the permeability of insulin from insulin- P(MAA-g-EG-co-Dextran) mixtures.

The permeabilities reported here are higher in comparison to the permeabilities obtained by Wood et al. [4] (1.61×10^{-9} cm/s to 15.20×10^{-9} cm/s) and Shofner et al. [8] (4.95×10^{-9} to 76.8×10^{-9} cm/s). Caco-2 cells are a heterogenous cell line. It is well known that the permeability of Caco-2 monolayers varies with passage number. In this case, Caco-2 cells between passage numbers 64 and 67 were used while the studies by Wood et al. and Shofner et al. were performed with Caco-2 cells with more than 70 passages.

8.4 Conclusions

Based on the effects of polysaccharide-modified P(MAA-g-EG) microparticles on the permeability across Caco-2/HT29-MTX cells, these systems are promising candidates for the oral delivery of insulin. The increased permeability observed for P(MAA-g-EG-co-Dextran 6000) hydrogels loaded with insulin further suggests that P(MAA-g-EG-co-Dextran 6000) are likely to perform well *in vivo*. Evaluation of the TEER of these materials shows the tight junctions remain intact without permanent damage to the epithelium.

Table 8.1 Apparent permeability of insulin across Caco-2/HT29-MTX cell monolayers in the presence of the oral delivery systems.

Formulation	Apparent Permeability Papp x 10^8 cm/s
Insulin	5.52
P(MAA-g-EG)	13.31
P(MAA-g-EG-co-Dextran 6000)	5.28

Table 8.2 Apparent permeability of insulin across Caco-2/HT29-MTX cell monolayers over 3 hours.

Formulation	Apparent Permeability Papp x 10^8 cm/s
Insulin	5.52
Loaded P(MAA-g-EG)	21.85
Loaded P(MAA-g-EG-co-Dextran 6000)	5.58

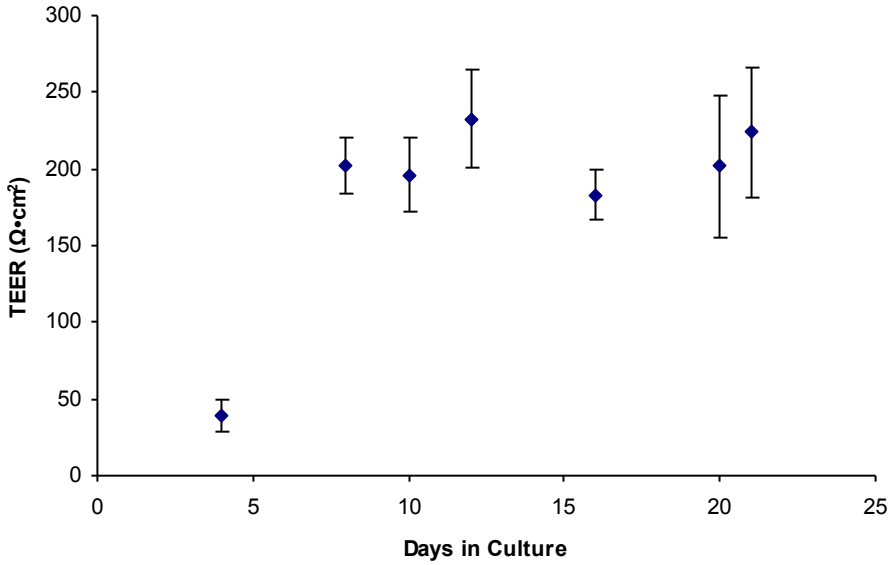

Figure 8.1 The average TEER of the developing Caco-2/HT29-MTX monolayer during formation of the monolayer during the 21 days prior to the transport and electrical resistance experiments.

Data are mean ± standard deviation.

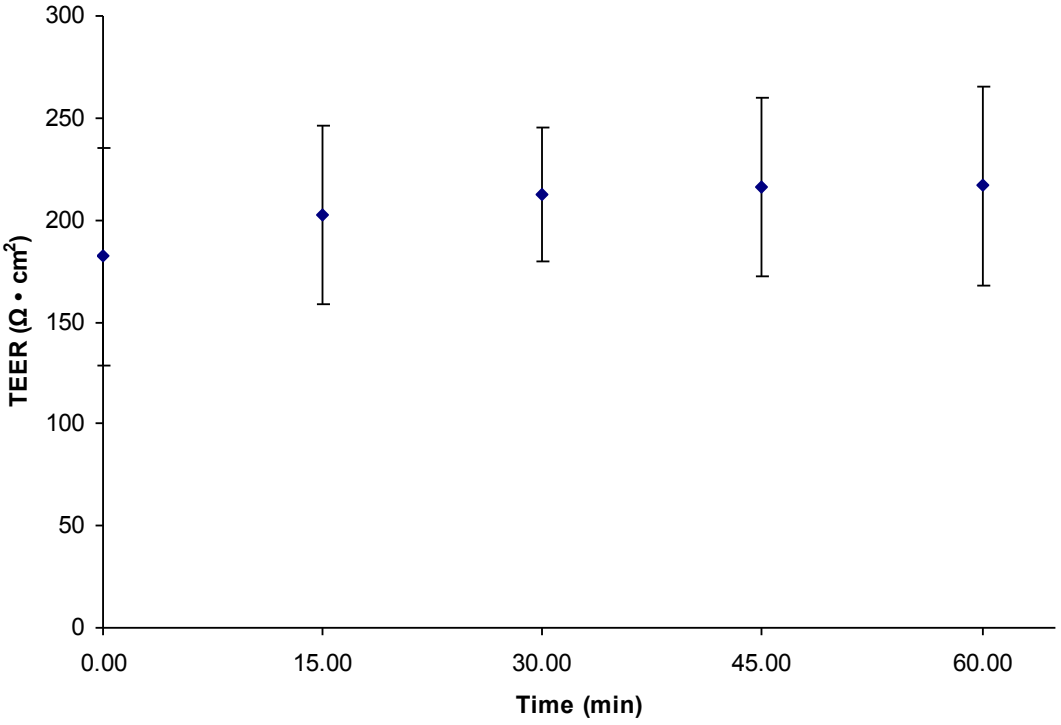

Figure 8.2 The average TEER of the Caco-2/HT29-MTX monolayer in the transport medium during a one hour equilibration period prior to drug transport studies.

Data are mean ± standard deviation. n = 48.

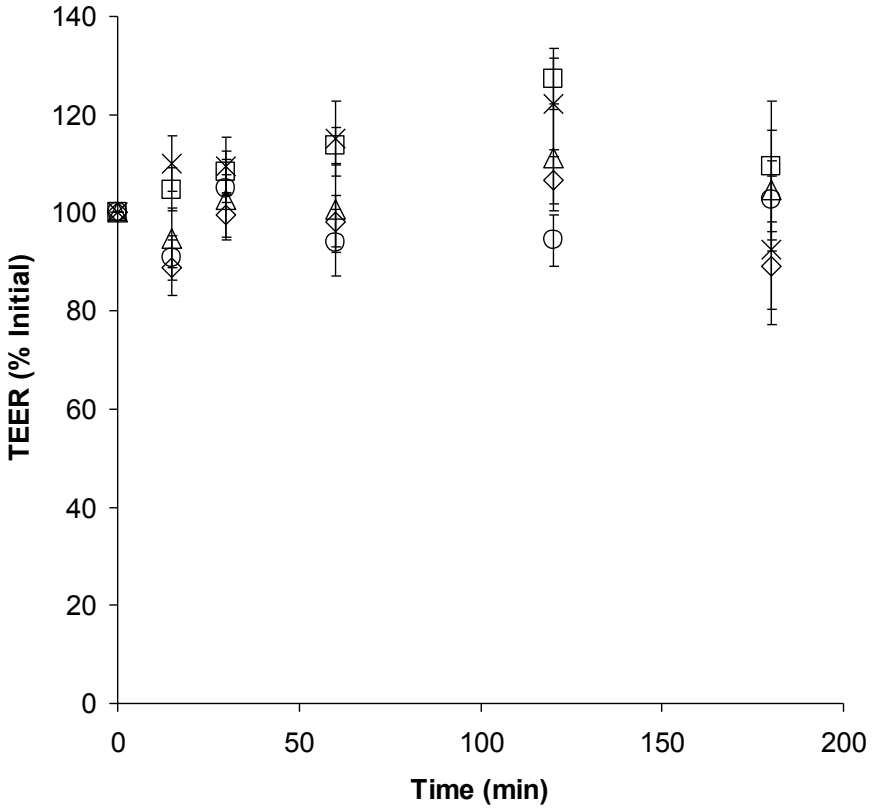

Figure 8.3 The average TEER of the Caco-2/HT29-MTX monolayer during drug transport studies with insulin in the presence of P(MAA-g-EG-co-Dextran 6000) (×), P(MAA-g-EG) (○). The TEER of Caco-2/HT29-MTX monolayers was also measured for systems loaded with drug including Insulin-loaded P(MAA-g-EG) (□) and Insulin-loaded P(MAA-g-EG-co-Dextran 6000) (Δ), and insulin alone (◇).

Data are mean ± standard deviation. n= 9.

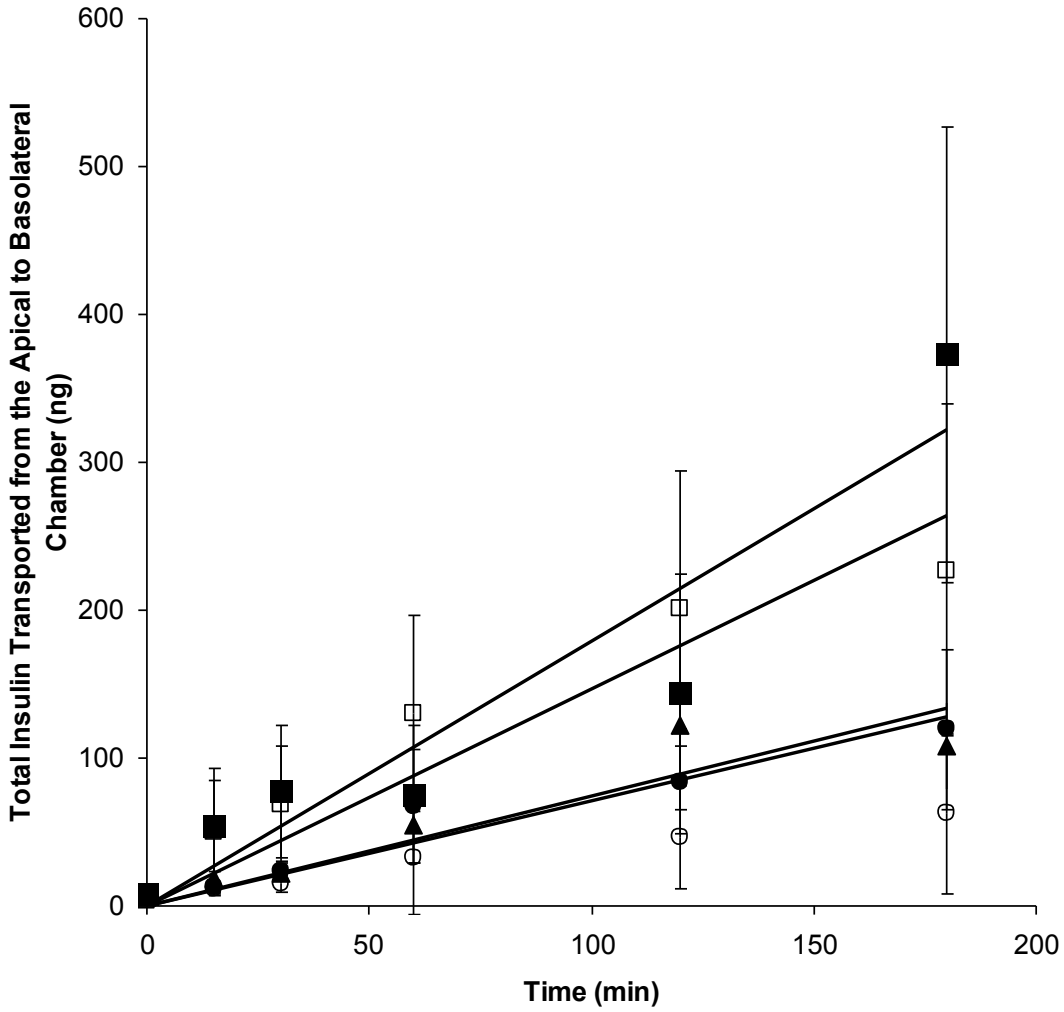

Figure 8.4 Cumulative insulin transport to the basolateral side of Caco-2/HT29-MTX monolayers from insulin-loaded P(MAA-*g*-EG) microparticles (□), insulin-loaded P(MAA-*g*-EG-co-Dextran 6000) (△) microparticles, insulin-P(MAA-*g*-EG) mixtures (■), insulin-P(MAA-*g*-EG-co-Dextran 6000) mixtures (●) in comparison to insulin controls (▲).

Data are mean ± standard error.

8.5 REFERENCES

1. Blanchette, J., N. Kavimandan and N. A. Peppas, Principles of transmucosal delivery of therapeutic agents. *Biomed. Pharmacother.*, 2004, 58, 142-151.

2. Peppas, N. A., J. B. Thomas and J. McGinty, Molecular Aspects of Mucoadhesive Carrier Development for Drug Delivery and Improved Absorption. *J. Biomater. Sci.-Polym. Ed.*, 2009, 20, 1-20.

3. Serra, L., J. Domenech and N. A. Peppas, Design of poly(ethylene glycol)-tethered copolymers as novel mucoadhesive drug delivery systems. *Eur. J. Pharm. Biopharm.*, 2006, 63, 11-18.

4. Wood, K. M., G. M. Stone and N. A. Peppas, The effect of complexation hydrogels on insulin transport in intestinal epithelial cell models. *Acta Biomater.*, 2010, 6, 48-56.

5. Fisher, O. Z. and N. A. Peppas, Quantifying tight junction disruption caused by biomimetic pH-sensitive hydrogel drug carriers. *J. Drug Deliv. Sci. Technol.*, 2008, 18, 47-50.

6. Hilgendorf, C., H. Spahn-Langguth, C. G. Regardh, E. Lipka, G. L. Amidon and P. Langguth, Caco-2 versus Caco-2/HT29-MTX co-cultured cell lines: Permeabilities via diffusion, inside- and outside-directed carrier-mediated transport. *J. Pharm. Sci.*, 2000, 89, 63-75.

7. Carr, D. A. and N. A. Peppas, Assessment of poly(methacrylic acid-co-N-vinyl pyrrolidone) as a carrier for the oral delivery of therapeutic proteins using Caco-2 and HT29-MTX cell lines. *J. Biomed. Mater. Res. Part A*, 2010, 92A, 504-512.

8. Shofner, J. P., M. A. Phillips and N. A. Peppas, Cellular Evaluation of Synthesized Insulin-Transferrin Bioconjugates for Oral Insulin Delivery Using Intelligent Complexation Hydrogels. *Macromol. Biosci.*, 2010, 10, 299-306.

9. Ichikawa, H. and N. A. Peppas, Novel complexation hydrogels for oral peptide delivery: In vitro evaluation of their cytocompatibility and insulin-transport enhancing effects using Caco-2 cell monolayers. *J. Biomed. Mater. Res. Part A*, 2003, 67A, 609-617.

10. Kavimandan, N. J. and N. A. Peppas, Confocal microscopic analysis of transport mechanisms of insulin across the cell monolayer. *Int. J. Pharm.*, 2008, 354, 143-148.

11. Torres-Lugo, M., M. Garcia, R. Record and N. A. Peppas, pH-sensitive hydrogels as gastrointestinal tract absorption enhancers: Transport mechanisms of salmon calcitonin and other model molecules using the Caco-2 cell model. *Biotechnol. Prog.*, 2002, 18, 612-616.

Chapter 9:

Conclusions

The use of protein drugs is a rapidly growing branch of pharmaceutics. While injection has been an effective administration route for protein drugs, alternative routes of administration are of interest. In particular, administration via the oral route is desirable. The oral delivery of proteins such as insulin has the potential to increase patient adherence, reduce waste, and eliminate adverse effects associated with repeated injections.

There are several major challenges associated with the oral delivery of protein drugs such as insulin. The activity of the therapeutic must be retained through the GI tract, and the active drug must reach the bloodstream at levels high enough to provide therapeutic efficacy. An oral protein delivery system must protect the drug from acid and enzymes in the stomach, but release the protein in the neutral environment of the small or large intestine. Anionic complexation hydrogels demonstrate pH responsive swelling behavior and have shown potential for use in such an oral protein fomulation.

In this work, a novel method for synthesizing complexation hydrogels containing poly(methacrylic acid), poly(ethylene glycol), and polysaccharides was developed. The synthesis of these materials was verified using FT-IR spectroscopy.

Based on analysis of the swelling of these hydrogels modified with either dextran or pullulan, pH-responsive swelling is conserved in the presence of the polysaccharide comonomers. These systems form collapsed structures with minimal swelling in acidic conditions and swell significantly in more neutral conditions. Analysis of the mesh size indicates that these gels could sufficiently entrap and release drugs as large as protein drugs including insulin. In comparison to unmodified P(MAA-g-EG) hydrogels,

polysaccharide-modified P(MAA-g-EG) hydrogels exhibited similar trends in swelling. Several differences such as increased $\upsilon_{2,s}$ at low pH and decreased $\upsilon_{2,s}$ at neutral pH suggest that polysaccharide-modified P(MAA-g-EG) gels may have some advantages for oral delivery with respect to their complexation and decomplexation behavior.

The data presented in this work show that polysaccharide-modified hydrogels have the potential to meet the requirements to overcome the major challenges to oral protein delivery. These systems can be used to entrap insulin, protect insulin in acidic conditions, release insulin in response to changes in pH, and the release profile can be controlled by the amount and type of polysaccharide tether.

Based on the *in vitro* cytotoxicity and mucoadhesion assessments of polysaccharide-modified hydrogels, these materials appear to be promising for the oral delivery of protein drugs. These materials do not cause a significant increase in cell death as measured by an MTS assay in a Caco-2 enterocyte model. In addition, these materials were shown to adhere to reconstituted mucin gels. The ability to adhere to mucus membranes and cause limited cell death is highly desirable for oral protein drug delivery systems.

Insulin drug transport from polysaccharide-modified P(MAA-g-EG) microparticles was evaluated by measuring the insulin permeability across Caco-2/HT29-MTX cells. Transport of insulin in the presence of and released from the polysaccharide-modified hydrogels demonstrate that they are promising candidates for the oral delivery of insulin. Evaluation of the TEER of epithelial monolayers exposed to these materials shows reversible opening and closing of tight junctions without permanent damage to the epithelium.

To fully evaluate these systems for oral insulin delivery, future work would include an in vivo assessment of the insulin bioavailability and ability to produce a

hypoglycemic affect. Additional optimization of these systems could include the evaluation of the influence of the polysaccharide diffusion coefficient in mucus as it relates to mucoadhesion. Overall these systems are promising candidates for the oral delivery insulin and other protein drugs.

Appendix A

Targeted Nanodelivery of Drugs and Diagnostics

Published in Nano Today, 2010.

Margaret A. Phillips, Martin L. Gran, Nicholas A. Peppas

Department of Biomedical Engineering, Department of Chemical Engineering, Division of Pharmacy, The University of Texas at Austin, Austin, TX 78712

ABSTRACT

Nanomaterials for targeted delivery are uniquely capable of localizing delivery of therapeutics and diagnostics to diseased tissues. The ability to achieve high, local concentrations of drugs or image contrast agents at a target site provides the opportunity for improved system performance and patient outcomes along with reduced systemic dosing. In this review, the design of targeted nanodelivery systems is discussed with an emphasis on *in vivo* performance, the physicochemical properties that affect localization at the target site, and the incorporation of therapeutic drugs into these systems.

INTRODUCTION

Successful targeted delivery systems are designed to allow delivery of therapeutic or diagnostic agents to a preferential site. As targeted nanodelivery involves local delivery of therapeutics and diagnostics at disease sites, this method has received considerable attention over the last 15 years and is poised to have a significant

impact on medicine. Efficient targeted delivery systems allow for a reduced systemic dosage while resulting in relatively higher or more efficient dosing at the target site. The promising benefits of reduced systemic side effects and simultaneously improved efficacy have fueled the development of this field. To date, targeted delivery has become a rich field of drug delivery and nanomaterials.

Nanoscale materials are a necessity for most targeted delivery systems as these systems must be allowed to transport through different tissue spaces in order to localize at the target site. For tumor delivery, intravenously administered particles must circulate in the bloodstream and be small enough to escape circulation through tumor microvasculature which typically requires the system to have a diameter less than 100 nm to 2 μm [1]. In other applications such as the treatment and diagnosis of atherosclerotic plaques, targeted delivery systems have been developed on the order of 10 nm to greater than 1 μm.

The ability of nanoparticles to localize at a target site is dependent on a number of factors. In general, it is unclear whether chemical properties, the presence of a targeting ligand, or size is the primary determinant for nanoparticle biodistribution. In many cases, it is a combination of these properties that shapes biodistribution. One of the advantages of nanoparticle delivery systems is that the circulation time of drugs and diagnostic agents can be prolonged, and delivery can be controlled through targeting. Even with targeted delivery, only a fraction of the administered dose localizes at the target site while the remaining nanoparticles distribute throughout the body. At this point, pharmacokinetics pertaining to the nanodelivery system determine the dose in nontargeted tissues. A furthered understanding of nanoparticle biodistribution and pharmacokinetics will be a significant contribution to the successful development and translation of targeted delivery systems.

An often overlooked design parameter in targeted delivery systems is the method and amount of incorporation of the drug or diagnostic agent. There are a variety of methods for incorporating these functions into a delivery system which depend on the nanomaterial and the agent of interest. The small volumes of nanomaterials inherently limit their maximum payloads, and their sizes present challenges to traditional purification and measurement techniques.

From current work in the field, it is evident that the design of optimized targeted delivery systems will be based on the drug or agent of interest, the nanoparticle type that allows sufficient loading of the drug, and the physicochemical properties that allow for targeting. We will highlight some of this recent work on targeted delivery systems and focus on *in vivo* performance, localization, and the incorporation of diagnostic and therapeutic agents in targeted delivery systems.

In vivo studies on targeted delivery: localization, uptake, and performance

One of the key features of targeted delivery systems is the addition of targeting ligands to the surface of the nanoparticle either through physical adsorption or more commonly chemical attachment. Various *in vitro* and *in vivo* studies have shown that the addition of these targeting ligands improves the therapeutic effects of the delivery systems compared to control systems without the targeting ligands. Nanodelivery systems with targeting ligands are often referred to as actively targeted systems but will be referred to as targeted delivery systems throughout this paper. Nanodelivery systems without targeting ligands can be passively targeted systems but will be referred to as nontargeted systems in this paper. Recent *in vivo* studies have shed light on some of the mechanisms behind this improvement in therapeutic efficacy. Findings from

these studies suggest that the targeting ligands act less like a homing device seeking out the target site but more like sticky shoes that improve nanoparticle association with the target cells' membranes or even uptake by the target cells. In this section, we will cite recent studies on targeted delivery systems focusing on comparisons against nontargeted delivery systems for the two most common applications of targeted delivery: targeting of tumors and atherosclerotic plaques.

Tumor targeting

Nanoparticles are well-suited materials for targeted tumor delivery due to their ability to circulate in the bloodstream for relatively long time periods and their ability to accumulate in tumor spaces. Often, actively targeted nanodelivery systems are modifications of passively targeted delivery systems. A number of studies have shown improved treatment in vivo and in vitro with targeted systems. However, there is growing evidence to suggest that for many nanoparticle delivery systems accumulation at the tumor site is independent of the presence or absence of a targeting ligand. In these cases, the enhanced permeability and retention (EPR) effect is the dominating mechanism for localization at the tumor site. Exploitation of the EPR effect requires careful size selection of nanoparticles that allows nanoparticles to extravasate leaky tumor vasculature and to be retained in the tumor due to insufficient lymphatic drainage. However, in a number of studies, nanodelivery systems with targeting ligands have performed better than nontargeted systems. This improved performance or more effective treatment has been attributed to improved nanoparticle association with target cell membranes and target cell internalization. We will discuss a variety of recent *in vivo* studies which have compared targeted and nontargeted nanodelivery systems towards understanding the relationship between active and passive tumor targeting.

Active Tumor Targeting

This relationship between cell uptake and performance of targeted nanodelivery systems has been demonstrated in several studies with folate targeted-nanoparticles. To target tumor cells overexpressing the folate receptor, folate was incorporated into the nanoparticle delivery system as a targeting ligand.

In a study by Wang et al [2], the biodistribution and performance of targeted nanoparticles composed of heparin-folate-paclitaxel conjugates loaded with paclitaxel (HFT-T) were compared to nontargeted nanoparticles of heparin-paclitaxel conjugates loaded with paclitaxel (HT-T). HFT-T targeted systems significantly reduced tumor volume over nanoparticle and paclitaxel controls in a KB-3-1 human nasopharyngeal carcinoma xenograft-bearing mouse model. Despite this, biodistribution studies revealed that the difference between accumulation of targeted and nontargeted systems in the tumor was not statistically significant. However, fluorescence microscopy of the tumor cells showed that the targeted systems were more commonly internalized. These results were confirmed by flow cytometry which showed that the targeted nanoparticles were found in three times more tumor cells than nontargeted nanoparticles (21.8 ± 2.9% cells compared to 5.6 ± 1.8% cells). This phenomenon was further evidenced by *in vitro* studies which showed the uptake of targeted nanoparticles was higher than nontargeted nanoparticles and was folate-dependent. In this study, the improved performance of targeted nanoparticles was due to enhanced cell uptake, rather than enhanced localization compared to nontargeted nanoparticles.

Likewise, comparable biodistributions and tumor accumulation between folate receptor-targeted and nontargeted gadolinium (Gd) nanoparticles has been observed in a KB xenograft-bearing athymic mouse model [3]. The results showed that the targeted and nontargeted systems had similar biodistributions and that there was no statistical

difference in tumor localization at either 5 or 8 hours. Furthermore, there was a higher tumor cell uptake of targeted nanoparticles *in vitro* and an enhanced retention following intratumor injection of nanoparticles *in vivo*. While this study did not examine the tumor microdistribution of nanoparticles *in vivo*, it relied on *in vitro* data to support the assertion that enhanced internalization was a feature of folate-coated Gd nanoparticles.

Tumor delivery via folate receptor targeting has also been evaluated using micelles with differing amounts of the targeting ligand [4]. Targeted micelles were formed with varying amounts of folate by increasing the molar ratio of folate-PEG-poly(aspartate-hydrazone-adriamycin) [Fol-PEG-p(Asp-Hyd-ADR)] to methoxy-PEG-poly(aspartate-hydrazone-adriamycin) [PEG-p(Asp-Hyd-ADR)] while nontargeted control micelles were formed entirely from PEG-p(Asp-Hyd-ADR). The effective dose for the targeted system improved upon the nontargeted system, which was also lower than the effective dosage for the free drug in *in vivo* studies with tumor-bearing CD-1 nude mice. These results indicated that targeted micelles (containing 10% of the folate-conjugated polymer) performed more effectively than nontargeted micelles despite similar pharmacokinetic profiles of micelle accumulation in the tumor and relatively close area under the curves (AUC) for the drug accumulation in tumors (132.67 and 143.60 percent initial dose (%ID)/g organ x h, respectively). While the internalization of targeted and nontargeted nanoparticles was not monitored *in vivo* in this study, the preferential internalization of targeted nanoparticles is hypothesized to be the reason for the improved effective dose.

Another common targeting ligand, transferrin (Tf), has been conjugated to a variety of targeted delivery systems to target overexpressed Tf receptors common to many cancers. As observed in folate receptor targeted systems, nanoparticles with Tf

targeting ligands improve delivery but have a biodistribution and tumor accumulation similar to nontargeted systems [5]. For example, Bartlett et al focused on delivery of siRNA using cyclodextrin-containing polycations and used positron emission tomography (PET) and bioluminescence imaging to simultaneously monitor the nanoparticle location and siRNA activity as shown in Figure 2. In this study, siRNA activity was higher for the targeted delivery systems (Figure 2c). The improved siRNA activity was attributed to a greater tumor cell internalization of the targeted nanoparticles versus the nontargeted nanoparticles, because the tumor accumulation of targeted and nontargeted nanoparticles was similar. Approximately 1% initial dose (ID) accumulated per tumor volume one day after injection. Additionally, Bartlett et al found that nanoparticle accumulation in tumors was independent of the Tf-receptor level.

In addition to the improvements in delivery via folate and transferrin targeting, enhanced performances due to nanoparticle internalization have been seen for multiple systems with antibody-directed targeting. In a study focused on spectroscopic detection of cancer using surface-enhanced Raman (SERS) via colloidal gold Raman nanotags, single-chain variable fragment antibodies for epidermal growth factor receptor (EGFR) were harnessed for targeting of 80 nm nanotags [6]. Transmission electron micrographs of tumor cells revealed that the targeted nanotags were more readily internalized. The enhanced internalization of targeted nanotags paralleled an increase in Raman signal intensity from tumors treated with the targeted nanotags. Biodistribution measurements showed that the accumulation and retention of EGFR targeted nanotags in the tumor was about 10 times greater than that of nontargeted controls.

Similar findings have been reported for antibody targeting of liposomes. For example, liposomes possessing an anti-HER2 monoclonal antibody (MAb) composed of phosphatidylcholine and polyethylene glycol (PEG)-modified

distearoylphoshphatidylethanolamine (DSPE) (PEG-DSPE) with an average particle diameter of 100 nm were shown to improve antitumor efficacy of doxorubicin over various control formulations [7]. Kirpotin et al further evaluated the biodistribution and uptake of these targeted liposomes containing the anti-HER2 MAb compared to nontargeted liposomes [8]. They found that the biodistribution of targeted and nontargeted liposomes was similar. In fact, localization of targeted and nontargeted liposomes in HER-2 overexpressing xenografts (BT-474) and non-HER-2-overexpressing xenografts (MCF-7) were not statistically different with a range of 7-8% of the injected dose per gram of tumor tissue (ID/g tumor). Targeted and nontargeted liposomes were shown to extravasate tumor blood vessels in both xenograft models, yet a significant difference between the targeted and nontargeted liposomes was observed in the microdistribution within HER-2-overexpressing tumor xenografts. Targeted liposomes were found predominantly in tumor cells while nontargeted liposomes were found in the extracellular spaces or in macrophages associated with tumor tissue. For targeted liposomes, there was a four-fold greater preference for nanoparticle localization in xenograft tumor cells rather than host cells while there was no statistical preference for tumor cells over host cells in the case of nontargeted liposomes.

Likewise, ElBayoumi and Torchilin used antibody targeting to enhance delivery of doxorubicin loaded PEGylated liposomes [9]. The targeting ligand, monoclonal antibody 2C5 (mAb 2C5) with nucleosome-restricted activity, increased accumulation of liposomes in Lewis lung carcinoma tumor models over nontargeted systems. Following administration of liposomes, a greater reduction in tumor volume was achieved by doxorubicin delivery from targeted liposomes.

Passive Targeting of Tumors

While the active targeting schemes described above involve the use of molecules designed to specifically interact with a physiological target, passive targeting takes advantage of natural properties and processes in tissues to localize a delivery agent at a desired target site. The most common type of passive targeting is tumor targeting by the EPR effect. To exploit this effect, the size of nanoparticles is designed to allow nanoparticles to extravasate from defects in tumor vasculature. Nanoparticles between 100-200 nm have been shown to accumulate in tumors by the EPR effect. Larger molecules such as nanoparticles can diffuse out of defective tumor vasculature but are retained in the tumor space due to insufficient venous and lymphatic clearance. The retention of large molecules such as nanoparticles is typically higher than small molecules which can more easily diffuse back into vasculature as shown in Figure 3 [10]. In addition to appropriate size, nanoparticles must have properties that allow for a long circulation time. Passive tumor targeting by the EPR effect requires a driving concentration gradient of nanoparticles for a sustained time period of at least 6 hours [10, 11]. As a result, PEGylation and surface charge are important design parameters due to their known effect on circulation times. *In vivo* targeting delivery studies suggested that the presence of a targeting ligand does not appear to significantly affect extravasation, but inefficient extravasation could significantly affect targeted delivery.

Challenges to Tumor Delivery

One of the challenges to developing a successful tumor targeting delivery platform, is that even with passive and active targeting only a fraction of the administered dose accumulates in the tumor. This brings two questions to light: is there enough accumulation at the target site and what is the systemic dose?

In short, effective delivery can be achieved at the tumor site. Whether the dose administered is an effective dose is easily gauged by a sufficient suppression in tumor growth. The effective dose is dependent on nanoparticle localization at the tumor site but also on the maximum payload that each nanoparticle can deliver. To put this into perspective, nanoparticles localize in tumors at much lower levels than the administered dose (Table 1). So, if the amount of drug or image contrast agent is increased in each nanoparticle, a higher dose arrives at the tumor site. However, there is a balance between the payload and the number of nanoparticles. The fraction of the administered dose that localizes in the tumor relative to the mass of the tumor (%ID/g tumor) is also lower than other in organs (the % ID/g tissue) such as the liver [12]. What this tells us is that other organs have an increased exposure per gram of tissue to the nanoparticles and their payloads than the tumor often does. So, an increase in the drug or contrast agent could be detrimental.

A greater cell internalization accompanied by a simultaneous improvement in performance of targeted nanodelivery systems is a recurring theme in cancer delivery. Clearly, the selection of the targeting ligand is important, but the nanoparticle properties that influence accumulation in the tumor are important design parameters as well.

Targeting of atherosclerotic plaques

Second to tumor targeting, the most common application of targeted imaging and treatment is atherosclerosis. In targeting atherosclerosis, the delivery system circulates in the bloodstream and must adhere to a specific region of the vasculature. The small size and relatively large surface area of nanoparticles makes them attractive candidates for this application. Because circulating nanodelivery systems must adhere

to atherosclerotic lesions, understanding nanoparticle adhesion and behavior in flow conditions is extremely important, although it is beyond the scope of this paper. To date, the majority of *in vivo* studies have focused on the delivery of image contrast agents. As a result, the preferential accumulation of targeted nanoparticles at atherosclerotic lesions has often been confirmed by improved image contrast or increases in the signal at the target site relative to the background.

In one such study, an improved contrast in fluorescence imaging and delivery of a heparin hirulog therapeutic was achieved using micelles with a clot-binding peptide, cysteine-arginine-glutamic acid-lysine-alanine (CREKA) to target fibrin deposits on atherosclerotic plaques [13]. The micelles were formed from PEG-DSPE polymers with variable head groups labeled with carboxyfluorescein (FAM-labeled) for imaging, CREKA for targeting, or a heparin hirulog for treatment. Results showed that the targeted micelles improved the fluorescence intensity of atherosclerotic plaques in the aortic tree over nontargeted micelles as well as the delivery of the heparin hirulog as seen in Figure 4. The CREKA targeting ligand was shown to be responsible for this improved contrast because through competitive inhibition studies. The contrast provided by targeted FAM-labeled micelles was depleted with the addition of excess unlabeled targeted micelles but remained the same with the addition of excess unlabeled nontargeted micelles. Additionally, CREKA targeted micelles were more effective than nontargeted control micelles in delivering hirulog to plaques in an ApoE-null mouse model. The ability to target delivery to diseased tissue using the CREKA targeted micelles by showing that hirulog delivery was significantly lower in nonatherosclerotic (wild-type) mice (Figure 3c).

Enhanced contrast of magnetic resonance imaging (MRI) of atherosclerotic plaques has also been achieved using targeted nanodelivery of contrast agents. For

example, magnetofluorescent nanoparticles targeted to vascular adhesion molecule-1 (VCAM-1), a biomarker for atherosclerosis, enhanced MRI and fluorescence image contrast agent delivery compared to nontargeted controls in a cholesterol-fed apoE$^{-/-}$ mouse model [14]. In another study, Neubauer et al examined targeted delivery of paramagnetic liquid perfluorocarbon nanoparticles which incorporated a peptidomimetic victronectin antagonist for targeting the $\alpha_v\beta_3$ integrins [15]. Targeted systems enhanced MRI images compared to the nontargeted systems with double the concentration at the aortic wall (0.38% ID compared to 0.18% ID for nontargeted, or 1.64 compared to 0.84 nmol Gd/g tissue/h, respectively) in a cholesterol-fed rabbit model.

Several other studies have focused on targeted delivery systems as platforms for image contrast agents in atherosclerosis and have shown significant image enhancement over controls. For example, Park et al. demonstrated that hydrophobically modified chitosan nanoparticles with a peptide targeting ligand selectively accumulate at atherosclerotic plaques [16]. In addition, magnetofluorescent nanoparticles were targeted to macrophages associated with atheroma using dextran [17]. Administration of the targeted nanoparticles resulted in significant image enhancement over saline controls in the blood-plaque contrast-to-noise ratio of MRI. Improvements were also observed in near infrared reflectance fluorescence images in the plaque-to-background ratio. While these studies and others have not compared targeted delivery with nontargeted delivery to atheroma, these results indicate that targeted delivery is a promising approach to treatment and diagnosis of cardiovascular diseases.

The "fate" of the nanoparticle delivery system

The systemic biodistribution of nanoparticle delivery systems after administration is one of the most important issues and design elements to consider in targeted delivery. There is an innate relationship between the physicochemical properties of the nanoparticle and what happens to the particle after administration. This section will focus on the biodistribution, opsonization, and clearance of nanoparticles related to targeted delivery.

Opsonization and Clearance

For targeted delivery applications, there is a delicate balance between the circulation time necessary for particle localization at the target site and a suitable time frame for elimination. The eventual elimination (or whole body elimination) of nanomaterials is particularly important due to concerns over long-term exposure and interference with other diagnostics and therapies.

Both renal filtration and opsonization result in removal of nanomaterials from the bloodstream. Nanoparticles smaller than the renal filtration cut-off of 50 kDa or 5-6 nm are rapidly cleared from the bloodstream and excreted as demonstrated by Choi et al and summarized in Figure 5 [18]. Larger nanoparticles can be removed from the bloodstream by the reticuloendothelial system (RES) through opsonization resulting in nanoparticle accumulation in the liver, spleen, and lungs. Both the size and charge of nanoparticles is known to affect opsonization. In general, smaller particles tend to circulate longer [19]. Surface engineering such as charge shielding and the reduction of the adsorption of opsonin proteins on the nanomaterial has been shown to slow opsonization by imparting 'stealth' properties to the nanoparticle. For example, the addition of hydrophilic molecules such as PEG has been used in a variety of studies to

slow opsonization. While we have alluded to the effect that PEGylation has on nanoparticle opsonization, there have been several extensive reviews that give a more in depth discussion of the factors affecting opsonization and strategies for slowing opsonization [19, 20].

In general, the selection of nanoparticle clearance rate is dependent on the application. For tumor targeting, the blood half-life in combination with the administered dose should afford a high blood concentration of nanoparticles for several hours [11]. Shorter blood half-lives may be desirable in other applications like image contrast agent delivery. Rapid localization and short half-lives would allow administration of contrast agent and imaging to be performed on a patient during a single appointment. Because nanoparticles are highly tunable, shorter or longer blood half-lives can be achieved on the order of minutes to hours. For example, quantum dots have been shown to have half-lives that range from 48 min to 20 h as demonstrated in Figure 5 [18].

An emerging issue in the field of nanoparticle delivery is the overall elimination of the nanoparticles. Clearance from the bloodstream is different than clearance or elimination from the body. Biodegradable polymeric systems do address the issue of elimination as long as they degrade to eliminable byproducts, but eventual elimination is an issue for organic and inorganic systems that are not degradable. One recent study has highlighted this issue by demonstrating that quantum dots can remain fluorescent *in vivo* for two years [21]. This nonelimination could cause significant problems if the quantum dots interfere with other treatments or diagnostics.

Biodistribution

Because understanding biodistribution is fundamental to the development of successful targeted nanodelivery systems, it is important to understand some of the

factors affecting biodistribution both from an experimental perspective and material design perspective. Currently, there are not standardized practices for evaluating the performance of targeted delivery systems. As a result, it is difficult to compare results across studies. For example, some of the experimental factors affecting the measured biodistribution of nanomaterials are the initial dose [4, 22] the method of administration [23], the experimental model (including the tumor mass in the case of tumor delivery) [12], and the experimental time range. As targeted nanodelivery systems continue to be developed, standardized practices and the effect of experimental conditions on results will become key experimental considerations.

Despite the fact that there are not standardized procedures in measuring biodistribution, there are some commonalities and trends in the development of new experimental techniques. Perhaps, the use of autoradiography in monitoring nanoparticle biodistribution of radiolabeled nanomaterials is one of the most common elements across studies [19]. The widespread usage of autoradiography is due to the ability to easily and quantitatively measure small concentrations, but there are several drawbacks to radiography. Autoradiography requires tissue excision so only one time point can be measured per sample, and there are safety considerations in practicing this technique. Because of this, there is a growing body of literature that has used alternative methods to quantify biodistribution (Table 2).

Similar biodistributions for systems with and without targeting ligands is a recurring theme in targeted delivery. In only a few studies, has the presence of targeting ligands been shown to affect biodistribution in tissues other than the target site [4, 6]. To the best of our knowledge, there have not been any studies to determine whether internalization is improved by a higher accumulation at the target site. However, it is evident that a higher concentration of nanodelivery systems at the target

site allows a greater availability for cell uptake. What this underscores is that the physicochemical properties affecting biodistribution are equally important for active and passive targeting. Size, shape, surface charge, and mechanical properties can be selected based on their effect on biodistribution.

It has been shown that the biodistribution of nanoparticles is size-dependent, as demonstrated by two recent studies on gold nanoparticles and PEGylated gold nanoparticles [24, 25]. For example, smaller gold nanoparticles (10 nm in diameter) were distributed in more tissues than larger particles (50, 100, or 250 nm) [25]. In all of the samples, nanoparticle accumulation occurred primarily in the liver, spleen, and the blood as measured by the concentration (ng/g tissue) and percent of the initial dose. Like gold nanoparticles, PEGylated gold nanoparticles exhibited a size-dependent biodistribution [24]. Accumulation of 20 nm gold nanoparticles in the tumor was significantly higher than that of 80 nm particles in an A341 xenograft-bearing mouse model. Outside of the tumor, nanoparticles of both sizes accumulated predominantly in the liver and spleen. As expected from a slow uptake by reticuloendothelial system (RES) organs, the 20 nm particles had a longer blood half-life than 80 nm particles and a lower accumulation in the liver and spleen.

Many studies have predicted that the shape of nanoparticles affects *in vivo* performance [26, 27], but the influence of shape on nanoparticle biodistribution is only beginning to be explored. To the best of our knowledge, only one study has compared the *in vivo* biodistributions of nanoparticles with different shapes. Park et al. evaluated the biodistribution of magnetic iron oxide nanoworms, elongated iron oxide nanoparticles, and compared them to spherical iron oxide nanoparticles [28]. They observed that nanoworms more readily accumulated in tumors in an MDA-MB-435 xenograft-bearing mouse model than nanospheres. After 48 h, nanoworms still

remained in the tumor while nanospheres did not. The overall biodistributions of the two systems after 24 h were similar, where each showed a lower accumulation in the kidney relative to the liver and a higher accumulation in the spleen relative to the liver. The circulation time for both systems was comparable with blood circulation half-lives between 15 and 18 h.

In conjunction with size, the composition of nanoparticles has been shown to affect biodistribution by determining the "flexibility or shape adaptability" of the nanoparticle [29]. When comparing the biodistribution of two relative sizes of shell cross-linked nanoparticles having diameters of approximately 20 nm or 37 nm and core compositions of either glassy polystyrene or fluid-like poly(methyl acrylate), Sun et al found that small particles with polystyrene cores (18 ± 3 nm) had a greater retention in the blood compared to small particles with poly(methyl acrylate) cores (24 ± 3 nm). The initial accumulation of nanoparticles in the liver, lung, and spleen was higher for small particles with a poly(methyl acrylate) core composition than particles with polystyrene core compositions at 10 min and 1 h. The authors suggested that increased shape adaptability imparted by the more flexible poly(methyl acrylate) core contributed to the observed differences.

Surface properties, such as surface charge and PEGylation, also affect the biodistribution of nanoparticles. Generally, the addition of neutral hydrophilic polymers to the surface of nanoparticles neutralizes the surface charge. Neutralization of surface charge has been associated with improved blood retention time and decreased opsonization by the RES giving rise to the term 'stealth properties' [30]. For example, the addition of PEG to poly(lactide-co-glycolic acid) (PLGA) liposomes (PLGA-mPEG liposomes) affects biodistribution in a manner dependent on the ratio of PLGA to PEG [31]. A comparison between similarly sized PLGA nanoparticles and PLGA-mPEG(256)

nanoparticles revealed that they had different surface charges (-54.2 mV and -5.9 mV, respectively). The neutralized surface charge of the PLGA-mPEG system increased nanoparticle retention in the blood after 3 hours to 42.6% ID in comparison to 4.1% ID of the PLGA dose. Meanwhile, the accumulation of PLGA-mPEG nanoparticles in the liver was generally lower than PLGA nanoparticles. Similar effects have been achieved with the PEGylation of poly(caprolactone) (PCL) nanoparticles [31]. For example, the surface charge of the PCL nanoparticles was increased from -27.17 mV to -6.046 mV by the addition of PEG, and a significant improvement in the blood retention time was accompanied by a drop in nanoparticle accumulation in the liver and lungs for PEGylated PCL nanoparticles.

The change in surface charge imparted by a polymer surface coating is not the only factor affecting biodistribution. The composition of the polymer is a determining factor as well. This phenomenon was explored with the adsorption of poloxamer 407, poloxamine 904, and poloxamine 908 onto the surface of polystyrene and PLGA nanoparticles [32]. Following administration in a rabbit model, the poloxamer 407 coating was the most effective in reducing nanoparticle clearance from the blood and liver accumulation after 3 hours even though the poloxamine 908 formulation had a more neutral surface charge than those with a poloxamer 407 coating.

For much smaller PEGylated nanoparticles, the length of PEG chains and end group functionality plays a greater role in determining biodistribution as demonstrated with 10 nm diameter Gadolinium nanoparticles [33]. The biodistribution of polymer coated Gadolinium nanoparticles was affected by the length of the PEG chains. Differences in the biodistribution of nanoparticles coated with similar lengths of PEG revealed that the end group (carboxylic acid, methoxy, or amine) of the PEG chain affected biodistribution.

Given that lowering systemic toxicity is a goal of targeted delivery and only a fraction of the total dose administered accumulates at the target site, the biodistribution in other tissues and clearance rate are extremely important.

Incorporation and Release of Therapeutics from Nanodelivery Systems

The importance of controlling nanoparticle localization for targeted delivery is inconsequential if a particle cannot carry a relevant amount of drug and release it at the target site. The ability to efficiently incorporate a drug into nanoparticle delivery systems is dependent on the drug itself, the design of the nanoparticle, and the method of loading. Countless strategies have been used to synthesize organic nanoparticles with an intended application in drug delivery, however, only a fraction of these systems have demonstrated a definitive ability to entrap a drug or model molecule, and most of these studies have focused on a relatively small number of nanodelivery systems, most commonly biodegradable PLGA. This section will focus specifically on nanoparticle systems designed to successfully entrap a therapeutic, the strategies used for loading, and data on drug release when available.

Selection of a general nanodelivery system, be it targeted or nontargeted, should reflect the properties of the drug and the intended application. For example, the nanodelivery system should maintain drug stability and should be hydrophilic or hydrophobic to ensure compatibility with the drug. Properties of the drug, such as size, charge, and hydrophilicity or hydrophobicity, typically determine whether the carrier can effectively entrap, protect, and release the drug. Mechanisms for drug entrapment vary depending on the type of nanoparticle and the drug itself. In many cases, the

method of drug loading determines the efficiency of the loading process and ultimately whether a nanodelivery system is suitable for the intended application.

Most nanodelivery systems can be placed into one or more of three large groups: biodegradable polymer nanoparticles; self-assembled carriers including micelles, liposomes, and polymersomes; or hydrophilic crosslinked systems such as nanoscale hydrogels, also called nanogels. While in the case of self-assembled carriers, therapeutics can be simply loaded during micelle or vesicle assembly, biodegradable nanoparticle matrices are loaded during post-polymerization nanoparticle formation using emulsion and solvent evaporation techniques. On the other hand, nanogel systems are typically loaded after nanoparticle formation by incubating the particles in a solution containing the drug. The drug becomes entrapped in the crosslinked network by simple partitioning effects, which allow the drug to diffuse into the nanoparticle matrix. The loading of hydrophilic and hydrophobic drugs in some of these types of nanodelivery systems is shown in Figure 6.

The amount of a drug that has been successfully loaded into a nanodelivery system is typically quantified in one of two ways. The most common measure cited is the entrapment efficiency, also referred to as the encapsulation or incorporation efficiency, which is defined as the fraction of the drug loaded per the total amount of drug used (or available for loading). The other number that is often reported is the loading capacity or loading efficiency, which refers simply to the ratio of the weight of drug incorporated to the weight of the carrier. These quantifications will be cited here as reported in the studies that are discussed.

Biodegradable Nanoparticles

Biodegradable nanoparticles have been widely investigated for use as drug delivery systems, and are versatile platforms for successful encapsulation of a range of therapeutics. These biodegradable polymer nanoparticles are formed most commonly using emulsion and solvent evaporation techniques, where the polymer is first dissolved in an organic phase that is subsequently dropped into a continuous aqueous phase and stirred until the solvent evaporates. Hydrophobic drugs can easily be incorporated into particles during this process by solvating the drug along with the polymer in the organic phase. These oil-in-water emulsions have been used to load a variety of hydrophobic drugs, such as anti-cancer therapeutics [34-36]. In addition to hydrophobic drugs, encapsulation of water-soluble drugs and biomolecules, including proteins and certain chemotherapeutics, has been achieved with water-in-oil-in-water double emulsion techniques [37-39]. Other synthesis techniques, such as nanoprecipitation and spray drying have also been used effectively to produce PLGA nanoparticles loaded with therapeutics [40].

Recent studies have carefully evaluated the effects of PLGA nanoparticle properties on drug loading. For example, smaller nanodelivery systems have a smaller volume, and therefore, would be expected to have a smaller maximum loading capacity. In the majority of studies, the maximum loading capacity is not determined for a carrier. The achieved loading capacity of a delivery system is dependent on factors beyond volume alone. For example, drug loading and release from PLGA micro- and nanospheres have been shown to be inversely correlated with size. In a study that compared two sizes of PLGA particles, dexamethasone was first loaded into PLGA microspheres using a typical oil-in-water solvent evaporation method to produce 20 mm particles. Smaller 1 mm particles loaded with dexamethasone were produced via

emulsion polymerization. The emulsion polymerization scheme for the smaller particles led to a dexamethasone encapsulation efficiency of 11.2% compared to 1% for the larger microparticles when incubating 100 mg of dexamethasone with 500 mg of polymer [41].

Drug delivery systems composed of polyanhydrides have been widely investigated because of their surface eroding mechanism which can lead to near zero-order release profiles [42, 43]. In general, drugs have been successfully incorporated in polyanhydride disks such as the Gliadel® system or microparticles [44]. However, there have been limited studies demonstrating loading and release from polyanhydride carriers on the nanoscale. In one study, paclitaxel or 2-hydroxypropyl-β-cyclodextrin (HPCD)-complexed paclitaxel was encapsulated in polyanhydride nanoparticles composed of poly(methyl vinyl ether-co-maleic anhydride) during particle formation using a solvent displacement method which simultaneously allowed nanoparticle formation and loading. Up to a 167 μg/mg loading capacity was obtained for nanoparticles with an average diameter of 302 nm. The controlled release of HPCD-paclitaxel was then demonstrated in different simulated biological fluids. No release was observed from particles in simulated gastric fluid (pH 1.2) whereas there was complete release over a 24 hour period in simulated intestinal fluid (pH 7.5) [45].

Like synthetic biodegradable systems, nanodelivery systems composed of naturally occurring biodegradable polymers have been investigated for drug delivery. Some of the most widely studied are systems based on the biodegradable and biocompatible polysaccharide chitosan. The potential use of chitosan carriers has been demonstrated for a vast number of drugs and applications. For example, chitosan carriers have received considerable attention for delivery of nucleic acids due to chitosan's net positive charge. One of the contributing factors to chitosan's versatility is

that a number of techniques have been developed to synthesize chitosan nanoparticles including ionic gelation, precipitation, reverse micelle formation, self-assembly, and spray drying [46, 47].

In one study examining the use of chitosan for delivery of biomolecules, a model protein, bovine serum albumin (BSA), was loaded into chitosan nanoparticles prepared by two different methods using tripolyphosphate (TPP) as an ionic crosslinker. In the first method termed "incorporation", BSA was incorporated into the polymer matrix during particle formation by adding BSA to a chitosan solution before the addition of the TPP crosslinker at which point particles spontaneously formed during mixing. Using the "incubation" method, BSA was simply adsorbed to the surface of nanoparticles during incubation following particle coacervation. Encapsulation efficiencies up to 88% were obtained and BSA release was primarily shown to be a fast release over a 6 hour period [48]. In another study, chitosan nanoparticles crosslinked with TPP were loaded with methotrexate disodium (MTX) using a post-polymerization incubation method. Loading capacities up to 52% and loading efficiencies up to 78% were obtained when an MTX concentration of 1.26 mg/mL was incubated with a 0.16 wt% nanogel solution [49].

Chitosan nanoparticles have also been formulated to deliver anticancer drugs. For example, a water-in-oil microemulsion method was used to entrap a doxorubicin-dextran conjugate in chitosan nanoparticles having a hydrodynamic diameter of 100 nm. Entrapment efficiencies were measured between 60-65%. In a mouse model, treatment with the loaded nanoparticles led to faster and more complete tumor regression than free drug or empty nanoparticles [50].

Another natural biodegradable material used to synthesize nanoparticles for drug delivery applications is the anionic biopolymer alginate. Most often calcium chloride is added to a solution of alginate to induce ionic crosslinking, resulting in micro-

and nanoparticle polymer networks. In one case, alginate gelation with calcium ions followed by coating with chitosan produced nanoparticles intended for oral insulin delivery applications. A maximum insulin encapsulation efficiency was measured at 92% with loading capacities up to 14.3% [51]. Isoniazid, rifampicin, and pyrazinamide were encapsulated in alginate particles using a cation gelation method in an effort to design aerosolized nanoparticles for treatment of tuberculosis. Calcium chloride was added to sodium alginate solution containing varying amounts of the three drugs to induce the gelation and encapsulation of the drug. Drug encapsulation efficiencies ranged from 70-90% in particles at the upper limit of so-called nanoparticles with an average size just around 1 μm [52].

Self-Assembled Nanoparticles

Self-assembled nanoparticles, including liposomes, micelles, and polymersomes, can be formed using various amphiphiles such as natural lipids or block copolymers. Liposomes are vesicles that consist of a spherical shaped lipid bilayer, or multilayers, containing an inner aqueous void space. Liposomal encapsulation is a versatile method to load therapeutics, because hydrophilic drugs and biomolecules can be loaded in the inner aqueous void, while hydrophobic molecules can be entrapped in the lipid bilayer. Liposomal delivery of chemotherapeutics has been established as an effective method to increase efficacy and decrease toxicity over free drug, evidenced by the success of liposomal doxorubicin, Doxil®, which has been approved for human use in cancer treatment [53].

In addition to the lipid structures, synthetic block copolymers built with one hydrophilic block and one hydrophobic block have been shown to exhibit a variety of self-assembled structures including spherical or cylindrical micelles and vesicles with

architectures that resemble liposomes known as polymersomes [54]. Micelles, nanoparticles with a hydrophobic core and hydrophilic outer layer, self-assembled from amphiphilic block copolymers in aqueous media, are frequently used to entrap hydrophobic drugs during micelle formation. During spontaneous micelle formation in an aqueous environment, hydrophobic drugs are localized in and around the hydrophobic core [55]. This loading method has been used to entrap a variety of therapeutics, particularly anticancer agents, in block copolymers of poloxamers, which consist of blocks of poly(ethylene oxide) (PEO) and poly(propylene oxide) (PPO), and NK105, which consists of blocks of PEG and a modified polyaspartate [56-58].

Using this method of drug loading, micelle nanoparticles have been used to entrap hydrophobic anticancer therapeutics. Biodegradable, cationic micelle nanoparticles were self-assembled using amphiphilic poly{(N-methyldietheneamine sebacate)-co-[(cholesteryl oxocarbonylamido ethyl) methyl bis(ethylene) ammonium bromide] sebacate}, P(MDS-co-CES). In this study, Herceptin®, which is a monoclonal antibody, was attached to the surface of the particles while paclitaxel was loaded into the micelles by dissolving the polymer and drug in DMF and dialyzing against a sodium acetate/acetic acid buffer. This method let to encapsulation efficiencies of paclitaxel of 58.1% and a loading capacity of 14.3%. Release studies demonstrated the that the drug could be released from the nanoparticles over a 69 hour period [59].

While traditional micelle systems have been used primarily to incorporate hydrophobic drugs, adapted systems have been used to entrap more hydrophilic species such as biomolecules. For example, drug carrier systems called polyion complex (PIC) micelles have been synthesized from PEG block copolymers. The PIC micelles are formed using block copolymers consisting of a hydrophilic block and a polyionic block. In this case, electrostatic interactions between the ionic polymer and an oppositely charged

species are a driving force for the formation of the micelles. Poly(ethylene glycol-grafted-chitosan), PEG-g-chitosan, block copolymers were used to entrap diammonium glycyrrhizinate (DG) in micelles assembled in acetate buffer after addition of TPP to induce chitosan aggregation. Loading efficiencies of DG over 96% have been obtained using these systems and the average diameter of micelles was between 20 and 30 nm. Release profiles varied based on the free ions in solution. In ionic solution, a burst release was observed, but there was limited release in DI water [60].

Polymer vesicles called polymersomes or polymerosomes have been used to entrap a variety of therapeutics and model drugs. For example, polymersomes with diameters around 100 nm were prepared from triblock copolymers, poly(caprolactone)-poly(ethylene glycol)-poly(caprolactone), PCL-PEG-PCL, using a double emulsion method. Insulin was incorporated during self-assembly of 122 nm particles [61]. In another study, triblock copolymers, poly(ethylene oxide)-b-poly(acrylic acid)-b-poly(N-isopropylacrylamide) (PEO-PAA-PNIPAM), were synthesized via RAFT polymerization. The resulting polymers were water soluble at room temperature, but formed polymer vesicles with diameters between 170 and 250 nm above 32º C. These polymersomes were loaded with FITC-dextran during self-assembly at elevated temperatures and then crosslinked using cystamine via carbodiimide chemistry. The crosslinks were shown to degrade in the presence of dithiothreitol, and therefore, it was hypothesized that these systems are degradable *in vitro* and in vivo. Loading capacity of these nanoparticles was measured at levels exceeding 85% by weight [62].

Recently, there has been interest in creating systems that are hybrid particles combining properties of liposomes and synthetic polymer systems for nanodelivery applications. Cationic lipids have been combined with peptide-lipid amphiphiles and 1,2-distearoyl-*sn*-glycero-3-phosphoethanolamine-*N*-carboxy(polyethylene glycol) to

design liposome nanoparticles targeted to the urokinase plasminogen activator receptor (uPAR) overexpressed on many tumors. The particles have an ABCD structure, an inner aqueous (A) layer of loaded anionic nucleic acids, a cationic lipid bilayer (B), a PEG layer for stealth characteristics (C), and a peptide sequence layer for targeting of uPAR (D). Loading efficiencies as high as 60% were achieved when 10 wt% docetaxel was added during the particle self-assembly process [63]. In another example, hybrid systems were formed through self-assembly to form nanoparticles with a lipid monolayer surrounding a PLGA core loaded with a hydrophobic drug. This unique system relied on PEG-conjugated lecithin to form a hydrophilic outer shell of PEG as the lipid monolayer formed around the hydrophobic PLGA polymer. Drug loading of docetaxel into the PLGA core was accomplished during this self-assembly process by first dissolving polymer and drug in an organic solvent and then dripping this solution into an aqueous solution containing PEG-lecithin. This process led to the formation of the particles via self-assembly and the solvent was allowed to evaporate. Encapsulation efficiencies of 62% were obtained using this method when adding 10 wt% docetaxel to the organic polymer solution. Controlled release was observed over a 100 h period and shown to be a function of lipid coverage, where the release rate could be slowed by increasing the lipid to polymer ratio [64].

Nanogels

Nanoscale hydrogels, or nanogels, are hydrophilic crosslinked polymer networks that imbibe water, but are insoluble in aqueous environments. Drugs can be loaded into the polymer matrix of these materials and controlled release is dependent on the diffusion coefficient of the drug through the hydrogel network. Additionally, hydrogel nanoparticle systems have been developed in a class of drug carriers know as

"intelligent" or "smart" delivery systems. Nanogels can swell in aqueous medium and also can respond to a variety of environmental stimuli such as pH, temperature, ionic strength, or electric field through an increase or decrease in volume [65, 66]. Typically, nanogels are used to carry a drug when the matrix is in a more collapsed state. Following a change in stimulus the nanogel swells, thereby increasing the mesh size and the rate of diffusion of the drug out of the polymer matrix. Alternatively, a method in which the drug is squeezed out of the nanogel has been used to obtain a fast release, where a drug is entrapped in a hydrogel in the swollen state, but upon deswelling the drug is squeezed out of the polymer matrix [67, 68].

While most biodegradable or self-assembled nanoparticle systems are formed from previously synthesized polymers, hydrogel nanoparticles are most commonly synthesized using heterogeneous polymerization techniques. Because the hydrogel nanoparticles are formed during polymerization, incorporating a therapeutic at this stage requires exposing the drug to polymerization conditions that could potentially damage or modify the drug. However, the porous characteristics of nanogel matrices allows for drug loading following polymerization by partitioning methods, which eliminates the need to subject the drug to harsh polymerization conditions. In most situations, the drug is loaded into the nanogel by incubating the nanoparticles with the drug in aqueous conditions such that the particles are in their most swollen state. After a period of time to allow the therapeutic to diffuse into the polymer matrix, a condition (most commonly pH or temperature) is altered, leading to a particle size transition to a more collapsed state with a smaller mesh size, physically entrapping the therapeutic in the polymer matrix.

The hydrophilic nature of hydrogel systems makes them an ideal candidate for the loading and delivery of water soluble therapeutics, of particular interest

biomacromolecules such as proteins or nucleic acids. Several nanogel systems have been investigated for the delivery of insulin to the small intestine. In addition to their ability to entrap the water soluble insulin, some of these systems have advantageous pH-sensitive properties allowing them to protect insulin in the acidic environment of the stomach and release it in the more neutral pH of the small intestine [69, 70]. Polybasic nanoparticles are cationic pH responsive hydrogels with PEG grafts. A UV-initiated free radical emulsion polymerization was used to synthesize poly[2-(diethylamino) ethyl methacrylate] surface grafted with PEG (PDGP) nanogels. Insulin as a model drug was added to a solution of the nanogels and the pH was adjusted to 6.5 to swell the nanoparticles. After a loading period the pH was raised quickly to 7.4 to collapse the particles and entrap the loaded protein. The loaded nanogels were dialyzed against water for 5 days to remove any excess protein not loaded. Encapsulation efficiencies were measured up to 92% for insulin in PDGP particles with low crosslinking densities when equal weights of particles and protein were added to the loading solution [71].

Controlled drug loading and release has also been shown in several studies using hydrogels based on the temperature-sensitive polymer poly(N-isopropylacrylamide) (PNIPAAm). PNIPAAm exhibits a negative swelling transition at 34 ºC, which makes it an attractive system from a physiological standpoint for applications in drug delivery. For example, poly(NIPAAm) and poly(NIPAAm-co-AA) nanoparticles were loaded with 5-fluorouracil and release was shown to be a function of pH and temperature [72].

Nanogels of poly(vinyl alcohol), PVA, and poly(vinyl pyrrolidone), PVP have also been investigated for drug delivery applications. For example, composite systems of PVA-crosslinked PVP nanogels were used to entrap ferromagnetic particles as well as bleomycin A5 hydrochloride. Nanogels were prepared using a water-in-oil emulsion polymerization initiated by gamma ray irradiation. For this emulsion polymerization,

the aqueous phase contained the PVA, PVP, and ferromagnetic particles. The resulting nanogels entrapped the ferromagnetic particles and were then used to load bleomycin A5 hydrochloride. Dry nanoparticles were allowed to swell in an aqueous solution containing the drug, sonicated, and then placed on a shaker plate for 12 h of storage until no apparent liquid was visible. Encapsulation efficiency was not reported, because it was assumed that all of the drug had been immobilized, but *in vitro* release occurred over a minimum period of 8 hours [73].

While most hydrogel nanodelivery systems have been used to entrap hydrophilic molecules, recent work on modified hydrogels has demonstrated the potential to load hydrophobic drugs as well. In order to do so, the hydrophobicity of the nanogels has been increased through the incorporation of amphiphiles into the hydrogel matrix. An acrylated PEG-PPG-PEG triblock copolymer with both hydrophobic and hydrophilic groups was used to synthesize crosslinked nanoparticles via an inverse microemulsion using a PEG crosslinker. Properties of the emulsion could be altered to control for particle sizes ranging from 50 to 500 nm. These nanogels were then loaded with doxorubicin to determine their ability to carry hydrophobic drugs. Doxorubicin, solubilized in $CHCl_3$ with triethylamine, was added to an aqueous solution of nanoparticles and the $CHCl_3$ was allowed to evaporate overnight. The results indicated that the formation of nanogels from amphiphilic macromers was a successful strategy for loading hydrophobic drugs in a hydrogel with up to 9.8% loading capacity of doxorubicin [74].

While the control and optimization of drug loading and release are key challenges in the field of nanodelivery, there is not a single carrier or loading mechanism that is ideal for any drug and any application. Each nanodelivery system and drug pairing is unique. Future studies on the interplay between the properties of the carrier,

properties of the drug, and the mechanisms of loading will to significantly improve nanodelivery from a drug loading and release vantage point.

Conclusion

As the field of targeted drug delivery continues to move forward, it will be increasingly important to design nanoscale systems with tailorable properties for efficient delivery and improved therapeutic efficacy. Important design considerations will include the physicochemical properties that govern targeting, biodistribution, and clearance as well as the system's effectiveness in carrying, protecting, and even releasing active therapeutic and diagnostic agents.

The selection and addition of targeting ligands to the surface of nanoparticles has already been shown to improve therapeutic efficacy over systems without targeting ligands. We are only beginning to understand the role that targeting ligands play in interfacing interactions of nanoparticles and cells. The few studies that have compared targeted and nontargeted systems have demonstrated that the role of targeting ligands in localization at the target site is application dependent. Targeted delivery to atherosclerotic lesions is greatly enhanced by targeting ligands which impart an improved ability to accumulate at the target site. However, in the case of tumor targeting, improved performances of targeted systems over nontargeted systems has been accomplished by improved cellular uptake as well as improved accumulation at the target site. Some of these studies have suggested that the primary benefit of incorporating targeting ligands is to mediate cell internalization. Only a small number of studies have focused on comparing the *in vivo* performance and biodistribution of

targeted and nontargeted delivery systems. Further study is necessary to truly determine how the presence of a targeting ligand affects targeted delivery.

Design of the physicochemical properties, including size, shape, surface charge, and mechanical characteristics, of the nanoparticle itself will continue to be key design parameters due to their effect on biodistribution. It is important to account for all of these factors in concert with targeting strategies to understand how to predict and control nanoparticle distribution. Many of the same properties that govern biodistribution also determine the clearance rate. The challenge in designing materials for targeted delivery is that the material properties should allow an appropriate residence time that is long enough for particle localization and delivery of the drug or diagnostic but does not prevent the system from being fully eliminated in an acceptable amount of time. The desired particle residence time will vary with the intended application, and this time frame can be tuned. Ultimately, the challenge lies in designing a system that has the perfect combination of properties to allow for sufficient interaction of the targeted nanoparticles with the target site, desirable biodistribution, and efficient removal.

The material properties that contribute to targeting, biodistribution, and elimination must also be balanced with the properties that affect the ability to entrap a therapeutic or diagnostic. The primary consideration in determining the ability of a nanoparticle system to entrap a molecule is the interaction between the polymer and the therapeutic. This relationship is often a balance of intermolecular interactions including hydrophobic/hydrophilic and electrostatic interactions. Another consideration is the method in which the drug can be incorporated into the material, and whether the available methods will allow an acceptable amount of the therapeutic to be loaded into the carrier. Both the loading strategy and stability of the entrapped drug must also be

carefully considered in order to design systems that are able to carry a sufficient amount of drug to the target site.

As we move towards developing optimally effective, high performance nanodelivery systems, it will be necessary to design new materials that incorporate the best properties for targeting, biodistribution, clearance, drug incorporation, and release at the target site.

Acknowledgments

This work was supported in part by the National Institutes of Health (grant EB000246 and a Physical Science-Oncology Centers U54 grant) and the National Science Foundation (grant DGE-03-33080).

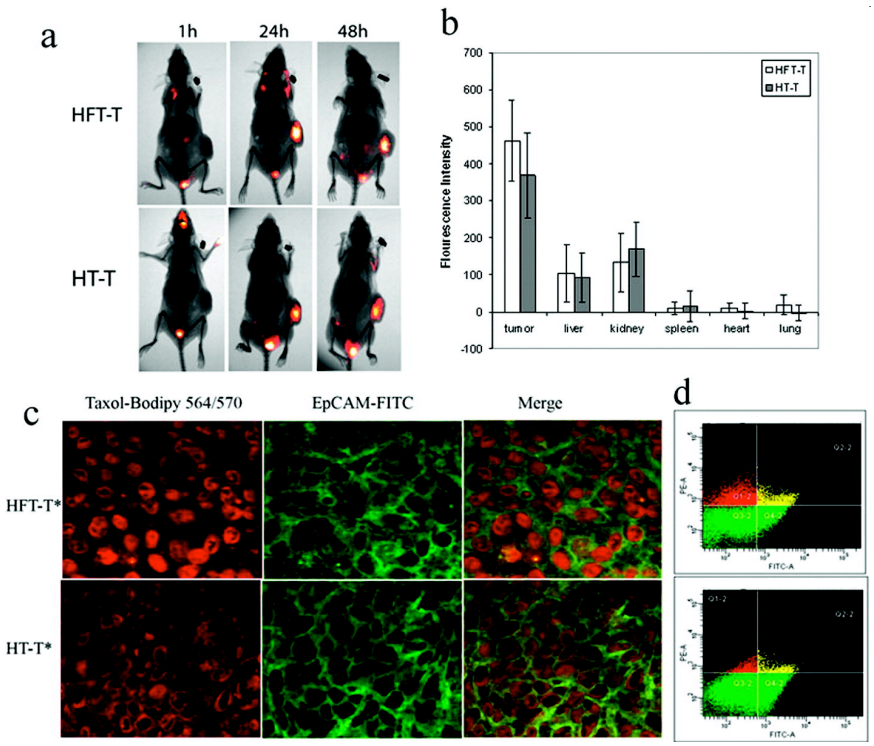

Figure A.1. The in vivo biodistribution of intravenously administered targeted HFT-T nanodelivery systems and nontargeted HT-T was investigated in a KB-3-1 xenograft-bearing mouse model.

Near-infrared fluorescence imaging of mice at 1, 24, and 48 h showed the biodistribution of nanodelivery systems. (b) At 48 h, the biodistribution of nanoparticles in various tissues was quantified by fluorescence intensity. (c) Nanoparticle (red) uptake by xenograft cells was shown by colocalization with EpCAM-positive (green) xenograft cells. Targeted systems were found predominantly in cells while nontargeted systems were less likely to be internalized remaining in the extracellular matrix. (d) Flow cytometry of disaggregated xenograft cells stained with a FITC-conjugated EpCAM antibody distinguished nanoparticle uptake in human xenograft tumor cells from nanoparticle uptake in host non-tumor cells for targeted and control nanoparticles. Human tumor cells were EpCAM positive in Q4-2 (green in lower right quadrant) and Q2-2 (yellow). Nanoparticle uptake by tumor cells are shown in Q2-2 (yellow), and nanoparticle uptake in host cells are shown in Q1-2 (red). Reprinted with permission from [2]. Copyright 2009 American Chemical Society.

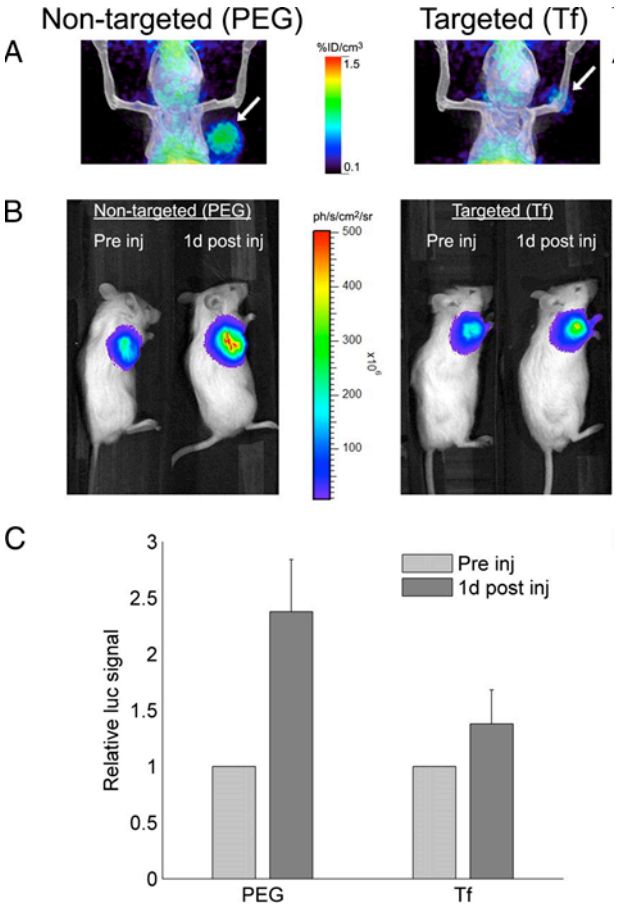

Figure A.2. The in vivo performance of siRNA administered via targeted and nontargeted nanodelivery systems.

(a) Micro-PET/CT images of mice show the distribution of targeted and nontargeted nanoparticles in tumors (arrow) 1 day after administration. (b) Bioluminescence imaging of mice shows luciferase expression in the tumor before and 1 day after administration of nontargeted and targeted nanoparticles. (c) A decrease in luciferase activity was associated with siRNA activity 1 day after administration of targeted (Tf) nanoparticles and nontargeted (PEG) nanoparticles. Error bars represent standard error. Reproduced from [5]. Copyright 2007 National Academy of Sciences, U.S.A.

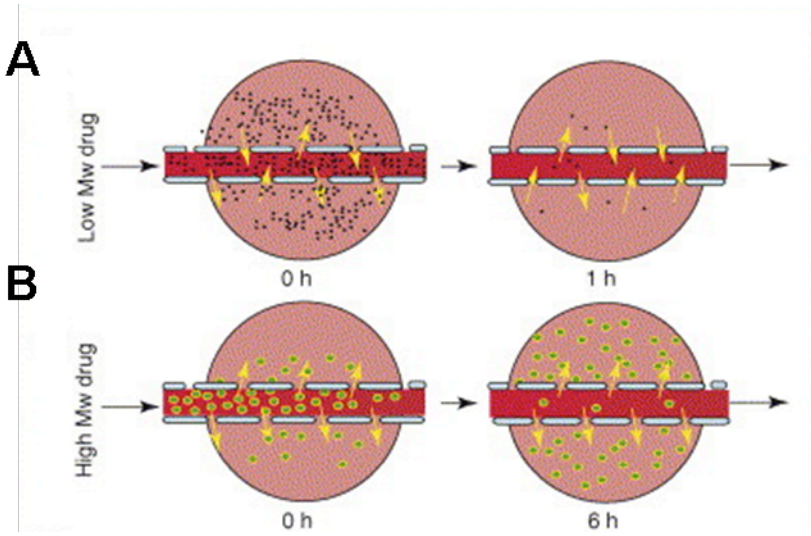

Figure A.3. Transport of small and large molecular weight drugs and nanoparticles from defective tumor vasculature into tumor space.

(a) Small molecular weight drugs (black) can diffuse out of tumor vasculature but can also diffuse back into tumor vasculature which allows clearance of these compounds from the tumor space. (b) Larger molecular weight drugs or nanoparticles (green) can diffuse into the tumor space but are retained due to the EPR effect. Reprinted from [10], Copyright 2006, with permission from Elsevier.

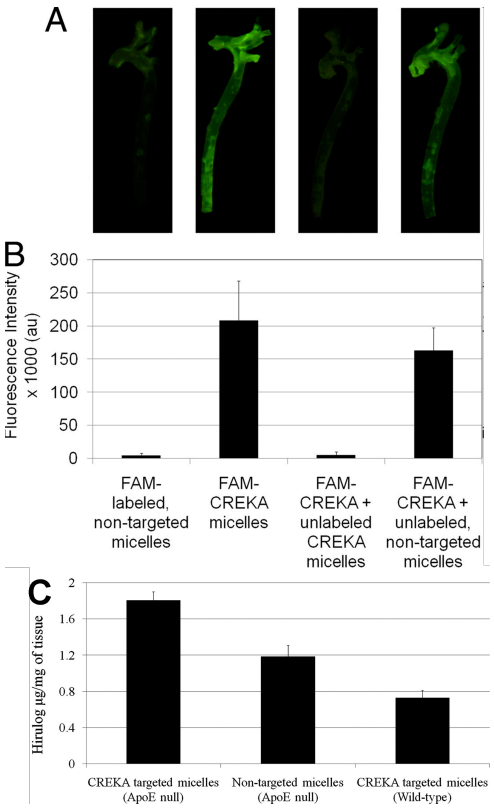

Figure A.4. Delivery of image contrast agent and a heparin hirulog to atherosclerotic plaques in the aortic tree of ApoE-null mice using micelles.

(a) Fluorescence images of excised aortic trees show that image contrast with fluorescently labeled (FAM-labeled) nontargeted micelles is improved upon by targeted (FAM-CREKA) micelles. The contrast provided by FAM-CREKA micelles disappears with the addition of excess targeted micelles lacking a fluorescent label. Contrast is not significantly decreased when FAM-CREKA targeted micelles are administered along with nontargeted micelles without a fluorescent label. (b) The average fluorescence intensity of image pixels for the various studies. (c) The delivery of the anticoagulant peptide hirulog-2 to atherosclerotic plaques from micelles was quantified with a thrombin activity assay. In an ApoE null mouse model, hirulog delivery was significantly improved using targeted micelles compared to nontargeted micelles. The delivery of hirulog via targeted micelles in wild-type mice was significantly lower than targeted delivery in the ApoE atherosclerotic model. Reproduced from [13]. Copyright 2009 National Academy of Sciences, U.S.A.

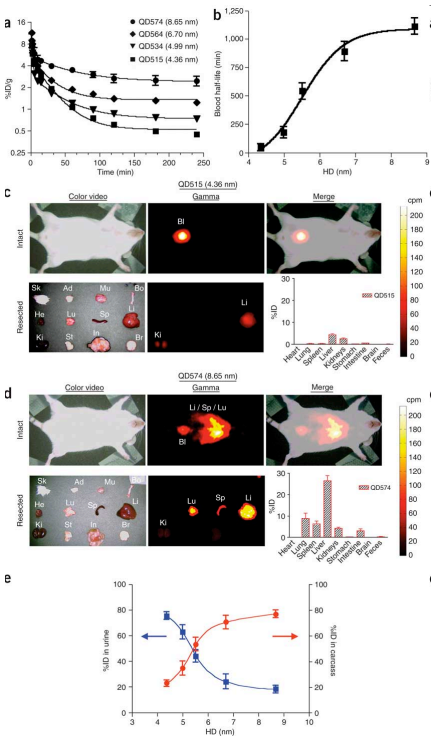

Figure A.5. CdSe core and ZnS shell quantum dot clearance from blood, biodistribution, and renal clearance.

(a) The concentration of radiolabeled quantum dots in blood after intravenous injection in a CD-1 mouse model decreases with nanoparticle size. (b) For quantum dots between 4 and 9 nm, the blood half-life of quantum dots increases with size. (c) Color video (left) and gamma-ray images taken with an Anger camera (middle) to show the biodistribution of 4.36 nm quantum dots in animals immediately after sacrifice (top row) and in organs (bottom row). The merged color image and gamma-ray image show nanoparticles in the bladder (Bl) (top right). The overall biodistribution of quantum dots in each organ is also quantified (bottom right). Abbreviations are: skin (Sk), adipose (Ad), muscle (Mu), bone (Bo), heart (He), lungs (Lu), spleen (Sp), liver (Li), kidneys (Ki), stomach (St), intestine (In), and brain (Br). (d) Biodistribution of 8.65 nm quantum dots following intravenous injection. Data corresponds to Figure 5c. (3) Quantum dot excretion via urine 4 h post-injection (blue) decreases with size and retention in the body (red) increases with size. Data is mean ± standard deviation. Reprinted by permission from Macmillan Publishers Ltd: [18], Copyright 2007.

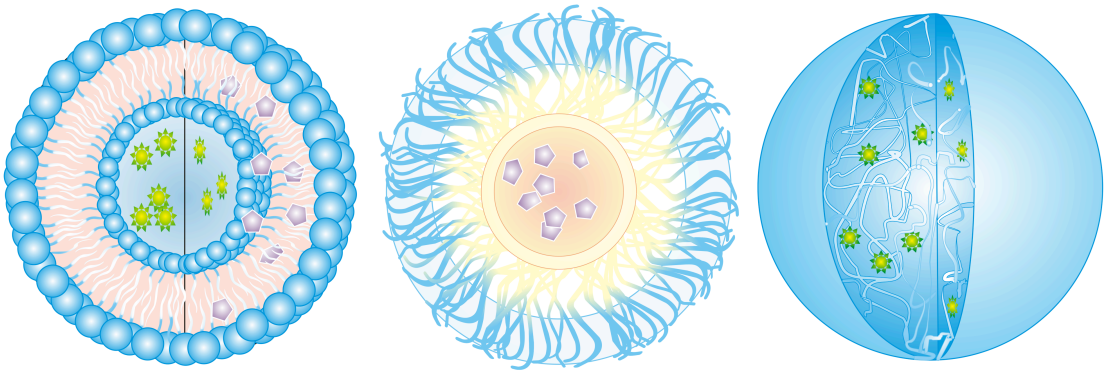

Figure A.6. Drug loading of various nanodelivery systems.

(a) Liposome loaded with hydrophilic (green) and hydrophobic drugs (purple). (b) Encapsulation of hydrophobic drugs in a micelle. (c) Entrapment of hydrophilic drugs in n**anogels.**

Table A.1. Summary of studies on tumor accumulation of nanodelivery systems

List of abbreviations for Table 1: initial dose (ID), nanoparticles (NPs), poly(ethylene glycol)-poly(aspartate-hydrazone-adriamycin) (PEG-p(ASP-Hyd-ADR)), Gadolinium (Gd), poly(acrylic acid-b-methyl acrylate) (PAA-b-PMA), epidermal growth factor receptor (EGFR), single-chain variable fragment antibody (ScFv), transferrin (Tf), α-melanocyte-stimulating hormone analog (NDP-MSH), PEGylated-hollow gold nanospheres (PEG-HauNS)

	Formulation	Tumor Accumulation	Dose	Tumor and Animal Model	Study
PEGylated Gadolinium nanoparticles	Folate and PEG-coated PEGylated	5% ID at 5 h, 7% ID at 8 h 4% ID at 5 h, 9% ID at 8 h	10 mg NPs/kg mouse weight (1.6 mg Gd/kg)	KB, athymic mice	[3]
PEG-p(ASP-Hyd-ADR) nanoparticles	Folate PEGylated	6-8% ID at 4 h, 4-7 % ID at 24 h ~6% ID at 4 h, ~4% ID at 24 h	10 mg/kg ADR	KB, CD-1 nude mice	[4]
^{64}Cu labeled shell-crosslinked nanoparticles of PAA-b-PMA	Folate Nontargeted	5.9 ± 2.8% ID/g, 0.04 ± 0.02 %ID 6.0 ± 1.9% ID/g, 0.13 ± 0.04 %ID at 4 h	370-440 kBq NPs or 3-5 mg/kg mouse weight	KB, folate-deficient athymic nude mice	[12]
^{64}Cu labeled nanoparticles with cyclo-dextrin containing polycations	Tf PEGylated	< 2% ID/cm^3 over 60 min < 2% ID/cm^3	100-300 μCi ^{64}Cu	Neuro2A-Luc, NOD/SCID mice	[5]
Colloidal gold nanoparticles	EGFR ScFv nanotags PEGylated nanotags	~ 8 ppm (gold/g tissue) at 5 h <1 ppm	45 femtomoles	Tu686, nude mice	[6]
Immunoliposomes	Anti-HER2 liposomes Nontargeted liposomes	8.34% ID/g tissue at 24 h 7.18% ID/g tissue 7.32% ID/g tissue 8.59% ID/g tissue	40 μmol/kg mouse weight	BT-474, mice MCF-7, mice BT-474 MCF-7	[8]
PEGylated gold nanoparticles	20 nm 80 nm	6.63 % ID at 48 hours 0.30% ID	2.6 x 10^{11} NPs /mouse	A431, mouse	[24]
Hollow gold nanospheres with α–melanocyte-stimulating hormone analog (NDP-MSH)	NDP-MSH-PEG-HauNS PEG-HAuNS	4.3 +-1.2% ID/g at 4 hours 12.6 +- 3.1% ID/g	2 x 10^{12} NPs/mouse	B16/F10, mouse	[75]

Table A.2. Measurement techniques for quantifying biodistribution

Technique	Agent	Study
Computed tomography (CT)	Iohexol	[76]
Fluorescence imaging	Cy5.5	[2]
Inductively coupled atomic emission spectroscopy (ICP-AES)	Gd	[3]
Inductively coupled plasma-mass spectrometry (ICP-MS)	Au	[6, 22, 25]
	Fe	[77]
Micro-positron emission tomography (PET)/computed tomography (CT)	^{64}Cu	[5]
MRI imaging	Gd	[15]
Radiography	^{111}In	[3, 9, 24, 32]
	^{67}Ga	[8]
	^{125}I-CA	[30]
	^{64}Cu	[12,29]
	Tc-O complex	[78]
	C^{14}	[79]
Superconducting quantum interference device (SQUID) magnetometer	Iron	[28]
Two-photon luminescence	Gold nanorods	[80]

REFERENCES

1. Byrne, J. D., T. Betancourt and L. Brannon-Peppas, Active targeting schemes for nanoparticle systems in cancer therapeutics. *Adv. Drug Deliv. Rev.*, 2008, 60, 1615-1626.

2. Wang, X., J. Li, Y. Wang, K. J. Cho, G. Kim, A. Gjyrezi, L. Koenig, P. Giannakakou, H. J. Shin, M. Tighiouart, S. Nie, Z. G. Chen and D. M. Shin, HFT-T, a Targeting Nanoparticle, Enhances Specific Delivery of Paclitaxel to Folate Receptor-Positive Tumors. *ACS Nano*, 2009, 3, 3165-3174.

3. Oyewumi, M. O., R. A. Yokel, M. Jay, T. Coakley and R. J. Mumper, Comparison of cell uptake, biodistribution and tumor retention of folate-coated and PEG-coated gadolinium nanoparticles in tumor-bearing mice. *J. Control. Release*, 2004, 95, 613-626.

4. Bae, Y., N. Nishiyama and K. Kataoka, In vivo antitumor activity of the folate-conjugated pH-Sensitive polymeric micelle selectively releasing adriamycin in the intracellular acidic compartments. *Bioconjugate Chem.*, 2007, 18, 1131-1139.

5. Bartlett, D. W., H. Su, I. J. Hildebrandt, W. A. Weber and M. E. Davis, Impact of tumor-specific targeting on the biodistribution and efficacy of siRNA nanoparticles measured by multimodality in vivo imaging. *Proc. Natl. Acad. Sci. U. S. A.*, 2007, 104, 15549-15554.

6. Qian, X., X. H. Peng, D. O. Ansari, Q. Yin-Goen, G. Z. Chen, D. M. Shin, L. Yang, A. N. Young, M. D. Wang and S. Nie, In vivo tumor targeting and spectroscopic detection with surface-enhanced Raman nanoparticle tags. *Nat. Biotechnol.*, 2008, 26, 83-90.

7. Park, J. W., K. Hong, D. B. Kirpotin, G. Colbern, R. Shalaby, J. Baselga, Y. Shao, U. B. Nielsen, J. D. Marks, D. Moore, D. Papahadjopoulos and C. C. Benz, Anti-HER2 immunoliposomes: Enhanced efficacy attributable to targeted delivery. *Clin. Cancer Res.*, 2002, 8, 1172-1181.

8. Kirpotin, D. B., D. C. Drummond, Y. Shao, M. R. Shalaby, K. Hong, U. B. Nielsen, J. D. Marks, C. C. Benz and J. W. Park, Antibody targeting of long-circulating lipidic nanoparticles does not increase tumor localization but does increase internalization in animal models. *Cancer Res.*, 2006, 66, 6732-6740.

9. ElBayoumi, T. A. and V. P. Torchilin, Tumor-Specific Anti-Nucleosome Antibody Improves Therapeutic Efficacy of Doxorubicin-Loaded Long-Circulating Liposomes against Primary and Metastatic Tumor in Mice. *Mol. Pharm.*, 2009, 6, 246-254.

10. Iyer, A. K., G. Khaled, J. Fang and H. Maeda, Exploiting the enhanced permeability and retention effect for tumor targeting. *Drug Discov. Today*, 2006, 11, 812-818.

11. Pirollo, K. F. and E. H. Chang, Does a targeting ligand influence nanoparticle tumor localization or uptake? *Trends Biotechnol.*, 2008, 26, 552-558.

12. Rossin, R., D. Pan, K. Qi, J. L. Turner, X. Sun, K. L. Wooley and M. J. Welch, Cu-64-labeled folate-conjugated shell cross-linked nanoparticles for tumor imaging and radiotherapy: Synthesis, radiolabeling, and biologic evaluation. *J. Nucl. Med.*, 2005, 46, 1210-1218.

13. Peters, D., M. Kastantin, V. R. Kotamraju, P. P. Karmali, K. Gujraty, M. Tirrell and E. Ruoslahti, Targeting atherosclerosis by using modular, multifunctional micelles. *Proc. Natl. Acad. Sci. U. S. A.*, 2009, 106, 9815-9819.

14. Kelly, K. A., J. R. Allport, A. Tsourkas, V. R. Shinde-Patil, L. Josephson and R. Weissleder, Detection of vascular adhesion molecule-1 expression using a novel multimodal nanoparticle. *Circ. Res.*, 2005, 96, 327-336.

15. Neubauer, A. M., H. Sim, P. M. Winter, S. D. Caruthers, T. A. Williams, J. D. Robertson, D. Sept, G. M. Lanza and S. A. Wickline, Nanoparticle Pharmacokinetic Profiling In Vivo Using Magnetic Resonance Imaging. *Magn. Reson. Med.*, 2008, 60, 1353-1361.

16. Park, Y., H. Y. Hong, H. J. Moon, B. H. Lee, I. S. Kim, I. C. Kwon and K. Rhee, A new atherosclerotic lesion probe based on hydrophobically modified chitosan nanoparticles functionalized by the atherosclerotic plaque targeted peptides. *J. Control. Release*, 2008, 128, 217-223.

17. Jaffer, F. A., M. Nahrendorf, D. Sosnovik, K. A. Kelly, E. Aikawa and R. Weissleder, Cellular imaging of inflammation in atherosclerosis using magnetofluorescent nanomaterials. *Mol. Imaging*, 2006, 5, 85-92.

18. Choi, H. S., W. Liu, P. Misra, E. Tanaka, J. P. Zimmer, B. Itty Ipe, M. G. Bawendi and J. V. Frangioni, Renal clearance of quantum dots. *Nat. Biotechnol.*, 2007, 25, 1165-1170.

19. Owens, D. E. and N. A. Peppas, Opsonization, biodistribution, and pharmacokinetics of polymeric nanoparticles. *Int. J. Pharm.*, 2006, 307, 93-102.

20. Moghimi, S. M. and J. Szebeni, Stealth liposomes and long circulating nanoparticles: critical issues in pharmacokinetics, opsonization and protein-binding properties. *Prog. Lipid Res.*, 2003, 42, 463-478.

21. Fitzpatrick, J. A., S. K. Andreko, L. A. Ernst, A. S. Waggoner, B. Ballou and M. P. Bruchez, Long-term Persistence and Spectral Blue Shifting of Quantum Dots in Vivo. *Nano Lett.*, 2009, 9, 2736-2741.

22. Akiyama, Y., T. Mori, Y. Katayama and T. Niidome, The effects of PEG grafting level and injection dose on gold nanorod biodistribution in the tumor-bearing mice. *J. Control. Release*, 2009, 139, 81-84.

23. Sun, W., W. Zou, G. Huang, A. Li and N. Zhang, Pharmacokinetics and targeting property of TFu-loaded liposomes with different sizes after intravenous and oral administration. *J. Drug Target.*, 2008, 16, 357-365.

24. Zhang, G., Z. Yang, W. Lu, R. Zhang, Q. Huang, M. Tian, L. Li, D. Liang and C. Li, Influence of anchoring ligands and particle size on the colloidal stability and in vivo biodistribution of polyethylene glycol-coated gold nanoparticles in tumor-xenografted mice. *Biomaterials*, 2009, 30, 1928-1936.

25. De Jong, W. H., W. I. Hagens, P. Krystek, M. C. Burger, A. J. Sips and R. E. Geertsma, Particle size-dependent organ distribution of gold nanoparticles after intravenous administration. *Biomaterials*, 2008, 29, 1912-1919.

26. Glangchai, L. C., M. Caldorera-Moore, L. Shi and K. Roy, Nanoimprint lithography based fabrication of shape-specific, enzymatically-triggered smart nanoparticles. 2008, 125, 263-272.

27. Gratton, S. E., P. A. Ropp, P. D. Pohlhaus, J. C. Luft, V. J. Madden, M. E. Napier and J. M. DeSimone, The effect of particle design on cellular internalization pathways. *Proc. Natl. Acad. Sci. U. S. A.*, 2008, 105, 11613-11618.

28. Park, J. H., G. von Maltzahn, L. Zhang, M. P. Schwartz, E. Ruoslahti, S. N. Bhatia and M. J. Sailor, Magnetic iron oxide nanoworms for tumor targeting and imaging. *Adv. Mater.*, 2008, 20, 1630-1635.

29. Sun, X., R. Rossin, J. L. Turner, M. L. Becker, M. J. Joralemon, M. J. Welch and K. L. Wooley, An assessment of the effects of shell cross-linked nanoparticle size, core composition, and surface PEGylation on in vivo biodistribution. *Biomacromolecules*, 2005, 6, 2541-2554.

30. Avgoustakis, K., A. Beletsi, Z. Panagi, P. Klepetsanis, E. Livaniou, G. Evangelatos and D. S. Ithakissios, Effect of copolymer composition on the physicochemical characteristics, in vitro stability, and biodistribution of PLGA-mPEG nanoparticles. *Int. J. Pharm.*, 2003, 259, 115-127.

31. Shan, X., Y. Yuan, C. Liu, X. Tao, Y. Sheng and F. Xu, Influence of PEG chain on the complement activation suppression and longevity in vivo prolongation of the PCL biomedical nanoparticles. *Biomed. Microdevices*, 2009, 11, 1187-1194.

32. Dunn, S. E., A. G. A. Coombes, M. C. Garnett, S. S. Davis, M. C. Davies and L. Illum, In vitro cell interaction and in vivo biodistribution of poly(lactide-co-glycolide) nanospheres surface modified by poloxamer and poloxamine copolymers. *J. Control. Release*, 1997, 44, 65-76.

33. Faure, A. C., S. Dufort, V. Josserand, P. Perriat, J. L. Coll, S. Roux and O. Tillement, Control of the in vivo Biodistribution of Hybrid Nanoparticles with Different Poly(ethylene glycol) Coatings. *Small*, 2009, 5, 2565-2575.

34. Govender, T., S. Stolnik, M. C. Garnett, L. Illum and S. S. Davis, PLGA nanoparticles prepared by nanoprecipitation: drug loading and release studies of a water soluble drug. *J. Control. Release*, 1999, 57, 171-185.

35. Mu, L. and S. S. Feng, A novel controlled release formulation for the anticancer drug paclitaxel (Taxol®): PLGA nanoparticles containing vitamin E TPGS. *J. Control. Release*, 2003, 86, 33-48.

36. Fonseca, C., S. Simões and R. Gaspar, Paclitaxel-loaded PLGA nanoparticles: preparation, physicochemical characterization and in vitro anti-tumoral activity. 2002, 83, 273-286.

37. Bilati, U., E. Allemann and E. Doelker, Poly(D,L-lactide-co-glycolide) protein-loaded nanoparticles prepared by the double emulsion method-processing and formulation issues for enhanced entrapment efficiency. *J. Microencapsul.*, 2005, 22, 205-214.

38. Li, Y. P., Y. Y. Pei, X. Y. Zhang, Z. H. Gu, Z. H. Zhou, W. F. Yuan, J. J. Zhou, J. H. Zhu and X. J. Gao, PEGylated PLGA nanoparticles as protein carriers: synthesis, preparation and biodistribution in rats. *J. Control. Release*, 2001, 71, 203-211.

39. Avgoustakis, K., A. Beletsi, Z. Panagi, P. Klepetsanis, A. G. Karydas and D. S. Ithakissios, PLGA-mPEG nanoparticles of cisplatin: in vitro nanoparticle

degradation, in vitro drug release and in vivo drug residence in blood properties. *J. Control. Release*, 2002, 79, 123-135.

40. Astete, C. E. and C. M. Sabliov, Synthesis and characterization of PLGA nanoparticles. *J. Biomater. Sci. Polym. Ed.*, 2006, 17, 247-289.

41. Dawes, G. J., L. E. Fratila-Apachitei, K. Mulia, I. Apachitei, G. J. Witkamp and J. Duszczyk, Size effect of PLGA spheres on drug loading efficiency and release profiles. *J. Mater. Sci. Mater M*, 2009, 20, 1089-1094.

42. Tabata, Y., S. Gutta and R. Langer, Controlled Delivery Systems for Proteins Using Polyanhydride Microspheres. *Pharm. Res.*, 1993, 10, 487-496.

43. Lopac, S. K., M. P. Torres, J. H. Wilson-Welder, M. J. Wannemuehler and B. Narasimhan, Effect of polymer chemistry and fabrication method on protein release and stability from polyanhydride microspheres. *J. Biomed. Mater. Res. B.*, 2009, 91, 938-947.

44. Langer, R., Polymer Implants for Drug Delivery in the Brain. *J. Control. Release*, 1991, 16, 53-59.

45. Agüeros, M., L. Ruiz-Gatón, C. Vauthier, K. Bouchemal, S. Espuelas, G. Ponchel and J. M. Irache, Combined hydroxypropyl-[beta]-cyclodextrin and poly(anhydride) nanoparticles improve the oral permeability of paclitaxel. *Eur. J. Pharm. Sci.*, 2009, 38, 405-413.

46. Agnihotri, S. A., N. N. Mallikarjuna and T. M. Aminabhavi, Recent advances on chitosan-based micro- and nanoparticles in drug delivery. *J. Control. Release*, 2004, 100, 5-28.

47. Berger, J., M. Reist, J. M. Mayer, O. Felt, N. A. Peppas and R. Gurny, Structure and interactions in covalently and ionically crosslinked chitosan hydrogels for biomedical applications. *Eur. J. Pharm. Biopharm.*, 2004, 57, 19-34.

48. Gan, Q. and T. Wang, Chitosan nanoparticle as protein delivery carrier--Systematic examination of fabrication conditions for efficient loading and release. *Colloid Surface B*, 2007, 59, 24-34.

49. Zhang, H., S. Mardyani, W. C. Chan and E. Kumacheva, Design of biocompatible chitosan microgels for targeted pH-mediated intracellular release of cancer therapeutics. *Biomacromolecules*, 2006, 7, 1568-1572.

50. Mitra, S., U. Gaur, P. C. Ghosh and A. N. Maitra, Tumour targeted delivery of encapsulated dextran-doxorubicin conjugate using chitosan nanoparticles as carrier. *J. Control. Release*, 2001, 74, 317-323.

51. Sarmento, B., A. J. Ribeiro, F. Veiga, D. C. Ferreira and R. J. Neufeld, Insulin-Loaded Nanoparticles are Prepared by Alginate Ionotropic Pre-Gelation Followed by Chitosan Polyelectrolyte Complexation. *J. Nanosci. Nanotechno.*, 2007, 7, 2833-2841.

52. Zahoor, A., S. Sharma and G. K. Khuller, Inhalable alginate nanoparticles as antitubercular drug carriers against experimental tuberculosis. *Int. J. Antimicrob. Ag.*, 2005, 26, 298-303.

53. Malam, Y., M. Loizidou and A. M. Seifalian, Liposomes and nanoparticles: nanosized vehicles for drug delivery in cancer. *Trends Pharmacol. Sci.*, 2009, 30, 592-599.

54. Discher, D. E., V. Ortiz, G. Srinivas, M. L. Klein, Y. Kim, D. Christian, S. Cai, P. Photos and F. Ahmed, Emerging applications of polymersomes in delivery: From molecular dynamics to shrinkage of tumors. *Prog. Polym. Sci.*, 2007, 32, 838-857.

55. Torchilin, V. P., Structure and design of polymeric surfactant-based drug delivery systems. *J. Control. Release*, 2001, 73, 137-172.

56. Kabanov, A. V., E. V. Batrakova and V. Y. Alakhov, Pluronic® block copolymers as novel polymer therapeutics for drug and gene delivery. *J. Control. Release*, 2002, 82, 189-212.

57. Hamaguchi, T., Y. Matsumura, M. Suzuki, K. Shimizu, R. Goda, I. Nakamura, I. Nakatomi, M. Yokoyama, K. Kataoka and T. Kakizoe, NK105, a paclitaxel-incorporating micellar nanoparticle formulation, can extend in vivo antitumour activity and reduce the neurotoxicity of paclitaxel. *Brit. J. Cancer*, 2005, 92, 1240-1246.

58. Kataoka, K., A. Harada and Y. Nagasaki, Block copolymer micelles for drug delivery: design, characterization and biological significance. *Adv. Drug Deliv. Rev.*, 2001, 47, 113-131.

59. Lee, A. L., Y. Wang, H. Y. Cheng, S. Pervaiz and Y. Y. Yang, The co-delivery of paclitaxel and Herceptin using cationic micellar nanoparticles. *Biomaterials*, 2009, 30, 919-927.

60. Yang, K. W., X. R. Li, Z. L. Yang, P. Z. Li, F. Wang and Y. Liu, Novel polyion complex micelles for liver-targeted delivery of diammonium glycyrrhizinate: in vitro and in vivo characterization. *J. Biomed. Mater. Res. A*, 2009, 88, 140-148.

61. Rastogi, R., S. Anand and V. Koul, Flexible polymerosomes-An alternative vehicle for topical delivery. *Colloid Surf. B*, 2009, 72, 161-166.

62. Xu, H., F. Meng and Z. Zhong, Reversibly crosslinked temperature-responsive nano-sized polymersomes: synthesis and triggered drug release. *J. Mater. Chem.*, 2009, 19, 4183-4190.

63. Wang, M., D. W. Lowik, A. D. Miller and M. Thanou, Targeting the Urokinase Plasminogen Activator Receptor with Synthetic Self-Assembly Nanoparticles. *Bioconjugate Chem.*, 2009, 20, 32-40.

64. Chan, J. M., L. Zhang, K. P. Yuet, G. Liao, J. W. Rhee, R. Langer and O. C. Farokhzad, PLGA-lecithin-PEG core-shell nanoparticles for controlled drug delivery. *Biomaterials*, 2009, 30, 1627-1634.

65. Ganta, S., H. Devalapally, A. Shahiwala and M. Amiji, A review of stimuli-responsive nanocarriers for drug and gene delivery. *J. Control. Release*, 2008, 126, 187-204.

66. Qiu, Y. and K. Park, Environment-sensitive hydrogels for drug delivery. *Adv. Drug Deliv. Rev.*, 2001, 53, 321-339.

67. Sershen, S. R., S. L. Westcott, N. J. Halas and J. L. West, Temperature-sensitive polymer-nanoshell composites for photothermally modulated drug delivery. *J. Biomed. Mater. Res.*, 2000, 51, 293-298.

68. Peppas, N. A., P. Bures, W. Leobandung and H. Ichikawa, Hydrogels in pharmaceutical formulations. *Eur. J. Pharm. Biopharm.*, 2000, 50, 27-46.

69. Yamagata, T., M. Morishita, N. J. Kavimandan, K. Nakamura, Y. Fukuoka, K. Takayama and N. A. Peppas, Characterization of insulin protection properties of complexation hydrogels in gastric and intestinal enzyme fluids. *J. Control. Release*, 2006, 112, 343-349.

70. Morishita, M., T. Goto, K. Nakamura, A. M. Lowman, K. Takayama and N. A. Peppas, Novel oral insulin delivery systems based on complexation polymer hydrogels: Single and multiple administration studies in type 1 and 2 diabetic rats. *J. Control. Release*, 2006, 110, 587-594.

71. Fisher, O. Z. and N. A. Peppas, Polybasic Nanomatrices Prepared by UV-Initiated Photopolymerization. *Macromolecules*, 2009, 42, 3391-3398.

72. Chen, H., Y. Gu, Y. Hu and Z. Qian, Characterization of pH- and Temperature-sensitive Hydrogel Nanoparticles for Controlled Drug Release. *PDA J. Pharm. Sci. Tech.*, 2007, 61, 303-313.

73. Guowei, D., K. Adriane, X. Chen, C. Jie and L. Yinfeng, PVP magnetic nanospheres: Biocompatibility, in vitro and in vivo bleomycin release. *Int. J. Pharm.*, 2007, 328, 78-85.

74. Missirlis, D., R. Kawamura, N. Tirelli and J. A. Hubbell, Doxorubicin encapsulation and diffusional release from stable, polymeric, hydrogel nanoparticles. *Eur. J. Pharm. Sci.*, 2006, 29, 120-129.

75. Lu, W., C. Xiong, G. Zhang, Q. Huang, R. Zhang, J. Z. Zhang and C. Li, Targeted Photothermal Ablation of Murine Melanomas with Melanocyte-Stimulating Hormone Analog-Conjugated Hollow Gold Nanospheres. *Clin. Cancer Res.*, 2009, 15, 876-886.

76. Zheng, J., D. Jaffray and C. Allien, Quantitative CT Imaging of the Spatial and Temporal Distribution of Liposomes in a Rabbit Tumor Model. *Mol. Pharm.*, 2009, 6, 571-580.

77. Jain, T. K., M. K. Reddy, M. A. Morales, D. L. Leslie-Pelecky and V. Labhasetwar, Biodistribution, clearance, and biocompatibility of iron oxide magnetic nanoparticles in rats. *Mol. Pharm.*, 2008, 5, 316-327.

78. Soman, N. R., S. L. Baldwin, G. Hu, J. N. Marsh, G. M. Lanza, J. E. Heuser, J. M. Arbeit, S. A. Wickline and P. H. Schlesinger, Molecularly targeted nanocarriers deliver the cytolytic peptide melittin specifically to tumor cells in mice, reducing tumor growth. *J. Clin. Invest.*, 2009, 119, 2830-2842.

79. Bazile, D. V., C. Ropert, P. Huve, T. Verrecchia, M. Marlard, A. Frydman, M. Veillard and G. Spenlehauer, BODY DISTRIBUTION OF FULLY BIODEGRADABLE [C-14] POLY(LACTIC ACID) NANOPARTICLES COATED WITH ALBUMIN AFTER PARENTERAL ADMINISTRATION TO RATS. *Biomaterials*, 1992, 13, 1093-1102.

80. Tong, L., W. He, Y. Zhang, W. Zheng and J. X. Cheng, Visualizing Systemic Clearance and Cellular Level Biodistribution of Gold Nanorods by Intrinsic Two-Photon Luminescence. *Langmuir*, 2009, 25, 12454-12459.

Appendix B

Cellular Evaluation of Synthesized Insulin-Transferrin Bioconjugates for Oral Insulin Delivery Using Intelligent Complexation Hydrogels

Justin P. Shofner,[†] Margaret A. Phillips,[‡] and Nicholas A. Peppas[†,‡,§]

[†]Department of Chemical Engineering, [‡]Department of Biomedical Engineering, and [§]Division of Pharmaceutics, University of Texas at Austin, Austin, Texas 78712

ABSTRACT

The oral delivery of insulin has been investigated through a variety of different approaches. One of the major barriers in achieving high bioavailability of insulin in the bloodstream is transport across the epithelial cell layer in the small intestine. To address this challenge, insulin-transferrin conjugates were synthesized to utilize the transport pathway of transferrin while retaining the bioactivity of insulin. In this work the effect on transport of insulin by using insulin-transferrin conjugates was investigated using cellular models. Transport studies were performed using the insulin-transferrin conjugates with and without the presence of P(MAA-g-EG) microparticles in contact with a co-culture of Caco-2/HT29-MTX cells. During the transport studies, the transepithelial electrical resistance was monitored to determine the effect of the proteins and particles on cell integrity. In the transport studies, the insulin-transferrin conjugate was shown to increase transport relative to insulin by a factor of 7, achieving an apparent permeability of 37 x 10^9 cm/s. Also, in the presence of polymer microparticles, the insulin-transferrin conjugate increased transport by a factor of 14

times relative to insulin, achieve an apparent permeability of 72.8 x 10^9 cm/s. The presence of the microparticles in solution was found to improve conjugate transport by nearly 100% with little to no change in cell monolayer integrity. Based on these cellular studies, it is concluded that the conjugation of a transporter molecule such as transferrin to proteins such as insulin is a promising option for overcoming the epithelial transport barrier and merits consideration in the design of future oral protein delivery systems.

INTRODUCTION

Bioavailability of orally administered therapeutic proteins depends on several factors such as the degree of protein degradation and residence time at the site of absorption. However, one of the most significant factors which affects absorption into the bloodstream is transport across the epithelial cell layer. The purpose of the epithelial cell layer is to absorb only required nutrients such as vitamins and minerals and to expel unrecognized or unwanted entities such as toxins or viruses. Additionally, tight junctions between the cells will only permit the transport of molecules with radii <11 Å [1]. Because of its ability to limit transport of large molecules, it is necessary to create strategies to significantly increase epithelial transport in order to effectively deliver therapeutic proteins.

We have successfully developed strategies to overcome the inherent challenges to oral protein delivery such as protein degradation and the narrow absorption window in the small intestine by incorporation into complexation hydrogels. Hydrogels are three-dimensional, hydrophilic polymer networks which can imbibe water and swell under certain conditions. Yamagata et al.[2] demonstrated the potential of the hydrogel carriers to protect proteins by encapsulating insulin within P(MAA-g-EG) microparticles

and achieving preservation of over 80% of the loaded insulin after being treated for one hour in gastric fluid. In contrast, only 20% of free insulin remained intact after the same treatment with gastric fluid. Also, increased residence time at the site of absorption has been achieved by the addition of polymers which are known to be mucoadhesive [3] and through the implementation of polymer tethers. Serra et al.[4] showed that the addition of PEG tethers to a poly(acrylic acid) (PAA) hydrogel system increased the mucoadhesive capacity of the microparticles, generating a work of adhesion of approximately 130 x 10^{-3} mJ, or five times that of a pure PAA system. Madsen and Peppas [5] were able to show that the calcium binding effect of the anionic hydrogels near the epithelial cell layer helped to reversibly loosen the cellular tight junctions and consequently allowed increased paracellular transport of therapeutic proteins. Finally, Morishita et al.[6] demonstrated the overall effectiveness and potential of the hydrogel system by performing *in vivo* studies in which insulin was administered in P(MAA-g-EG) carriers to diabetic rats, resulting in a bioavailability of 12.8%, a significant increase over insulin administered alone. Hydrogels have been shown to effectively protect the protein in the stomach, to create extended residence time in the small intestine for protein release, and even to enhance paracellular transport of therapeutic proteins, altogether demonstrating the promise of complexation hydrogels as carriers for the oral delivery of proteins.

The use of complexation hydrogels addresses many of the challenges of oral protein delivery, but further design strategies are required to significantly increase cellular transport in order to increase bioavailability in the bloodstream. A large portion of the design strategies to improve epithelial transport focuses on paracellular protein transport, or protein transport between the cells. System designs based on large molecule absorption through the paracellular route contain an inherent disadvantage.

Because of naturally poor protein transport across the epithelial cell layer, the monolayer must be disrupted or loosened to allow for increased protein transport. The monolayer disruption is typically non-specific to the protein of interest, translating to an increased probability of toxins or viruses entering.

An alternative to protein absorption through the paracellular route is to absorb the protein through the cell itself, utilizing the transcellular route for absorption. Transcellular transport can be utilized to be specific to the protein and may result in increased bioavailability as well. In our laboratory, we have been able to successfully synthesize and characterize protein-transporter conjugates which utilize the specific targeting mechanisms of ligand-receptor interactions for use with complexation hydrogels to ultimately deliver a significant amount of protein to the bloodstream through the transcellular route [7].

The goal of this work was to synthesize insulin-transferrin conjugates for evaluation of cellular transport characteristics using a Caco-2/HT29-MTX cellular model. This work achieves several objectives beyond the scope of the prior work from our laboratory on the subject [7]. As evident in the results and discussion section, this work addresses new factors related to the insulin-transferrin oral delivery system such as conjugate size related to diffusion, the use of a co-culture for more reliable diffusion and permeability results, and determination of a more realistic microparticle concentration for cellular studies, resulting in an increased understanding of their effect on transcellular transport versus the previous work on the subject.

The addition of the transporter transferrin to the therapeutic protein insulin allows for specific targeting of the bioconjugate entity as well as potentially increased transport. Transferrin is a glycoprotein which is normally involved in iron transport. The transferrin receptor is expressed on human intestinal epithelial cells. When evaluating

the potential of a novel oral dosage form for oral delivery, it is necessary to examine cellular interactions with the therapeutic entity using cellular models. The cellular model used for evaluation of insulin-transferrin bioconjugates was a co-culture consisting of both absorptive enterocyte-like Caco-2 cells which are commonly used to determine molecule permeability [8-11] and mucus-producing HT29-MTX goblet cells [12]. The advantage of using a Caco-2/HT29-MTX co-culture versus a simpler Caco-2 cellular model is in observing the effect that intestinal mucus will play in the diffusion of the large insulin-transferrin conjugate molecules, resulting in a more accurate depiction of overall permeability. A system consisting solely of Caco-2 cells used to measure permeability of large molecules the size of the insulin-transferrin conjugates would disregard the significant effect that diffusion through the mucus has on permeability. The Caco-2/HT29MTX co-culture was used to compare the permeability and transport of insulin-transferrin conjugates to native insulin. Additionally, cellular studies were performed in the presence of the P(MAA-g-EG) microparticles to give insight into the effect of complexation hydrogels on the transport processes of the epithelial cell monolayer. Based on the results of the cellular transport studies, the overall rate of transport was quantified as an overall apparent permeability, P_{app}, for the study. By comparing the apparent permeability values for each set of conditions, conclusions were drawn regarding the effect of protein-transporter conjugation and the presence of complexation hydrogels on epithelial transport of insulin.

MATERIALS AND METHODS

Hydrogel Synthesis. P(MAA-g-EG) was prepared using a free radical UV polymerization in solution. P(MAA-g-EG) was prepared by mixing MAA (Sigma-Aldrich

Inc., St. Louis, MO) with poly(ethylene glycol) monomethyl ether monomethacrylate with a approximate molecular weight of 1000 (PEGMA1000, Polysciences Inc., Warrington, PA) in a 1:1 molar ratio of MAA:EG. The crosslinker used within the polymer network was poly(ethylene glycol) dimethacrylate with an approximately molecular weight of 1000 (PEGDMA1000, Polysciences Inc., Warrington, PA). The amount of crosslinker added to each monomer mixture was equal to 1 mol% of the total amount of monomer. In order to eventually initiate the polymerization, the photoinitiator 1-hydroxycyclohexyl phenyl ketone (Irgacure 184, Sigma-Aldrich Inc., St. Louis, MO) was added to the polymerization mixture in the amount of 1 wt% of the total monomer added. A solvent mixture consisting of 50:50 by weight deionized water (Milli-Q Plus system, Millipore) and ethanol (AAPER Alcohol, Shelbyville, KY) was added to the polymer mixture in a 1:1 ratio by weight relative to monomer present in the prepolymer mixture. The presence of the solvent solution is essential to prevent autopolymerization as well as to produce a workable thin polymer film.

To ensure all components dissolved and went into a homogenous solution, the polymer mixture was sonicated for 15 minutes. After sonication, nitrogen was bubbled through the polymer solution within a nitrogen environment to eliminate oxygen. Oxygen is a free radical scavenger and significant oxygen levels could prematurely end the polymerization process. After removal of oxygen by nitrogen purging, the polymer mixture was poured between two glass slides (153 x 153 x 3 mm) separated by a Teflon spacer (0.7 mm) while still in a nitrogen environment. The glass slide apparatus containing the polymer solution spread into a thin film was then placed under a UV light source while still in a nitrogen environment. The solution was allowed to polymerize under the light source within an intensity range of 16-17 mW/cm^2 for 30 minutes. After the polymerization was completed, the polymer gels were removed from the nitrogen

environment, separated from the glass slides, and placed in deionized water. The polymer films were washed in the deionized water for 7 days to remove excess monomer and contaminants. After washing was completed, the polymers were dried in a vacuum oven at approximately 30° C for 2 days. After completely drying the polymer films, they were crushed into microparticles using a mortar and pestle to sizes less than 75 microns. The sieved microparticles were then stored in a vial within a desiccator to prevent moisture entering until further use.

Synthesis of Insulin-Transferrin Conjugates

The method for protein conjugation outlined in this section was originally developed by Carlsson et al [13]. The protein conjugation method was first utilized for the conjugation of insulin to transferrin by Shah and Shen [14]. The conjugation scheme consists of using N-succinimidyl 3-(2-pyridyldithio)propionate (SPDP) as a protein crosslinker to conjugate insulin (Ins) to transferrin (Tf) to form insulin-transferrin (Ins-Tf) heteroconjugates.

To begin the reaction, the n-terminal primary amines of the insulin chains were effectively "blocked" by reaction of insulin with dimethylmaleic anhydride (DMMA, Fluka/Sigma Aldrich Inc., St. Louis, MO), excluding possible reactive sites for SPDP. To begin the reaction, 10.5 mg of DMMA was added to a stock solution of insulin (Sigma Aldrich Inc., St. Louis, MO) and reacted for approximately one hour. During the reaction period, the pH was maintained within the pH range of 6.8-6.9 by adding small volumes of a 1 M Na_2CO_3 (Fisher Scientific, Fair Lawn, NJ) solution. After the reaction had finished, the insulin-DMMA intermediate was purified by dialysis (MWCO 3,500, Spectrum Laboratories Inc., Rancho Dominguez, CA) for at least 24 hours to remove unreacted DMMA.

Insulin-DMMA was reacted with 6.0 mg of SPDP (Pierce Biotechnology Inc., Rockford, IL) to add disulfide bonds to the remaining unblocked primary amine at B29-Lysine. The reaction was performed at 4°C under constant stirring within a pH range of 8.8-9.0. The pH was maintained by adding small volumes of 1 M Na_2CO_3. Upon completion of the reaction time period, the insulin-PDP product was purified by dialysis (MWCO 3,500) at 4°C for at least 24 hours to remove unreacted SPDP reagent.

In addition to the modification of insulin, transferrin (Sigma Aldrich Inc., St. Louis, MO) was also reacted with SPDP to form PDP groups on the transferrin molecule. To initiate the reaction, 8.0 mg of SPDP was added to a solution containing 120 mg of human holo-transferrin in PBS buffer (pH 7.0). The reaction was held at approximately 4°C and allowed to react for 2 hours. The transferrin-PDP product was purified through dialysis (MWCO 12,000-14,000, Spectrum Laboratories Inc., Rancho Dominguez, CA) in a solution of PBS buffer (pH 8.0) overnight to remove unreacted SPDP. After formation of PDP groups on transferrin, the modified protein was reduced by the addition of 1 M dithiothreitol (DTT, Sigma Aldrich Inc., St. Louis, MO). The transferrin-PDP was reduced using DTT for one hour, forming a product with attached sulfohydryl groups (Tf-SH). The transferrin-SH product was purified by dialysis for at least 24 hours to remove unreacted DTT.

Upon formation of transferrin-SH, the product was purified by elution from D-Salt Dextran Desalting Columns (10 mL, Pierce Biotechnology Inc., Rockford, IL). To initiate the final step in the conjugation reaction, the product solutions of Ins-PDP and Tf-SH were combined and allowed to react under constant stirring. The reaction was allowed to proceed for approximately 90 minutes before it was stopped by the addition of n-ethylmaleimide (NEM, ACROS Organics, Geel, Belgium), which reacts with free thiol groups [15] and prevents further crosslinking. The final insulin-transferrin product was

purified by dialysis (MWCO 12,000-14,000) for at least 48 hours to remove unreacted reagents. To determine the concentration of the conjugate solution, the product was analyzed using HPLC (Waters Corporation, Milford, MA). After analysis, the conjugate solution was refrigerated until further use.

Development of Caco-2/HT29-MTX Monolayers

To form the Caco-2/HT29-MTX monolayer, both Caco-2 and HT29-MTX cells were initially cultured in culturing flasks (75 cm^2, VWR Scientific, West Chester, PA) with 10 mL of culture media (DMEM, Biofluids Inc., Rockville, MD) containing additional supplements. Cultivation was performed at a seeding density of 2.5 x 10^5 cells per flask for the Caco-2 cells and 1.25 x 10^5 cells per flask for the HT29-MTX cells. During cultivation, the cells were incubated at 37° C, 95% relative humidity, and 5% CO_2 while the culture media was replaced every other day until the cells reached 70-80% confluency. After reaching the desired confluency, both types of cells were passaged at least once prior to combination of the cell types. After passaging, the Caco-2 and HT29-MTX cells were transferred at the desired seeding density to experimental wells in a 1:1 ratio as to obtain a 50% Caco-2/50% HT29-MTX experimental co-culture monolayer.

For the transport studies, a co-culture of Caco-2/HT29-MTX cells was grown in 6-well Transwell® plates (4.71 cm^2/well, Costar Corning Inc., Corning, NY). The cell density in the experimental wells was approximately 3 x 10^5 cells/well with the composition being 50% of each cell type. The co-culture was grown in the culture medium for approximately 21-23 days until the monolayer achieved a constant transepithelial electrical resistance (TEER) as measured by a chopstick electrode (World Precision Instrument, Sarasota, FL). Typically, a constant TEER value indicates that the monolayer

has formed tight junctions [16, 17]. During the formation of the monolayer, the culture media was changed every other day and the TEER was monitored regularly.

Upon the formation of tight junctions, the transport studies began by allowing the cells to equilibrate with Hank's Balanced Salt Solution (HBSS, HyClone, Logan, UT), the experimental medium for the study. HBSS is typically listed having a pH of 7.1, which closely mimics the conditions at the targeted site of delivery in the upper ileum. Though the pH of the small intestine varies throughout its length, the mucoadhesive nature of the hydrogels ensures that delivery should occur early in transit and in the upper ileum[4]. The HBSS also contained Ca^{2+} ions to ensure regulation of intracellular Ca^{2+} ions, which are instrumental in maintaining the integrity of the tight junctions. After addition of the HBSS, the TEER of the cell monolayer was monitored for the next hour with samples regularly withdrawn. The conclusion of the equilibration period was marked by the achievement of a constant TEER, indicating adjustment to the HBSS solution as well as the ability to begin the transport studies.

Protein Transport Across the Cell Monolayer

For the studies in which only protein was present in the apical chamber, insulin or insulin-transferrin was dissolved in warm HBSS at a concentration of 0.2 mg/mL. To begin the study, the previous HBSS solution was removed from the apical chamber. Approximately 1.5 mL of the solution containing either the insulin or insulin-transferrin was placed in the apical chamber. The Transwell® plates were then placed in an incubator at 37° C. Samples of 100 µL were withdrawn from the basolateral chambers at time points of 0, 0.5, 1, 2, and 3 hours after the addition of protein solution to the well. The TEER of the monolayer was also measured at the withdrawal of each sample. Throughout the course of the transport study, all measurements were taken while

maintaining the Transwell® plate at 37° C, ensuring no changes in the integrity of the tight junctions or in the amount of transcellular transport as both vary significantly as temperature varies. The samples were placed in small vials and refrigerated until they could be analyzed. Analysis of protein concentration of the apical chamber was performed by HPLC and protein concentration in the basolateral chamber was determined by use of an ELISA kit.

Protein Transport Across the Cell Monolayer in the Presence of P(MAA-g-EG) Microparticles

In addition to transport studies using only proteins, more transport studies were performed to determine the effect of the presence of P(MAA-g-EG) microparticles on the cellular transport of both insulin and insulin-transferrin conjugates.

As with the previous transport studies, solutions of either insulin or insulin-transferrin conjugates were prepared at a concentration of 0.2 mg/mL in warm HBSS. After removing the HBSS used for equilibration of the monolayer from the apical chamber, approximately 1.5 mL of either of the protein solutions was added to refill the apical chamber with sample. Immediately after addition of the protein solutions to the apical side, dry P(MAA-g-EG) microparticles were added to the apical chamber at a concentration of 1 mg/mL. Sampling of both the apical and basolateral chambers occurred in the same manner as previously described and all samples were analyzed by either HPLC (apical samples) or using an ELISA kit (basolateral samples).

RESULTS AND DISCUSSION

Protein Transport Across the Cell Monolayer

Solutions of either insulin or insulin-transferrin conjugates were investigated through transport studies. In the studies, samples were withdrawn from the basolateral chamber at regular time points to determine the amount of protein transported over time. The transport profiles were fit using a linear regression model and the slope of the fit was used to calculate apparent permeability values, P_{app}, for each of the protein samples.

In order to calculate an apparent permeability for protein transport, the following equation was used:

$$P_{app} = \frac{dQ(t)}{dt} \times \frac{1}{A \times C_{A0}}$$

In the equation above, Q(t) is the cumulative amount of protein (mg) transported at time t, A is the area of the cell monolayer (cm^2), and C_{A0} is the initial protein concentration in the apical (donor) compartment (mg/cm^3). The term dQ(t)/dt is represented by the slope of the linear fit to the data plotting cumulative protein transported (Q(t)) versus time (t). It should be noted that the lines drawn on Figures 1, 3, 4, and 6 are slope lines representative of the dQ(t)/dt term in determining apparent permeability values. The lines are only a reflection of average protein transport over the entire course of the study, not a predictive model intended to represent the data trends. In fact, certain types of transport, particularly transcellular transport, may not transport protein linearly but instead in a non-linear fashion based on the timing of cellular processes. Apparent permeability values were calculated over the course of the entire study versus between each data point to provide an overall comparison of protein transport within the different transport mechanisms that may be occurring.

As an experimental control, a solution of insulin dissolved in HBSS was added to the apical chamber and was allowed to interact with the cell monolayer. The apparent permeability of the insulin relative to the cell monolayer was determined to be 4.95 x 10^9 cm/s using the equation shown above. The extent of transport as well as the apparent permeability of the insulin control served as a standard of comparison for the experimental protein solutions. To determine the effect of the conjugation of a transporter protein to insulin, the transport of a solution of insulin-transferrin conjugates across the cell monolayer was measured and analyzed. In comparison to the insulin control, the transport occurred to a much greater extent and also in a much more linear fashion. The linearity of the transport can most likely be attributed to the timing of cellular mechanisms involved in transcellular transport, leading to a slower but more linear transport profile. The apparent permeability, P_{app}, of the insulin-transferrin conjugates across the Caco-2/HT29-MTX monolayer was calculated and found to be 37.0 x 10^9 cm/s. The transport profiles of the insulin control and insulin-transferrin are shown in Figure B1. To compare the protein transport studies, the most simple and direct method is to compare the apparent permeability values between the different protein solutions. According to the values, the insulin-transferrin molecule has more than seven times the permeability compared to unmodified insulin. Increasing transport of a potential therapeutic more than sevenfold has dramatic potential ramifications on the bioavailability of the drug in the bloodstream. Based on the results of the transport studies conducted using solutions containing only protein, the transport of an orally administered therapeutic protein can be greatly increased by conjugating the drug to a transporter molecule such as transferrin.

While performing the transport studies, it was important to monitor the integrity of the cell monolayer and the tight junctions as to ensure that administration of such

therapeutics would not cause the epithelial cell layer to have a lessened ability to expel dangerous viruses or toxins. Over the course of each transport study, the transepithelial electrical resistance was measured as a means of monitoring tight junction integrity. The TEER values throughout both transport studies are shown as Figure B2. As evident in Figure B.2, the TEER of the Caco-2/HT29-MTX monolayer stayed near 100% of the initial value throughout the course of each transport study. The absolute TEER values for all the co-cultures in the transport studies were recorded in the range of 85-95 $\Omega*cm^2$. It should be noted that Caco-2/HT29-MTX co-cultures have been shown to have lower TEER values relative to pure Caco-2 cell monolayers [18]. However, it should also be noted that the typical TEER values of Caco-2/HT29-MTX co-cultures more closely represent the TEER values of the human intestine, known to range from 50-100 $\Omega*cm^2$.[19] The maintenance of steady TEER values in these experiments indicates that the proteins (insulin and insulin-transferrin) do not have a disruptive effect on the cell monolayer, ensuring their presence upon administration will not cause illness due to uptake of dangerous toxins or viruses through a weakened epithelial cell barrier.

Protein Transport Across the Cell Monolayer in the Presence of P(MAA-g-EG) Microparticles

To determine the effect of the presence of polymer microparticles on cellular insulin transport, a prepared solution of insulin dissolved in HBSS with added P(MAA-g-EG) microparticles was added to the apical chamber and was allowed to interact with the cell monolayer. The apparent permeability, P_{app}, of the insulin in the presence of polymer microparticles was determined to be 5.20×10^{9} cm/s. The apparent permeability of insulin in the presence of polymer microparticles is slightly higher than the value obtained for insulin alone, indicating that the presence of the microparticles may have a slight permeation enhancing effect for the paracellular transport of insulin.

However, while the apparent permeability value is slightly higher for transport in the presence of microparticles, the difference in amount of protein transported is not significant between the cases. Therefore, the presence of microparticles at this concentration has little to no effect on insulin transport. The transport profiles of insulin with and without the presence of microparticles are shown in Figure B3. A higher concentration of microparticles in solution would have most likely caused a significant increase in insulin transport due to concurrently increased calcium binding capacity, further loosening the tight junctions of the cell monolayer as shown in previous work from our laboratory[5].

Similar transport studies were also conducted which used solutions of insulin-transferrin conjugates in the presence of P(MAA-g-EG) microparticles to determine if the microparticles had a more pronounced effect on insulin transport. The apparent permeability of the insulin-transferrin conjugates across the Caco-2/HT29-MTX monolayer in the presence of polymer microparticles was calculated and found to be 72.8×10^{9} cm/s. In comparison to the transport of insulin-transferrin conjugates alone, the permeability of the conjugate nearly doubled in the presence of polymer microparticles. The transport profiles of insulin-transferrin with and without the presence of microparticles are shown in Figure B4. Though it is not completely clear whether the presence of the microparticles enhanced transcellular transport of the conjugate or simply opened up paracellular pathways, it is evident that transport was greatly increased. The previous study showed that the presence of polymer microparticles had little to no effect on insulin transport at the given microparticle concentration. However, at the same concentration, the microparticles were able to enhance insulin-transferrin transport by nearly 100%. The drastic difference in enhanced transport suggests that P(MAA-g-EG) microparticles act as better enhancers

for transport that has been hypothesized to be transcellular versus that which has been thought to be paracellular. In this study, while improved conjugate transport could be attributed to newly opened paracellular pathways, the absence of improved transport in the previous case seems to negate this idea. Our hypothesis is that the microparticles facilitated transcellular transport, possibly through calcium binding, the consequent loss of intracellular calcium, and the resultant effect which lowered calcium has on transcytotic processes. However, to rigorously determine the effect of the microparticles on the transport mechanism of insulin-transferrin conjugates, further investigation into the cellular transport mechanisms of intestinal cells as well as more in-depth public knowledge about the intracellular transferrin mechanisms would be required.

To gain a greater understanding of the effect of microparticles on the integrity of the tight junctions and the monolayer, the transepithelial electrical resistance (TEER) was measured over the course of the transport studies. The TEER values throughout the two transport studies are shown as Figure B5. As can be seen in Figure B5, the TEER of the Caco-2/HT29-MTX monolayer stayed near 100% of the initial value throughout the course of both transport studies. Steady TEER values throughout the studies indicate little to no disruption of the monolayer in the presence of both proteins and P(MAA-g-EG) microparticles. While previous studies have shown that the TEER values and the tight junctions will be affected by the presence of polymer microparticles [20,21], the microparticles used in this study were likely not introduced at a high enough concentration to achieve the significant disruptive effect that had been observed in previous studies.

Combinatorial Effect of Transferrin Conjugation and Presence of Microparticles

It is also useful to determine the effect of transferrin conjugation on insulin transport while in the presence of microparticles. The transport profiles of insulin and insulin-transferrin in the presence of microparticles can be compared in Figure B6. Simply replacing insulin with insulin-transferrin conjugates at the same concentration but in the presence of microparticles increased the apparent permeability by a factor of nearly fourteen. Assuming that a formulation of insulin-transferrin conjugates loaded into P(MAA-g-EG) microparticles could deliver the same amount of protein to the site of absorption as an insulin-loaded microparticle, the benefit of having potentially fourteen times the cellular transport would translate into a much more effective drug with significantly higher bioavailability.

To compare all of the transport studies quantitatively, it is important to compare the apparent permeability values. The apparent permeability values for all of the transport studies can be directly examined in Table 1. Based on the permeability values, the insulin-transferrin conjugate alone achieves more than seven times the transport of insulin alone. Meanwhile, the addition of P(MAA-g-EG) microparticles increases insulin-transferrin transport by nearly 100%. Due to the ability of the microparticles to enhance conjugate transport, the insulin-transferrin conjugate achieves nearly fourteen times the transport that insulin does in the presence of the microparticles. The progress achieved in this work is significant relative to previous work from the laboratory in the area [7]. While the protein (insulin) and transporter ligand (transferrin) used are the same, the conjugates in this work were constructed to be slightly smaller (i.e. lower insulin to transferrin ratio) than the previous work to improve epithelial transport. The conjugate size can have a profound effect on the diffusion of the entity through the mucosa of the small intestine. Thus, the use of a smaller conjugate has resulted in increased transport

characteristics relative to studies performed previously in our laboratory [7]. The effect of conjugate size is magnified by the use of a co-culture of Caco-2/HT29-MTX cells; the use of these cells provides a more accurate depiction of condition in the small intestine as well as more accurate conditions for diffusion due to the mucus secreted by the HT29-MTX cells. A simple Caco-2 cell study is acceptable for determining permeability of small molecules, but the diffusion in the mucus of the intestine cannot be ignored for large molecules such as the insulin-transferrin conjugate, thus requiring the need for the co-culture permeability study as contrasted with the previous work from our laboratory [7]. Also, this study is the first from our laboratory to accurately measure the effect of the microparticles on overall transport of insulin-transferrin conjugates. In previous studies, the concentration of particles used was too high to the point of adversely affecting cell integrity. Using a more realistic concentration yields no loss of cell integrity but instead a possible enhancement to transcellular transport. Moreover, the concentration of microparticles used in the transport study more accurately reflects the estimated amount of particles per approximate area of the small intestine. All of these factors combined result in significant research findings that further the possibility of insulin-transferrin systems being used in future drug delivery designs.

Considering all of the transport studies performed in this work, modification of therapeutic proteins by conjugation to transporter molecules remains an attractive option for increasing epithelial transport and achieving high bioavailability.

CONCLUSIONS

Cellular evaluation of the insulin-transferrin conjugate was performed using a co-culture Caco-2/HT29-MTX cell model. The conjugate was investigated by conducting

transport studies on both the insulin-transferrin conjugate and an insulin control with and without the presence of microparticles. The results of the transport studies indicated a sevenfold increase in transport by replacing insulin with insulin-transferrin conjugates. Also, the presence of P(MAA-g-EG) microparticles enhanced transport for the insulin-transferrin conjugate by nearly 100% while having minimal effect on pure insulin transport, indicating that the polymer microparticles may assist in transcytotic processes. Finally, the transport studies also demonstrated that a 14-fold increase in transport can be achieved by switching from insulin in the presence of polymer microparticles to insulin-transferrin conjugates in the presence of polymer microparticles. The specific targeting and increased transport of the insulin-transferrin conjugate in combination with the protection and site-specific release capabilities of P(MAA-g-EG) microparticles combine synergistically to form a potential dosage form which could effectively deliver therapeutics to the small intestine and across the epithelium, resulting in high bioavailability in the bloodstream.

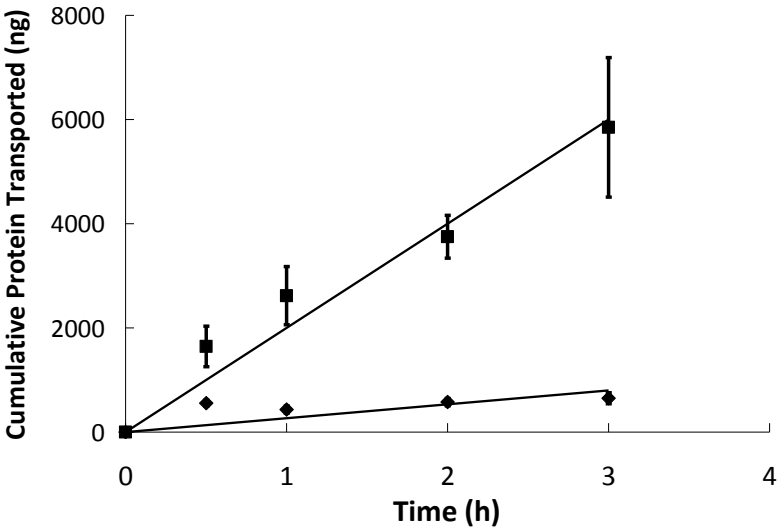

Figure B.1. Insulin and insulin-transferrin conjugates were placed in the apical chamber at a concentration of 0.2 mg/mL and were allowed to diffuse through a cell monolayer of Caco-2/HT29-MTX for 3 hours. The protein concentrations in the basolateral chamber were measured at time points of 0.5, 1, 2, and 3 hours using ELISA and compared to standards of known concentrations. n = 9 ± SD

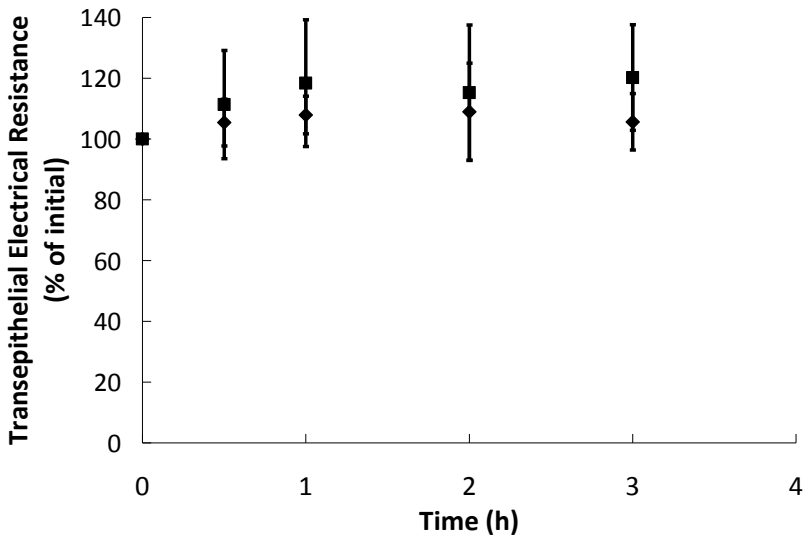

Figure B.2. Transepithelial electrical resistances (TEER) of cell monolayers of Caco-2/HT29-MTX co-cultures over the course of a 3 hour transport study using insulin and insulin-transferrin conjugates at a protein concentration of 0.2 mg/mL. The values are percentages of the TEER as compared to the initial values before the study began. n = 9 ± SD

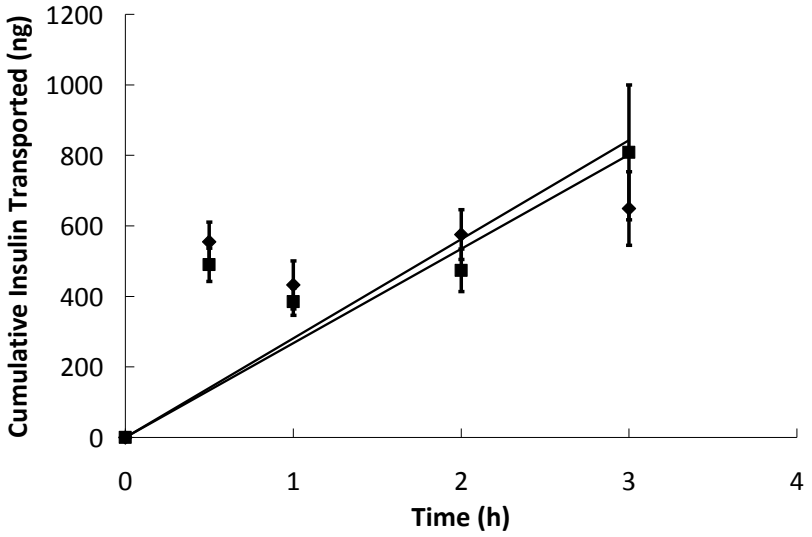

Figure B.3. Insulin was placed in the apical chamber without the presence of P(MAA-g-EG) microparticles and while in the presence of P(MAA-g-EG) microparticles at a protein concentration of 0.2 mg/mL and a microparticle concentration of 1 mg/mL.

The insulin was allowed to diffuse through a cell monolayer of Caco-2/HT29-MTX for 3 hours. The protein concentrations in the basolateral chamber were measured at time points of 0.5, 1, 2, and 3 hours using ELISA and compared to standards of known concentrations. *n = 9 ± SD*

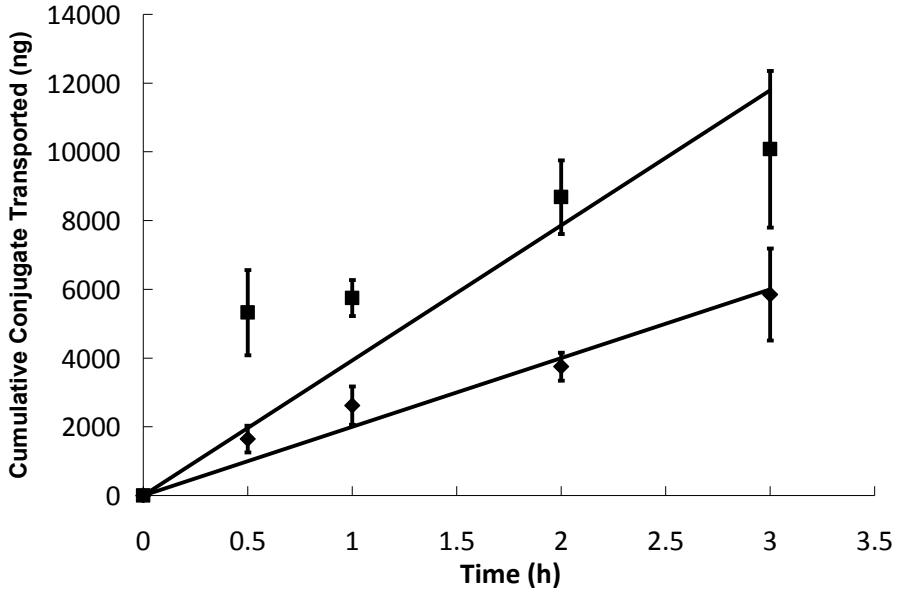

Figure B.4. Insulin-transferrin was placed in the apical chamber without the presence of P(MAA-g-EG) microparticles and while in the presence of P(MAA-g-EG) microparticles at a protein concentration of 0.2 mg/mL and a microparticle concentration of 1 mg/mL.

The insulin-transferrin conjugates were allowed to diffuse through a cell monolayer of Caco-2/HT29-MTX for 3 hours. The protein concentrations in the basolateral chamber were measured at time points of 0.5, 1, 2, and 3 hours using ELISA and compared to standards of known concentrations. *n = 9 ± SD*

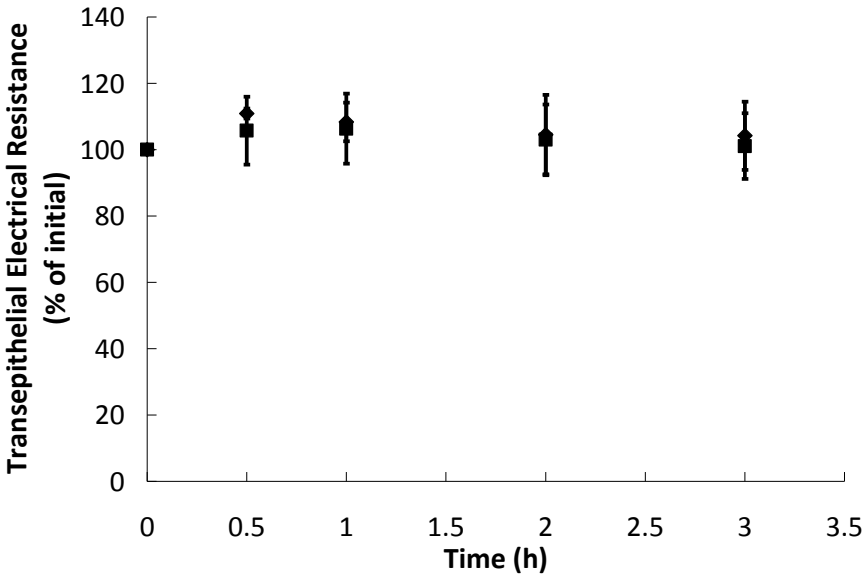

Figure B.5. Transepithelial electrical resistances (TEER) of cell monolayers of Caco-2/HT29-MTX co-cultures over the course of a 3 hour transport study using insulin and insulin-transferrin conjugates at protein concentrations of 0.2 mg/mL. Also present in the apical chamber were P(MAA-g-EG) microparticles at a concentration of 1 mg/mL.

The values are percentages of the TEER as compared to the initial values before the study began. *n = 9 ± SD*

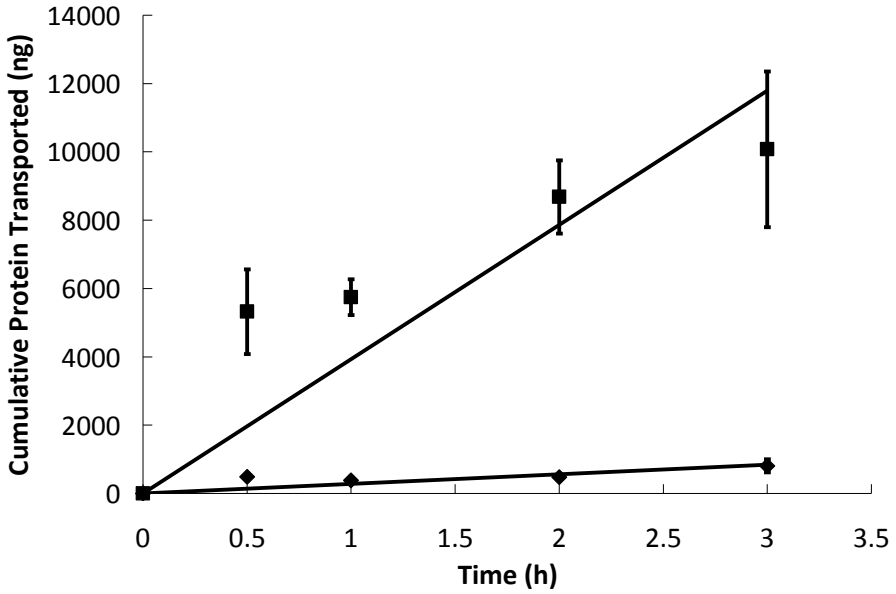

Figure B.6. Insulin and insulin-transferrin conjugates were placed in the apical chamber at a protein concentration of 0.2 mg/mL while in the presence of P(MAA-g-EG) microparticles at a particle concentration of 1 mg/mL and were allowed to diffuse through a cell monolayer of Caco-2/HT29-MTX for 3 hours.

The protein concentrations in the basolateral chamber were measured at time points of 0.5, 1, 2, and 3 hours using ELISA and compared to standards of known concentrations. *n = 9 ± SD*

REFERENCES

1. Fasano, A., Novel approaches for oral delivery of macromolecules. *J. Pharm. Sci.*, 1998, 87, 1351-1356.

2. Yamagata, T., M. Morishita, N. J. Kavimandan, K. Nakamura, Y. Fukuoka, K. Takayama and N. A. Peppas, Characterization of insulin protection properties of complexation hydrogels in gastric and intestinal enzyme fluids. *J. Control. Release*, 2006, 112, 343-349.

3. Peppas, N. A. and J. J. Sahlin, Hydrogels as mucoadhesive and bioadhesive materials: a review. 1996, 17, 1553-1561.

4. Serra, L., J. Domenech and N. A. Peppas, Design of poly(ethylene glycol)-tethered copolymers as novel mucoadhesive drug delivery systems. *Eur. J. Pharm. Biopharm.*, 2006, 63, 11-18.

5. Madsen, F. and N. A. Peppas, Complexation graft copolymer networks: swelling properties, calcium binding and proteolytic enzyme inhibition. *Biomaterials*, 1999, 20, 1701-1708.

6. Morishita, M., T. Goto, N. A. Peppas, J. I. Joseph, M. C. Torjman, C. Munsick, K. Nakamura, T. Yamagata, K. Takayama and A. M. Lowman, Mucosal insulin delivery systems based on complexation polymer hydrogels: effect of particle size on insulin enteral absorption. *J. Control. Release*, 2004, 97, 115-124.

7. Kavimandan, N. J., E. Losi and N. A. Peppas, Novel delivery system based on complexation hydrogels as delivery vehicles for insulin-transferrin conjugates. *Biomaterials*, 2006, 27, 3846-3854.

8. Artursson, P., T. Lindmark, S. S. Davis and L. Illum, Effect of chitosan on the permeability of monolayers of intestinal epithelial cells (Caco-2). *Pharm. Res.*, 1994, 11, 1358-1361.

9. Artursson, P. and R. T. Borchardt, Intestinal drug absorption and metabolism in cell cultures: Caco-2 and beyond. *Pharm. Res.*, 1997, 14,

10. Artursson, P., K. Parlm and K. Luthman, Caco-2 monolayers in experimental and theoretical predictions of drug transport. *Adv. Drug Deliver. Rev.*, 2001, 46, 27-43.

11. Ungell, A.-L. N., Caco-2 replace or refine? *Drug Discov. Today: Technologies*, 2004, 1, 423-430.

12. Walter, E., S. J. Blake, J. Roessler, J. M. Hilfinger and G. L. Amidon, HT29-MTX/Caco-2 cocultures as an in vitro model for the intestinal epithelium: In vitro-in vivo correlation with permeability data from rats and humans. *J. Pharm. Sci.*, 1996, 85, 1070-1076.

13. Carlsson, J., H. Drevin and R. Axen, Protein thiolation and reversible protein-protein conjugation. N-Succinimidyl 3-(2-pyridyldithio)propionate, a new heterobifunctional reagent. *Biochem J.*, 1978, 173, 723-737.

14. Widera, A., F. Norouziyan and W. C. Shan, Mechanisms of TfR-mediated transcytosis and sorting in epithelial cells and applications toward drug delivery. *Adv. Drug Deliver. Rev.*, 2003, 55, 1439-1466.

15. Faulstich, H., S. Zobeley, D. Heintz and G. Drewes, Probing the phalloidin binding site of actin. *FEBS Lett.*, 1993, 318, 218-222.

16. Denker, B. M. and S. K. Nigam, Molecular structure and assembly of the tight junction. *Am. J. Physiol. Renal Physiol.*, 1998, 274, F1-9.

17. Gumbiner, B., Structure, biochemistry, and assembly of epithelial tight junctions. *Am. J. Physiol. Cell Physiol.*, 1987, 253, C749-758.

18. Wood, K. M., G. M. Stone and N. A. Peppas, The effect of complexation hydrogels on insulin transport in intestinal epithelial cell models. *Acta Biomater.*, 2010, 6, 48-56.

19. Balimane, P. V. and S. Chong, Cell culture-based models for intestinal permeability: a critique. *Drug Discover. Today*, 2005, 10, 335-343.

20. Foss, A. C. and N. A. Peppas, Investigation of the cytotoxicity and insulin transport of acrylic-based copolymer protein delivery systems in contact with Caco-2 cultures. *Eur. J. Pharm. Biopharm.*, 2004, 57, 447-455.

21. Ichikawa, H. and N. A. Peppas, Novel complexation hydrogels for oral peptide delivery: In vitro evaluation of their cytocompatibility and insulin-transport enhancing effects using Caco-2 cell monolayers. *J. Biomed. Mater. Res. Part A*, 2003, 67A, 609-617.

Appendix C

Anionic Complexation Hydrogels for the Oral Delivery of Protein Vaccines

INTRODUCTION

Oral administration of vaccines is the preferred route of administration and has the potential to improve vaccine efficacy by directly targeting the GI tract mucosa for generation of mucosal immunity. Oral administration of vaccines is particularly attractive because it would reduce production costs as well as administration costs by eliminating needles and the requirement of trained personnel to administer them [1].

The generation of mucosal immunity offers an alternative mechanism to systemic immunity generated by parenteral vaccine administration. The mucosal immune system is distinct in function and anatomy from the peripheral (systemic) immune system. The mucosal immune system functions to locally protect against microbe colonization and entry, to prevent entry of undegraded antigens, and to prevent harmful systemic immune responses in the event that antigens do enter the body [2].

One of the most interesting features of the common mucosal immune system is that exposure to antigens at one mucosal site can lead to IgA secretion at distant mucosal sites and antigen-specific IgA can also be found in serum [3, 4]. Immunization at one site can generate protective immunity at the local mucosal site, at distant mucosal sites, and may also lead to a systemic immunity.

The common mucosal immune system consists of mucosa-associated lymphoid tissue (MALT), which contains 80% of all immune cells [2]. MALT tissue can be classified by its function as either organized inductive sites where naïve B and T cells are primed

after antigen exposure or diffuse effector sites where activated B and T cells reside. Mucosal immunity is associated primarily with secretory IgA dominant responses to antigens.

The intestinal mucosal immune system, or the gut-associated lymphoid tissue (GALT), includes Peyer's patches, mesenteric lymph nodes, and lymphoid cells in the epithelium and in the lamina propria. A schematic overview of the gut mucosal immune system is shown in Figure 1. Peyer's patches are aggregated lymphoid nodules that act as inductive sites in the GALT. Peyer's patches appear as dome like regions that extend into the lumen of the GI tract. The Peyer's patch epithelium is composed of specialized follicle-associated epithelium (FAE) including enterocyte-like cells and microfold (M-) cells. These epithelial cells have no mucosal layer and have a thin glycocalyx, which allows Peyer's patch FAE cells to directly contact luminal contents [5]. M-cells endocytose or phagacytose antigens adhered to their membrane [6-10]. M-cell anatomy, such as short microvilli, cytoplasmic vesicles, and few lysosomes, allows antigen transport across the M-cell below the dome region of the Peyer's patch [5].

Beneath the dome region of the Peyer's patch, a variety of immune cells are present including B cells, T cells, dendritic cells, and macrophages. Antigens transported across the dome region are then taken up by professional antigen presenting cells (APCs) (dendritic cells or possibly neighboring epithelial cells). APCs present the antigen to $CD4^+$ T cells causing activation shown in Figure C1. Activated $CD4^+$ T cells in turn activate B cells via CD40L and TGF-beta and cause them to switch to IgA isotype [11, 12]. Following, T cell activation and B cell IgA switching, B and T cells migrate out of the inductive site to effector sites. These cells typically leave the Peyer's patch follicle inductive site via the mesenteric lymph node and circulate back (through the bloodstream) to differentiate into memory cells at mucosal effector sites typically at the

tissue of origin (the GI tract lamina propria) [2]. The mechanism for relocation of the B and T cells is attributed to addressins on the surface of the cells. The cells associated with the lamina propria include B cells, J-chain expressing IgA and IgM plasma cells, IgG plasma cells, and $CD4^+$ T cells shown in Figure C1. Of these antibodies produced, IgA is the most abundant and protects the GI tract from infection by preventing pathogens from binding enterocytes [13].

Because most pathogens enter the body through mucosal membranes, vaccination to produce mucosal immunity is highly desirable. Generation of mucosal immune responses is highest when the antigen is administered directly to the mucosa [14]. In addition, there is some indication that stimulation of local mucosal immunity can lead to immunity at other mucosal membranes as well as systemic immunity as activated B and T cells at mucosal inductive sites can relocate to other mucosal effector sites. Therefore, it is thought that mucosal immunization and, in some cases, systemic immunity, may be achieved by inoculation at just a single mucosal inductive site [2]. Furthermore, the highly effective protective, local immune responses associated with mucosal immunity could improve vaccine efficacy as most pathogens enter the body via mucosal membranes, and infection would not be required for generating an immune response as infection is required for a systemic immune response due to systemic immunization by parenteral vaccination.

Vaccines may consist of either a killed or attenuated form of a pathogen, a protein from the pathogen, DNA, or a toxoid produced by a pathogen. One of the main challenges to oral delivery of a vaccine is maintaining the immunogenicity of the antigen in the GI tract and uptake of a large molecular weight compound by Peyer's patches. Often, vaccines are administered through injection because of the challenges associated with delivering a sufficient amount of an intact antigen orally. Several vaccines have

been shown to be effective after oral administration. Most notably Sabin's polio vaccine was one of the vaccines used to eradicate polio in the 1960s. The safety concerns associated with a live vaccine were not attributed to the oral route of administration but rather that the vaccine was an attenuated live polio virus that in rare cases could lead to infection [2]. Other examples of licensed oral mucosal vaccines include cholera (Dukoral, Orochol), typhoid (TyphimVi, Vivotif), rotavirus (RotaRix), and influenza (FluMist) [2].

Safety concerns regarding the possibility of attenuated virus vaccines to cause infection in addition to the rapid development of genetic and protein engineering technologies have shifted focus to the design of DNA, protein, and peptide vaccines. The development of oral vaccine formulations especially of protein-based vaccines faces similar challenges to the oral delivery of protein drugs. For example, the vaccine must arrive in tact at the site of absorption, the ileum, must retain its immunogenicity, must be absorbed by Peyer's patches, and taken up by APCs [1].

To address these challenges, polymer particulate drug delivery systems have been investigated for oral protein vaccine delivery. Most strategies have focused on biodegradable microparticle formulations designed for uptake by M-cells [15, 16]. For example, poly(lactic acid-co-glycolic acid) (PLGA) microparticles have been the most widely studied polymer microparticles to deliver antigens orally. Antigens delivered using PLGA have been shown to elicit increased serum immune responses and mucosal immune responses (via increased antibody titers) [17, 18]. Generation of secretory IgA responses locally and at distant mucosa has also be demonstrated [18]. Systemic cytotoxic T lymphocytes have also been detected after orally administered antigens via PLGA [19]. In one study, oral immunization using PLGA delivery systems provided protective immunity upon a nasal challenge with *Bordetella pertussis* [20]. Other

biodegradable polymers have also been investigated for oral delivery of vaccines including alginate, sodium alginate and spermine hydrochloride [21-23], starch [24-26], poly(ε-caprolactone) (PCL) [27, 28], and chitosan [29, 30].

The majority of these studies have highlighted that microparticle uptake by M-cells is important for the generation of an immune response, and as a result, biodegradable polymers are necessary. In a recent study by Yamamoto et al., it was shown that protective immunity, IgA responses, can be achieved outside Peyer's patches in mice [31]. Therefore, it may not be entirely necessary for an oral vaccine to be taken up only at M-cells. Delivery of an intact antigen to the intestinal wall may be sufficient. In this work, we take an alternative approach in which non-degradable hydrogel microparticles are designed to orally deliver a vaccine via bioadhesion to M-cells. One of the advantages of a non-degradable system is the increased stability of the formulation in the GI tract [1].

Our laboratory has developed anionic complexation hydrogels composed of poly(methacrylic acid-grafted-ethylene glycol) (P(MAA-g-EG) for oral delivery of protein drugs, and we believe that these systems can successfully deliver a protein based vaccine orally. P(MAA-g-EG) microgels protect protein drugs from degradation in the GI tract through the formation of interpolymer complexes in stomach conditions which limit diffusion into and out of the gel [32]. Release of the drug occurs in intestinal conditions due to decomplexation and subsequent swelling of the gels. P(MAA-g-EG) gels have the ability to interact with intestinal mucosa through mucoadhesion as well as reversibly open tight junctions between neighboring epithelial cells [32-36]. Both mucoadhesion and the ability to improve absorption make P(MAA-g-EG) gels attractive vaccine delivery systems. For example, mucoadhesion improves the residence time of the carrier at the site of absorption allowing for a longer window for drug release and

therefore more drug absorption. These systems have been shown to effectively deliver a variety of protein drugs including insulin, growth hormone, calcitonin, and interferon-β.

Because Peyer's patches are the major inductive site of the intestinal mucosal immune system, localizing P(MAA-g-EG) microgels to Peyer's patches could enhance vaccine absorption and the resulting immune response. For example, PLGA microparticles have been modified with RGD [37] and other peptides [38] to target the apical surface of M-cells. Because multiple pathogens target and invade M-cells very effectively, we believe that a biomimetic approach using invasin, a bacterial protein that mediates M-cell invasion, may be high affinity and high specificity targeting ligands for localizing P(MAA-g-EG) microgels at Peyer's patches.

The main objectives in this work were 1) to develop and optimize P(MAA-g-EG) gels for the delivery of a model protein vaccine, ovalbumin, and 2) to optimize a method for conjugation of targeting ligands to the surface of P(MAA-g-EG) hydrogels.

MATERIALS AND METHODS

Preparation of P(MAA-g-EG) Hydrogels

Thin films of P(MAA-g-EG) hydrogels were synthesized using a UV-initiated free solution radical polymerization. A solution of the monomers, crosslinker, initiator, and solvent were prepared. The solvent was 50 wt% water and 50 wt% ethanol. The solvent and an equal mass of the monomers were combined. The monomers, methacrylic acid (Sigma Aldrich) and poly(ethylene glycol) monomethyl ether monomethacrylate (PEGMA; Polysciences) with an average molecular weight of 1000, were added to the solvent such that there was an equal molar ratio between the methacrylic acid and

PEGMA ethylene glycol mer units. A 1% molar feed ratio of the crosslinker, poly(ethylene glycol) dimethacrylate (Polysciences), was added to the monomers and solvent mixture. Irgacure 184 (1-hydroxycyclohexy benzoephenone; Sigma Aldrich), the photoinitiator, was added at 0.5 wt% of the total monomers.

The solution was sonicated for 20 minutes to ensure full dissolution of reactants. After sonication, the solution was placed in a glove box which was sealed and then purged with nitrogen. The glove box was purged with nitrogen to reduce the amount of oxygen (in the glove box and dissolved in the solution of reactants) which acts as a free radical scavenger. The solution of reactants was placed in a glass mold and irradiated with UV light for 30 minutes. The polymer film was washed in Ultrapure water for 5-7 days to remove any unreacted components and noncrosslinked polymer. The water was changed twice every day.

After washing the film was drawer dried for 24 hours followed by drying in a vacuum oven at 37 ^{o}C for 24 hours. The dry P(MAA-g-EG) film was crushed using a mortar and pestle to form microparticles. The microparticles were sieved to achieve a microparticle size range of 53-75 µm.

Fourier Transform Infrared Spectroscopy

To confirm the synthesis of P(MAA-g-EG) hydrogels, Fourier transform infrared spectroscopy was used to show the functional groups present in the polymer. The sample was prepared from 2 mg of dry P(MAA-g-EG) and 198 mg of dry KBr. The sample powder was mixed using a mortar and pestle then placed in a steel die. A hydraulic press was used to form a 13 mm sample pellet in the die. The sample pellet was then placed in a FTIR sample holder. Infrared spectroscopy was performed using a Nicolet FT-IR. Samples were read at 4 cm^{-1} at either 40 or 100 scans.

HPLC of Ovalbumin

A method for performing high throughput liquid chromatography for ovalbumin was developed in order to accurately measure the amount of ovalbumin loaded and released. A Waters Alliance Chromatography instrument equipped with a Symmetry C4 5 µm column was used. The mobile phase consisted of 95% water with 0.1% trifluoroacetic acid (TFA) and 5% acetonitrile with 0.8% TFA. A gradient was applied to the column in the reverse direction (to 40% water, 60% acetonitrile). Typically, a 0.6 mL/min flowrate was used and a gradient time of 6-10 minutes was sufficient. The concentration of ovalbumin was measured by an inline dual wavelength UV detector (at 220 nm and 280 nm). The performance of the HPLC method was determined by comparing spectra of ovalbumin with spectra from a water sample run immediately after the sample. The HPLC spectra were used to determine ovalbumin concentrations by integrating the area under the curve (AUC) of the absorbance peak corresponding to ovalbumin and comparing to the AUC for a set of known concentrations.

Loading of Ovalbumin

P(MAA-g-EG) microgels were loaded with ovalbumin (Sigma Aldrich) by equilibrium partitioning. All glassware used in protein loading was first cleaned in a base bath and then coated with Sigmacote (Sigma Aldrich). A stock solution of ovalbumin (0.5 mg/ml) was prepared fresh in phosphate buffered saline at pH 7.4. A 100 µl sample of the original stock solution was taken and passed through a 0.2 µm filter.

Dry P(MAA-g-EG) microgels were slowly added to the solution to achieve a final concentration of 2 mg/ml of microgels. After addition of the P(MAA-g-EG) gels, the pH of the solution was checked. The suspension was allowed to stir for 4 hours. At 4 hours,

a 200 µl sample was removed from the suspension and passed through a 0.2 µm filter. The pH of the suspension was lowered to pH 3 by adding 0.1 N HCl. The volume of HCl added was recorded. After briefly stirring the suspension, the suspension was filtered through a Whatman 54 filter using vacuum aspiration. The collected microparticles were washed with a fixed volume of Ultrapure water, and the wash was filtered off the particles. The microparticles were collected from the filter paper. Loaded microparticles were dried by lyophilization overnight and stored in a -80 ^{o}C freezer until use.

Release Studies

In order to determine the release kinetics of ovalbumin from P(MAA-g-EG) gels, release studies were performed in phosphate buffered saline with a pH of 7.4. Release studies were carried out in a USP 2 dissolution apparatus to maintain a constant temperature of 37 ^{o}C and solutions were constantly stirred at 100 rpm. Dry P(MAA-g-EG) gels loaded with ovalbumin (20 mg) were slowly added to 20 ml of pre-warmed PBS. Over the 8 hour period, 200 µl samples were taken with replacement (with pre-warmed PBS) using a Norm-Eject Syringe and 19 gauge needle. Each sample was filtered through a 0.22 µm PVDF syringe filter (Millipore) and placed in an HPLC sample vial. The sample time points were 0, 5 minutes, 10 minutes, 15 minutes, 30 minutes, 60 minutes (1 h), 120 minutes (2 h), 240 minutes (4 h), and 480 minutes (8 h).

Samples were stored at 4 ^{o}C until the concentration in each sample was measured with HPLC. For HPLC of samples from release studies, the HPLC procedures remained the same, but the injected sample volume was increased from 20 µl to 40 µl.

Attachment of Ligands to Hydrogels

Optimization of Reaction with a Model Protein

Ovalbumin was attached to the P(MAA-g-EG) microgels as a model protein ligand. A variety of different reaction parameters were tested to optimize the protein conjugation protocol. A list of the reaction parameter can be found in Table 1.

Briefly, dry P(MAA-g-EG) microgels were suspended in the reaction buffer at a given concentration. Then, varying amounts of EDC and sulfo-NHS were added to the suspension. The suspension was mixed for varying activation times. The pH of the suspension was increased from 6 to ~8 with the addition of 1 N sodium hydroxide. A solution of ovalbumin was then added to the reaction mixture at various concentrations. The reaction was allowed to proceed for a set reaction time. The reaction conditions are given in Table 1. The suspension was centrifuged and the supernatant removed. The supernatant was used to measure the concentration of un-reacted protein. The particles were washed with water several times by centrifugation and resuspension in Ultrapure water.

Attachment of Invasin to P(MAA-g-EG) Hydrogels

Based on the optimized method for covalently attaching ovalbumin to P(MAA-g-EG) gels, invasin, an M-cell targeting ligand, was covalently attached to the P(MAA-g-EG) hydrogels. Briefly, CONC P(MAA-g-EG) was suspended in 1X PBS buffer. EDC was added and then the reaction mixture was placed on a shaker overnight. Finally, NaOH was added to the solution to raise the pH and a solution of invasin composed of 50% conc and 50% conc was added to the reaction mixture. The solution was placed on the shaker for 24 hours. The microparticles were removed by centrifugation. The concentration of invasin in the supernatant of the conjugation reaction was determined

by measuring the UV absorbance at 280 nm. The conjugation efficiency was calculated by mass balance.

UV/Vis Spectroscopy

The concentration of ovalbumin before and after conjugation to the P(MAA-g-EG) microgels was measured by UV absorbance at 280 nm. The supernatant of the conjugation reaction was read in a UV free 96-well plate on a Biotek UV/Vis plate reader. A calibration curve from ovalbumin at several different concentrations was used to calculate the concentration of ovalbumin in the supernatant of the conjugation reaction. The mass of ovalbumin after conjugation was subtracted from the starting mass of ovalbumin to determine the amount of ovalbumin conjugated to the P(MAA-g-EG) gels.

RESULTS AND DISCUSSION

Material Synthesis and Characterization

P(MAA-g-EG) hydrogels were successfully synthesized by a UV-initiated free radical solution polymerization. The resulting hydrogel films were transparent and flexible. After washing and drying, the film was brittle and easily crushed and sieved to form microparticles.

The synthesis of P(MAA-g-EG) gels was confirmed with FT-IR spectroscopy shown in Figure C2. The spectrum clearly shows the presence of both the PEG grafts and poly(methacrylic acid) backbone. The broad peak 2500-3500 cm^{-1} is due to hydroxyl stretching on the carboxylic acid groups and O-H groups associated with water. The peak and shoulders near this region 2850-3000 cm^{-1} corresponds to asymmetric and symmetric vibrations from PEG's methylene groups. A peak at 1730 cm^{-1} appears which corresponds to the carboxylic acid groups. The C=O vibration band for pure

poly(methacrylic acid) would be expected to fall closer to 1700 cm^{-1}, but hydrogen bonding is known to shift the peak (cite 20). The smaller band at 1390 cm^{-1} is associated with C-O stretching and O-H deformation vibrations on the MAA.

HPLC of Ovalbumin

In order to quantify loading and release of ovalbumin, an HPLC procedure was developed. First, the run time was set to 1 hour to make sure that there was enough time for gradient elution to occur. Next, the mobile phase and gradient were optimized. Ovalbumin is readily soluble aqueous solutions, and starting with a mostly aqueous mobile phase allows elution with a steeper gradient in the reverse direction. Therefore, the solubility of ovalbumin in 95% water and 5% acetonitrile was tested. In addition, an acidic mobile phase is highly desirable in HPLC of proteins so the solubility of ovalbumin in 95% water containing 0.1% TFA and 5% acetronitrile containing 0.08% TFA was verified.

Optimization of the reverse gradient took into account several important variables: the steepness of the gradient, the solubility of ovalbumin in a solvent with a greater percentage of organic solvent, and the ability of ovalbumin to elute from the column. The steepness of the gradient depends on the time period that the gradient runs over as well as the change in solvent composition. We found that a reverse gradient that changed the solvent composition to 40% water with 0.1% TFA and 60% acetonitrile with 0.08% TFA. It was important to note that as the organic component to the solvent increases, it becomes increasingly more likely that protein precipitation can occur. This caveat was taken into account in optimization of the gradient by determining the amount of sample retention after a sample run by running a water sample through the column.

The total run time and the gradient time were optimized to allow for relatively fast sample runs without causing peak broadening. Several spectra from the optimized procedure are shown in Figure C3 and 4. Ovalbumin appears as a sharp peak at 10.8 minutes when absorbance was measured at either a wavelength of 220 nm (Figure C3) or 280 nm (Figure C4).

Loading and release of ovalbumin

P(MAA-g-EG) microparticles were loaded with ovalbumin by equilibrium partitioning for 4 hours. In previous work by Shofner et al., a 4 hour loading time was shown to be sufficient for loading of large molecular weight proteins into P(MAA-g-EG) hydrogel microparticles. The results from loading studies with ovalbumin confirm these results. We achieved up to 40% loading in one study. However, the average loading efficiency obtained was 23%. This loading efficiency is lower than what has been achieved with P(MAA-g-EG) microparticles in part due to the size and hydrophobicity of ovalbumin. Ovalbumin is a relatively hydrophobic protein so a lower loading efficiency than more hydrophilic proteins in a hydrogel is expected.

In order to verify that release of ovalbumin from P(MAA-g-EG) gels was possible, a release study was carried out. In the first iteration of the release study, no release was measured by HPLC. It was assumed that no ovalbumin release was detected due to the low amount of loading and dilution by the relatively volume of buffer used for the release solution. In subsequent release studies, the release buffer volume was reduced to 20 ml. The release data is shown in Figure C5.

There are a few phenomena that may explain the unexpected release profile. First, ovalbumin is a relatively hydrophobic drug. It is possible that the protein interacts with the P(MAA-g-EG) network and preferentially stays in the network rather than

diffusing out into an aqueous buffer. Because the release buffer volume was decreased relative to the amount of P(MAA-g-EG) microparticles, it is possible that released ovalbumin adsorbed to neighboring microparticles instead of staying dissolved in the release media. In addition, a comparison between the AUCs used to determine protein concentration are less than 50000. If the AUCs are very low, detector resolution and signal-to-noise ratio may have significant effects on the data. Therefore, further investigation of the release of ovalbumin from P(MAA-g-EG) microgels are needed to fully understand the phenomena affecting ovalbumin release. Despite this, we were able to confirm that ovalbumin is released from P(MAA-g-EG) gels at neutral pH although there are still questions to be answered regarding the release kinetics.

Covalent Attachment of Ligands

For the covalent attachment of protein targeting ligands such as invasin, a method for attachment of proteins to P(MAA-g-EG) microparticles was optimized. Bioconjugation of molecules via reaction of carboxylic acid groups with primary amines under mild, aqueous reaction conditions is most commonly performed with carbodiimide coupling. Typically, EDC and sulfo-NHS are used to activate and stabilize a carboxylic acid groups, respectively. The activated carboxylic acid group and primary amine react forming an amide bond.

We chose to use EDC/NHS chemistry to form an amide bond between the carboxylic acid groups of P(MAA-g-EG) microparticles and primary amine groups on a protein targeting ligand. In this work, we optimized the reaction mechanism for attaching ovalbumin to the surface of P(MAA-g-EG) microgels as a model for invasin. The reason that we used a model protein instead of invasin was primarily based on cost and time efficiency. The Maynard Laboratory at the University of Texas at Austin

synthesizes an invasin ligand using *E. coli*. However, the process to synthesize invasin is time consuming and yields a relatively small amount of product.

A variety of conjugation reaction conditions were tested to determine what yielded the largest amount of conjugation. We found that the reaction efficiency increased when sulfo-NHS was omitted from the reaction. Sulfo-NHS forms an NHS ester with carboxylic acid groups and increases the half life of the activated carboxylic acid. In the conjugation reaction, the NHS ester serves as a leaving group in the conjugation reaction. Our results show that EDC is sufficient in activating carboxylic acid groups and that 24 hours is a sufficient activation time. Our results coincide with findings in which greater conjugation efficiencies in carbodiimide coupling of poly(N-isopropylacrylamide-co-acrylic acid) hydrogel particles were observed with EDC alone. They hypothesized that the NHS esters formed on the acrylic acid groups of the copolymer were much more stable than in aqueous solutions and was not a good leaving group.

Our results for using EDC without sulfo-NHS are summarized in Figures 6-8. We were primarily interested in determining the optimal ratios of EDC to polymer, protein to polymer, and reaction time. At low protein feed ratios, we saw a range of outcomes. The supernatant for several had high absorbance values which corresponded to protein concentrations higher than the initial concentrations and negative conjugation efficiencies as well as several absorbance values that were lower than the range of the calibration curve which caused the conjugation efficiency to exceed 100%. At higher protein feed ratios, we saw more reasonable data. At protein concentrations of 2 mg/ml and 0.2 mg/ml, we saw a reduction in the concentration of the protein after incubation with activated P(MAA-g-EG) microparticles. Similarly, we saw more protein conjugation at greater concentrations of EDC. While a 24 hour reaction time achieved

the highest conjugation efficiency compared to shorter reaction times, it is recommended that future work focus on reaction times less than 4 hours to prevent a significant amount of protein loading.

In performing the conjugation reaction with invasin, very low conjugation efficiencies were observed (1%). The data suggest that optimized protocol for ovalbumin may not be the optimal procedure for covalent attachment of invasin to the surface of P(MAA-g-EG) gels.

CONCLUSIONS

In this work, we developed P(MAA-g-EG) hydrogels for potential use as oral vaccine delivery systems. The methods to measure ovalbumin concentration for loading and release studies were optimized. We demonstrated as a proof of concept for invasin attachment to P(MAA-g-EG) microgels that conjugation of ovalbumin to the surface of the P(MAA-g-EG) microgels was possible. The ability to load and release a model protein vaccine, ovalbumin, was demonstrated. Future work includes optimization of the conjugation of invasin to the surface of the P(MAA-g-EG) microgels and optimization of loading and release of a vaccine from invasin modified-P(MAA-g-EG) microgels. *In vivo* studies would need to be performed to determine whether vaccine formulations with P(MAA-g-EG) elicit an immune response, generate protective immunity, and generate systemic immunity.

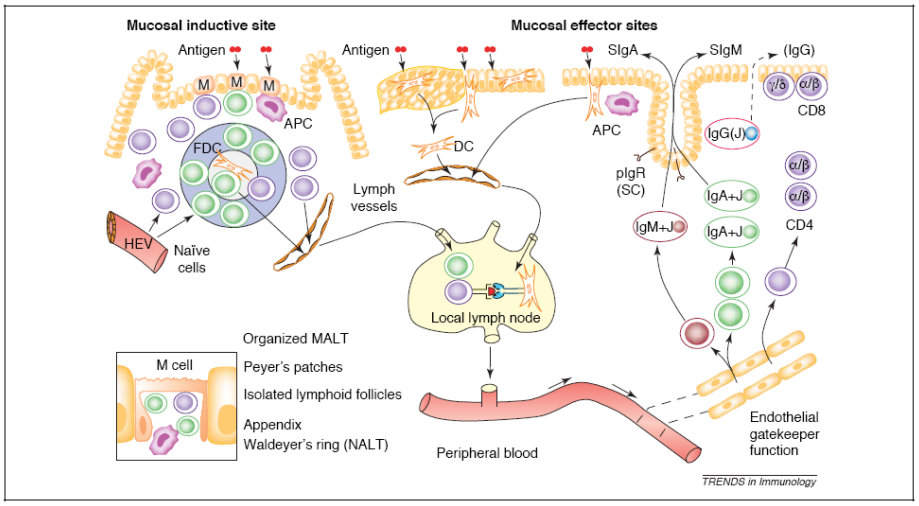

Figure C.1. Overview of the gut mucosal immune system

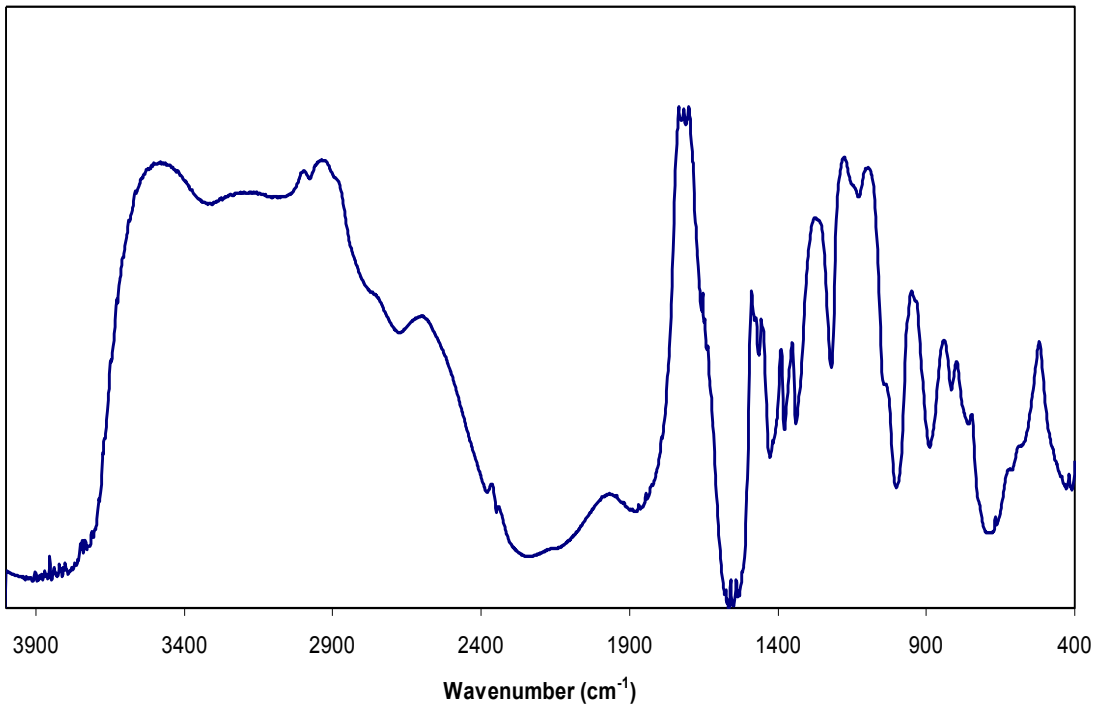

Figure C.2. FT-IR spectrum of P(MAA-g-EG) microparticles

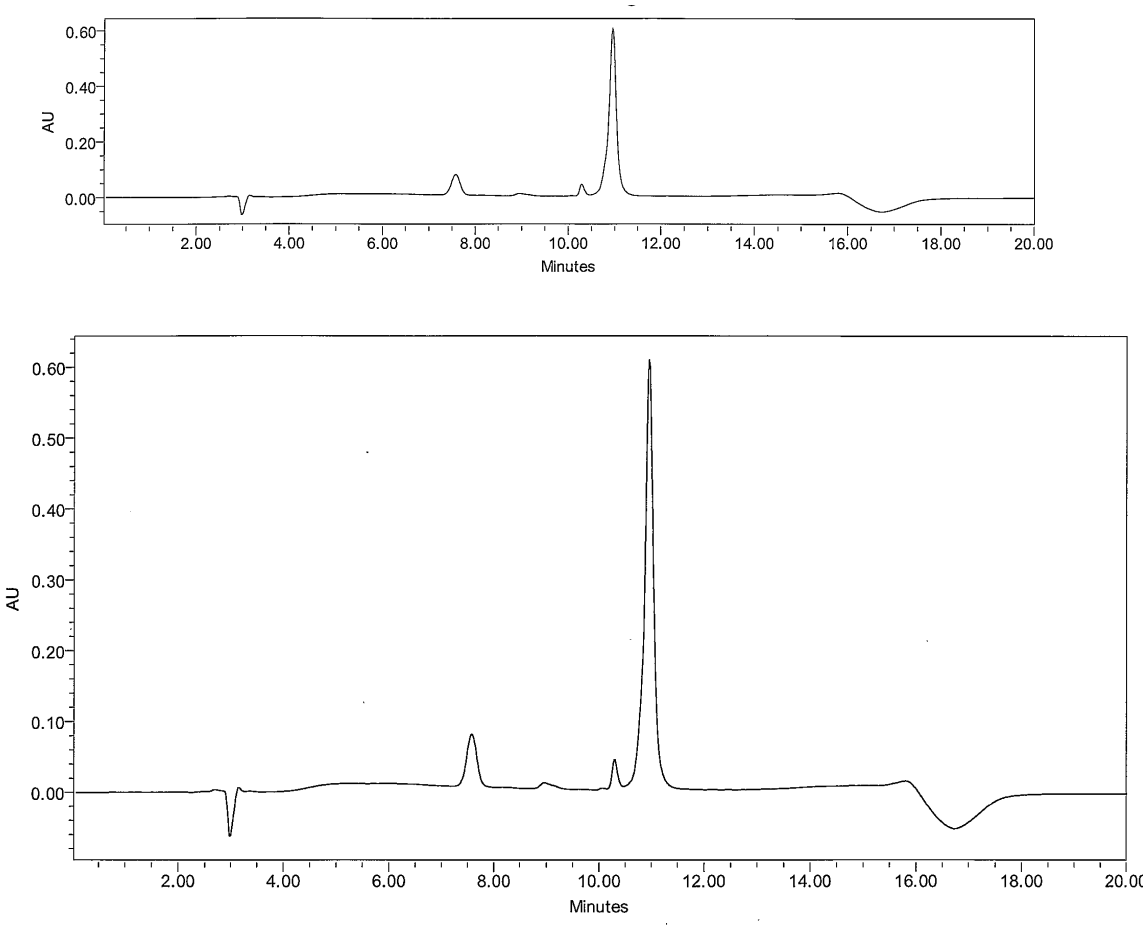

Figure C.3. HPLC absorbance spectrum of ovalbumin (wavelength of 220 nm)

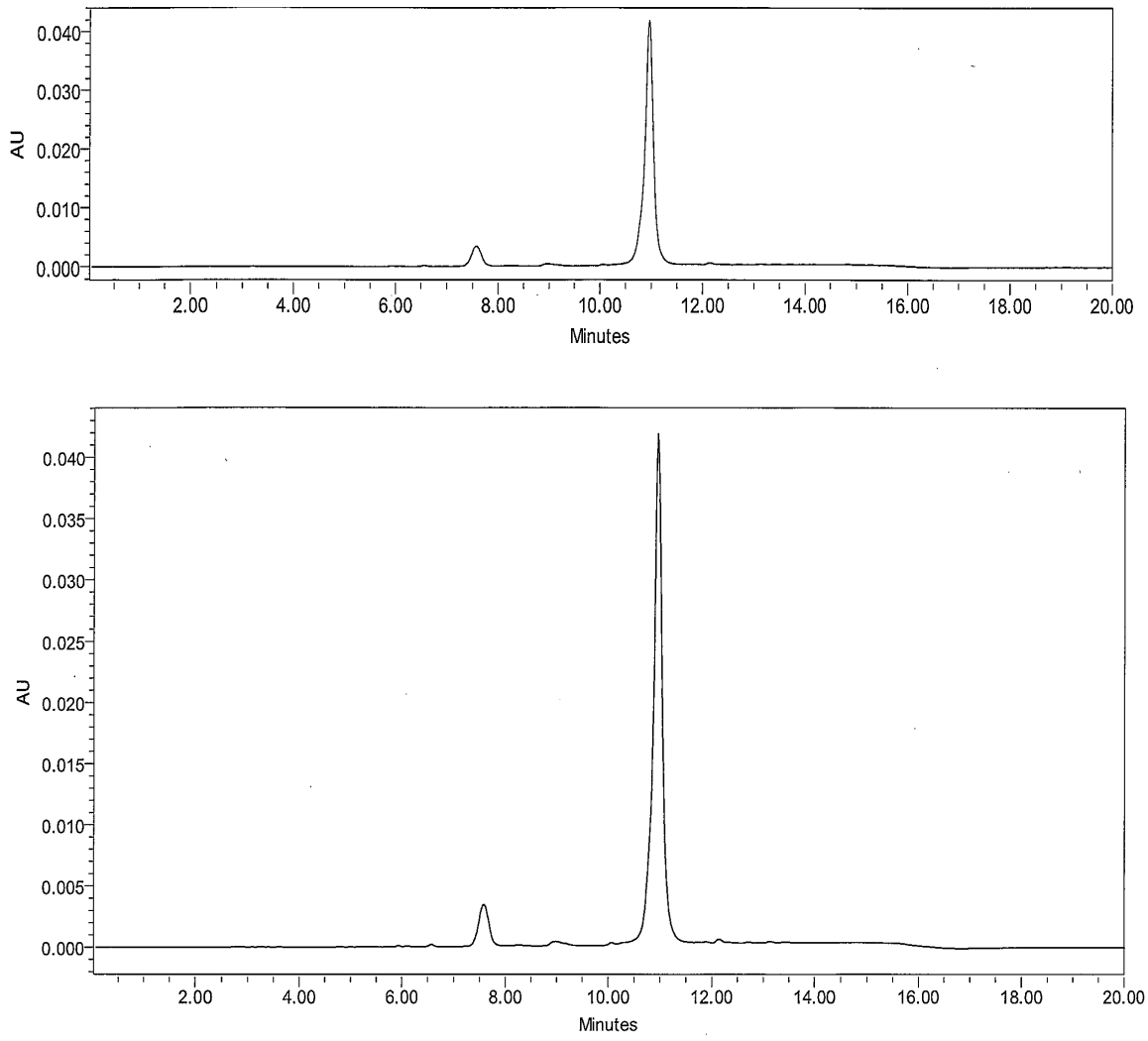

Figure C.4. HPLC absorbance spectrum of ovalbumin (wavelength 280 nm)

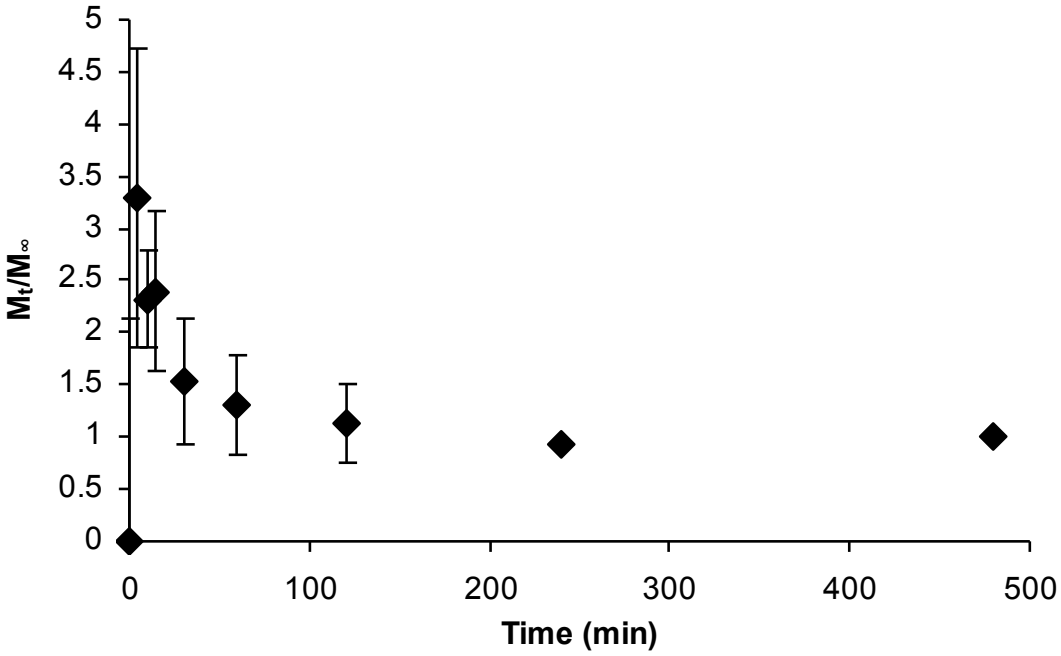

Figure C.5. Release profile of ovalbumin from P(MAA-g-EG) microparticles

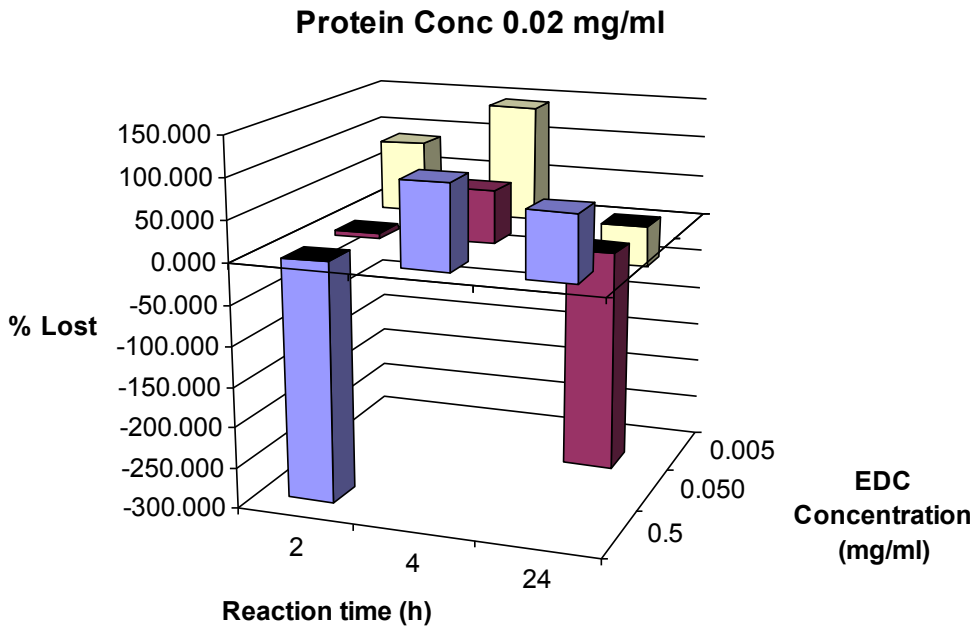

Figure C.6. Optimization of attachment of proteins to the surface of P(MAA-g-EG)

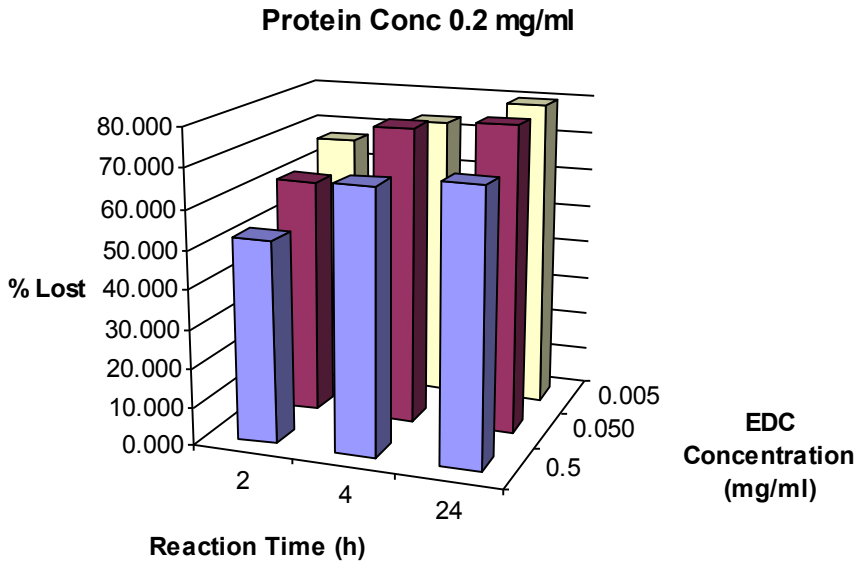

Figure C.7. Optimization of attachment of proteins to the surface of P(MAA-g-EG)

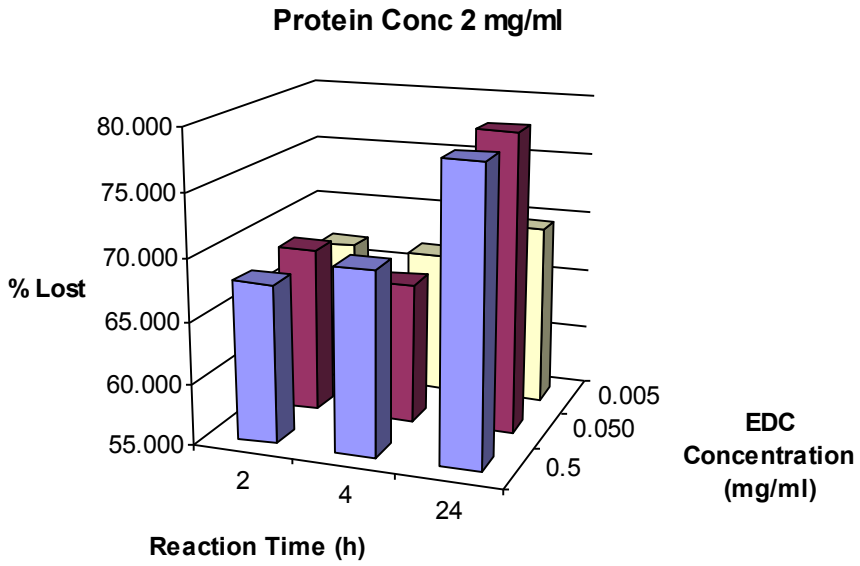

Figure C.8. Optimization of attachment of proteins to the surface of P(MAA-g-EG)

Table C.1. Variables used to optimize surface decoration

Polymer: Sulfo-NHS	Polymer: EDC	Polymer: Protein	Activation time	Reaction time
1:0	1:0.5	1:2	15 min	2 hours
1:1	1:0.05	1:0.2	30 min	4 hours
1:0.1	1:0.005	1:0.02	2 hours	24 hours
1:0.01			24 hours	

REFERENCES

1. Lavelle, E. C. and D. T. O'Hagan, Delivery systems and adjuvants for oral vaccines. *Expert Opin. Drug Deliv.*, 2006, 3, 747-762.

2. Holmgren, J. and C. Czerkinsky, Mucosal immunity and vaccines. *Nat. Med.*, 2005, 11, S45-S53.

3. Czerkinsky, C., S. J. Prince, S. M. Michalek, S. Jackson, M. W. Russell, Z. Moldoveanu, J. R. McGhee and J. Mestecky, IGA ANTIBODY-PRODUCING CELLS IN PERIPHERAL-BLOOD AFTER ANTIGEN INGESTION - EVIDENCE FOR A COMMON MUCOSAL IMMUNE-SYSTEM IN HUMANS. *Proc. Natl. Acad. Sci. U. S. A.*, 1987, 84, 2449-2453.

4. Mestecky, J., THE COMMON MUCOSAL IMMUNE-SYSTEM AND CURRENT STRATEGIES FOR INDUCTION OF IMMUNE-RESPONSES IN EXTERNAL SECRETIONS. *J. Clin. Immunol.*, 1987, 7, 265-276.

5. Macdonald, T. T., The mucosal immune system. *Parasite Immunol.*, 2003, 25, 235-246.

6. Bockman, D. E. and M. D. Cooper, PINOCYTOSIS BY EPITHELIUM ASSOCIATED WITH LYMPHOID FOLLICLES IN BURSA OF FABRICIUS, APPENDIX, AND PEYERS PATCHES - ELECTRON-MICROSCOPIC STUDY. 1973, 136, 455-477.

7. Neutra, M. R., T. L. Phillips, E. L. Mayer and D. J. Fishkind, TRANSPORT OF MEMBRANE-BOUND MACROMOLECULES BY M-CELLS IN FOLLICLE-ASSOCIATED EPITHELIUM OF RABBIT PEYER PATCH. 1987, 247, 537-546.

8. Owen, R. L., SEQUENTIAL UPTAKE OF HORSERADISH-PEROXIDASE BY LYMPHOID FOLLICLE EPITHELIUM OF PEYERS PATCHES IN NORMAL UNOBSTRUCTED MOUSE INTESTINE - ULTRASTRUCTURAL-STUDY. 1977, 72, 440-451.

9. Pappo, J. and T. H. Ermak, UPTAKE AND TRANSLOCATION OF FLUORESCENT LATEX-PARTICLES BY RABBIT PEYERS PATCH FOLLICLE EPITHELIUM - A QUANTITATIVE MODEL FOR M CELL UPTAKE. 1989, 76, 144-148.

10. Frey, A., K. T. Giannasca, R. Weltzin, P. J. Giannasca, H. Reggio, W. I. Lencer and M. R. Neutra, Role of the glycocalyx in regulating access of microparticles to apical plasma membranes of intestinal epithelial cells: Implications for microbial attachment and oral vaccine targeting. *J. Exp. Med.*, 1996, 184, 1045-1059.

11. Brandtzaeg, P. and R. Pabst, Let's go mucosal: communication on slippery ground. *Trends Immunol.*, 2004, 25, 570-577.

12. Boursier, L., J. N. Gordon, S. Thiagamoorthy, J. D. Edgeworth and J. Spencer, Human intestinal IgA response is generated in the organized gut-associated lymphoid tissue but not in the lamina propria. *Gastroenterology*, 2005, 128, 1879-1889.

13. Brandtzaeg, P., Mucosal Immunity: Induction, Dissemination, and Effector Functions. *Scand. J. Immunol.*, 2009, 70, 505-515.

14. Neutra, M. R. and P. A. Kozlowski, Mucosal vaccines: the promise and the challenge. *Nat. Rev. Immunol.*, 2006, 6, 148-158.

15. Brayden, D. J. and A. W. Baird, Apical membrane receptors on intestinal M cells: potential targets for vaccine delivery. *Adv. Drug Deliv. Rev.*, 2004, 56, 721-726.

16. Brayden, D. J., M. A. Jepson and A. W. Baird, Intestinal Peyer's patch M cells and oral vaccine targeting. *Drug Discov. Today*, 2005, 10, 1145-1157.

17. Challacombe, S. J., D. Rahman, H. Jeffery, S. S. Davis and D. T. Ohagan, ENHANCED SECRETORY IGA AND SYSTEMIC IGG ANTIBODY-RESPONSES AFTER ORAL IMMUNIZATION WITH BIODEGRADABLE MICROPARTICLES CONTAINING ANTIGEN. *Immunology*, 1992, 76, 164-168.

18. Challacombe, S. J., D. Rahman and D. T. Ohagan, Salivary, gut, vaginal and nasal antibody responses after oral immunization with biodegradable microparticles. *Vaccine*, 1997, 15, 169-175.

19. Maloy, K. J., A. M. Donachie, D. T. Ohagan and A. M. Mowat, INDUCTION OF MUCOSAL AND SYSTEMIC IMMUNE-RESPONSES BY IMMUNIZATION WITH OVALBUMIN ENTRAPPED IN POLY(LACTIDE-CO-GLYCOLIDE) MICROPARTICLES. *Immunology*, 1994, 81, 661-667.

20. Jones, D. H., B. W. McBride, C. Thornton, D. T. Ohagan, A. Robinson and G. H. Farrar, Orally administered microencapsulated Bordetella pertussis fimbriae protect mice from B-pertussis respiratory infection. *Infect. Immun.*, 1996, 64, 489-494.

21. Griffin, P., P. A. Offit, H. F. Clark and M. E. Conley, INVITRO PRODUCTION OF ROTAVIRUS SPECIFIC IGA AFTER ORAL IMMUNIZATION OF HUMANS. *Gastroenterology*, 1984, 86, 1099-1099.

22. Khoury, C. A., C. A. Moser, T. J. Speaker and P. A. Offit, ORAL INOCULATION OF MICE WITH LOW-DOSES OF MICROENCAPSULATED, NONINFECTIOUS ROTAVIRUS INDUCES VIRUS-SPECIFIC ANTIBODIES IN GUT-ASSOCIATED LYMPHOID-TISSUE. *J. Infect. Dis.*, 1995, 172, 870-874.

23. Offit, P. A., C. A. Khoury, C. A. Moser, H. F. Clark, J. E. Kim and T. J. Speaker, ENHANCEMENT OF ROTAVIRUS IMMUNOGENICITY BY MICROENCAPSULATION. *Virology*, 1994, 203, 134-143.

24. Larhed, A., L. Stertman, E. Edvardsson and I. Sjoholm, Starch microparticles as oral vaccine adjuvant: Antigen-dependent uptake in mouse intestinal mucosa. *J. Drug Target.*, 2004, 12, 289-296.

25. Stertman, L., E. Lundgren and I. Sjoholm, Starch microparticles as a vaccine adjuvant: Only uptake in Peyer's patches decides the profile of the immune response. *Vaccine*, 2006, 24, 3661-3668.

26. Stertman, L., L. Strindelius and I. Sjoholm, Starch microparticles as an adjuvant in immunisation: effect of route of administration on the immune response in mice. *Vaccine*, 2004, 22, 2863-2872.

27. Murillo, M., M. M. Goni, J. M. Irache, M. A. Arangoa, J. M. Blasco and C. Gamazo, Modulation of the cellular immune response after oral or subcutaneous immunization with microparticles containing Brucella ovis antigens. *J. Control. Release*, 2002, 85, 237-246.

28. Murillo, M., M. J. Grillo, J. Rene, C. M. Marin, M. Barberan, M. M. Goni, J. M. Blasco, J. M. Irache and C. Gamazo, A Brucella ovis antigenic complex bearing poly-epsilon-caprolactone microparticles confer protection against experimental brucellosis in mice. *Vaccine*, 2001, 19, 4099-4106.

29. Kadiyala, I., Y. H. Loo, K. Roy, J. Rice and K. W. Leong, Transport of chitosan-DNA nanoparticles in human intestinal M-cell model versus normal intestinal enterocytes. *Eur. J. Pharm. Sci.*, 39, 103-109.

30. Roy, K., H. Q. Mao, S. K. Huang and K. W. Leong, Oral gene delivery with chitosan-DNA nanoparticles generates immunologic protection in a murine model of peanut allergy. *Nat. Med.*, 1999, 5, 387-391.

31. Yamamoto, M., P. Rennert, J. R. McGhee, M. N. Kweon, S. Yamamoto, T. Dohi, S. Otake, H. Bluethmann, K. Fujihashi and H. Kiyono, Alternate mucosal immune system: Organized Peyer's patches are not required for IgA responses in the gastrointestinal tract. *J. Immunol.*, 2000, 164, 5184-5191.

32. Lowman, A. M., M. Morishita, M. Kajita, T. Nagai and N. A. Peppas, Oral delivery of insulin using pH-responsive complexation gels. 1999, 88, 933-937.

33. Fisher, O. Z. and N. A. Peppas, Quantifying tight junction disruption caused by biomimetic pH-sensitive hydrogel drug carriers. *J. Drug Deliv. Sci. Technol.*, 2008, 18, 47-50.

34. Lowman, A. M. and N. A. Peppas, Molecular analysis of interpolymer complexation in graft copolymer networks. *Polymer*, 2000, 41, 73-80.

35. Morishita, M., T. Goto, K. Nakamura, A. M. Lowman, K. Takayama and N. A. Peppas, Novel oral insulin delivery systems based on complexation polymer hydrogels: Single and multiple administration studies in type 1 and 2 diabetic rats. 2006, 110, 587-594.

36. Sahlin, J. J. and N. A. Peppas, Enhanced hydrogel adhesion by polymer interdiffusion: Use of linear poly(ethylene glycol) as an adhesion promoter. *J. Biomater. Sci.-Polym. Ed.*, 1997, 8, 421-436.

37. Garinot, M., V. Fievez, V. Pourcelle, F. Stoffelbach, A. des Rieux, L. Plapied, I. Theate, H. Freichels, C. Jerome, J. Marchand-Brynaert, Y. J. Schneider and V. Preat, PEGylated PLGA-based nanoparticles targeting M cells for oral vaccination. *J. Control. Release*, 2007, 120, 195-204.

38. Fievez, V., L. Plapied, C. Plaideau, D. Legendre, A. des Rieux, V. Pourcelle, H. Freichels, C. Jerome, J. Marchand, V. Preat and Y. J. Schneider, In vitro identification of targeting ligands of human M cells by phage display. *Int. J. Pharm.*, 394, 35-42.

References

Achar, L. and N. A. Peppas, Preparation, Characterization And Mucoadhesive Interactions Of Poly(Methacrylic Acid) Copolymers With Rat Mucosa. *J. Control. Release*, 1994, 31, 271-276.

Agnihotri, S. A., N. N. Mallikarjuna and T. M. Aminabhavi, Recent advances on chitosan-based micro- and nanoparticles in drug delivery. *J. Control. Release*, 2004, 100, 5-28.

Agüeros, M., L. Ruiz-Gatón, C. Vauthier, K. Bouchemal, S. Espuelas, G. Ponchel and J. M. Irache, Combined hydroxypropyl-[beta]-cyclodextrin and poly(anhydride) nanoparticles improve the oral permeability of paclitaxel. *Eur. J. Pharm. Sci.*, 2009, 38, 405-413.

Aigner, J., J. Tegeler, P. Hutzler, D. Campoccia, A. Pavesio, C. Hammer, E. Kastenbauer and A. Naumann, Cartilage tissue engineering with novel nonwoven structured biomaterial based on hyaluronic acid benzyl ester. *J. Biomed. Mater. Res.*, 1998, 42, 172-181.

Akiyama, Y., T. Mori, Y. Katayama and T. Niidome, The effects of PEG grafting level and injection dose on gold nanorod biodistribution in the tumor-bearing mice. *J. Control. Release*, 2009, 139, 81-84.

Albertsson, P. A., Particle Fractionation in Liquid Two-Phase Systems: The Composition of Some Phase Systems and the Behaviour of Some Model Particles in them Application to the Isolation of Cell Walls from Microorganisms. *Biochim. Biophys. Acta*, 1958, 27, 378-395.

amEnde, M. T., D. Hariharan and N. A. Peppas, Factors influencing the drug and protein transport and release from ionic hydrogels. React. Polym., 1995, 25, 127-137.

Aoki, Y., M. Morishita and K. Takayama, Role of the mucous/glycocalyx layers in insulin permeation across the rat ileal membrane. *Int. J. Pharm.*, 2005, 297, 98-109.

Artursson, P. and R. T. Borchardt, Intestinal drug absorption and metabolism in cell cultures: Caco-2 and beyond. *Pharm. Res.*, 1997, 14,

Artursson, P., T. Lindmark, S. S. Davis and L. Illum, Effect of chitosan on the permeability of monolayers of intestinal epithelial cells (Caco-2). *Pharm. Res.*, 1994, 11, 1358-1361.

Artursson, P., K. Parlm and K. Luthman, Caco-2 monolayers in experimental and theoretical predictions of drug transport. *Adv. Drug Deliver. Rev.*, 2001, 46, 27-43.

Astete, C. E. and C. M. Sabliov, Synthesis and characterization of PLGA nanoparticles. *J. Biomater. Sci. Polym. Ed.*, 2006, 17, 247-289.

Augst, A. D., H. J. Kong and D. J. Mooney, Alginate hydrogels as biomaterials. *Macromol. Biosci.*, 2006, 6, 623-633.

Aungst, B. J., Intestinal Permeation Enhancers. *J. Pharm. Sci.*, 2000, 89, 429-442.

Avgoustakis, K., A. Beletsi, Z. Panagi, P. Klepetsanis, A. G. Karydas and D. S. Ithakissios, PLGA-mPEG nanoparticles of cisplatin: in vitro nanoparticle degradation, in vitro drug release and in vivo drug residence in blood properties. *J. Control. Release*, 2002, 79, 123-135.

Avgoustakis, K., A. Beletsi, Z. Panagi, P. Klepetsanis, E. Livaniou, G. Evangelatos and D. S. Ithakissios, Effect of copolymer composition on the physicochemical characteristics, in vitro stability, and biodistribution of PLGA-mPEG nanoparticles. *Int. J. Pharm.*, 2003, 259, 115-127.

Bae, Y., N. Nishiyama and K. Kataoka, In vivo antitumor activity of the folate-conjugated pH-Sensitive polymeric micelle selectively releasing adriamycin in the intracellular acidic compartments. *Bioconjugate Chem.*, 2007, 18, 1131-1139.

Balimane, P. V. and S. Chong, Cell culture-based models for intestinal permeability: a critique. *Drug Discover. Today*, 2005, 10, 335-343.

Banting, F. G., C. H. Best, J. B. Collip, W. R. Campbell and A. A. Fletcher, Pancreatic Extracts in the Treatment of Diabetes Mellitus. *Can. Med. Assoc. J.*, 1922, 12, 141-146.

Barsbay, M. and A. Guner, Miscibility of dextran and poly(ethylene glycol) in solid state: Effect of the solvent choice. *Carbohyd. Polym.*, 2007, 69, 214-223.

Bartlett, D. W., H. Su, I. J. Hildebrandt, W. A. Weber and M. E. Davis, Impact of tumor-specific targeting on the biodistribution and efficacy of siRNA nanoparticles measured by multimodality in vivo imaging. *Proc. Natl. Acad. Sci. U. S. A.*, 2007, 104, 15549-15554.

Bazile, D. V., C. Ropert, P. Huve, T. Verrecchia, M. Marlard, A. Frydman, M. Veillard and G. Spenlehauer, BODY DISTRIBUTION OF FULLY BIODEGRADABLE [C-14] POLY(LACTIC ACID) NANOPARTICLES COATED WITH ALBUMIN AFTER PARENTERAL ADMINISTRATION TO RATS. *Biomaterials*, 1992, 13, 1093-1102.

Behravesh, E., V. I. Sikavitsas and A. G. Mikos, Quantification of ligand surface concentration of bulk-modified biomimetic hydrogels. Biomaterials, 2003, 24, 4365-4374.

Berger, J., M. Reist, J. M. Mayer, O. Felt, N. A. Peppas and R. Gurny, Structure and interactions in covalently and ionically crosslinked chitosan hydrogels for biomedical applications. *Eur. J. Pharm. Biopharm.*, 2004, 57, 19-34.

Bergmann, N. M. and N. A. Peppas, Molecularly imprinted polymers with specific recognition for macromolecules and proteins. Prog. Polym. Sci., 2008, 33, 271-288.

Bergmann, N. M. and N. A. Peppas, Configurational Biomimetic Imprinting for Protein Recognition: Structural Characteristics of Recognitive Hydrogels. Ind. Eng. Chem. Res., 2008, 47, 9099-9107.

Bertozzi, C. R. and L. L. Kiessling, Chemical glycobiology. 2001, 291, 2357-2364.

Besheer, A., K. M. Wood, N. A. Peppas and K. Mader, Loading and mobility of spin-labeled insulin in physiologically responsive complexation hydrogels intended for oral administration. *J. Control. Release*, 2006, 111, 73-80.

Betancourt, T., J. Pardo, K. Soo and N. A. Peppas, Characterization of pH-responsive hydrogels of poly(itaconic acid-g-ethylene glycol) prepared by UV-initiated free radical polymerization as biomaterials for oral delivery of bioactive agents. *J. Biomed. Mater. Res. Part A*, 93A, 175-188.

Bigucci, F., B. Luppi, L. Monaco, T. Cerchiara and V. Zecchi, Pectin-based microspheres for colon-specific delivery of vancomycin. *J. Pharm. Pharmacol.*, 2009, 61, 41-46.

Bilati, U., E. Allemann and E. Doelker, Poly(D,L-lactide-co-glycolide) protein-loaded nanoparticles prepared by the double emulsion method-processing and formulation issues for enhanced entrapment efficiency. *J. Microencapsul.*, 2005, 22, 205-214.

Bilous, R. and R. Donnelly, *Handbook of Diabetes*. John Wiley & Sons Ltd., Chichester, 2010,

Blanchette, J., N. Kavimandan and N. A. Peppas, Principles of transmucosal delivery of therapeutic agents. *Biomed. Pharmacother.*, 2004, 58, 142-151.

Bockman, D. E. and M. D. Cooper, PINOCYTOSIS BY EPITHELIUM ASSOCIATED WITH LYMPHOID FOLLICLES IN BURSA OF FABRICIUS, APPENDIX, AND PEYERS PATCHES - ELECTRON-MICROSCOPIC STUDY. 1973, 136, 455-477.

Bouhadir, K. H., E. Alsberg and D. J. Mooney, Hydrogels for combination delivery of antineoplastic agents. 2001, 22, 2625-2633.

Boursier, L., J. N. Gordon, S. Thiagamoorthy, J. D. Edgeworth and J. Spencer, Human intestinal IgA response is generated in the organized gut-associated lymphoid tissue but not in the lamina propria. *Gastroenterology*, 2005, 128, 1879-1889.

Bowman, K. and K. W. Leong, Chitosan nanoparticles for oral drug and gene delivery. *Int. J. Nanomed.*, 2006, 1, 117-128.

Brandtzaeg, P. and R. Pabst, Let's go mucosal: communication on slippery ground. *Trends Immunol.*, 2004, 25, 570-577.

Brandtzaeg, P., Mucosal Immunity: Induction, Dissemination, and Effector Functions. *Scand. J. Immunol.*, 2009, 70, 505-515.

Brayden, D. J. and A. W. Baird, Apical membrane receptors on intestinal M cells: potential targets for vaccine delivery. *Adv. Drug Deliv. Rev.*, 2004, 56, 721-726.

Brayden, D. J., M. A. Jepson and A. W. Baird, Intestinal Peyer's patch M cells and oral vaccine targeting. *Drug Discov. Today*, 2005, 10, 1145-1157.

Bucior, I. and M. M. Burger, Carbohydrate-carbohydrate interaction as a major force initiating cell-cell recognition. *Glycoconjugate J.*, 2004, 21, 111-123.

Bucior, I., S. Scheuring, A. Engel and M. M. Burger, Carbohydrate-carbohydrate interaction provides adhesion force and specificity for cellular recognition. *J. Cell Biol.*, 2004, 165, 529-537.

Bulpitt, P. and D. Aeschlimann, New strategy for chemical modification of hyaluronic acid: Preparation of functionalized derivatives and their use in the formation of novel biocompatible hydrogels. 1999, 47, 152-169.

Burdick, J. A., C. Chung, X. Q. Jia, M. A. Randolph and R. Langer, Controlled degradation and mechanical behavior of photopolymerized hyaluronic acid networks. *Biomacromolecules*, 2005, 6, 386-391.

Burke, S. D., Q. Zhao, M. C. Schuster and L. L. Kiessling, Synergistic formation of soluble lectin clusters by a templated multivalent saccharide ligand. *J. Am. Chem. Soc.*, 2000, 122, 4518-4519.

Byrne, J. D., T. Betancourt and L. Brannon-Peppas, Active targeting schemes for nanoparticle systems in cancer therapeutics. *Adv. Drug Deliv. Rev.*, 2008, 60, 1615-1626.

Cakal, E. and S. Cavus, Novel Poly(N-vinylcaprolactam-co-2-(diethylamino)ethyl methacrylate) Gels: Characterization and Detailed Investigation on Their Stimuli-Sensitive Behaviors and Network Structure. Ind. Eng. Chem. Res., 2010, 49, 11741-11751.

Camby, I., M. Le Mercier, V. Mathieu, L. Ingrassia, F. Lefranc and R. Kiss, Galectin-1 as potential therapeutic target for cancer progression. *Drug Future*, 2008, 33, 1057-1069.

Carlsson, J., H. Drevin and R. Axen, Protein thiolation and reversible protein-protein conjugation. N-Succinimidyl 3-(2-pyridyldithio)propionate, a new heterobifunctional reagent. *Biochem J.*, 1978, 173, 723-737.

Carr, D. A., Molecular Design of Biomaterial Systems for the Oral Delivery of Therapeutic Proteins. 2008, Ph.D., 225, Thesis. Academic, DepartmentThe University of Texas at Austin.

Carr, D. A., M. Gomez-Burgaz, M. C. Boudes and N. A. Peppas, Complexation Hydrogels for the Oral Delivery of Growth Hormone and Salmon Calcitonin. *Ind. Eng. Chem. Res.*, 2010, 49, 11991-11995.

Carr, D. A. and N. A. Peppas, Assessment of poly(methacrylic acid-co-N-vinyl pyrrolidone) as a carrier for the oral delivery of therapeutic proteins using Caco-2 and HT29-MTX cell lines. J. Biomed. Mater. Res. Part A, 2010, 92A, 504-512.

Caterson, E. J., L. J. Nesti, W. J. Li, K. G. Danielson, T. J. Albert, A. R. Vaccaro and R. S. Tuan, Three-dimensional cartilage formation by bone marrow-derived cells seeded ion polylactide/alginate amalgam. *J. Biomed. Mater. Res.*, 2001, 57, 394-403.

Challacombe, S. J., D. Rahman, H. Jeffery, S. S. Davis and D. T. Ohagan, ENHANCED SECRETORY IGA AND SYSTEMIC IGG ANTIBODY-RESPONSES AFTER ORAL IMMUNIZATION WITH BIODEGRADABLE MICROPARTICLES CONTAINING ANTIGEN. *Immunology*, 1992, 76, 164-168.

Challacombe, S. J., D. Rahman and D. T. Ohagan, Salivary, gut, vaginal and nasal antibody responses after oral immunization with biodegradable microparticles. *Vaccine*, 1997, 15, 169-175.

Chan, J. M., L. Zhang, K. P. Yuet, G. Liao, J. W. Rhee, R. Langer and O. C. Farokhzad, PLGA-lecithin-PEG core-shell nanoparticles for controlled drug delivery. *Biomaterials*, 2009, 30, 1627-1634.

Chen, H., Y. Gu, Y. Hu and Z. Qian, Characterization of pH- and Temperature-sensitive Hydrogel Nanoparticles for Controlled Drug Release. *PDA J. Pharm. Sci. Tech.*, 2007, 61, 303-313.

Cheng, J. J., B. A. Teply, S. Y. Jeong, C. H. Yim, D. Ho, I. Sherifi, S. Jon, O. C. Farokhzad, A. Khademhosseini and R. S. Langer, Magnetically responsive polymeric microparticles for oral delivery of protein drugs. *Pharm. Res.*, 2006, 23, 557-564.

Cheng, M. Y., W. L. Cao, Y. Cao, Y. D. Gong, N. M. Zhao and X. F. Zhang, Studies on nerve cell affinity of biodegradable modified chitosan films. *J. Biomater. Sci.-Polym. Ed.*, 2003, 14, 1155-1167.

Cheng, M. Y., J. U. Deng, F. Yang, Y. D. Gong, N. M. Zhao and X. F. Zhang, Study on physical properties and nerve cell affinity of composite films from chitosan and gelatin solutions. *Biomaterials*, 2003, 24, 2871-2880.

Cho, C. S., S. J. Seo, I. K. Park, S. H. Kim, T. H. Kim, T. Hoshiba, I. Harada and T. Akaike, Galactose-carrying polymers as extracellular matrices for liver tissue engineering. *Biomaterials*, 2006, 27, 576-585.

Choi, H. S., W. Liu, P. Misra, E. Tanaka, J. P. Zimmer, B. Itty Ipe, M. G. Bawendi and J. V. Frangioni, Renal clearance of quantum dots. *Nat. Biotechnol.*, 2007, 25, 1165-1170.

Chupa, J. M., A. M. Foster, S. R. Sumner, S. V. Madihally and H. W. T. Matthew, Vascular cell responses to polysaccharide materials: in vitro and in vivo evaluations. *Biomaterials*, 2000, 21, 2315-2322.

Clark, M. A., B. H. Hirst and M. A. Jepson, Lectin-mediated mucosal delivery of drugs and microparticles. 2000, 43, 207-223.

Collier, J. H., J. P. Camp, T. W. Hudson and C. E. Schmidt, Synthesis and characterization of polypyrrole-hyaluronic acid composite biomaterials for tissue engineering applications. *J. Biomed. Mater. Res.*, 2000, 50, 574-584.

Csaky, T. Z., Intestinal Permeation and Permeability: an Overview. 1984, 61-88.

Cui, F. D., A. J. Tao, D. M. Cun, L. Q. Zhang and K. Shi, Preparation of insulin loaded PLGA-Hp55 nanoparticles for oral delivery. *J. Pharm. Sci.*, 2007, 96, 421-427.

Czerkinsky, C., S. J. Prince, S. M. Michalek, S. Jackson, M. W. Russell, Z. Moldoveanu, J. R. McGhee and J. Mestecky, IGA ANTIBODY-PRODUCING CELLS IN PERIPHERAL-BLOOD AFTER ANTIGEN INGESTION - EVIDENCE FOR A COMMON MUCOSAL IMMUNE-SYSTEM IN HUMANS. *Proc. Natl. Acad. Sci. U. S. A.*, 1987, 84, 2449-2453.

Damge, C., M. Socha, N. Ubrich and P. Maincent, Poly(epsilon-Caprolactone)/Eudragit Nanoparticles for Oral Delivery of Aspart-Insulin in the Treatment of Diabetes. *J. Pharm. Sci.*, 99, 879-889.

Damge, C., P. Maincent and N. Ubrich, Oral delivery of insulin associated to polymeric nanoparticles in diabetic rats. *J. Control. Release*, 2007, 117, 163-170.

Dang, J. M. and K. W. Leong, Natural polymers for gene delivery and tissue engineering. *Adv. Drug Deliv. Rev.*, 2006, 58, 487-499.

Daugherty, A. L. and R. J. Mrsny, Regulation of the intestinal epithelial paracellular barrier. *Pharm. Sci. Tech. Today*, 1999, 2, 281-287.

David, A., P. Kopeckova, T. Minko, A. Rubinstein and J. Kopecek, Design of a multivalent galactoside ligand for selective targeting of HPMA copolymer-doxorubicin conjugates to human colon cancer cells. 2004, 40, 148-157.

Dawes, G. J., L. E. Fratila-Apachitei, K. Mulia, I. Apachitei, G. J. Witkamp and J. Duszczyk, Size effect of PLGA spheres on drug loading efficiency and release profiles. *J. Mater. Sci. Mater M*, 2009, 20, 1089-1094.

Deascentiis, A., J. L. Degrazia, C. N. Bowman, P. Colombo and N. A. Peppas, Mucooadhesion of Poly(2-Hydroxy Ethyl Methacrylate) is Improved when Linear Poly(Ethylene Oxide) Chains are Added to the Polymer Network. *J. Control. Release*, 1995, 33, 197-201.

De Groot, C. J., M. J. A. Van Luyn, W. N. E. Van Dijk-Wolthuis, J. A. Cadee, J. A. Plantinga, W. Den Otter and W. E. Hennink, In vitro biocompatibility of biodegradable dextran-based hydrogels tested with human fibroblasts. *Biomaterials*, 2001, 22, 1197-1203.

De Jong, W. H., W. I. Hagens, P. Krystek, M. C. Burger, A. J. Sips and R. E. Geertsma, Particle size-dependent organ distribution of gold nanoparticles after intravenous administration. *Biomaterials*, 2008, 29, 1912-1919.

Delacour, D., C. I. Cramm-Behrens, H. Drobecq, A. Le Bivic, H. Y. Naim and R. Jacob, Requirement for galectin-3 in apical protein sorting. *Curr. Biol.*, 2006, 16, 408-414.

Delacour, D., C. Greb, A. Koch, E. Salomonsson, H. Leffler, A. Le Bivic and R. Jacob, Apical sorting by galectin-3-dependent glycoprotein clustering. *Traffic*, 2007, 8, 379-388.

Denker, B. M. and S. K. Nigam, Molecular structure and assembly of the tight junction. *Am. J. Physiol. Renal Physiol.*, 1998, 274, F1-9.

De Smedt, S. C., A. Lauwers and D. J., Characterization of the Network Structure of Dextran Glycidyl Methacrylate Hydrogels by Studying the Rheological and Swelling Behavior. *Macromolecules*, 1995, 28, 5082-5088.

Deutel, B., M. Greindl, M. Thaurer and A. Bernkop-Schnuerch, Novel insulin thiomer nanoparticles: In vivo evaluation of an oral drug delivery system. *Biomacromolecules*, 2008, 9, 278-285.

Diabetes Atlas. International Diabetes Federation, Brussels, 2006, 387.

Diamond, A. D. and J. T. Hsu, Phase Diagrams for Dextran-PEG Aqueous Two-Phase Systems at 22 Degrees C. *Biotechnol. Tech.*, 1989, 3, 119-124.

Diduch, D. R., L. C. M. Jordan, C. M. Mierisch and G. Balian, Marrow stromal cells embedded in alginate for repair of osteochondral defects. *Arthroscopy*, 2000, 16, 571-577.

Discher, D. E., V. Ortiz, G. Srinivas, M. L. Klein, Y. Kim, D. Christian, S. Cai, P. Photos and F. Ahmed, Emerging applications of polymersomes in delivery: From molecular dynamics to shrinkage of tumors. *Prog. Polym. Sci.*, 2007, 32, 838-857.

Dunn, S. E., A. G. A. Coombes, M. C. Garnett, S. S. Davis, M. C. Davies and L. Illum, In vitro cell interaction and in vivo biodistribution of poly(lactide-co-glycolide) nanospheres surface modified by poloxamer and poloxamine copolymers. *J. Control. Release*, 1997, 44, 65-76.

Eckel, R. H., S. M. Grundy and P. Z. Zimmet, The metabolic syndrome. *Lancet*, 2005, 365, 1415-1428.

Eichenbaum, G. M., P. F. Kiser, A. V. Dobrynin, S. A. Simon and D. Needham, Investigation of the swelling response and loading of ionic microgels with drugs and proteins: The dependence on cross-link density. Macromolecules, 1999, 32, 4867-4878.

ElBayoumi, T. A. and V. P. Torchilin, Tumor-Specific Anti-Nucleosome Antibody Improves Therapeutic Efficacy of Doxorubicin-Loaded Long-Circulating Liposomes against Primary and Metastatic Tumor in Mice. *Mol. Pharm.*, 2009, 6, 246-254.

Eniola, A. O. and D. A. Hammer, Characterization of biodegradable drug delivery vehicles with the adhesive properties of leukocytes - II: effect of degradation on targeting activity. *Biomaterials*, 2005, 26, 661-670.

Eniola, A. O. and D. A. Hammer, Artificial polymeric cells for targeted drug delivery. *J. Control. Release*, 2003, 87, 15-22.

Esposito, A., A. Mezzogiorno, A. Sannino, A. De Rosa, D. Menditti, V. Esposito and L. Ambrosio, Hyaluronic acid based materials for intestine tissue engineering: A morphological and biochemical study of cell-material interaction. *J. Mater. Sci.-Mater. Med.*, 2006, 17, 1365-1372.

Fasano, A., Novel approaches for oral delivery of macromolecules. *J. Pharm. Sci.*, 1998, 87, 1351-1356.

Faulstich, H., S. Zobeley, D. Heintz and G. Drewes, Probing the phalloidin binding site of actin. *FEBS Lett.*, 1993, 318, 218-222.

Faure, A. C., S. Dufort, V. Josserand, P. Perriat, J. L. Coll, S. Roux and O. Tillement, Control of the in vivo Biodistribution of Hybrid Nanoparticles with Different Poly(ethylene glycol) Coatings. *Small*, 2009, 5, 2565-2575.

Fetih, G., S. Lindberg, K. Itoh, N. Okada, T. Fujita, F. Habib, P. Artersson, M. Attia and A. Yamamoto, Improvement of absorption enhancing effects of n-dodecyl-beta-D-maltopyranoside by its colon-specific delivery using chitosan capsules. *Int. J. Pharm.*, 2005, 293, 127-135.

Fievez, V., L. Plapied, C. Plaideau, D. Legendre, A. des Rieux, V. Pourcelle, H. Freichels, C. Jerome, J. Marchand, V. Preat and Y. J. Schneider, In vitro identification of targeting ligands of human M cells by phage display. *Int. J. Pharm.*, 394, 35-42.

Finney, S. J., P. B. Anning, T. V. Cao, M. Perretti, T. W. Evans and A. Burke-Gaffney, Butanol-extracted lipoteichoic acid induces in vivo leukocyte adhesion. *Biochem. Biophys. Res. Commun.*, 2007, 364, 831-837.

Fisher, O. Z. and N. A. Peppas, Polybasic Nanomatrices Prepared by UV-Initiated Photopolymerization. *Macromolecules*, 2009, 42, 3391-3398.

Fisher, O. Z. and N. A. Peppas, Quantifying tight junction disruption caused by biomimetic pH-sensitive

Fitzpatrick, J. A., S. K. Andreko, L. A. Ernst, A. S. Waggoner, B. Ballou and M. P. Bruchez, Long-term Persistence and Spectral Blue Shifting of Quantum Dots in Vivo. *Nano Lett.*, 2009, 9, 2736-2741.

Fonseca, C., S. Simões and R. Gaspar, Paclitaxel-loaded PLGA nanoparticles: preparation, physicochemical characterization and in vitro anti-tumoral activity. 2002, 83, 273-286.

Foss, A. C. and N. A. Peppas, Investigation of the cytotoxicity and insulin transport of acrylic-based copolymer protein delivery systems in contact with Caco-2 cultures. *Eur. J. Pharm. Biopharm.*, 2004, 57, 447-455.

Freeze, H. H., Genetic defects in the human glycome. *Nat. Rev. Genet.*, 2006, 7, 537-551.

Frey, A., K. T. Giannasca, R. Weltzin, P. J. Giannasca, H. Reggio, W. I. Lencer and M. R. Neutra, Role of the glycocalyx in regulating access of microparticles to apical plasma membranes of intestinal epithelial cells: Implications for microbial attachment and oral vaccine targeting. *J. Exp. Med.*, 1996, 184, 1045-1059.

Fu, A. Z., Y. Qiu and L. Radican, Impact of fear of insulin or fear of injection on treatment outcomes of patients with diabetes. *Curr. Med. Res. Opin.*, 2009, 25, 1413-1420.

Fukuda, M., Roles of mucin-type O-glycans in cell adhesion. *Biochim. Biophys. Acta-Gen. Subj.*, 2002, 1573, 394-405.

Gabius, H. J., H. C. Siebert, S. Andre, J. Jimenez-Barbero and H. Rudiger, Chemical biology of the sugar code. *Chembiochem*, 2004, 5, 741-764.

Gabor, F. and M. Wirth, Lectin-mediated drug delivery: fundamentals and perspectives. *STP Pharma Sci.*, 2003, 13, 3-16.

Gabor, F., M. Stangl and M. Wirth, Lectin-mediated bioadhesion: binding characteristics of plant lectins on the enterocyte-like cell lines Caco-2, HT-29 and HCT-8. *J. Control. Release*, 1998, 55, 131-142.

Gan, Q. and T. Wang, Chitosan nanoparticle as protein delivery carrier--Systematic examination of fabrication conditions for efficient loading and release. *Colloid Surface B*, 2007, 59, 24-34.

Ganta, S., H. Devalapally, A. Shahiwala and M. Amiji, A review of stimuli-responsive nanocarriers for drug and gene delivery. *J. Control. Release*, 2008, 126, 187-204.

Garinot, M., V. Fievez, V. Pourcelle, F. Stoffelbach, A. des Rieux, L. Plapied, I. Theate, H. Freichels, C. Jerome, J. Marchand-Brynaert, Y. J. Schneider and V. Preat, PEGylated PLGA-based nanoparticles targeting M cells for oral vaccination. *J. Control. Release*, 2007, 120, 195-204.

George, M. and T. E. Abraham, Polyionic hydrocolloids for the intestinal delivery of protein drugs: Alginate and chitosan - a review. *J. Control. Release*, 2006, 114, 1-14.

Glangchai, L. C., M. Caldorera-Moore, L. Shi and K. Roy, Nanoimprint lithography based fabrication of shape-specific, enzymatically-triggered smart nanoparticles. 2008, 125, 263-272.

Goeddel, D. V., D. G. Kleid, F. Bolivar, H. L. Heyneker, D. G. Yansura, R. Crea, T. Hirose, A. Kraszewski, K. Itakura and A. D. Riggs, Expression in Escherichia coli of chemically synthesized genes for human insulin. *P. Natl. Acad. Sci. U.S.A.*, 1979, 76, 106-110.

Gombotz, W. R. and S. F. Wee, Protein release from alginate matrices. *Adv. Drug Deliv. Rev.*, 1998, 31, 267-285.

Goto, T., M. Morishita, N. J. Kavimandan, K. Takayama and N. A. Peppas, Gastrointestinal transit and mucoadhesive characteristics of complexation hydrogels in rats. *J. Pharm. Sci.*, 2006, 95, 462-469.

Govender, T., S. Stolnik, M. C. Garnett, L. Illum and S. S. Davis, PLGA nanoparticles prepared by nanoprecipitation: drug loading and release studies of a water soluble drug. *J. Control. Release*, 1999, 57, 171-185.

Guowei, D., K. Adriane, X. Chen, C. Jie and L. Yinfeng, PVP magnetic nanospheres: Biocompatibility, in vitro and in vivo bleomycin release. *Int. J. Pharm.*, 2007, 328, 78-85.

Granato, D., F. Perotti, I. Masserey, M. Rouvet, M. Golliard, A. Servin and D. Brassart, Cell surface-associated lipoteichoic acid acts as an adhesion factor for

attachment of Lactobacillus johnsonii La1 to human enterocyte-like Caco-2 cells. *Appl. Environ. Microbiol.*, 1999, 65, 1071-1077.

Gratton, S. E., P. A. Ropp, P. D. Pohlhaus, J. C. Luft, V. J. Madden, M. E. Napier and J. M. DeSimone, The effect of particle design on cellular internalization pathways. *Proc. Natl. Acad. Sci. U. S. A.*, 2008, 105, 11613-11618.

Green, D. W., S. Mann and R. O. C. Oreffo, Mineralized polysaccharide capsules as biomimetic microenvironments for cell, gene and growth factor delivery in tissue engineering. *Soft Matter*, 2006, 2, 732-737.

Griffin, P., P. A. Offit, H. F. Clark and M. E. Conley, INVITRO PRODUCTION OF ROTAVIRUS SPECIFIC IGA AFTER ORAL IMMUNIZATION OF HUMANS. *Gastroenterology*, 1984, 86, 1099-1099.

Griffith, L. G. and S. Lopina, Microdistribution of substratum-bound ligands affects cell function: hepatocyte spreading on PEO-tethered galactose. 1998, 19, 979-986.

Gumbiner, B., Structure, biochemistry, and assembly of epithelial tight junctions. *Am. J. Physiol. Cell Physiol.*, 1987, 253, C749-758.

Gunning, A. P., R. J. M. Bongaerts and V. J. Morris, Recognition of galactan components of pectin by galectin-3. *Faseb J.*, 2009, 23, 415-424.

Hama, Y., Y. Urano, Y. Koyama, P. L. Choyke and H. Kobayashi, Targeted optical imaging of cancer cells using lectin-binding BODIPY conjugated avidin. *Biochem. Biophys. Res. Commun.*, 2006, 348, 807-813.

Hama, Y., Y. Urano, Y. Koyama, M. Kamiya, M. Bernardo, R. S. Paik, M. C. Krishna, P. L. Choyke and H. Kobayashi, In vivo spectral fluorescence imaging of submillimeter peritoneal cancer implants using a lectin-targeted optical agent. *Neoplasia*, 2006, 8, 607-U2.

Hamaguchi, T., Y. Matsumura, M. Suzuki, K. Shimizu, R. Goda, I. Nakamura, I. Nakatomi, M. Yokoyama, K. Kataoka and T. Kakizoe, NK105, a paclitaxel-incorporating

micellar nanoparticle formulation, can extend in vivo antitumour activity and reduce the neurotoxicity of paclitaxel. *Brit. J. Cancer*, 2005, 92, 1240-1246.

Hasa, J. and M. Ilavsky, Deformational, Swelling and Potentiometric Behavior of Ionized Poly(Methacrylic Acid) Gels. 2. Experimental Results. J. Polym. Sci., Part B: Polym. Phys., 1975, 13, 263-274.

Hastewell, J., S. Lynch, R. Fox, I. Williamson, P. Skeltonstroud and M. Mackay, Enhancement of Human Calcitonin Absorption Across the Rat Colon In-vivo. *Int. J. Pharm.*, 1994, 101, 115-120.

Heinemann, L., The Failure of Exubera: Are We Beating a Dead Horse? 2008, 2, 518-529.

Hirabayashi, J., Y. Arata and K. Kasai, Glycome project: Concept, strategy and preliminary application to Caenorhabditis elegans. *Proteomics*, 2001, 1, 295-303.

Holmgren, J. and C. Czerkinsky, Mucosal immunity and vaccines. *Nat. Med.*, 2005, 11, S45-S53.

Holt, T. and S. Kumar, *ABC of Diabetes*. John Wiley & Sons Ltd, Chichester, 2010, 114.

Hsu, K. L., K. T. Pilobello and L. K. Mahal, Analyzing the dynamic bacterial glycome with a lectin microarray approach. *Nat. Chem. Biol.*, 2006, 2, 153-157.

Huang, Y. B., W. Leobandung, A. Foss and N. A. Peppas, Molecular aspects of muco- and bioadhesion: Tethered structures and site-specific surfaces. *J. Control. Release*, 2000, 65, 63-71

Huang, Y. B., I. Szleifer and N. A. Peppas, A molecular theory of polymer gels. *Macromolecules*, 2002, 35, 1373-1380.

Hwang, S.-J., H. Park and K. Park, Gastric Retentive Drug-Delivery Systems. *Crit. Rev. Ther Drug Carrier Syst.*, 1998, 15, 243-284.

Ichikawa, H. and N. A. Peppas, Novel complexation hydrogels for oral peptide delivery: In vitro evaluation of their cytocompatibility and insulin-transport enhancing effects using Caco-2 cell monolayers. *J. Biomed. Mater. Res. Part A*, 2003, 67A, 609-617.

Itakura, K., T. Hirose, R. Crea, A. D. Riggs, H. L. Heyneker, F. Bolivar and H. W. Boyer, Expression in Escherichia coli of a Chemically Synthesized Gene for the Hormone Somatostatin. *Science*, 1977, 198, 1056-1063.

Iwaki, J., T. Minamisawa, H. Tateno, J. Kominami, K. Suzuki, N. Nishi, T. Nakamura and J. Hirabayashi, Desulfated galactosaminoglycans are potential ligands for galectins: Evidence from frontal affinity chromatography. *Biochem. Biophys. Res. Commun.*, 2008, 373, 206-212.

Iwasaki, N., S. T. Yamane, T. Majima, Y. Kasahara, A. Minami, K. Harada, S. Nonaka, N. Maekawa, H. Tamura, S. Tokura, M. Shiono, K. Monde and S. I. Nishimura, Feasibility of polysaccharide hybrid materials for scaffolds in cartilage tissue engineering: Evaluation of chondrocyte adhesion to polyion complex fibers prepared from alginate and chitosan. *Biomacromolecules*, 2004, 5, 828-833.

Iyer, A. K., G. Khaled, J. Fang and H. Maeda, Exploiting the enhanced permeability and retention effect for tumor targeting. *Drug Discov. Today*, 2006, 11, 812-818.

Jaffer, F. A., M. Nahrendorf, D. Sosnovik, K. A. Kelly, E. Aikawa and R. Weissleder, Cellular imaging of inflammation in atherosclerosis using magnetofluorescent nanomaterials. *Mol. Imaging*, 2006, 5, 85-92.

Jain, T. K., M. K. Reddy, M. A. Morales, D. L. Leslie-Pelecky and V. Labhasetwar, Biodistribution, clearance, and biocompatibility of iron oxide magnetic nanoparticles in rats. *Mol. Pharm.*, 2008, 5, 316-327.

Janes, K. A., P. Calvo and M. J. Alonso, Polysaccharide colloidal particles as delivery systems for macromolecules. *Adv. Drug Deliv. Rev.*, 2001, 47, 83-97.

D. H., B. W. McBride, C. Thornton, D. T. Ohagan, A. Robinson and G. H. Farrar, Orally administered microencapsulated Bordetella pertussis fimbriae protect mice from B-pertussis respiratory infection. *Infect. Immun.*, 1996, 64, 489-494.

Jepson, M. A., M. A. Clark and B. H. Hirst, M cell targeting by lectins: a strategy for mucosal vaccination and drug delivery. 2004, 56, 511-525.

Joseph, J. W., J. Kalitsky, S. St-Pierre and P. L. Brubaker, Oral delivery of glucagon-like peptide-1 in a modified polymer preparation normalizes basal glycaemia in diabetic db/db mice. *Diabetologia*, 2000, 43, 1319-1328.

Kabanov, A. V., E. V. Batrakova and V. Y. Alakhov, Pluronic® block copolymers as novel polymer therapeutics for drug and gene delivery. *J. Control. Release*, 2002, 82, 189-212.

Kadiyala, I., Y. H. Loo, K. Roy, J. Rice and K. W. Leong, Transport of chitosan-DNA nanoparticles in human intestinal M-cell model versus normal intestinal enterocytes. *Eur. J. Pharm. Sci.*, 39, 103-109.

Kamei, N., M. Morishita, H. Chiba, N. J. Kavimandan, N. A. Peppas and K. Takayama, Complexation hydrogels for intestinal delivery of interferon beta and calcitonin. *J. Control. Release*, 2009, 134, 98-102.

Kataoka, K., A. Harada and Y. Nagasaki, Block copolymer micelles for drug delivery: design, characterization and biological significance. *Adv. Drug Deliv. Rev.*, 2001, 47, 113-131.

Kavimandan, N. J., E. Losi and N. A. Peppas, Novel delivery system based on complexation hydrogels as delivery vehicles for insulin-transferrin conjugates. *Biomaterials*, 2006, 27, 3846-3854.

Kavimandan, N. J. and N. A. Peppas, Confocal microscopic analysis of transport mechanisms of insulin across the cell monolayer. *Int. J. Pharm.*, 2008, 354, 143-148.

Kelly, K. A., J. R. Allport, A. Tsourkas, V. R. Shinde-Patil, L. Josephson and R. Weissleder, Detection of vascular adhesion molecule-1 expression using a novel multimodal nanoparticle. *Circ. Res.*, 2005, 96, 327-336.

Khoury, C. A., C. A. Moser, T. J. Speaker and P. A. Offit, ORAL INOCULATION OF MICE WITH LOW-DOSES OF MICROENCAPSULATED, NONINFECTIOUS ROTAVIRUS INDUCES VIRUS-SPECIFIC ANTIBODIES IN GUT-ASSOCIATED LYMPHOID-TISSUE. *J. Infect. Dis.*, 1995, 172, 870-874.

Kim, S. H. and C. C. Chu, Synthesis and characterization of dextran-methacrylate hydrogels and structural study by SEM. *J. Biomed. Mater. Res.*, 2000, 49, 517-527.

Kim, S. H., T. Hoshiba and T. Akaike, Effect of carbohydrates attached to polystyrene on hepatocyte morphology on sugar-derivatized polystyrene matrices. *J. Biomed. Mater. Res. Part A*, 2003, 67A, 1351-1359.

Kim, B. S. and D. J. Mooney, Development of biocompatible synthetic extracellular matrices for tissue engineering. *Trends Biotechnol.*, 1998, 16, 224-230.

Kirpotin, D. B., D. C. Drummond, Y. Shao, M. R. Shalaby, K. Hong, U. B. Nielsen, J. D. Marks, C. C. Benz and J. W. Park, Antibody targeting of long-circulating lipidic nanoparticles does not increase tumor localization but does increase internalization in animal models. *Cancer Res.*, 2006, 66, 6732-6740.

Kryscio, D. R. and N. A. Peppas, Mimicking Biological Delivery Through Feed back-Controlled Drug Release Systems Based on Molecular Imprinting. Aiche J., 2009, 55, 1311-1324.

Langer, R., Polymer Implants for Drug Delivery in the Brain. *J. Control. Release*, 1991, 16, 53-59.

Larhed, A., L. Stertman, E. Edvardsson and I. Sjoholm, Starch microparticles as oral vaccine adjuvant: Antigen-dependent uptake in mouse intestinal mucosa. *J. Drug Target.*, 2004, 12, 289-296.

Lavelle, E. C. and D. T. O'Hagan, Delivery systems and adjuvants for oral vaccines. *Expert Opin. Drug Deliv.*, 2006, 3, 747-762.

Lawrence, M. B. and T. A. Springer, Neutrophils Roll on E-Selectin. *J. Immunol.*, 1993, 151, 6338-6346.

Leach, J. B., K. A. Bivens, C. N. Collins and C. E. Schmidt, Development of photocrosslinkable hyaluronic acid-polyethylene glycol-peptide composite hydrogels for soft tissue engineering. *J. Biomed. Mater. Res. Part A*, 2004, 70A, 74-82.

Leader, B., Q. J. Baca and D. E. Golan, Protein therapeutics: A summary and pharmacological classification. *Nat. Rev. Drug Discov.*, 2008, 7, 21-39.

Lee, A. L., Y. Wang, H. Y. Cheng, S. Pervaiz and Y. Y. Yang, The co-delivery of paclitaxel and Herceptin using cationic micellar nanoparticles. *Biomaterials*, 2009, 30, 919-927.

Lee, W. C., S. Balu, D. Cobden, A. V. Joshi and C. L. Pashos, Medication adherence and the associated health-economic impact among patients with type 2 diabetes mellitus converting to insulin pen therapy: An analysis of third-party managed care claims data. *Clin. Ther.*, 2006, 28, 1712-1725.

.Lee, Y. C., R. R. Townsend, M. R. Hardy, J. Lonngren, J. Arnarp, M. Haraldsson and H. Lonn, Binding Of Synthetic Oligosaccharides To The Hepatic Gal Galnac Lectin - Dependence On Fine-Structural Features. *J. Biol. Chem.*, 1983, 258, 199-202.

Leitner, V. M., M. K. Marschutz and A. Bernkop-Schnurch, Mucoadhesive and cohesive properties of poly(acrylic acid)-cysteine conjugates with regard to their molecular mass. *Eur. J. Pharm. Sci.*, 2003, 18, 89-96.

Leitner, V. M., G. F. Walker and A. Bernkop-Schnurch, Thiolated polymers: evidence for the formation of disulphide bonds with mucus glycoproteins. *Eur. J. Pharm. Biopharm.*, 2003, 56, 207-214.

Leslie-Barbick, J. L., J. J. Moon and J. L. West, Covalently-immobilized vascular endothelial growth factor promotes endothelial cell tubulogenesis in poly(ethylene glycol) diacrylate hydrogels. J. Biomater. Sci., 2009, 20, 1763-1779.

Lewis, G. F., A. Carpentier, K. Adeli and A. Giacca, Disordered fat storage and mobilization in the pathogenesis of insulin resistance and type 2 diabetes. *Endocr. Rev.*, 2002, 23, 201-229.

Li, Y. P., Y. Y. Pei, X. Y. Zhang, Z. H. Gu, Z. H. Zhou, W. F. Yuan, J. J. Zhou, J. H. Zhu and X. J. Gao, PEGylated PLGA nanoparticles as protein carriers: synthesis, preparation and biodistribution in rats. *J. Control. Release*, 2001, 71, 203-211.

Lim, S. T., G. P. Martin, D. J. Berry and M. B. Brown, Preparation and evaluation of the in vitro drug release properties and mucoadhesion of novel microspheres of hyaluronic acid and chitosan. *J. Control. Release*, 2000, 66, 281-292.

Lopac, S. K., M. P. Torres, J. H. Wilson-Welder, M. J. Wannemuehler and B. Narasimhan, Effect of polymer chemistry and fabrication method on protein release and stability from polyanhydride microspheres. *J. Biomed. Mater. Res. B.*, 2009, 91, 938-947.

Lopina, S. T., G. Wu, E. W. Merrill and L. GriffithCima, Hepatocyte culture on carbohydrate-modified star polyethylene oxide hydrogels. *Biomaterials*, 1996, 17, 559-569.

Lowman, A. M., M. Morishita, M. Kajita, T. Nagai and N. A. Peppas, Oral delivery of insulin using pH-responsive complexation gels. 1999, 88, 933-937.

Lowman, A. M. and N. A. Peppas, Molecular analysis of interpolymer complexation in graft copolymer networks. *Polymer*, 2000, 41, 73-80.

Lu, J. X., F. Prudhommeaux, A. Meunier, L. Sedel and G. Guillemin, Effects of chitosan on rat knee cartilages. *Biomaterials*, 1999, 20, 1937-1944.

Lu, W., C. Xiong, G. Zhang, Q. Huang, R. Zhang, J. Z. Zhang and C. Li, Targeted Photothermal Ablation of Murine Melanomas with Melanocyte-Stimulating Hormone Analog-Conjugated Hollow Gold Nanospheres. *Clin. Cancer Res.*, 2009, 15, 876-886.

Luchansky, S. J., S. Goon and C. R. Bertozzi, Expanding the diversity of unnatural cell-surface sialic acids. *Chembiochem*, 2004, 5, 371-374.

Ludwig, A., The use of mucoadhesive polymers in ocular drug delivery. *Adv. Drug Deliv. Rev.*, 2005, 57, 1595-1639.

Macadam, A., The Effect of Gastrointestinal Mucus on Drug Absorption. *Adv. Drug Deliv. Rev.*, 1993, 11, 201-220.

Macdonald, T. T., The mucosal immune system. *Parasite Immunol.*, 2003, 25, 235-246.

Madihally, S. V. and H. W. T. Matthew, Porous chitosan scaffolds for tissue engineering. *Biomaterials*, 1999, 20, 1133-1142.

Madsen, F. and N. A. Peppas, Complexation graft copolymer networks: swelling properties, calcium binding and proteolytic enzyme inhibition. *Biomaterials*, 1999, 20, 1701-1708.

Mahal, L. K., K. J. Yarema and C. R. Bertozzi, Engineering chemical reactivity on cell surfaces through oligosaccharide biosynthesis. 1997, 276, 1125-1128.

Malam, Y., M. Loizidou and A. M. Seifalian, Liposomes and nanoparticles: nanosized vehicles for drug delivery in cancer. *Trends Pharmacol. Sci.*, 2009, 30, 592-599.

Maloy, K. J., A. M. Donachie, D. T. Ohagan and A. M. Mowat, INDUCTION OF MUCOSAL AND SYSTEMIC IMMUNE-RESPONSES BY IMMUNIZATION WITH OVALBUMIN ENTRAPPED IN POLY(LACTIDE-CO-GLYCOLIDE) MICROPARTICLES. *Immunology*, 1994, 81, 661-667.

Mammen, M., S. K. Choi and G. M. Whitesides, Polyvalent interactions in biological systems: Implications for design and use of multivalent ligands and inhibitors. *Angew. Chem.-Int. Edit.*, 1998, 37, 2755-2794.

Mann, D. A., M. Kanai, D. J. Maly and L. L. Kiessling, Probing low affinity and multivalent interactions with surface plasmon resonance: Ligands for concanavalin A. 1998, 120, 10575-10582.

Mann, B. K., R. H. Schmedlen and J. L. West, Tethered-TGF-beta increases extracellular matrix production of vascular smooth muscle cells. Biomaterials, 2001, 22, 439-444.

Masuko, T., N. Iwasaki, S. Yamane, T. Funakoshi, T. Majima, A. Minami, N. Ohsuga, T. Ohta and S. I. Nishimura, Chitosan-RGDSGGC conjugate as a scaffold material for musculoskeletal tissue engineering. *Biomaterials*, 2005, 26, 5339-5347.

Maury, J., A. Bernadac, A. Rigal and S. Maroux, Expression and Glycosylation of the Filamentous Brush-Border Glycocalyx (FBBG) during Rabbit Enterocyte Differentiation along the Crypt-Villus Axis. *J. Cell Sci.*, 1995, 108, 2705-2713.

Mestecky, J., THE COMMON MUCOSAL IMMUNE-SYSTEM AND CURRENT STRATEGIES FOR INDUCTION OF IMMUNE-RESPONSES IN EXTERNAL SECRETIONS. *J. Clin. Immunol.*, 1987, 7, 265-276.

Mikos, A. G. and N. A. Peppas, Bioadhesive Analysis Of Controlled-Release Systems .4. An Experimental-Method For Testing The Adhesion Of Microparticles With Mucus. 1990, 12, 31-37.

Missirlis, D., R. Kawamura, N. Tirelli and J. A. Hubbell, Doxorubicin encapsulation and diffusional release from stable, polymeric, hydrogel nanoparticles. *Eur. J. Pharm. Sci.*, 2006, 29, 120-129.

Mitra, S., U. Gaur, P. C. Ghosh and A. N. Maitra, Tumour targeted delivery of encapsulated dextran-doxorubicin conjugate using chitosan nanoparticles as carrier. *J. Control. Release*, 2001, 74, 317-323.

Moghimi, S. M. and J. Szebeni, Stealth liposomes and long circulating nanoparticles: critical issues in pharmacokinetics, opsonization and protein-binding properties. *Prog. Lipid Res.*, 2003, 42, 463-478.

Molineux, G., Pegylation: engineering improved pharmaceuticals for enhanced therapy. *Cancer Treat. Rev.*, 2002, 28, 13-16.

Morishita, M., T. Goto, K. Nakamura, A. M. Lowman, K. Takayama and N. A. Peppas, Novel oral insulin delivery systems based on complexation polymer hydrogels: Single and multiple administration studies in type 1 and 2 diabetic rats. *J. Control. Release*, 2006, 110, 587-594.

Morishita, M., M. Goto, K. Takayama and N. A. Peppas, Oral insulin delivery systems based on complexation polymer hydrogels. *J. Drug Deliv. Sci. Technol.*, 2006, 16, 19-24.

Morishita, M., I. Morishita, K. Takayama, Y. Machida and T. Nagai, Novel Oral Microspheres of Insulin with Protease Inhibitor Protecting Enzymatic Degradation. *Int. J. Pharm.*, 1992, 78, 1-7.

Morishita, I., M. Morishita, K. Takayama, Y. Machida and T. Nagai, Enteral Insulin Delivery by Microspheres in 3 Different Formulations Using Eudragit-L-100 and Eudragit-S100. *Int. J. Pharm.*, 1993, 91, 29-37.

Morishita, M. and N. A. Peppas, Is the oral route possible for peptide and protein drug delivery. *Drug Discov. Today*, 2006, 11, 905-910.

Moriyama, K. and N. Yui, Regulated insulin release from biodegradable dextran hydrogels containing poly(ethylene glycol) (vol 42, pg 237, 1996). *J. Control. Release*, 1997, 45, 209-209.

Mu, L. and S. S. Feng, A novel controlled release formulation for the anticancer drug paclitaxel (Taxol®): PLGA nanoparticles containing vitamin E TPGS. *J. Control. Release*, 2003, 86, 33-48.

Murillo, M., M. M. Goni, J. M. Irache, M. A. Arangoa, J. M. Blasco and C. Gamazo, Modulation of the cellular immune response after oral or subcutaneous immunization with microparticles containing Brucella ovis antigens. *J. Control. Release*, 2002, 85, 237-246.

Murillo, M., M. J. Grillo, J. Rene, C. M. Marin, M. Barberan, M. M. Goni, J. M. Blasco, J. M. Irache and C. Gamazo, A Brucella ovis antigenic complex bearing poly-epsilon-caprolactone microparticles confer protection against experimental brucellosis in mice. *Vaccine*, 2001, 19, 4099-4106.

National diabetes fact sheet: general information and national estimates on diabetes in the United States. 2007,

Neubauer, A. M., H. Sim, P. M. Winter, S. D. Caruthers, T. A. Williams, J. D. Robertson, D. Sept, G. M. Lanza and S. A. Wickline, Nanoparticle Pharmacokinetic Profiling In Vivo Using Magnetic Resonance Imaging. *Magn. Reson. Med.*, 2008, 60, 1353-1361.

Neutra, M. R. and P. A. Kozlowski, Mucosal vaccines: the promise and the challenge. *Nat. Rev. Immunol.*, 2006, 6, 148-158.

Neutra, M. R., T. L. Phillips, E. L. Mayer and D. J. Fishkind, TRANSPORT OF MEMBRANE-BOUND MACROMOLECULES BY M-CELLS IN FOLLICLE-ASSOCIATED EPITHELIUM OF RABBIT PEYER PATCH. 1987, 247, 537-546.

Nishikawa, M., A. Kamijo, T. Fujita, Y. Takakura, H. Sezaki and M. Hashida, Synthesis And Pharmacokinetics Of A New Liver-Specific Carrier, Glycosylated Carboxymethyl-Dextran, And Its Application To Drug Targeting. *Pharm. Res.*, 1993, 10, 1253-1261.

Offit, P. A., C. A. Khoury, C. A. Moser, H. F. Clark, J. E. Kim and T. J. Speaker, ENHANCEMENT OF ROTAVIRUS IMMUNOGENICITY BY MICROENCAPSULATION. *Virology*, 1994, 203, 134-143.

Owens, D. E. and N. A. Peppas, Opsonization, biodistribution, and pharmacokinetics of polymeric nanoparticles. *Int. J. Pharm.*, 2006, 307, 93-102.

Owen, R. L., SEQUENTIAL UPTAKE OF HORSERADISH-PEROXIDASE BY LYMPHOID FOLLICLE EPITHELIUM OF PEYERS PATCHES IN NORMAL UNOBSTRUCTED MOUSE INTESTINE - ULTRASTRUCTURAL-STUDY. 1977, 72, 440-451.

Oyewumi, M. O., R. A. Yokel, M. Jay, T. Coakley and R. J. Mumper, Comparison of cell uptake, biodistribution and tumor retention of folate-coated and PEG-coated gadolinium nanoparticles in tumor-bearing mice. *J. Control. Release*, 2004, 95, 613-626.

Pan, Y., Y. J. Li, H. Y. Zhao, J. M. Zheng, H. Xu, G. Wei, J. S. Hao and F. D. Cui, Bioadhesive polysaccharide in protein delivery system: chitosan nanoparticles improve the intestinal absorption of insulin in vivo. *Int. J. Pharm.*, 2002, 249, 139-147.

Pappo, J. and T. H. Ermak, UPTAKE AND TRANSLOCATION OF FLUORESCENT LATEX-PARTICLES BY RABBIT PEYERS PATCH FOLLICLE EPITHELIUM - A QUANTITATIVE MODEL FOR M CELL UPTAKE. 1989, 76, 144-148.

Park, J. H., G. von Maltzahn, L. Zhang, M. P. Schwartz, E. Ruoslahti, S. N. Bhatia and M. J. Sailor, Magnetic iron oxide nanoworms for tumor targeting and imaging. *Adv. Mater.*, 2008, 20, 1630-1635.

Park, J. W., K. Hong, D. B. Kirpotin, G. Colbern, R. Shalaby, J. Baselga, Y. Shao, U. B. Nielsen, J. D. Marks, D. Moore, D. Papahadjopoulos and C. C. Benz, Anti-HER2 immunoliposomes: Enhanced efficacy attributable to targeted delivery. *Clin. Cancer Res.*, 2002, 8, 1172-1181.

Park, Y., H. Y. Hong, H. J. Moon, B. H. Lee, I. S. Kim, I. C. Kwon and K. Rhee, A new atherosclerotic lesion probe based on hydrophobically modified chitosan nanoparticles functionalized by the atherosclerotic plaque targeted peptides. *J. Control. Release*, 2008, 128, 217-223.

Park, I. K., T. H. Kim, Y. H. Park, B. A. Shin, E. S. Choi, E. H. Chowdhury, T. Akaike and C. S. Cho, Galactosylated chitosan-graft-poly(ethylene glycol) as hepatocyte-targeting DNA carrier. *J. Control. Release*, 2001, 76, 349-362.

Patel, T. R., S. E. Harding, A. Ebringerova, M. Deszczynski, Z. Hromadkova, A. Togola, B. S. Paulsen, G. A. Morris and A. J. Rowe, Weak self-association in a carbohydrate system. *Biophys. J.*, 2007, 93, 741-749.

Peppas, N. A., P. Bures, W. Leobandung and H. Ichikawa, Hydrogels in pharmaceutical formulations. *Eur. J. Pharm. Biopharm.*, 2000, 50, 27-46.

Peppas, N. A. and J. J. Sahlin, Hydrogels as mucoadhesive and bioadhesive materials: a review. 1996, 17, 1553-1561.

Peppas, N. A., J. B. Thomas and J. McGinty, Molecular Aspects of Mucoadhesive Carrier Development for Drug Delivery and Improved Absorption. *J. Biomater. Sci.-Polym. Ed.*, 2009, 20, 1-20.

Peppas, N. A., K. M. Wood and J. O. Blanchette, Hydrogels for oral delivery of therapeutic proteins. Expert Opin. Biolog. Ther., 2004, 4, 881-887.

Peters, D., M. Kastantin, V. R. Kotamraju, P. P. Karmali, K. Gujraty, M. Tirrell and E. Ruoslahti, Targeting atherosclerosis by using modular, multifunctional micelles. *Proc. Natl. Acad. Sci. U. S. A.*, 2009, 106, 9815-9819.

Petrus, A. K., A. R. Vortherms, T. J. Fairchild and R. P. Doyle, Vitamin B-12 as a carrier for the oral delivery of insulin. *ChemMedChem*, 2007, 2, 1717-1721.

Peyrot, M., R. R. Rubin, D. F. Kruger and L. B. Travis, Correlates of Insulin Injection Omission. *Diabetes Care*, 2010, 33, 240-245.

Pilobello, K. T., D. E. Slawek and L. K. Mahal, A ratiometric lectin microarray approach to analysis of the dynamic mammalian glycome. *Proc. Natl. Acad. Sci. U. S. A.*, 2007, 104, 11534-11539.

Pirollo, K. F. and E. H. Chang, Does a targeting ligand influence nanoparticle tumor localization or uptake? *Trends Biotechnol.*, 2008, 26, 552-558.

Podual, K., F. J. Doyle and N. A. Peppas, Glucose-sensitivity of glucose oxidase-containing cationic copolymer hydrogels having poly(ethylene glycol) grafts. J. Control. Release, 2000, 67, 9-17.

Podual, K., F. J. Doyle and N. A. Peppas, Preparation and dynamic response of cationic copolymer hydrogels containing glucose oxidase. Polymer, 2000, 41, 3975-3983.

Poretsky, L., Principles of Diabetes of Diabetes Mellitus. 2010, 868.

Prabaharan, M. and J. F. Mano, Chitosan-based particles as controlled drug delivery systems. 2005, 12, 41-57.

Qian, X., X. H. Peng, D. O. Ansari, Q. Yin-Goen, G. Z. Chen, D. M. Shin, L. Yang, A. N. Young, M. D. Wang and S. Nie, In vivo tumor targeting and spectroscopic detection with surface-enhanced Raman nanoparticle tags. *Nat. Biotechnol.*, 2008, 26, 83-90.

Qiu, Y. and K. Park, Environment-sensitive hydrogels for drug delivery. *Adv. Drug Deliv. Rev.*, 2001, 53, 321-339.

Raetz, C. R. H. and C. Whitfield, Lipopolysaccharide endotoxins. *Annu. Rev. Biochem.*, 2002, 71, 635-700.

Rastogi, R., S. Anand and V. Koul, Flexible polymerosomes-An alternative vehicle for topical delivery. *Colloid Surf. B*, 2009, 72, 161-166.

Ratner, D. M., E. W. Adams, M. D. Disney and P. H. Seeberger, Tools for glycomics: Mapping interactions of carbohydrates in biological systems. 2004, 5, 1375-1383.

Rossin, R., D. Pan, K. Qi, J. L. Turner, X. Sun, K. L. Wooley and M. J. Welch, Cu-64-labeled folate-conjugated shell cross-linked nanoparticles for tumor imaging and radiotherapy: Synthesis, radiolabeling, and biologic evaluation. *J. Nucl. Med.*, 2005, 46, 1210-1218.

Roy, K., H. Q. Mao, S. K. Huang and K. W. Leong, Oral gene delivery with chitosan-DNA nanoparticles generates immunologic protection in a murine model of peanut allergy. *Nat. Med.*, 1999, 5, 387-391.

Rudiger, H., H. C. Siebert, D. Solis, J. Jimenez-Barbero, A. Romero, C. W. von der Lieth, T. Diaz-Maurino and H. J. Gabius, Medicinal chemistry based on the sugar code: Fundamentals of lectinology and experimental strategies with lectins as targets. 2000, 7, 389-416.

Roy, R., Syntheses and some applications of chemically defined multivalent glycoconjugates. 1996, 6, 692-702.

Russell-Jones, G. J., S. W. Westwood and A. D. Habberfield, Vitamin-B-12 Mediated Oral Delivery Systems for Granulocyte-colony-stimulating Factor and Erythropoieitin. *Bioconjugate Chem.*, 1995, 6, 459-465.

Russell-Jones, G. J., S. W. Westwood, P. G. Farnworth, J. K. Findlay and H. G. Burger, Synthesis of LHRH Antagonists Suitable for Oral-Administration via the Vitamin-B-12 Uptake System. *Bioconjugate Chem.*, 1995, 6, 34-42.

Sadeghi, A. M. M., M. R. Avadi, S. Ejtemaimehr, S. Abashzadeh, A. Partoazar, F. Dorkoosh, M. Faghihi, M. Rafiee-Tehrani and H. E. Junginger, Development of a Gas Empowered Drug Delivery system for peptide delivery in the small intestine. *J. Control. Release*, 2009, 134, 11-17.

Sahlin, J. J. and N. A. Peppas, Enhanced hydrogel adhesion by polymer interdiffusion: Use of linear poly(ethylene glycol) as an adhesion promoter. *J. Biomater. Sci.-Polym. Ed.*, 1997, 8, 421-436.

Sarmento, B., A. J. Ribeiro, F. Veiga, D. C. Ferreira and R. J. Neufeld, Insulin-Loaded Nanoparticles are Prepared by Alginate Ionotropic Pre-Gelation Followed by Chitosan Polyelectrolyte Complexation. *J. Nanosci. Nanotechno.*, 2007, 7, 2833-2841.

Sarmento, B., A. Ribeiro, F. Veiga, P. Sampaio, R. Neufeld and D. Ferreira, Alginate/Chitosan nanoparticles are effective for oral insulin delivery. 2007, 24, 2198-2206.

Sarmento, B., A. Ribeiro, F. Veiga, D. Ferreira and R. Neufeld, Oral bioavailability of insulin contained in polysaccharide nanoparticles. 2007, 8, 3054-3060.

Schar-Zammaretti, P. and J. Ubbink, The cell wall of lactic acid bacteria: Surface constituents and macromolecular conformations. *Biophys. J.*, 2003, 85, 4076-4092.

Sechriest, V. F., Y. J. Miao, C. Niyibizi, A. Westerhausen-Larson, H. W. Matthew, C. H. Evans, F. H. Fu and J. K. Suh, GAG-augmented polysaccharide hydrogel: A novel biocompatible and biodegradable material to support chondrogenesis. *J. Biomed. Mater. Res.*, 1999, 49, 534-541.

Seksek, O., J. Biwersi and A. S. Verkman, Translational Diffusion of Macromolecule-sized Solutes in Cytoplasm and Nucleus. *J. Cell. Biol.*, 1997, 138, 131-142.

Senel, S., M. J. Kremer, S. Kas, P. W. Wertz, A. A. Hincal and C. A. Squier, Enhancing effect of chitosan on peptide drug delivery across buccal mucosa. *Biomaterials*, 2000, 21, 2067-2071.

Serra, L., J. Domenech and N. A. Peppas, Design of poly(ethylene glycol)-tethered copolymers as novel mucoadhesive drug delivery systems. *Eur. J. Pharm. Biopharm.*, 2006, 63, 11-18.

Sershen, S. R., S. L. Westcott, N. J. Halas and J. L. West, Temperature-sensitive polymer-nanoshell composites for photothermally modulated drug delivery. *J. Biomed. Mater. Res.*, 2000, 51, 293-298.

Shah, D. and W. C. Shen, Transcellular delivery of an insulin-transferrin conjugate in enterocyte-like Caco-2 cells. *J. Pharm. Sci.*, 1996, 85, 1306-1311.

Shan, X., Y. Yuan, C. Liu, X. Tao, Y. Sheng and F. Xu, Influence of PEG chain on the complement activation suppression and longevity in vivo prolongation of the PCL biomedical nanoparticles. *Biomed. Microdevices*, 2009, 11, 1187-1194.

Shofner, J. P., Oral Delivery of Protein-Transporter Bioconjugates Using Intelligent Complexation Hydrogels. 2008, Ph.D., 325, Thesis, Department of Chemical Engineering, The University of Texas at Austin.

Shofner, J. P., M. A. Phillips and N. A. Peppas, Cellular Evaluation of Synthesized Insulin/Transferrin Bioconjugates for Oral Insulin Delivery Using Intelligent Complexation Hydrogels. *Macromol. Biosci.*, 10, 299-306.

Shogren, R., T. A. Gerken and N. Jentoft, Role of Glycosylation on the Conformation and Chain Dimensions of O-Linked Glycoproteins - Light-Scattering-Studies of Ovine Submaxillary Mucin. *Biochemistry*, 1989, 28, 5525-5536.

Sigal, G. B., M. Mammen, G. Dahmann and G. M. Whitesides, Polyacrylamides bearing pendant alpha-sialoside groups strongly inhibit agglutination of erythrocytes by

influenza virus: The strong inhibition reflects enhanced binding through cooperative polyvalent interactions. *J. Am. Chem. Soc.*, 1996, 118, 3789-3800.

Sinha, V. R. and R. Kumria, Polysaccharides in colon-specific drug delivery. 2001, 224, 19-38.

Solchaga, L. A., J. S. Temenoff, J. Z. Gao, A. G. Mikos, A. I. Caplan and V. M. Goldberg, Repair of osteochondral defects with hyaluronan- and polyester-based scaffolds. *Osteoarthritis Cartilage*, 2005, 13, 297-309.

Soman, N. R., S. L. Baldwin, G. Hu, J. N. Marsh, G. M. Lanza, J. E. Heuser, J. M. Arbeit, S. A. Wickline and P. H. Schlesinger, Molecularly targeted nanocarriers deliver the cytolytic peptide melittin specifically to tumor cells in mice, reducing tumor growth. *J. Clin. Invest.*, 2009, 119, 2830-2842.

Spillmann, D. and M. M. Burger, Carbohydrate-carbohydrate interactions in adhesion. *J. Cell. Biochem.*, 1996, 61, 562-568.

Sriamornsak, P. and N. Wattanakorn, Rheological synergy in aqueous mixtures of pectin and mucin. *Carbohydr. Polym.*, 2008, 74, 474-481.

Stenekes, R. J. H., O. Franssen, E. M. G. van Bommel, D. J. A. Crommelin and W. E. Hennink, The preparation of dextran microspheres in an all-aqueous system: Effect of the formulation parameters on particle characteristics. *Pharm. Res.*, 1998, 15, 557-561.

Stertman, L., E. Lundgren and I. Sjoholm, Starch microparticles as a vaccine adjuvant: Only uptake in Peyer's patches decides the profile of the immune response. *Vaccine*, 2006, 24, 3661-3668.

Stertman, L., L. Strindelius and I. Sjoholm, Starch microparticles as an adjuvant in immunisation: effect of route of administration on the immune response in mice. *Vaccine*, 2004, 22, 2863-2872.

Suh, J. K. F. and H. W. T. Matthew, Application of chitosan-based polysaccharide biomaterials in cartilage tissue engineering: a review. *Biomaterials*, 2000, 21, 2589-2598.

Sun, S. P., N. Liang, H. Z. Piao, H. Yamamoto, Y. Kawashima and F. D. Cui, Insulin-S.O (sodium oleate) complex-loaded PLGA nanoparticles: Formulation, characterization and in vivo evaluation. *J. Microencapsul.*, 27, 471-478.

Sun, W., W. Zou, G. Huang, A. Li and N. Zhang, Pharmacokinetics and targeting property of TFu-loaded liposomes with different sizes after intravenous and oral administration. *J. Drug Target.*, 2008, 16, 357-365.

Sun, X., R. Rossin, J. L. Turner, M. L. Becker, M. J. Joralemon, M. J. Welch and K. L. Wooley, An assessment of the effects of shell cross-linked nanoparticle size, core composition, and surface PEGylation on in vivo biodistribution. *Biomacromolecules*, 2005, 6, 2541-2554.

Swenson, E. S., W. B. Milisen and W. Curatolo, Intestinal Permeability Enhancement-Efficacy, Acute Local Toxicity, and Reversibility. *Pharm. Res.*, 1994, 11, 1132-1142.

Tabata, Y., S. Gutta and R. Langer, Controlled Delivery Systems for Proteins Using Polyanhydride Microspheres. *Pharm. Res.*, 1993, 10, 487-496.

Temenoff, J. S. and A. G. Mikos, Review: tissue engineering for regeneration of articular cartilage. *Biomaterials*, 2000, 21, 431-440.

Thijssen, V., R. Postel, R. Brandwijk, R. P. M. Dings, I. Nesmelova, S. Satijn, N. Verhofstad, Y. Nakabeppu, L. G. Baum, J. Bakkers, K. H. Mayo, F. Poirier and A. W. Griffioen, Galectin-1 is essential in tumor angiogenesis and is a target for antiangiogenesis therapy. *Proc. Natl. Acad. Sci. U. S. A.*, 2006, 103, 15975-15980.

Thomas, J. B., J. H. Tingsanchali, A. M. Rosales, C. M. Creecy, J. W. McGinity and N. A. Peppas, Dynamics of poly(ethylene glycol)-tethered, pH responsive networks. *Polymer*, 2007, 48, 5042-5048.

Tobio, M., A. Sanchez, A. Vila, I. Soriano, C. Evora, J. L. Vila-Jato and M. J. Alonso, The role of PEG on the stability in digestive fluids and in vivo fate of PEG-PLA nanoparticles following oral administration. *Colloid Surf. B-Biointerfaces*, 2000, 18, 315-323.

Tong, L., W. He, Y. Zhang, W. Zheng and J. X. Cheng, Visualizing Systemic Clearance and Cellular Level Biodistribution of Gold Nanorods by Intrinsic Two-Photon Luminescence. *Langmuir*, 2009, 25, 12454-12459.

Torchilin, V. P., Structure and design of polymeric surfactant-based drug delivery systems. *J. Control. Release*, 2001, 73, 137-172.

Torres-Lugo, M. and N. A. Peppas, Preparation and characterization of P(MAA-g-EG) nanospheres for protein delivery applications. *J. Nanopart. Res.*, 2002, 4, 73-81.

Townsend, R. R., M. R. Hardy, T. C. Wong and Y. C. Lee, Binding Of N-Linked Bovine Fetuin Glycopeptides To Isolated Rabbit Hepatocytes - Gal/Galnac Hepatic Lectin Discrimination Between Galbeta(1,4)Glcnac And Galbeta(1,3)Glcnac In A Triantennary Structure. *Biochemistry*, 1986, 25, 5716-5725.

Tuesca, A., K. Nakamura, M. Morishita, J. Joseph, N. Peppas and A. Lowman, Complexation hydrogels for oral insulin delivery: Effects of polymer dosing on in vivo efficacy. J. Pharm. Sci., 2008, 97, 2607-2618.3

Tuesca, A. D., C. Reiff, J. I. Joseph and A. M. Lowman, Synthesis, Characterization and In Vivo Efficacy of PEGylated Insulin for Oral Delivery with Complexation Hydrogels. *Pharm. Res.*, 2009, 26, 727-739.

Ulevitch, R. J. and P. S. Tobias, Receptor-Dependent Mechanisms of Cell Stimulation by Bacterial-Endotoxicin. *Annu. Rev. Immunol.*, 1995, 13, 437-457.

Umamaheshwari, R. B. and N. K. Jain, Receptor mediated targeting of lectin conjugated gliadin nanoparticles in the treatment of Helicobacter pylori. *J. Drug Target.*, 2003, 11, 415-424.

Ungell, A.-L. N., Caco-2 replace or refine? *Drug Discov. Today: Technologies*, 2004, 1, 423-430.Wang, M., D. W. Lowik, A. D. Miller and M. Thanou, Targeting the Urokinase Plasminogen Activator Receptor with Synthetic Self-Assembly Nanoparticles. *Bioconjugate Chem.*, 2009, 20, 32-40.

Vacanti, C. A., R. Langer, B. Schloo and J. P. Vacanti, Synthetic-Polymers Seeded With Chondrocytes Provide A Template For New Cartilage Formation. *Plast. Reconstr. Surg.*, 1991, 88, 753-759.

Vandamme, T. F., A. Lenourry, C. Charrueau and J. Chaumeil, The use of polysaccharides to target drugs to the colon. 2002, 48, 219-231.

Van Dijk-Wolthuis, W. N. E., O. Franssen, H. Talsma, M. J. van Steenbergen, J. J. Kettenes-van den Bosch and W. E. Hennink, Synthesis, Characterization, and Polymerization of Glycidyl Methacrylate Derivitized Dextran. Macromolecules, 1995, 28, 6317-6322.

vanDijkWolthuis, W. N. E., J. J. KettenesvandenBosch, A. vanderKerkvanHoof and W. E. Hennink, Reaction of dextran with glycidyl methacrylate: An unexpected transesterification. *Macromolecules*, 1997, 30, 3411-3413.

Walter, E., S. J. Blake, J. Roessler, J. M. Hilfinger and G. L. Amidon, HT29-MTX/Caco-2 cocultures as an in vitro model for the intestinal epithelium: In vitro-in vivo correlation with permeability data from rats and humans. *J. Pharm. Sci.*, 1996, 85, 1070-1076.

Wang, X. D., W. Hu, Y. Cao, J. Yao, J. Wu and X. S. Gu, Dog sciatic nerve regeneration across a 30-mm defect bridged by a chitosan/PGA artificial nerve graft. *Brain*, 2005, 128, 1897-1910.

Wang, X., J. Li, Y. Wang, K. J. Cho, G. Kim, A. Gjyrezi, L. Koenig, P. Giannakakou, H. J. Shin, M. Tighiouart, S. Nie, Z. G. Chen and D. M. Shin, HFT-T, a Targeting Nanoparticle, Enhances Specific Delivery of Paclitaxel to Folate Receptor-Positive Tumors. *ACS Nano*, 2009, 3, 3165-3174.

Wells, C. L., R. P. Jechorek, S. B. Olmsted and S. L. Erlandsen, Effect of LPC on Epithelial Integrity and Bacterial Uptake in the Polarized Human Enterocyte-Like Cell-Line Caco-2. *Circ. Shock*, 1993, 40, 276-288.

Werle, M. and H. Takeuchi, Chitosan-aprotinin coated liposomes for oral peptide delivery: Development, characterisation and in vivo evaluation. *Int. J. Pharm.*, 2009, 370, 2

Widera, A., F. Norouziyan and W. C. Shan, Mechanisms of TfR-mediated transcytosis and sorting in epithelial cells and applications toward drug delivery. *Adv. Drug Deliver. Rev.*, 2003, 55, 1439-1466.

Wood, K. M., Molecular design of advanced oral protein delivery systems using complexation hydrogels. 2006, Ph.D., Thesis. Academic, DepartmentThe University of Texas at Austin.

Wood, K. M., G. M. Stone and N. A. Peppas, The effect of complexation hydrogels on insulin transport in intestinal epithelial cell models. *Acta Biomater.*, 2010, 6, 48-56.

Wood, K. M., G. M. Stone and N. A. Peppas, Wheat germ agglutinin functionalized complexation hydrogels for oral insulin delivery. *Biomacromolecules*, 2008, 9, 1293-1298.

World Health Organization *Preventing Chronic Diseases: A Vital Investment*. 2006,

Xu, H., F. Meng and Z. Zhong, Reversibly crosslinked temperature-responsive nano-sized polymersomes: synthesis and triggered drug release. *J. Mater. Chem.*, 2009, 19, 4183-4190.

Yamagata, T., M. Morishita, N. J. Kavimandan, K. Nakamura, Y. Fukuoka, K. Takayama and N. A. Peppas, Characterization of insulin protection properties of complexation hydrogels in gastric and intestinal enzyme fluids. *J. Control. Release*, 2006, 112, 343-349.

Yamamoto, A., T. Taniguchi, K. Rikyuu, T. Tsuji, T. Fujita, M. Murakami and S. Muranishi, Effects of Various Protease Inhibitors on the Intestinal Absorption and Degradation of Insulin in Rats. *Pharm. Res.*, 1994, 11, 1496-1500.

Yamamoto, M., P. Rennert, J. R. McGhee, M. N. Kweon, S. Yamamoto, T. Dohi, S. Otake, H. Bluethmann, K. Fujihashi and H. Kiyono, Alternate mucosal immune system: Organized Peyer's patches are not required for IgA responses in the gastrointestinal tract. *J. Immunol.*, 2000, 164, 5184-5191.

Yang, K. W., X. R. Li, Z. L. Yang, P. Z. Li, F. Wang and Y. Liu, Novel polyion complex micelles for liver-targeted delivery of diammonium glycyrrhizinate: in vitro and in vivo characterization. *J. Biomed. Mater. Res. A*, 2009, 88, 140-148.

Yang, T. Z., J. J. Arnold and F. Ahsan, Tetradecylmaltoside (TDM) enhances in vitro and in vivo intestinal absorption of enoxaparin, a low molecular weight heparin. *J. Drug Target.*, 2005, 13, 29-38.

Yarema, K. J. and C. R. Bertozzi, Chemical approaches to glycobiology and emerging carbohydrate-based therapeutic agents. *Curr. Opin. Chem. Biol.*, 1998, 2, 49-61.

Zhang, G., Z. Yang, W. Lu, R. Zhang, Q. Huang, M. Tian, L. Li, D. Liang and C. Li, Influence of anchoring ligands and particle size on the colloidal stability and in vivo biodistribution of polyethylene glycol-coated gold nanoparticles in tumor-xenografted mice. *Biomaterials*, 2009, 30, 1928-1936.

Zhang, H., S. Mardyani, W. C. Chan and E. Kumacheva, Design of biocompatible chitosan microgels for targeted pH-mediated intracellular release of cancer therapeutics. *Biomacromolecules*, 2006, 7, 1568-1572.

Zhang, N., Q. N. Ping, G. H. Huang and W. F. Xu, Investigation of lectin-modified insulin liposomes as carriers for oral administration. *Int. J. Pharm.*, 2005, 294, 247-259.

Zheng, J., D. Jaffray and C. Allien, Quantitative CT Imaging of the Spatial and Temporal Distribution of Liposomes in a Rabbit Tumor Model. *Mol. Pharm.*, 2009, 6, 571-

Zheng, Y. Q., Y. H. Qiu, M. Y. F. Lu, D. Hoffman and T. L. Reiland, Permeability and absorption of leuprolide from various intestinal regions in rabbits and rats. *Int. J. Pharm.*, 1999, 185, 83-92.

Vita

Margaret Phillips is from St. Louis, MO where she attended Saint Louis Univeristy to pursue an Honors Bachelors of Science Degree in Biomedical Engineering and Mathematics. Margaret gradauated with her Honors B.S. degree in 2006. After finishing her undergraduate studies, Margaret Phillips began her graduate studies to pursue a Ph.D. in Biomedical Engineering at the University of Texas at Austin. Margaret carried out her graduate studies and research under the guidance of Prof. Nicholas Peppas.

Permanent address (or email): margaretaphillips@mail.utexas.edu

This dissertation was typed by the author.